Identification of response amplitude operators for ships based on full scale measurements

September 2015

D. Skandali

MARINE CONTRACTORS

TU Delft

Offshore & Dredging Engineering

Identification of response amplitude operators for ships based on full scale measurements

Master of Science

Thesis

For the degree of Master of Science in Offshore & Dredging Engineering at Delft University of Technology

D. Skandali

September, 2015

Author:
D. Skandali

Thesis Committee:

Prof. Dr. A. V. Metrikine	Delft University of Technology
Dr. Eliz-Mari Lourens	Delft University of Technology
Dr. K.N. van Dalen	Delft University of Technology
Ir. R. Ogink	Heerema Marine Contractors

Educational Institute:
Delft University of Technology

Under the authority of:
Heerema Marine Contractors

Year to be released: 2015

Acknowledgements

This report is the result of the research I conducted at Heerema Marine Contractors for the master degree in Offshore & Dredging Engineering at Delft University of Technology. In order to complete this graduation study successfully, I received support and advice from many people. I would like to take this opportunity to thank every person that helped me during this thesis.

First of all I am very grateful to Heerema Marine Contractors for giving me the chance to perform my research on a very interesting and challenging topic. Working at HMC was a great experience for the past nine months. The friendly working environment as well as the experienced and highly qualified employees helped me to expand my knowledge on hydromechanics and other engineering disciplines.

At this point, I would like to thank my daily supervisor in HMC, Richard Ogink, for his support and advice. His feedback provided me with the guidance that I needed for this study. Also, I am grateful for our cooperation during the whole period of the graduation study and the fact that he was always available for questions and discussion.

Also, I would like to thank my daily supervisor in TU Delft, Eliz-Mari Lourens, for her advice and suggestions. Her input, especially on the field of identification problems, was important for the completion of this thesis.

Moreover, I would also like to thank the chairman of my graduation committee, Professor Andrei Metrikine, for his guidance and his remarks during this graduation study. His valuable advice and especially his to-the-point questions, helped me deeply understand the physics of the problem and face the challenges of this graduation study.

Finally, I would like to thank my friends and family for their encouragement, patience and mental support.

Danai Skandali

Leiden, September 2015

Abstract

Heerema Marine Contractors (HMC) operates several crane vessels, barges and tug boats for the transportation, the installation and the removal of offshore facilities. To achieve safe and successful projects, the accurate prediction of vessel motions is of great importance. Vessel motions are calculated on the basis of wave energy spectra and motion Response Amplitude Operators (RAOs). The wave energy spectra are received from meteorological services or from wave rider buoys and the RAOs are typically calculated using diffraction software, based on potential theory.

In order to validate the numerical models, HMC regularly monitors the motions of its vessels. In a number of cases, HMC has noticed that the calculated vessel motions do not fully match with the full scale measurements. This inaccuracy can occur due to several reasons such as forward speed of the vessel, awkward draught, viscous damping forces or the variations of mass distribution during the projects.

The main objective of this graduation study is to develop a mathematical method which determines the motion RAOs using the full scale motion measurements and the available wave data. Basically, it is examined whether it is possible to calibrate the following model properties of the vessels:

- The hydrodynamic properties: the potential added mass, the potential damping and the potential wave forces.
- The mass matrix. It is examined whether the radii of gyration can be determined when measured wave data and vessel motions are available.
- The viscous damping matrix.
- The coordinates of the CoG.

The procedure for the identification of the RAOs is applied on a specific vessel with a certain draft: the semi-submersible crane vessel Thialf at 22m draft in deep water.

The first challenge of this graduation study is to find a method to express each element of the hydrodynamic database with a limited number of parameters for the entire frequency range. This is accomplished by applying the vector fitting method. According to this method, the hydrodynamic elements are fitted to approximation functions with a certain number of coefficients.

In order to calibrate the motion RAOs, a sensitivity analysis is first be performed. The sensitivity analysis leads to the minimization of the number of parameters that is to be examined.

The identification process is repeated several times until the best possible modifications are found. In order to choose the correct modification, the normalized root mean square error between the calculated and the measured vessel motions is determined. Apart from the normalised root mean square error, the selection of the possible modifications should be based on logical criteria as well. For this graduation study, the identification method is tested by several cases. These test cases are based on simulated data.

The results of this study shows that we can identify several parameters that lead to more accurate response spectra. However, in most cases the solution is not unique and we have to choose between the calibration of two parameters or more. For instance, the same results can be achieved by either changing the radius of gyration or a diagonal element of the hydrodynamic added mass and damping. This can be solved by examining the causes of inaccuracies. If the draft of the vessel is such that the awkward draft does not occur, then the hydrodynamic data base should not be modified. Small changes of the viscous damping could not be identified for the SSCV ‘Thialf’. The viscous damping is much lower than the hydrodynamic damping and as a consequence, it doesn’t have noticeable impact on the vessel responses. However, this is not valid for rolling ships such as the deep-water construction vessel Aegir. Finally, it should be mentioned that the errors of the data processing influence the accuracy of the identification procedure.

Table of contents

ACKNOWLEDGEMENTS ..... **I**

ABSTRACT ..... **III**

TABLE OF CONTENTS ..... **V**

LIST OF FIGURES ..... **IX**

LIST OF TABLES ..... **XIII**

LIST OF SYMBOLS ..... **XV**

CHAPTER 1. INTRODUCTION **1**

1.1 PROBLEM DEFINITION 1

1.2 OBJECTIVES 2

1.3 APPROACH 2

CHAPTER 2. CALCULATION OF SHIP MOTIONS **3**

2.1 EQUATION OF MOTION 3

2.2 MASS MATRIX 6

2.3 STIFFNESS MATRIX 7

2.4 HYDRODYNAMIC PROPERTIES 8

2.4.1 Potential theory: added mass and damping *8*

2.4.2 Potential theory: wave forces and moments *13*

2.5 VISCOUS DAMPING 14

2.6 WAVE SPECTRUM 15

CHAPTER 3. VECTOR FITTING **17**

3.1 RATIONAL FUNCTION APPROXIMATION 17

3.2 THEORY ABOUT THE VECTOR FITTING METHOD 22

3.2.1 Stage 1 ..... *23*

3.2.2 Stage 2 ..... *26*

3.2.3 Starting poles *27*

3.3 VECTOR FITTING: ADDED MASS AND DAMPING 27

3.3.1 Added mass and Damping-Stage 1 ..... *28*

3.3.2 Added mass and Damping-Stage 2 ..... *30*

3.4 VECTOR FITTING –WAVE FORCES AND MOMENTS 32

3.4.1 Wave forces and moments-Stage 1 ..... *33*

3.4.2 Wave forces and moments-Stage 2 ..... *34*

3.4.3 Interpolation of wave forces and moments *38*

3.5 REMARKS FOR THE VECTOR FITTING METHOD 43

CHAPTER 4. COG TRANSFORMATIONS **45**

4.1 TRANSFORMATION MATRICES 45

4.2 TRANSFORMATION OF THE HYDRODYNAMIC DATA BASE 47

CHAPTER 5. MOTION RESPONSE SPECTRA 49
5.1 MOTION RAOS 49
5.2 MOTION RESPONSE SPECTRA 54
CHAPTER 6. SENSITIVITY ANALYSIS 57
6.1 SENSITIVITY ANALYSIS FOR COG 57
6.2 SENSITIVITY ANALYSIS FOR THE RADIUS OF GYRATION 59
6.3 SENSITIVITY ANALYSIS OF VISCOUS DAMPING 61
6.4 SENSITIVITY ANALYSIS: ADDED MASS AND DAMPING 65
6.5 SENSITIVITY ANALYSIS: WAVE FORCES AND MOMENTS 68
CHAPTER 7. IDENTIFICATION OF RAOS 73
7.1 IDENTIFICATION PROCCEDURE 73
7.1.1 Golden section method 73
CHAPTER 8. TEST CASES 81
8.1 DATA PROCESSING 81
8.1.1 Impact of data processing 82
8.2 TEST CASE 1 83
8.3 TEST CASE 2 84
8.4 TEST CASE 3 98
8.5 TEST CASE 4 106
8.6 TEST CASE 5 113
CHAPTER 9. CONCLUSIONS-RECOMMENDATIONS 123
9.1 CONCLUSIONS 123
9.1.1 Vector fitting 123
9.1.2 Sensitivity analysis 124
9.1.3 Identification procedure 124
9.2 RECOMMENDATIONS 125
REFERENCES 127
APPENDIX A1 PEAK SELECTION ..... - 1 -
APPENDIX A2 STAGE1-IDENTIFICATION OF POLES ..... - 2 -
APPENDIX A3 STAGE 2-VECTOR FITTING ..... - 4 -
APPENDIX B1 STAGE 1-IDENTIFICATION OF POLES ..... - 5 -
APPENDIX B2 STAGE 2-VECTOR FITTING ..... - 7 -
APPENDIX B3 POLES AND RESIDUES ..... - 8 -
APPENDIX B4 INTERPOLATION ..... - 9 -
APPENDIX C1 TRANSFORMATION OF HYD. DATA ..... - 10 -
APPENDIX C2 SPRING MATRIX TRANSFORMATION ..... - 14 -
APPENDIX D1 GOLDEN SECTION METHOD ..... - 16 -
APPENDIX D1 IDENTIFICATION OF COG ..... - 17 -

APPENDIX D2 IDENTIFICATION OF MASS MATRIX ..... - 26 -

APPENDIX D3 IDENTIFICATION OF VISCOUS DAMP. ..... - 30 -

APPENDIX D4 IDENTIFICATION OF ADDED MASS-DAMPING ..... - 34 -

APPENDIX D5 IDENTIFICATION OF WAVE FORCES ..... - 44 -

List of figures

Figure 1: Vessels of HMC 1
Figure 2: Calculation of motion response spectra for a floating structure 3
Figure 3: Ship motions, SSCV Thialf 4
Figure 4: Amplitude of Heave-RAO for the SSCV Thialf in deep water at 22m draft 5
Figure 5: Phase of Heave-RAO for the SSCV Thialf in deep water at 22m draft 6
Figure 6: Potential theory and equation of motion 9
Figure 7: Radiation potential 9
Figure 8: Added mass matrix: SSCV Thialf, deep water, 22m draft 11
Figure 9: Damping matrix: SSCV Thialf, deep water, 22m draft 12
Figure 10: Amplitude of wave forces and moments: 15° wave heading, SSCV Thialf, deep water, 22m draft 14
Figure 11: Phase of wave forces and moments: 15° wave heading, SSCV Thialf, deep water, 22m draft 14
Figure 12: Wave spectrum $S_\zeta(\omega)$ where $\zeta(t)$=wave elevation, ζ_α=wave amplitude, ω=wave frequency 15
Figure 13: Directional wave spectrum 15
Figure 14: Wave types 16
Figure 15: Amplitude, real part and imaginary part of approximation function, case 1 18
Figure 16: Examination of imaginary part of pole, case 2 19
Figure 17: Examination of real part of pole, case 3 19
Figure 18: Examination of real part of residue, case 4 20
Figure 19: Examination of imaginary part of residue, case 5 20
Figure 20: Examination of both imaginary and real parts of residue, case 6 21
Figure 21: Examination of real quantity 'd', case 7 21
Figure 22: Examination of real quantity 'h', case 8 22
Figure 23: Peak Selection, ab_{33} 29
Figure 24: New set of poles, ab_{33} 29
Figure 25: Vector fitting for hydrodynamic added mass a_{33} 30
Figure 26: Vector fitting for hydrodynamic damping b_{33} 31
Figure 27: Vector fitting for hydrodynamic added mass a_{66} 31
Figure 28: Vector fitting for hydrodynamic damping b_{66} 32
Figure 29: Amplitude of F_3, wave directions = 0° -180° 33
Figure 30: Peak selection, amplitude of $F3(\omega, 180°)$ 34
Figure 31: New set of poles, $F3(\omega, 180°)$ 34
Figure 32: Vector fitting for $F3(\omega, 180°)$, real part 35

Figure 33: Vector fitting for $F3(\omega, 180°)$, imaginary part 35
Figure 34: Real part of F_3, directions=0°-180°, fitted curve=red color, original curve=blue color 36
Figure 35: Imaginary part of F_3, directions=0°-180°, fitted curve=red color, original curve=blue color 37
Figure 36: Vector fitting for $F1(\omega, 90°)$, real part 38
Figure 37: Vector fitting for $F1(\omega, 90°)$, imaginary part 38
Figure 38: Real part of residues of F_3 over the wave directions 39
Figure 39: Imaginary part of residues of F3 over the wave directions 40
Figure 40: Interpolated real part of residues of F_3 40
Figure 41: Interpolated imaginary part of residues of F_3 41
Figure 42: Interpolation of F_3, real part 41
Figure 43: Interpolation of F_3, imaginary part 42
Figure 44: Amplitude of $F3(\omega, 5°)$, verification of interpolated forces 42
Figure 45: CoG, Hyd.Origin, CoB for SSCV Thialf 45
Figure 46: Azimuth angle β and elevation angle γ 46
Figure 47: Heave RAO, real part, fitted curve=red color, original curve=blue color 49
Figure 48: Heave RAO, imaginary part, fitted curve=red color, original curve=blue color 49
Figure 49: Roll RAO, real part, fitted curve=red color, original curve=blue color 50
Figure 50: Roll RAO, imaginary part, fitted curve=red color, original curve=blue color 50
Figure 51: Surge RAO, amplitude, fitted curve=red color, original curve=blue color 51
Figure 52: Sway RAO, amplitude, fitted curve=red color, original curve=blue color 51
Figure 53: Yaw RAO, amplitude, fitted curve=red color, original curve=blue color 52
Figure 54: Roll-RAO, amplitude, 165° wave heading 53
Figure 55: Yaw-RAO, amplitude, 90° wave heading 53
Figure 56: 1D Jonswap Spectrum, T_p=8.5s, H_s=5m 54
Figure 57: 2D Jonswap Spectrum, main wave direction=30° 54
Figure 58: Motion Response Spectra 55
Figure 59: CoG of the SSCV Thialf 57
Figure 60: Sensitivity analysis for the 'x' coordinate of the CoG 58
Figure 61: Sensitivity analysis for the 'y' coordinate of the CoG 58
Figure 62: Sensitivity analysis for the 'z' coordinate of the CoG 59
Figure 63: Sensitivity analysis for the radius of gyration 'r_{xx}' 60
Figure 64: Sensitivity analysis for the radius of gyration 'r_{yy}' 60
Figure 65: Sensitivity analysis for the radius of gyration 'r_{zz}' 61
Figure 66: Sensitivity analysis for viscous damping element $B_{ad}(1,1)$ 62
Figure 67: Sensitivity analysis for viscous damping element $B_{ad}(2,2)$ 62
Figure 68: Sensitivity analysis for viscous damping element $B_{ad}(3,3)$ 63

Figure 69: Sensitivity analysis for viscous damping element $B_{ad}(4,4)$ 63
Figure 70: Sensitivity analysis for viscous damping element $B_{ad}(5,5)$ 64
Figure 71: Sensitivity analysis for viscous damping element $B_{ad}(6,6)$ 64
Figure 72: Modification of ab_{33}, real part 65
Figure 73: Modification of ab_{33}, imaginary part 66
Figure 74: Response spectra, sensitivity analysis, ab_{33} 66
Figure 75: Modification of ab_{35}, real part 67
Figure 76: Modification of $ab_{35,}$ imaginary part 67
Figure 77: Response spectra, sensitivity analysis, ab_{35} 68
Figure 78: Modification of $F_3(\omega,30^o)$, real part 69
Figure 79: Modification of $F_3(\omega,30^o)$, imaginary part 69
Figure 80: Response spectra, sensitivity analysis, $F_3(\omega,30^o)$ 70
Figure 81: Modification of $F_3(\omega,90^o)$, real part 70
Figure 82: Modification of $F_3(\omega,90^o)$, imaginary part 71
Figure 83: Response spectra, sensitivity analysis, $F_3(\omega,90^o)$ 71
Figure 84: Golden section method 74
Figure 85: Identification of the CoG 76
Figure 86: Identification of radius of gyration 77
Figure 87: Identification of added mass and damping 78
Figure 88: Identification of wave forces 79
Figure 89: Final identification procedure 80
Figure 90: Coordinate system for the ship and the 2D wave spectrum 82
Figure 91: 1D and 2D wave spectra, test case 1 83
Figure 92: 2D wave spectrum, local coordinate system of the vessel, test case 1 83
Figure 93: Comparison of motion response spectra, interpolation of wave forces, data set=blue, calculations=red 84
Figure 94: Comparison of motion response spectra, interpolation of RAOs, data set=blue, calculations=red 84
Figure 95: 1D and 2D wave spectra, test case 2 85
Figure 96: 2D wave spectrum, local coordinate system of the vessel, test case 2 85
Figure 97: Comparison of response spectra, test case 2, data set=blue, calculations=red 86
Figure 98: Motion response spectra, identification method, test case 2, data set=blue, calculations=red 93
Figure 99: Motion response spectra, solution, test case 2, data set=blue, calculations=red 93
Figure 100: Comparison of RAOs, amplitude of Surge-RAO, test case 2 95
Figure 101: Comparison of RAOs, amplitude of Sway-RAO, test case 2 95
Figure 102: Comparison of RAOs, amplitude of Heave-RAO, test case 2 96
Figure 103: Comparison of RAOs, amplitude of Roll-RAO, test case 2 96

Figure 104: Comparison of RAOs, amplitude of Pitch-RAO, test case 2 97
Figure 105: Comparison of RAOs, amplitude of Yaw-RAO, test case 2 97
Figure 106: 1D and 2D wave spectra, test case 3 99
Figure 107: 2D wave spectrum, local coordinate system of the vessel, test case 3 99
Figure 108: Comparison of motion response spectra, test case 3 100
Figure 109: Motion response spectra, identification method, test case 3, data set=blue, calculations=red 101
Figure 110: Motion response spectra, solution, test case 3, data set=blue, calculations=red 101
Figure 111: Comparison of RAOs: Amplitude of Surge-RAO, test case 3 102
Figure 112: Comparison of RAOs: Amplitude of Sway-RAO, test case 3 103
Figure 113: Comparison of RAOs: Amplitude of Heave-RAO, test case 3 103
Figure 114: Comparison of RAOs: Amplitude of Roll-RAO, test case 3 104
Figure 115: Comparison of RAOs: Amplitude of Pitch-RAO, test case 3 104
Figure 116: Comparison of RAOs: Amplitude of Yaw-RAO, test case 3 105
Figure 117: 1D and 2D wave spectra, test case 4 106
Figure 118: 2D wave spectrum, local coordinate system of the vessel, test case 4 106
Figure 119: Comparison of motion response spectra, test case 4 107
Figure 120: Motion response spectra, identification method, test case 4, data set=blue, calculations=red 108
Figure 121: Motion response spectra, solution, test case 4, data set=blue, calculations=red 108
Figure 122: Comparison of RAOs: Amplitude of Surge-RAO, test case 4 109
Figure 123: Comparison of RAOs: Amplitude of Sway-RAO, test case 4 110
Figure 124: Comparison of RAOs: Amplitude of Heave-RAO, test case 4 110
Figure 125: Comparison of RAOs: Amplitude of Roll-RAO, test case 4 111
Figure 126: Comparison of RAOs: Amplitude of Pitch-RAO, test case 4 111
Figure 127: Comparison of RAOs: Amplitude of Yaw-RAO, test case 4 112
Figure 128: 1D and 2D wave spectra, test case 5 113
Figure 129: 2D wave spectrum, local coordinate system of the vessel, test case 5 113
Figure 130: Comparison of motion response spectra, test case 5, data set=blue, calculations=red 114
Figure 131: Motion response spectra, identification 1, test case 5, data set=blue, calculations=red 115
Figure 132: Motion response spectra, identification 2, test case 5, data set=blue, calculations=red 115
Figure 133: Motion response spectra, solution, test case 5, data set=blue, calculations=red 116
Figure 134: Comparison of RAOs, amplitude of Heave-RAO, identification 1, test case 5 117
Figure 135: Comparison of RAOs, amplitude of Heave-RAO, identification 2, test case 5 117
Figure 136: Comparison of RAOs, amplitude of Roll-RAO, identification 1, test case 5 118
Figure 137: Comparison of RAOs, amplitude of Roll-RAO, identification 2, test case 5 118
Figure 138: Comparison of RAOs, amplitude of Pitch-RAO, identification 1, test case 5 119
Figure 139: Comparison of RAOs, amplitude of Pitch-RAO, identification 2, test case 5 119

List of tables

Table 1: Investigation of the coefficients of the approximation functions 18
Table 2: Normalized Root Mean Square Error: Hydrodynamic added mass and damping 31
Table 3: Normalized Root Mean Square Error: Wave forces and moments 37
Table 4: NRMSE of the vector fitting of motion RAOs 52
Table 5: Significant responses: Fitted and original response spectra 55
Table 6: Results of sensitivity analysis 72
Table 7: Golden section method-Vessel properties 75
Table 8: Identification of CoG, x coordinate, test case 2 86
Table 9: Identification of CoG, y coordinate, test case 2 86
Table 10: Identification of CoG, z coordinate, test case 2 87
Table 11: Identification of radii of gyration, test case 2 87
Table 12: Identification of hydrodynamic added mass and damping, test case 2 87
Table 13: Identification of hydrodynamic forces, test case 2 87
Table 14: Identification of viscous damping, test case 2 88
Table 15: Identification of CoG, x coordinate, 2nd repetition, test case 2 88
Table 16: Identification of CoG, y coordinate, 2nd repetition, test case 2 89
Table 17: Identification of CoG, z coordinate, 2nd repetition, test case 2 89
Table 18: Identification of hydrodynamic added mass and damping, 2nd repetition, test case 2 89
Table 19: Identification of hydrodynamic forces, 2nd repetition, test case 2 89
Table 20: Identification of viscous damping, 2nd repetition, test case 2 90
Table 21: Identification of CoG, x coordinate, 3rd repetition, test case 2 90
Table 22: Identification of CoG, y coordinate, 3rd repetition, test case 2 90
Table 23: Identification of CoG, z coordinate, 3rd repetition, test case 2 91
Table 24: Identification of hydrodynamic added mass and damping, 3rd repetition, test case 2 91
Table 25: Identification of hydrodynamic forces, 2nd repetition, test case 2 91
Table 26: Identification of viscous damping, 3rd repetition, test case 2 91
Table 27: Identification of CoG, z coordinate, 4th repetition, test case 2 92
Table 28: Final results: Test case 2 92
Table 29: Final NRMSEs: Test case 2 92
Table 30: Significant values of motions: Test case 2 94
Table 31: Comparison of RAOs: Test case 2 98
Table 32: Final results: Test case 3 100
Table 33: Final NRMSEs: Test case 3 100
Table 34: Significant values of motions: Test case 3 102

Table 35: Comparison of RAOs: test case 3 105
Table 36: Final results: Test case 4 107
Table 37: Final NRMSEs: Test case 4 107
Table 38: Significant values of motions: Test case 4 109
Table 39: Comparison of RAOs: Test case 4 112
Table 40: Calibration of all the parameters, **Table 41:** Calibration of the hyd. database 114
Table 42: Final NRMSEs: Test case 5 115
Table 43: Significant values of motions: Test case 5 116
Table 44: Comparison of RAOs: Test case 5, Identification 1 120
Table 45: Comparison of RAOs: Test case 5, Identification 2 121

List of symbols

CHAPTER 2 Calculation of ship motions:

a=	Added mass for the single mass spring system
A_{WL}=	Wetted plane area
b=	Damping for the single mass spring system
c=	Spring stiffness of the single mass spring system
CoB=	Centre of Buoyancy
CoF=	Centre of Floatation
dir=	Wave direction
F=	External force for the single mass spring system
F_a=	Amplitude of wave force
g=	Acceleration of gravity
GM_L=	Longitudinal metacentric height
GM_T=	Transverse metacentric height
I=	Moment of inertia
I_L=	Longitudinal moment of inertia
I_T=	Transverse moment of inertia
k=	Wave number
KB=	Vertical distance from CoB to keel point
KG=	Vertical distance from CoG to keel point
m=	Mass of the single mass spring system
mdir=	Main wave direction
p=	Pressure
r_{xx}=	Radius of gyration along x axis
r_{yy}=	Radius of gyration along y axis
r_{zz}=	Radius of gyration along z axis
S=	Mean wetted surface

S_i= Motion response spectrum

S_ζ= Wave spectrum

t= Time

$\tilde{\nabla}$= Submerged volume

x= Motion of mass spring system

x_j= Complex amplitude of vessel motion ‘j’

$x_{a,j}$= Amplitude of vessel motion ‘j’

$X_{a\_complex}$= Complex amplitude of motion of the mass spring system

z= Wave elevation

Greek letters:

γ= Gamma factor for Jonswap wave spectrum

ε_F= Phase of wave forces

ε_x= Phase of motion

ζ_a= Wave amplitude

ζ_{unit}= Wave amplitude of unit wave

λ= Spreading factor

ρ_w= Water density

φ_d= Space dependent term of potential due to diffracted waves

φ_j= Space dependent term of radiation potential

φ_w= Space dependent term of potential due to undisturbed waves

Φ= Potential of a floating body

Φ_d= Potential due to diffracted waves

Φ_r= Radiation potential

Φ_w= Potential due to undisturbed incoming waves

ω= Wave frequency

ω_n= Natural frequency

ω_p= Peak frequency

Matrices:

A=	Matrix of hydrodynamic added mass
B=	Matrix of hydrodynamic damping
C=	Stiffness matrix
C_{ad}=	Additional stiffness matrix
B_{ad}=	Matrix of viscous damping
F=	Matrix of wave forces
F_d=	Forces and moments due to the diffracted waves
F_r=	Forces and moments due to the waves radiating from the oscillating body
F_s=	Forces and moments due to hydrostatic buoyancy
F_{total}=	Matrix of all the hydrodynamic forces and moments
F_w=	Forces and moments due to the incoming undisturbed waves
M=	Mass matrix
n=	Direction cosines of mean wetted surface S
RAO=	Response Amplitude Operators
RAO_a=	Amplitude of RAOs
X=	Matrix of ship motions

CHAPTER 3 ***Vector fitting:***

a=	Element of hydrodynamic added mass matrix
ab=	Complex number of the combination of hydrodynamic added mass and damping
ab_{OR} =	Original values of element ab
ab_{VF} =	Approximated values of element ab
b=	Element of hydrodynamic damping matrix
c_I =	Imaginary part of residue
c_n=	Residues of approximation function
$c_{n,ab}$ =	Residues of approximation function f_{ab}
$c_{n,F}$ =	Residues of approximation function f_i

c_R= Real part of residue

d= Real quantity of approximation function

d_{ab} = Real quantity of approximation function f_{ab}

d_1= 1

f= Approximation function

f_{ab} = Approximation function of elements ab

f_i = Approximation function of wave force ‘i’

F= Hydrodynamic force

h= Real quantity of approximation function

h_{ab} = Real quantity of approximation function f_{ab}

k= Number of wave frequencies

M= Hydrodynamic moment

N= Number of poles for approximation function

NRMSE = Normalized Root Mean Square Error

p_I = Imaginary part of pole

p_n= Poles of approximation function

$p_{n,ab}$ = Poles of approximation function f_{ab}

$p_{n,F}$ = Poles of approximation function f_i

p_R = Real part of pole

r_n = Residues of scaling function σ

s= iω

u= 1

y= Output of system of equations that gives the values of ‘σ’

Greek letters:

α_{cn} = Real part of residue

α_{pn} = Real part pole

β_{cn} = Imaginary part of residue

α_{pn} = Real part pole

β_{pn} = Imaginary part of pole

σ = Scaling function

ω= Wave frequency

Matrices:

A= Matrix of hydrodynamic added mass

$\mathbf{A_{sigma}}$= Diagonal matrix with starting poles

$\mathbf{b_{sigma}}$= Vector of ones

B= Matrix of hydrodynamic damping

H= Matrix of which the eigenvalues are the new poles of the approximation function

$\mathbf{r_{sigma}}$= Matrix with residues of scaling function σ

$\mathbf{x_{sigma}}$= Matrix of partial fractions of 'σ'

CHAPTER 4 CoG transformations:

a= Point on the vessel defined by three coordinates

a_x= X coordinate of point a

a_y= Y coordinate of point a

a_z= Z coordinate of point a

b= Point on the vessel defined by three coordinates

b_x= X coordinate of point b

b_y= Y coordinate of point b

b_z= Z coordinate of point b

Greek letters:

β= Azimuth angle in the horizontal plane

γ = Elevation angle between the x-axes.

Matrices:

$\mathbf{A_{CoG}}$= Matrix of hydrodynamic added mass with respect to the CoG of the vessel

$\mathbf{A_{hyd}}$= Matrix of hydrodynamic added mass with respect to the hydrodynamic origin

$\mathbf{A_{local}}$=	Matrix of hydrodynamic added mass with respect to the local axes system
$\mathbf{B_{CoG}}$ =	Matrix of the hydrodynamic damping with respect to the CoG of the vessel
$\mathbf{B_{hyd}}$ =	Matrix of hydrodynamic damping with respect to the hydrodynamic origin
$\mathbf{B_{local}}$ =	Matrix of the hydrodynamic damping with respect to the local axes system
CoG =	Matrix with the three coordinates of the CoG of the vessel
$\mathbf{F_a}$ =	Matrix of wave forces at point 'a'
$\mathbf{F_{a,CoG}}$ =	Matrix of the added inertia forces with respect to the CoG of the vessel
$\mathbf{F_{a,hyd}}$ =	Matrix of the added inertia forces with respect to the hydrodynamic origin
$\mathbf{F_{a,local}}$ =	Matrix of the added inertia forces with respect to the local axes system
$\mathbf{F_b}$=	Matrix of wave forces at point 'b'
$\mathbf{F_{global}}$ =	Matrix of wave forces with respect to the global axes system
$\mathbf{F_{local}}$ =	Matrix of wave forces with respect to the local axes system
$\mathbf{F_{v,CoG}}$ =	Matrix of forces related to the velocities of the vessel, expressed at the CoG of the vessel
$\mathbf{F_{v,hyd}}$ =	Matrix of forces related to the velocities of the vessel with respect to the hydrodynamic origin
$\mathbf{F_{v,local}}$ =	Matrix of forces related to the velocities of the vessel, expressed at the local axes system
Hyd.Origin=	Matrix of the three coordinates of the hydrodynamic origin
$\mathbf{T_{F\_Shift}}$=	Transformation matrix for the translation of forces
$\mathbf{T_{M\_Shift}}$=	Transformation matrix for the translation of motions
$\mathbf{T_{Rot}}$ =	Matrix for the rotation of motions
$\mathbf{X_a}$ =	Matrix of vessel motions at point 'a'
$\mathbf{X_b}$ =	Matrix of vessel motions at point 'b'
$\mathbf{X_{CoG}}$=	Matrix of vessel motions with respect to the CoG of the vessel
$\mathbf{X_{global}}$ =	Matrix of vessel motions with respect to the global axes system
$\mathbf{X_{hyd}}$ =	Matrix of vessel motions with respect to the hydrodynamic origin
$\mathbf{X_{local}}$ =	Matrix of vessel motions with respect to the local axes system

CHAPTER 5 Motion Response Spectra:

dir= Wave direction

H_s= Significant wave height

S= Motion response spectrum

S_ζ= Wave spectrum

T_p= Peak period

X_s= Significant response

Greek letters:

ω= Wave frequency

Matrices:

A = Matrix of hydrodynamic added mass

B = Matrix of hydrodynamic damping

$\mathbf{B_{ad}}$ = Matrix of viscous damping

F= Matrix of wave forces

M= Mass matrix

RAO= Matrix of motion RAO's

CHAPTER 6 Sensitivity analysis:

ab= Complex number of the combination of hydrodynamic added mass and damping

dv = Relative difference between the new and the original value of the parameter

F= Hydrodynamic wave force

r_{xx}= Radius of gyration along x axis

r_{yy}= Radius of gyration along y axis

r_{zz}= Radius of gyration along z axis

v_{new} = New value of parameter

$v_{original}$ = Original value of parameter

x= Coordinate of CoG regarding the x axis

y= Coordinate of CoG regarding the y axis

z = Coordinate of CoG regarding the z axis

Matrices:

$\mathbf{B_{ad}}$= Additional viscous damping matrix

$\mathbf{B_{ad\_original}}$= Viscous damping matrix with original values

CHAPTER 7 *Identification of RAOs*:

ab= Element of the matrix with the combination of hydrodynamic added mass and damping

c= Residues of approximation functions

dir_{waves}= Wave headings according to the axis system of the 2D wave spectrum

f_{ab}= Approximation function for element ab

f_F= Approximation function for wave force F

F= Hydrodynamic wave force

M= Hydrodynamic moment

NRMSE= Normalized root mean square error

r_{xx}= Radius of gyration along x axis

r_{yy}= Radius of gyration along y axis

r_{zz}= Radius of gyration along z axis

x= Coordinate of CoG regarding the x axis

y= Coordinate of CoG regarding the y axis

z = Coordinate of CoG regarding the z axis

Greek letters:

α= Left end of the triplet of values for the golden section method

β= Middle value of triplet for golden section method

γ= Right end of the triplet of values for the golden section method

χ= Random value within the triplet of golden section method

Matrices:

$\mathbf{B_{ad}}$= Additional viscous damping matrix

$\mathbf{RAO_{final}}$= Matrix of directional RAOs corresponding to the wave headings of the 2D wave spectrum

$\mathbf{RAO_{calc.}}$= Matrix of directional RAOs corresponding to the wave headings regarding the local axis system of the vessel

CHAPTER 1. Introduction

Heerema Marine Contractors (HMC) is a contractor that transports and installs large structures at sea. For this purpose, HMC operates 4 crane vessels of which 3 are semi-submersible vessels (Thialf, Balder and Hermod) and one is a mono hull vessel (Aegir). Additionally, HMC operates a number of transport barges. To achieve safe and successful projects, the accurate prediction of vessel motions during transportation and installation is of great importance.

Vessel motions are calculated on the basis of wave energy spectra and Response Amplitude Operators (RAOs). During projects, HMC receives forecasted wave energy spectra from a meteorological services provider. In addition, HMC measures the local frequency and direction dependent wave spectra with wave rider buoys. Regarding the RAOs, they are typically calculated using diffraction software. Wave energy spectra and motion RAOs are both frequency and direction dependent. Given the wave spectra and the RAOs, the vessel motions can be determined. Vessel motions are also measured and recorded with the help of Motion Reference Units (MRUs).

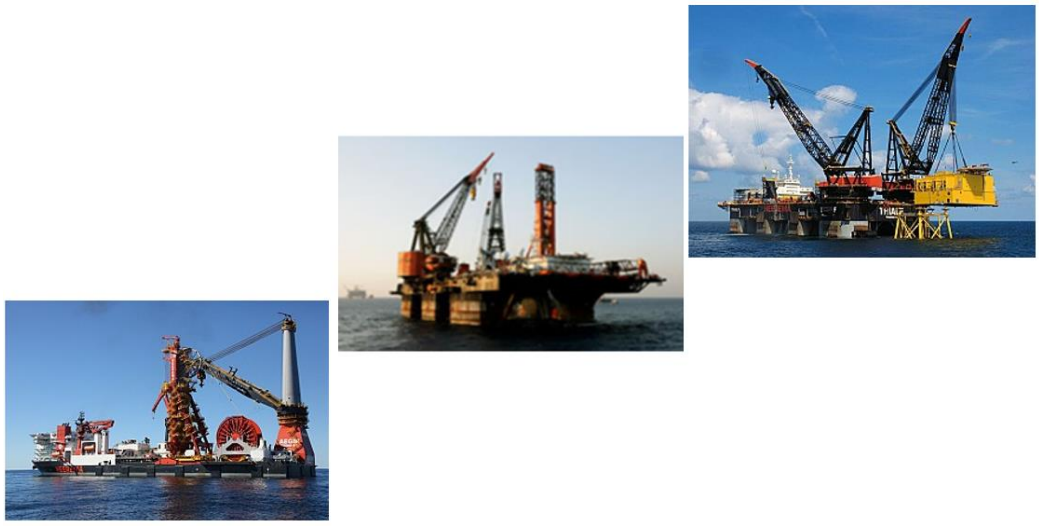

Figure 1: Vessels of HMC

1.1 PROBLEM DEFINITION

In a number of cases, HMC has noticed that the calculated vessel motions do not fully match with the measured vessel motions. This inaccuracy can occur because of the following:

- The vessel has forward speed. In this case, the wave frequency of encounter changes due to the vessel speed. This effect cannot directly be accounted for in most diffraction software suites.
- The semi-submersible vessels are on a draught with a small amount of water on the floaters: the so-called awkward draught. The diffraction software cannot cope with the flowing of water off and onto the floaters.
- The influence of viscous damping forces on the vessel motion is of importance. Viscous damping forces have to be added separately when determining RAOs based on diffraction calculations.
- The mass distribution and the centre of gravity of the vessel changes during projects. Due to fuel consumption, the mass distribution cannot remain constant. In addition, the position of several objects on the vessel changes during operations. In order to calculate the RAOs, however, standard values for the radii of gyration and the coordinates of the CoG are applied for each vessel.

1.2 OBJECTIVES

In this graduation study, a method should be developed to determine the RAOs based on full scale motion measurements (MRU) and the available wave data. It is examined whether it is possible to calibrate the particular properties of the vessel:

- The hydrodynamic properties, the added mass, the damping and the wave forces and moments.
- The mass matrix. It is examined whether the radii of gyration can be determined when measured wave data and vessel motions are available.
- The viscous damping matrix.
- The coordinates of the CoG.

It should be noted that to calculate the vessel motions, waves approach the vessel in one direction only. Therefore, the RAOs of the 6 vessel motions (surge, sway, heave, roll, pitch and yaw) can be determined directly. However, when using full scale measurements, determining the motion RAOs is much more difficult, as the 6 resulting vessel motions are caused by wave energy approaching from all directions.

1.3 APPROACH

In most cases the RAOs are accurate enough and thereby they can be used as good initial guesses. Based on these initial guesses, the aim is to find a method to adjust the elements of the RAOs and predict an accurate motion response spectrum.

With respect to the hydrodynamic added mass and damping matrices, each element should be calibrated for a large number of wave frequencies. In addition, for the wave forces that are frequency and direction dependent, the amount of parameters to be investigated is even higher. Thus, one of the challenges of this graduation study is to find a method to express each element of the hydrodynamic database (added mass, damping and wave forces) with limited number of parameters for the entire frequency range.

Also, it is important to perform a sensitivity analysis and show the influence of each parameter on the vessel motions. The sensitivity analysis leads to the minimization of the amount of parameters that is to be examined. Therefore, the identification procedure becomes faster.

For this graduation study, the identification method is tested by several cases. These test cases are based on simulated data. The simulated data contain the simulated wave spectrum and the simulated response spectra. The simulated response spectra are obtained by modifying several vessel properties. The identification procedure, which is going to be developed, should be able to identify these modifications.

Finally, the procedure for the identification of the RAOs is applied to a specific vessel with a certain draft: the semi-submersible crane vessel Thialf (SSCV Thialf) at 22m draft in deep water.

CHAPTER 2. Calculation of ship motions

In some cases, the calculated vessel motions do not fully match with full-scale measurements. In order to identify the possible causes of this inaccuracy, this chapter provides a full description of the calculation of the ship motions. The ship motions are determined on the basis of the RAOs and the wave energy spectrum. The aim of this chapter is to identify the key parameters contributing to the calculation of the RAOs as well as provide further information on the wave energy spectrum.

2.1 EQUATION OF MOTION

In order to describe the motions of a vessel, which mainly has a linear behaviour, a frequency domain analysis is performed. According to this analysis, the resulting motions of a vessel in irregular waves are calculated by adding together the vessel's response to regular harmonic waves of different amplitudes, frequencies and propagation directions. In short, given the wave spectrum and the frequency characteristics of the vessel, the motion response spectra can be determined (Figure 2).

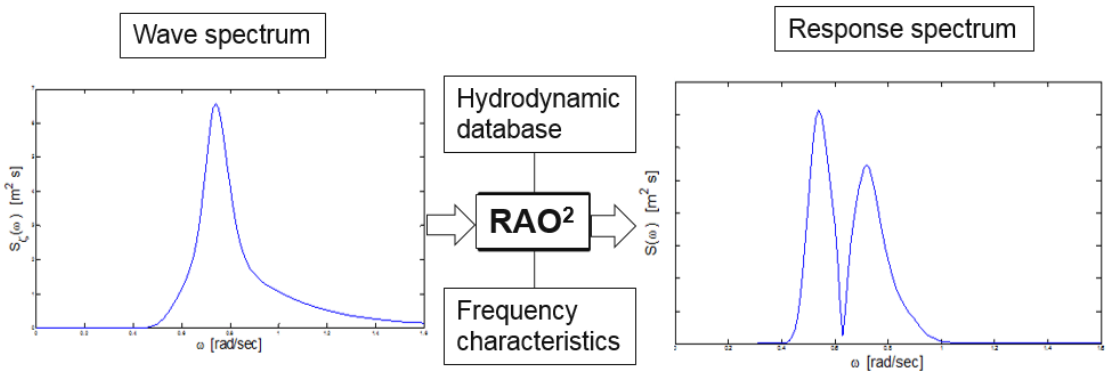

Figure 2: Calculation of motion response spectra for a floating structure

The detail description of the wave spectrum, the RAOs and the response spectra, shown in the above figure, is given in the next sections.

The resulting six vessel motions are defined by three translations and three rotations of the ship's centre of gravity in the directions x, y and z [1]:

- Surge: translation along X axis
- Sway: translation along Y axis
- Heave: translation along Z axis
- Roll: rotation around X axis
- Pitch: rotation around Y axis
- Yaw: rotation around Z axis

The following figure shows the motions of the semi-submersible crane vessel Thialf.

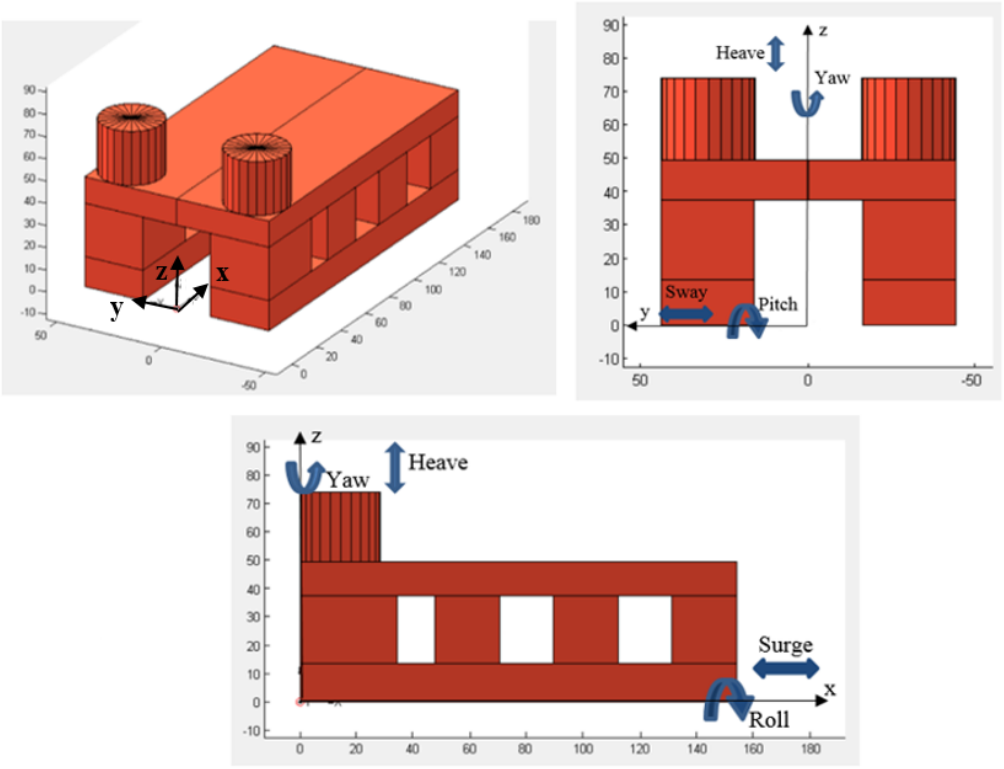

Figure 3: Ship motions, SSCV Thialf

To obtain the RAOs, we should analyse the dynamic behaviour of the vessel due to an incoming harmonic wave. First, the hydromechanics of a single mass-spring system are described.

For a simple mass-spring system without any damping and external forces, the following equations are applied:

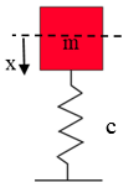

- Newton 2nd law:

$$F = m\ddot{x}(t) => -cx(t) = m\ddot{x}(t) => m \cdot \ddot{x}(t) + c \cdot x(t) = 0$$

- Solution: $x(t) = X_a cos(\omega t + \varepsilon_x)$ where

$$X_a = \sqrt{x(0)^2 + \left(\frac{\dot{x}(0)}{\omega_n}\right)^2}\ ,\ \varepsilon_x = \arctan\left(\frac{\dot{x}(0)}{x(0)\cdot\omega_n}\right) \text{ and } \omega_n = \sqrt{\frac{c}{m}}$$

To describe vessel motions, the mass term should be modified. The mass term is modified by implementing the hydrodynamic added mass, a(ω), which is a frequency dependent function: m=m +a(ω). Regarding the restoring spring term 'c', it is related to the hydrostatic stability of the vessel. A detailed description of the added mass and the restoring terms is given in the next paragraphs.

Consider a damped mass-spring system subjected to a harmonic external force. The hydrodynamic damping term is also a function of frequency.

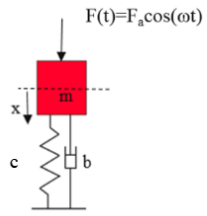

- Newton's 2nd law: $\big(m + a(\omega)\big)\ddot{x}(t) + b(\omega)\dot{x}(t) + cx(t) = F(t)$
- The harmonic wave force has the following form:

$$F(t) = F_a cos(\omega t) => F(t) = Re\{F_a \cdot e^{i(\omega t)}\}$$

- We assume that the particular solution of the equation of motion is:

$x(t) = \Re\{X_a \cdot e^{i(\omega t)}\}$. The solution for Newton's 2nd law gives the following relation for the complex amplitude of x(t): $X_a = \frac{F_a}{-(m+a(\omega))\omega^2 + i\omega b(\omega) + c}$

Based on the above mass-spring system, the motion RAOs for the 6 degrees of freedom are determined by solving the following relation for **X**:

$$\{-\boldsymbol{\omega}^2 \cdot (\mathbf{M} + \mathbf{A}(\boldsymbol{\omega})) + \mathbf{i}\boldsymbol{\omega} \cdot \mathbf{B}(\boldsymbol{\omega}) + \mathbf{C}\} \cdot \mathbf{X}(\boldsymbol{\omega}, \mathbf{dir}) = \mathbf{F}(\boldsymbol{\omega}, \mathbf{dir}) \qquad \text{Eq. 2-1}$$

where **C** is the vessel stiffness matrix (section 2.3), **B**(ω) is the hydrodynamic damping matrix (section 2.4.1), **M** is the mass matrix of the vessel (section 2.2), **A**(ω) is the hydrodynamic added mass matrix (section 2.4.1), **F**(ω,dir) is the hydrodynamic force vector (section 2.4.2) and **X**(ω,dir) is the 6X1 matrix of vessel motions for the wave frequency 'ω' and the wave direction 'dir'. The hydrodynamic wave forces are calculated for a unit wave with amplitude ζ.

The equation for the resulting motion RAOs is shown below:

$$\boldsymbol{RAO}(\omega, dir) = \{-\omega^2 \cdot (\mathbf{M} + \mathbf{A}(\omega)) + i\omega \cdot \boldsymbol{B}(\omega) + \boldsymbol{C}\}^{-1} \cdot \mathbf{F}(\omega, \mathrm{dir}) \qquad \text{Eq. 2-2}$$

The amplitude of the RAOs represents the motion amplitude per unit wave amplitude: $\boldsymbol{RAO_a}(\omega, \mathrm{dir}) = \left(\frac{\boldsymbol{X}(\omega, dir)}{\zeta}\right)$. The phase of the RAOs indicates the phase difference between the motions and the waves.

The following figures show the resulting amplitude and phase of the heave RAO for the semi-submersible Thialf.

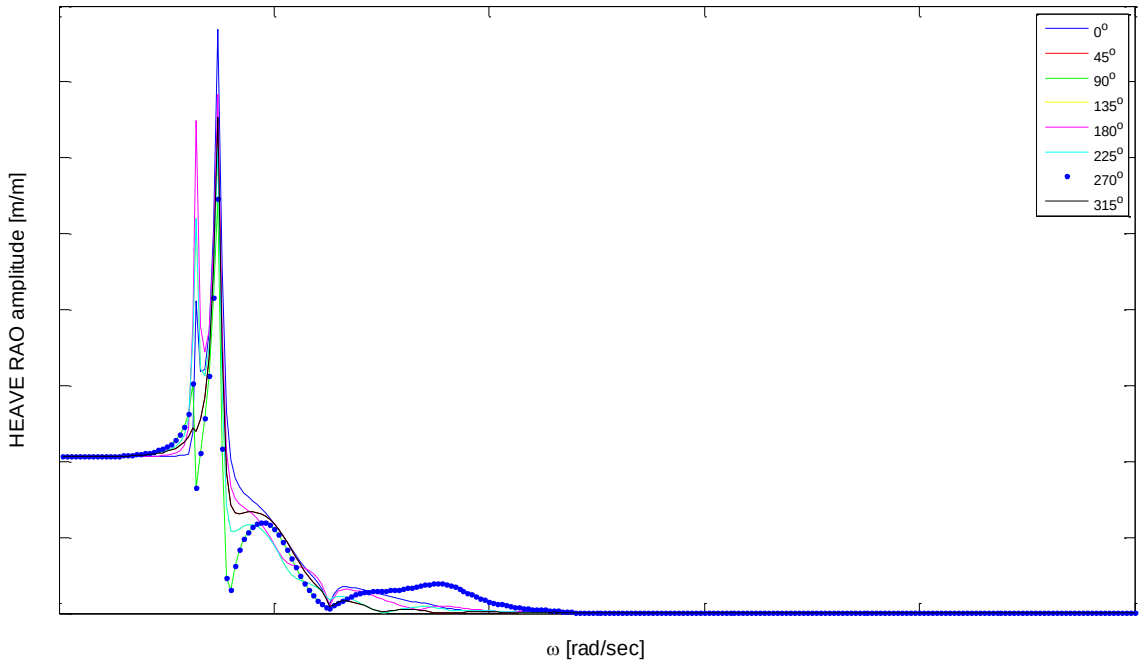

Figure 4: Amplitude of Heave-RAO for the SSCV Thialf in deep water at 22m draft

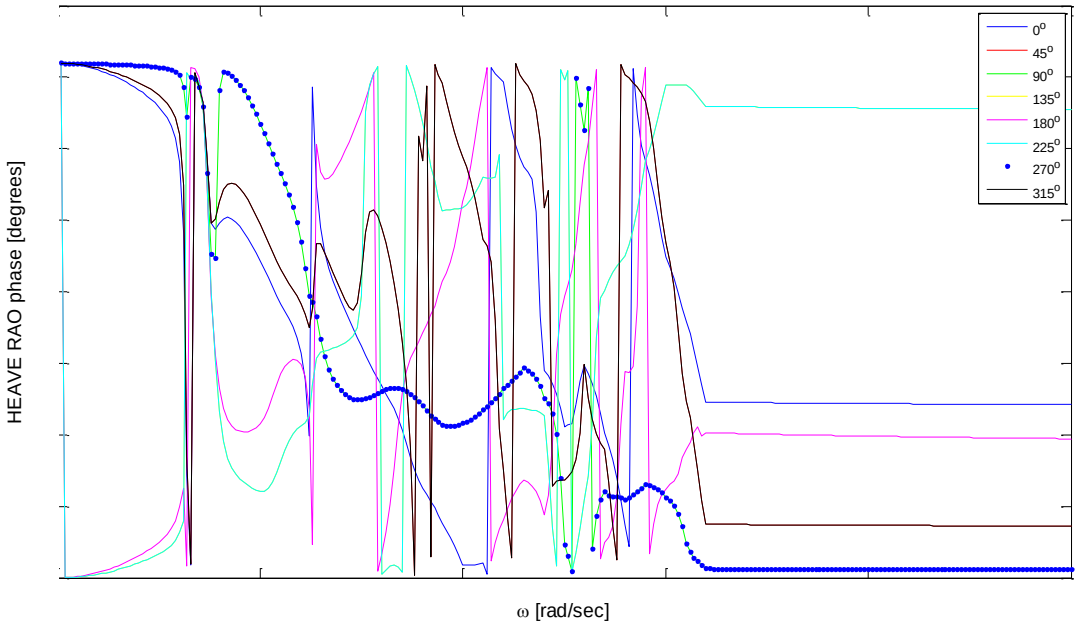

Figure 5: Phase of Heave-RAO for the SSCV Thialf in deep water at 22m draft

Finally, the motion response spectra are obtained by multiplying the wave spectrum with the RAO squared and integrating over the wave directions.

$$S_i(\omega) = \int_{-\pi}^{\pi} S_\zeta(\omega, dir) \cdot RAO_i(\omega, dir)^2 \, d(dir) \qquad \text{Eq. 2-3}$$

where i indicates the degree of freedom, S_i is the response spectrum and S_ζ is the wave spectrum.

In order to identify possible sources of inaccuracy of the RAOs, special attention should be given to the parameters that contribute to their calculation Eq.2-2.

2.2 MASS MATRIX

The mass matrix is defined by the body mass and radius of gyration of the vessel. The 6X6 mass matrix is given below:

$$\boldsymbol{M} = \begin{bmatrix} m & 0 & 0 & 0 & 0 & 0 \\ 0 & m & 0 & 0 & 0 & 0 \\ 0 & 0 & m & 0 & 0 & 0 \\ 0 & 0 & 0 & {r_{xx}}^2 m & 0 & 0 \\ 0 & 0 & 0 & 0 & {r_{yy}}^2 m & 0 \\ 0 & 0 & 0 & 0 & 0 & {r_{zz}}^2 m \end{bmatrix}$$

where m is the mass of the vessel and r_{xx}, r_{yy}, r_{zz}, are the radii of gyration with respect to x, y and z axes respectively.

The radius of gyration is determined as follows:

$$r_{xx} = \sqrt{\frac{I_{xx}}{m}}, r_{yy} = \sqrt{\frac{I_{yy}}{m}}, r_{zz} = \sqrt{\frac{I_{zz}}{m}} \qquad \text{Eq. 2-4}$$

where I_{xx}, I_{yy} and I_{zz} are the moments of inertia regarding the x, y and z axes respectively.

In order to determine the radius of gyration, the moment of inertia of the vessel should be calculated. However, the moment of inertia is related with the mass distribution of the vessel which is not constant during projects. For example, the decrease of the mass due to fuel consumption is ignored for the calculations of the moment of inertia. In addition, while the position of a load on the deck of the vessel is changing, so does the radius of gyration. Thus, the possible inaccuracies of the radius of gyration should be investigated.

2.3 STIFFNESS MATRIX

The stiffness matrix contains the restoring spring terms which influence the heave, roll and pitch motions. The 6X6 spring matrix of the Thialf is shown below:

$$\boldsymbol{C} = \begin{bmatrix} 0 & 0 & 0 & 0 & 0 & 0 \\ 0 & 0 & 0 & 0 & 0 & 0 \\ 0 & 0 & \rho g A_{wL} & 0 & -\rho g A_{wL}(CoF - CoB) & 0 \\ 0 & 0 & 0 & \rho g \bar{V} GM_T & 0 & 0 \\ 0 & 0 & -\rho g A_{wL}(CoF - CoB) & 0 & \rho g \bar{V} GM_L & 0 \\ 0 & 0 & 0 & 0 & 0 & 0 \end{bmatrix}$$

where ρ is the fluid density, $\bar{V}$ is the submerged volume of the vessel, g is the acceleration of gravity, A_{WL} is the wetted plane area, CoF is the center of floatation, CoB is the center of buoyancy and GM_T, GM_L, are the transverse and longitudinal metacentric heights.

To determine the elements of the stiffness matrix, the hydrostatic stability of the vessel should be analysed. If the wetted plane area, the centre of floatation (CoF) and the centre of buoyancy (CoB) are known, then, elements C_{33}, C_{35} and C_{53} can be calculated. Regarding the elements C_{44} and C_{55}, the transverse and longitudinal metacentric heights should be determined. For small angles of heel or trim, the metacentric heights GM_T and GM_L are calculated as follows [2]:

$$GM_T = KB + BM_T - KG \qquad \text{Eq. 2-5}$$

$$GM_L = KB + BM_L - KG \qquad \text{Eq. 2-6}$$

where KB is the vertical distance from the CoB to the keel point of the ship and KG is the vertical distance from CoG to the keel point of the ship.

The terms BM_L and BM_T are defined below:

$$BM_T = \frac{I_T}{\bar{V}} \qquad \text{Eq. 2-7}$$

$$BM_L = \frac{I_L}{\bar{V}} \qquad \text{Eq. 2-8}$$

where I_L is the longitudinal and I_T is the transverse moment of inertia of the wetted area, respectively.

Because of the ballasting system of the semi-submersible vessels, the submerged volume and the draft of the vessel can be kept constant during projects. As a consequence, the wetted plane area, CoF and CoB are known and the elements C_{33}, C_{35}, C_{53} do not contain any inaccuracies.

On the other hand, when the distribution of the mass changes, so does the CoG of the vessel. As a result, the elements C_{44} and C_{55} that are influenced by the distance KG should be modified.

For surge, sway and yaw motions, the following additional spring matrix should be implemented:

$$\boldsymbol{C_{ad}} = \begin{bmatrix} [redacted]\ \frac{kN}{m} & 0 & 0 & 0 & 0 & 0 \\ 0 & [redacted]\ \frac{kN}{m} & 0 & 0 & 0 & 0 \\ 0 & 0 & 0 & 0 & 0 & 0 \\ 0 & 0 & 0 & 0 & 0 & 0 \\ 0 & 0 & 0 & 0 & 0 & 0 \\ 0 & 0 & 0 & 0 & 0 & [redacted]\ \frac{kNm}{rad} \end{bmatrix}$$

The additional spring matrix is such that the resonances for surge, sway and yaw are obtained for long wave frequencies.

2.4 HYDRODYNAMIC PROPERTIES

The added mass, the wave damping and the hydrodynamic wave forces and moments constitute the hydrodynamic database of the vessel. The wave damping is caused by the oscillations of the vessel that generate waves and withdraw energy from the vessel motion. The damping matrix B(ω) contains the hydrodynamic damping coefficients expressed as functions of the frequency of oscillation. Regarding the added mass, it is the mass of the fluid particles near the vessel that oscillate with the same frequency as the vessel and cause an extra hydro-mechanical reaction force. The added mass matrix A(ω) contains the hydrodynamic mass coefficients, which are also dependent to the frequency of oscillation [3]. Finally, the wave forces and moments are written as functions of wave frequency and wave direction as follows:

$$F(\omega, dir) = F_a \cos(\omega t + \varepsilon_F) \quad \text{Eq. 2-9}$$

where F_a and ε_F are the amplitude and the phase of the hydrodynamic forces, respectively.

The hydrodynamic database of a vessel is in practice calculated by diffraction software based on potential theory.

2.4.1 Potential theory: added mass and damping

The added mass and damping coefficients as well as the wave forces are determined from the pressure distribution on the hull which is calculated from the velocity potentials [4]. The potential of a floating body is expressed as the sum of the potential due to an undisturbed incoming wave Φ_w, the potential due to the diffraction of the undisturbed incoming wave, Φ_d, and the radiation potential due to six body motions Φ_r.

$$\Phi = \Phi_r + \Phi_w + \Phi_d \quad \text{Eq. 2-10}$$

It should be mentioned that the fluid is assumed to be incompressible, inviscid and irrotational without any effects of surface tension. In addition, the potential theory is developed for unidirectional regular waves.

Using the velocity potentials, the hydrodynamic pressures on the surface of the body can be obtained from the linearized Bernoulli equation:

$$p = -\rho \frac{d\Phi}{dt} - \rho g z = -\rho \left(\frac{d\Phi_r}{dt} + \frac{d\Phi_w}{dt} + \frac{d\Phi_d}{dt} \right) - \rho g z \quad \text{Eq. 2-11}$$

where ρ is the water density and the term ρgz is the hydrostatic pressure.

The integration of this pressure over the submerged surface S of the body, provides the hydrodynamic force or moment [5].

$$\boldsymbol{F_{total}} = -\iint (p * \boldsymbol{n}) \cdot dS = \rho \iint \left(\frac{d\Phi_r}{dt} + \frac{d\Phi_w}{dt} + \frac{d\Phi_d}{dt} + \rho g z \right) \boldsymbol{n} \cdot dS \quad \text{Eq. 2-12}$$

where **n** is the matrix of the direction cosines of the surface elements dS:

$$\boldsymbol{n} = \begin{bmatrix} \cos(n,x) \\ \cos(n,y) \\ \cos(n,z) \\ y\cos(n,z) - z\cos(n,y) \\ z\cos(n,x) - x\cos(n,z) \\ x\cos(n,y) - y\cos(n,x) \end{bmatrix}$$

Then, the hydrodynamic forces and moments can be split into four parts:

$$\boldsymbol{F_{total}} = \boldsymbol{F_r} + \boldsymbol{F_w} + \boldsymbol{F_d} + \boldsymbol{F_s} \quad \text{Eq. 2-13}$$

where:

- $\mathbf{F_r}$: hydrodynamic forces and moments due to the waves radiating from the oscillating body.

- $\mathbf{F_w}$: hydrodynamic forces and moments on the body due to the undisturbed approaching wave.
- $\mathbf{F_d}$: hydrodynamic forces and moments due to the diffracted waves.
- $\mathbf{F_s}$: hydrodynamic forces and moments due to the hydrostatic buoyancy.

The forces and moments which are associated with the radiation potential, can also be expressed in terms of potential mass and damping. To explain this, the equation of motion can be written as shown below:

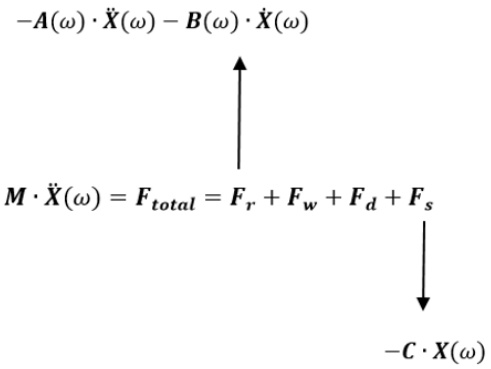

Figure 6: Potential theory and equation of motion

If the radiation potential due to the six body motions is known, the added mass and damping coefficients can be calculated. The radiation potential is a harmonic function with the same frequency as the harmonic motion, a certain space dependent amplitude and a certain space dependent phase angle [6]:

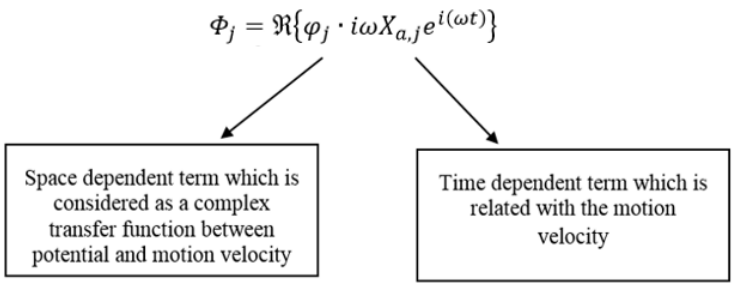

Figure 7: Radiation potential

The oscillating hydrodynamic force which is associated with the radiation potential can be written as follows:

$$F_{r,i}=-a_{ij}\ddot{x}_j-b_{ij}\dot{x}_j \qquad \text{Eq. 2-14}$$

where i represents the direction of the oscillating force or moment (i=1-6) , j represents the vessel motions (j=1-6), a_{ij} is the added mass coefficient, b_{ij} is the damping coefficient, and $F_{r,i}$ is the oscillating hydrodynamic force at direction i due to motion at direction j: $F_{r,i}=\iint_S\left(\rho\frac{d\Phi_j}{dt}\cdot n_i\right)dS.$

Furthermore, the motion of the vessel is expressed by the following equation:

$$x_j=X_{a,j}\cdot\cos(\omega t+\varepsilon_{x,j}) \qquad \text{Eq. 2-15}$$

where $X_{a,j}$ is the amplitude of the motion at direction j, ω is the frequency of oscillations and $\varepsilon_{x,j}$ is the phase of the vessel motion.

By solving the following system of equations, the added mass and damping coefficients can be determined:

$$\left.\begin{aligned} F_{r,i} &= -a_{ij}\ddot{x}_j - b_{ij}\dot{x}_j \\ F_{r,i} &= \iint_S \left(\rho \frac{d\Phi_j}{dt} \cdot n_i\right) dS \end{aligned}\right\} \qquad \iint_S \left(\rho \frac{d\Phi_j}{dt} \cdot n_i\right) dS = -a_{ij}\ddot{x}_j - b_{ij}\dot{x}_j$$

where:

$x_j = X_{a,j} \cdot \cos(\omega t + \varepsilon_{x,j}) = \Re\left\{X_{a,j} e^{i(\omega t + \varepsilon_{x,j})}\right\} = \Re\{X_{a,j} e^{i\varepsilon_{x,j}} e^{i\omega t}\} = \Re\{X_j e^{i\omega t}\}$

$X_j = X_{a,j} e^{i\varepsilon_{x,j}}$: complex amplitude of motion

$\Phi_j = \Re\{\varphi_j \cdot i\omega X_j e^{i\omega t}\}$: radiation potential

$\dot{x}_j = \Re\{i\omega X_j e^{i\omega t}\}$: motion velocity

$\ddot{x}_j = \Re\{-\omega^2 X_j e^{i\omega t}\}$: motion acceleration

$$\iint_S \left(\rho \frac{d\Phi_j}{dt} \cdot n_i\right) dS = -a_{ij}\ddot{x}_j - b_{ij}\dot{x}_j =>$$

$$\Re\left\{\iint_S \left(\rho \frac{d(\varphi_j \cdot i\omega X_j e^{i\omega t})}{dt} n_i\right) dS\right\} = -a_{ij} \cdot \Re\{-\omega^2 X_j e^{i\omega t}\} - b_{ij} \cdot \Re\{i\omega X_j e^{i\omega t}\} =>$$

$$\Re\left\{\rho \cdot -\omega^2 \cdot X_j \cdot e^{i\omega t} \iint_S (\varphi_j \cdot n_i) dS\right\} = \Re\{a_{ij} \cdot \omega^2 \cdot X_j \cdot e^{i\omega t} - b_{ij} \cdot i\omega \cdot X_j \cdot e^{i\omega t}\} =>$$

$$-\rho \cdot \iint_S (\varphi_j \cdot n_i) dS = a_{ij} - \frac{b_{ij}}{\omega} \cdot i \qquad \text{Eq. 2-16}$$

Both real and imaginary parts should be equaled:

$$a_{ij} = \Re\{-\rho \iint (\varphi_j \cdot n_i) dS\} \qquad \text{Eq. 2-17}$$

$$b_{ij} = -\omega \Im\{-\rho \iint (\varphi_j \cdot n_i) dS\} \qquad \text{Eq. 2-18}$$

The only unknown of Eq. 2-17 and Eq. 2-18 is the space dependent term of the radiation potential (φ_j). This term can be found by the panel method. According to this method, the mean wetted part of the vessel hull is approximated by a large number of panel elements. The distribution of source singularities on these panels, describes the fluid flow around the vessel hull [6]. Further details about this method are not given. However, it is important to know that the added mass and damping depend on the geometry of the submerged hull.

It should also be noticed that the added mass and damping coefficients are related to the same complex number. This means that the effects of these two hydrodynamic properties should not be investigated separately. The next figures show the curves of the frequency domain elements of the added mass and damping matrices.

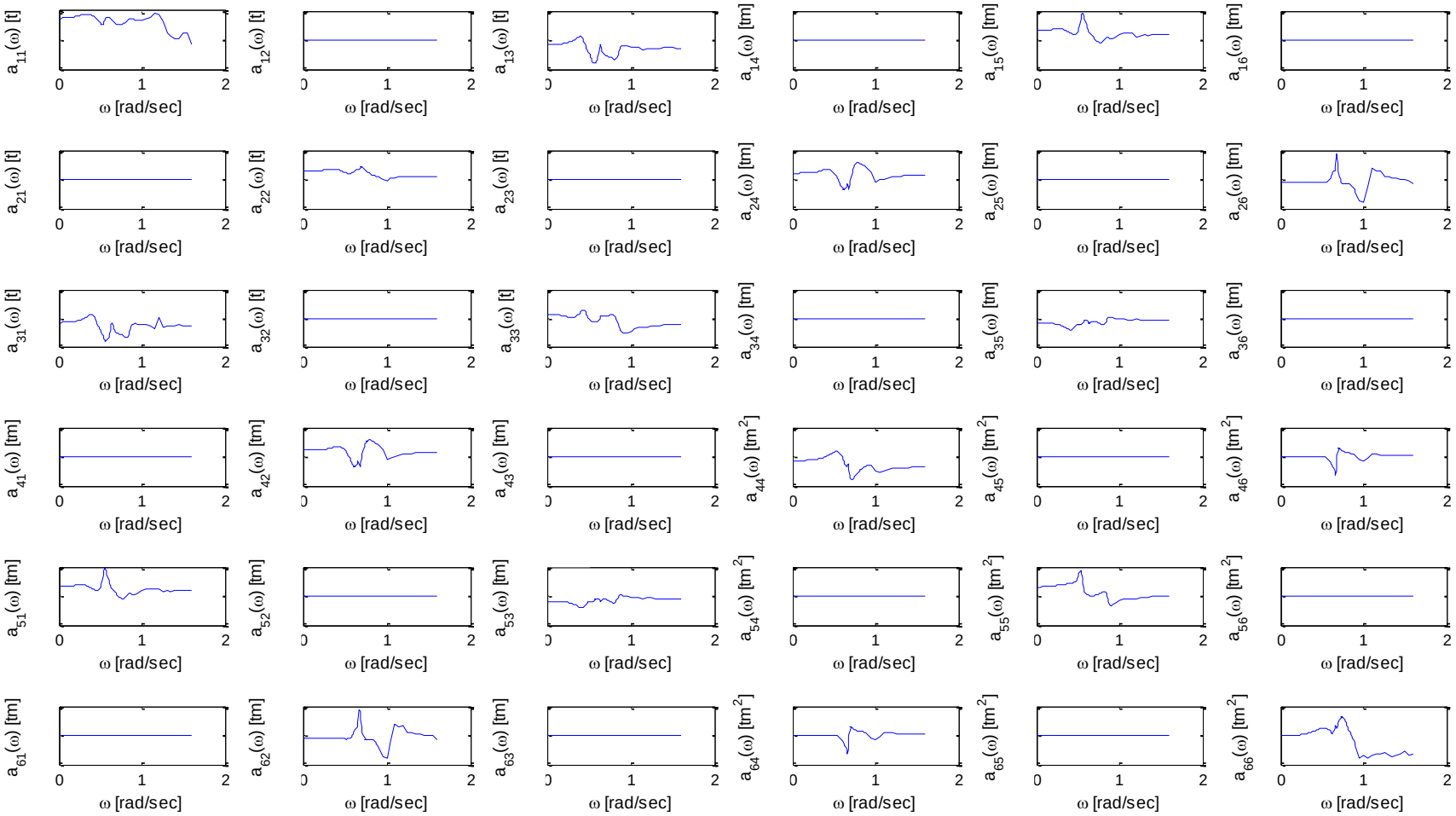

Figure 8: Added mass matrix: SSCV Thialf, deep water, 22m draft

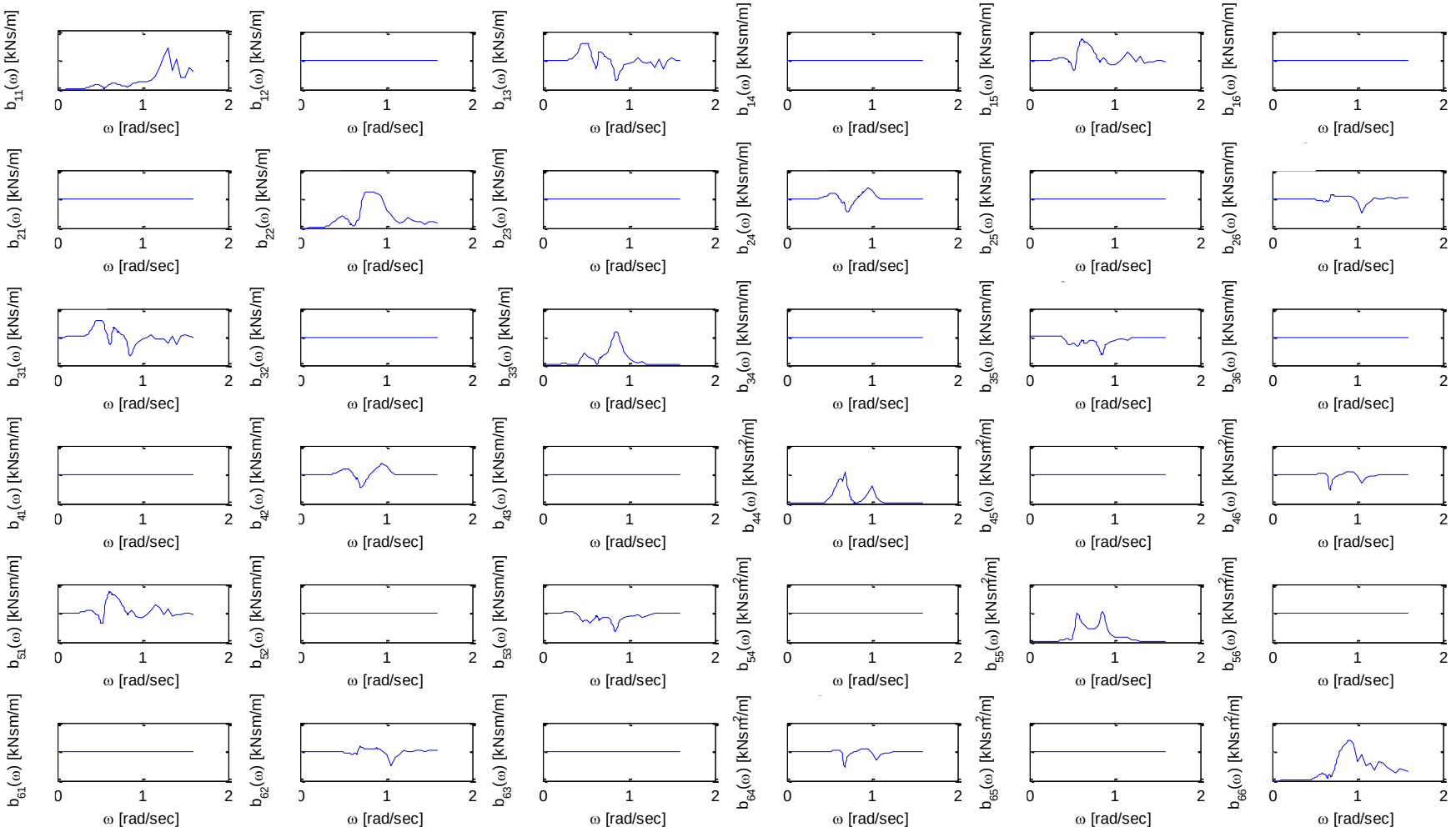

Figure 9: Damping matrix: SSCV Thialf, deep water, 22m draft

2.4.2 Potential theory: wave forces and moments

As it was mentioned in the previous paragraph, the wave forces are expressed in terms of the undisturbed and diffracted waves.

$$\big(\boldsymbol{M} + \boldsymbol{A}(\omega)\big) \cdot \ddot{\boldsymbol{X}}(\omega) + \boldsymbol{B}(\omega) \cdot \dot{\boldsymbol{X}}(\omega) + (\boldsymbol{C} + \boldsymbol{C_{ad}}) \cdot \boldsymbol{X}(\omega) = \boldsymbol{F_w} + \boldsymbol{F_D} \quad \text{Eq. 2-19}$$

where $\mathbf{F_w}$ is the undisturbed wave force (Froude-Krilov) and $\mathbf{F_D}$ is the diffracted wave force.

Given a regular wave, propagating in direction 'dir', the equation of the velocity potential for deep water is obtained [7]:

$$\Phi_w = \frac{\zeta_a g}{\omega} e^{kz} \sin(kxcos(dir) + kysin(dir) - \omega t) \quad \text{Eq. 2-20}$$

where g=acceleration of gravity, ζ_a=amplitude of undisturbed wave, k=wave number, h=water depth, dir=wave direction which is zero for wave travelling in the positive z direction and ω=wave frequency.

Similar to the radiation potential, the potential of the undisturbed wave is written as a function of a space dependent term multiplied by the velocity of the undisturbed wave elevation.

$$\Phi_w = Re\{\varphi_w \cdot i\omega\zeta_a e^{i\omega t}\} \quad \text{Eq. 2-21}$$

where φ_w is the space dependent term:

$$\varphi_w = \frac{g}{\omega^2} e^{kz} e^{i(kxcos(dir)+kysin(dir))} \quad \text{Eq. 2-22}$$

With respect to the diffraction potential, there is a linear relation with the undisturbed wave potential:

$$\Phi_d = Re\{\varphi_d \cdot i\omega\zeta_a e^{i\omega t}\} \quad \text{Eq. 2-23}$$

where φ_d is the unknown space dependent term of the diffraction potential.

In order to determine the first order wave exciting forces and moments, the pressure due to the incoming and diffracted wave should be calculated:

$$p_w = -\rho \frac{d(\Phi_w + \Phi_d)}{dt} = \rho\omega^2(\varphi_w + \varphi_d)\zeta_a e^{i\omega t} \quad \text{Eq. 2-24}$$

Thus, the hydrodynamic forces and moments are determined by the following equation:

$$\boldsymbol{F_w} + \boldsymbol{F_D} = -\iint_S (p * \boldsymbol{n}) \cdot dS = \rho\omega^2\zeta_a e^{i\omega t} \iint_S \big((\varphi_w + \varphi_d) \cdot \boldsymbol{n}\big) \cdot dS \quad \text{Eq. 2-25}$$

As with the space dependent term of the radiation potential, the unknown term of the diffraction potential, φ_d, is determined by the panel method.

The following figures show the amplitude and the phase of the wave forces and moments of 15° of wave heading.

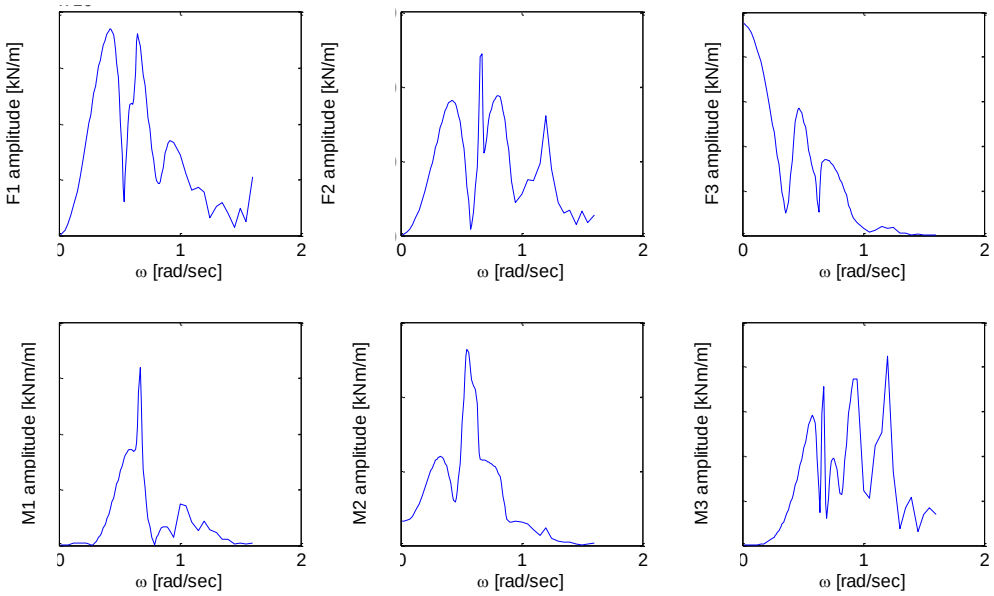

Figure 10: Amplitude of wave forces and moments: 15º wave heading, SSCV Thialf, deep water, 22m draft

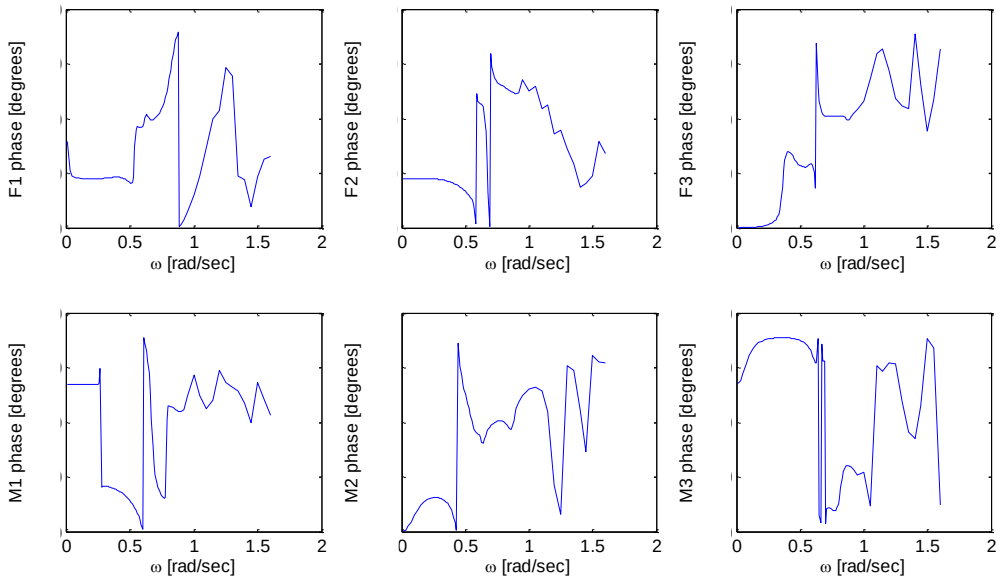

Figure 11: Phase of wave forces and moments: 15º wave heading, SSCV Thialf, deep water, 22m draft

The diffraction software calculates the hydrodynamic effects on the vessel hull below the still water level. A possible case of inaccuracy for the hydrodynamic database is when there is a small amount of water on the floaters of the semi-submersible vessels. Unfortunately, the hydrodynamic effects of this water cannot be analysed by the diffraction software.

The hydrodynamic properties are functions of the wave frequency, thus another cause of inaccuracy is the forward speed of the vessel. When the vessel has forward speed, the frequency at which it encounters the waves is different from the wave frequency.

2.5 VISCOUS DAMPING

The motion damping can also be caused by viscous effects such as skin friction, vortices, etc. Because of these viscous effects, an additional damping matrix should be added to the equation for calculating the RAOs. Empirical methods can estimate the additional viscous damping due

to skin friction, eddy making, lift and bilge keels [8]. After the implementation of the additional damping, the equation of motion for the RAOs becomes as follows:

$$\boldsymbol{RAO}(\omega, dir) = \left\{-\omega^2 \cdot \left(\mathbf{M} + \mathbf{A}(\omega)\right) + i\omega \cdot (\boldsymbol{B}(\omega) + \boldsymbol{B_{ad}}) + (\boldsymbol{C} + \boldsymbol{C_{ad}})\right\}^{-1} \cdot \mathbf{F}(\omega, \mathrm{dir}) \qquad \text{Eq. 2-26}$$

The fact that the viscous damping is estimated by empirical methods can also cause inaccuracies.

2.6 WAVE SPECTRUM

In order to describe the surface elevation of the ocean waves, the wave spectrum is determined. The wave spectrum represents the irregular waves travelling across the ocean. These irregular waves can be represented as the sum of a large number of harmonic wave components with different periods, directions, amplitudes and phases. A wave spectrum is created by distributing the variance of the amplitudes of these harmonic components over a frequency band, as is shown in the following figure [9].

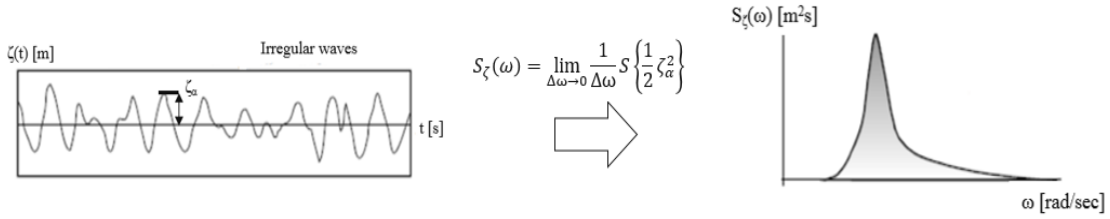

Figure 12: Wave spectrum $S_\zeta(\omega)$ where $\zeta(t)$=wave elevation, ζ_α=wave amplitude, ω=wave frequency

The above figure shows the one-dimensional wave energy spectrum that represents the surface elevation as a function of time. However, to describe the actual, three-dimensional, moving waves, the horizontal dimension has to be added [9]. An example of a 2D wave spectra is indicated in the following figure:

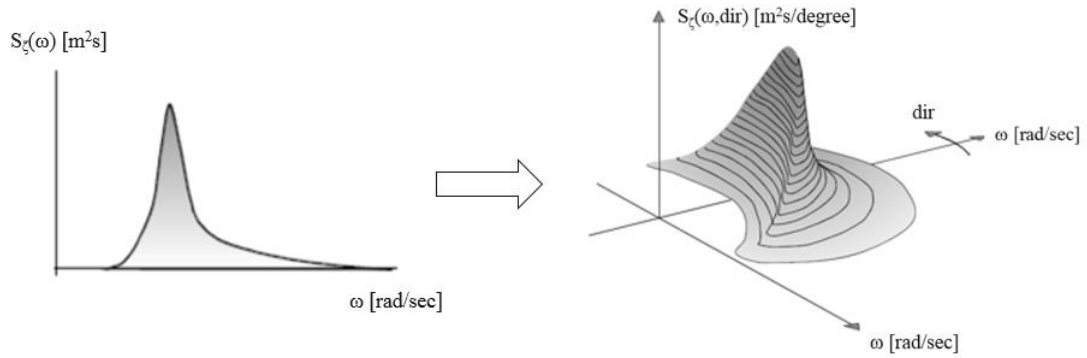

Figure 13: Directional wave spectrum

The motions of the vessels during projects are mainly influenced by the swell and the wind sea. When the wind-generated waves leave the generation area, they take on a regular and long-crested appearance. This is what we call swell. The swell has larger period than the wind generated waves and it is spread in a narrow band of wave directions. Moreover, the swell is not affected by the local wind and as a consequence, it is possible to have sea state with swell and wind sea coming from different directions. The swell and wind sea are characterised by a period of 4s to 30s [10].

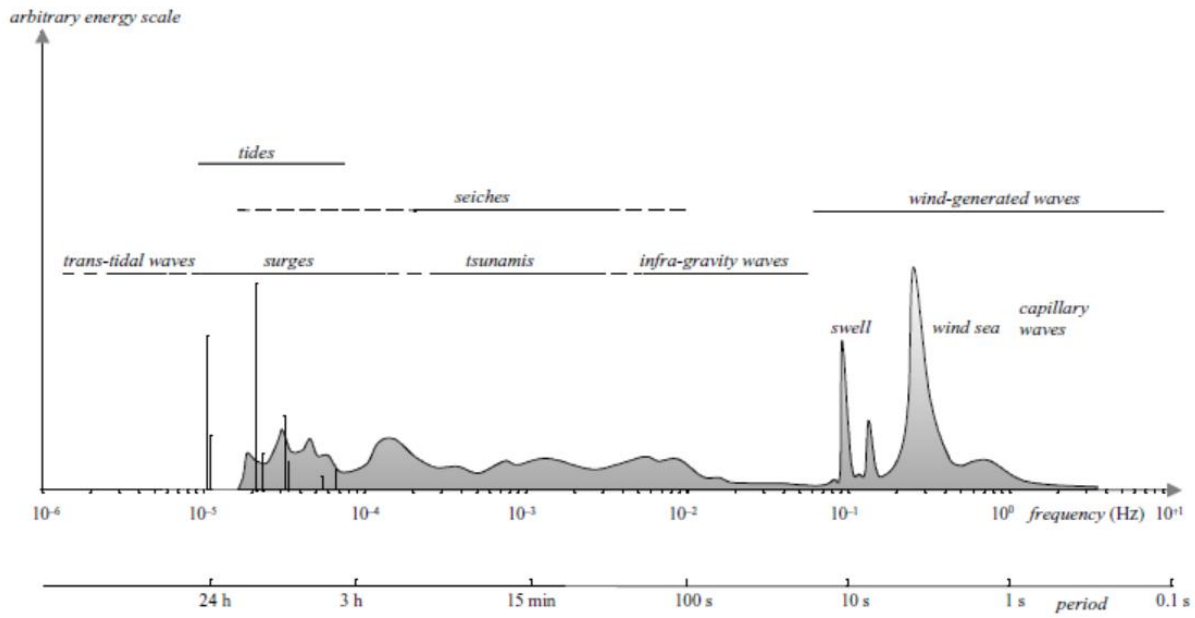

Figure 14: Wave types

Under idealised conditions and if the significant wave height and the peak period are known, the one-dimensional frequency spectrum can be calculated by specific formulas. For example, we can determine the JONSWAP spectrum by selecting a specific wave height, peak period and a peakness factor γ. In addition, we can also use the formula of the Ochi-Hubble spectrum to describe a double peak spectrum.

Given the one–dimensional frequency spectrum, the 2D wave spectrum can be also determined by adding a spreading function of cosφ. The following equations can be used to create a 2D wave spectrum [11].

$$S_\zeta(\omega, \omega_p, dir) = \lambda \cdot cos^2(dir - mdir) \cdot S_\zeta(\omega, \omega_p) \qquad \text{Eq. 2-27}$$

where: $mdir$ =main wave direction, ω=wave frequency , ω_p=peak frequency,

$$\lambda = \frac{1}{\int_{-\pi/2}^{\pi/2} cos^2(dir - mdir) \cdot ddir}, \quad -\pi/2 \leq (dir - mdir) \leq \pi/2.$$

It should be mentioned that the 2D wave spectrum shows the wave directions which influence the final vessel responses. For example, when the main wave direction is 0degrees, most of the wave energy is concentrated among -45degrees to +45degrees of wave heading. As a result, the RAOs corresponding to the before-mentioned wave headings are more important for the calculation of the final vessel motions.

CHAPTER 3. Vector fitting

In most cases the RAOs are accurate enough and thereby they can be used as good initial guesses. Based on these initial guesses, the aim is to find a method to adjust the elements of the RAOs and predict an accurate motion response spectrum. However, the amount of elements which should be calibrated is high. Regarding the hydrodynamic added mass and damping, we should investigate a great number of wave frequencies. With respect to the hydrodynamic forces that are frequency and direction dependent, the amount of elements is even higher. To solve this problem, we try to express the hydrodynamic properties using a limited number of parameters by means of the 'vector fitting' method. According to this method, the frequency domain data are approximated by functions of certain coefficients over the entire frequency interval. These coefficients are a set of poles, a set of residues and in some cases two additional real quantities. In this chapter, the main principles of the vector fitting method are described. Also, this chapter shows the results of the approximated hydrodynamic properties of the semi-submersible crane vessel Thialf.

3.1 RATIONAL FUNCTION APPROXIMATION

An approximation function can be found by fitting a ratio of two polynomials to the given frequency dependent data [12]:

$$f(s) = \frac{a_0 + a_1 s + a_2 s^2 + \cdots + a_N s^N}{b_0 + b_1 s + b_2 s^2 + \cdots + b_N s^N} \qquad \text{Eq. 3-1}$$

where $s=i\omega$ and f(s) stands for the frequency domain data.

In order to find the unknown coefficients of the polynomial, the above mentioned equation can be written as a linear problem of type **Ax**=**b**. However, the resulting problem is badly scaled as the columns of **A** are multiplied by different powers of s. Only low order approximations can be found by that relation [12]. To avoid this limitation, the data are approximated by fitting partial fractions with pre-calculated resonant complex poles. The equation now becomes [12]:

$$\mathrm{f}(s) = \sum_{n=1}^{N} \left(\frac{c_n}{s - p_n}\right) + d + s \cdot h \qquad \text{Eq. 3-2}$$

where c_n are the complex residues, p_n are the complex resonant poles, d and h are real quantities and N is the total amount of resonant poles. Both the residues and the poles come in complex conjugate pairs.

To understand the role of each parameter, we investigate a low order approximation function, considering only one pole.

Given the following coefficients:

- c_R: Real part of residue
- c_I: Imaginary part of residue
- p_R: Real part of pole
- p_I: Imaginary part of pole

The polynomial of the approximation function becomes:

$$f(s) = \frac{c_R + c_I i}{s - p_R - p_I i} + d + s \cdot h$$

After multiplying with the conjugate of the denominator, the following relation is obtained:

$$f(\omega) = \frac{(c_R + c_I \cdot i) \cdot [-p_R + (p_I - \omega) \cdot i]}{{p_R}^2 + (p_I - \omega)^2} + \frac{(d + h \cdot \omega \cdot i) \cdot [{p_R}^2 + (p_I - \omega)^2]}{{p_R}^2 + (p_I - \omega)^2}$$

For a specific frequency, the real and imaginary parts of the approximation function are shown below:

$$\Re\{f(\omega)\} = \frac{d \cdot {p_I}^2 - 2 \cdot d \cdot p_I \cdot \omega - c_I \cdot p_I + d \cdot {p_R}^2 - c_R \cdot p_R + d \cdot \omega^2 + c_I \cdot \omega}{{p_R}^2 + (p_I - \omega)^2}$$

$$\Im\{f(\omega)\} = \frac{h \cdot {p_I}^2 \cdot \omega - 2 \cdot h \cdot p_I \cdot \omega^2 + c_R \cdot p_I + h \cdot {p_R}^2 \cdot \omega - c_I \cdot p_R + h \cdot \omega^3 + c_R \cdot \omega}{{p_R}^2 + (p_I - \omega)^2}$$

The real and imaginary parts of f(s) show that a resonant peak at a specific frequency can be found by setting the denominators close to zero. The denominator becomes zero if the imaginary part of the pole (p_I) equals the frequency of the resonant peak and the real part of the pole (p_R) is zero. To gain more insight into the coefficients, the next step is to set several values for the pole, the residue and the real quantities, and analyze the results.

The frequency range is set from 0rad/sec to 1rad/sec with a step of 0.01 rad/sec. Then the following cases are examined:

Table 1: Investigation of the coefficients of the approximation functions

CASES:	*1*	*2*	*3*	*4*	*5*	*6*	*7*	*8*
c_R	10	10	10 →	1 →	10 →	1	1	1
c_I	10	10	10	10 →	1 →	1	1	1
p_R	10^{-3}	10^{-3} →	10^{-1}	10^{-1}	10^{-1}	10^{-1}	10^{-1}	10^{-1}
p_I	0.8 →	0.2	0.2	0.2	0.2	0.2	0.2	0.2
d	0	0	0	0	0	0 →	10 →	0
h	0	0	0	0	0	0	0 →	10

For each case, the curves of the amplitude, the real and the imaginary part of the approximation function are shown in the following figures.

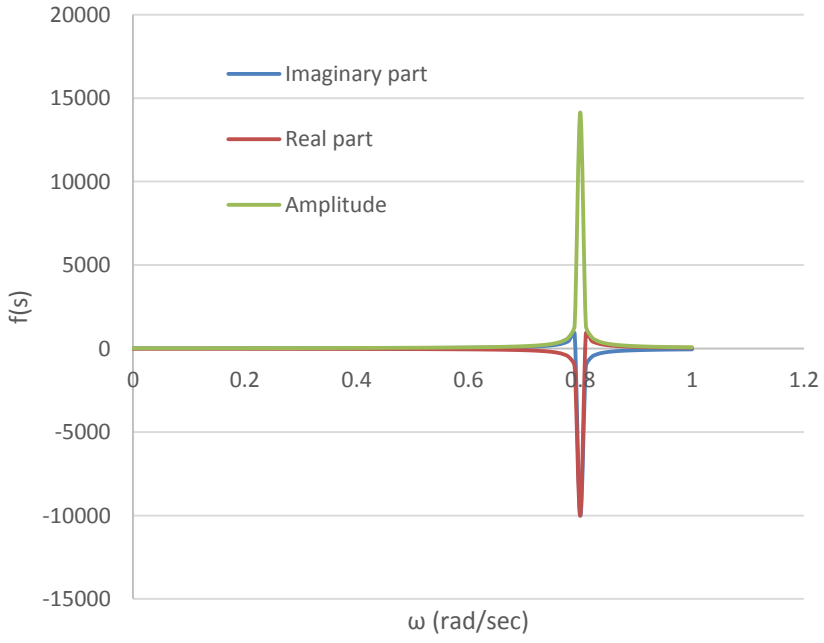

Figure 15: Amplitude, real part and imaginary part of approximation function, case 1

Regarding the first case, the imaginary part of the pole is 0.8. As it was expected, the resonant peak appears at the frequency of 0.8 rad/sec.

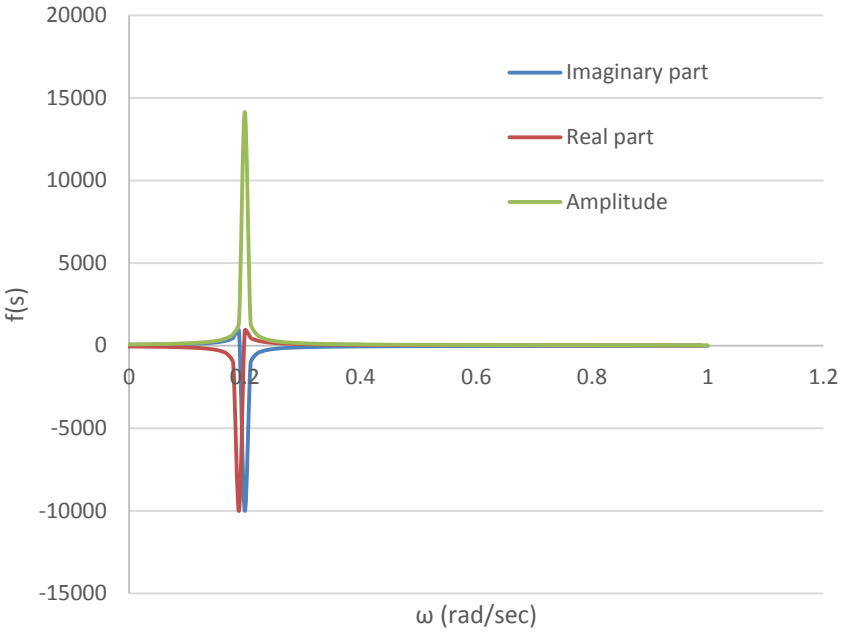

Figure 16: Examination of imaginary part of pole, case 2

For case 2, we only changed the imaginary part of the pole, from 0.8 to 0.2. The figure above showed that the resonant peak transferred from 0.8rad/sec to 0.2rad/sec.

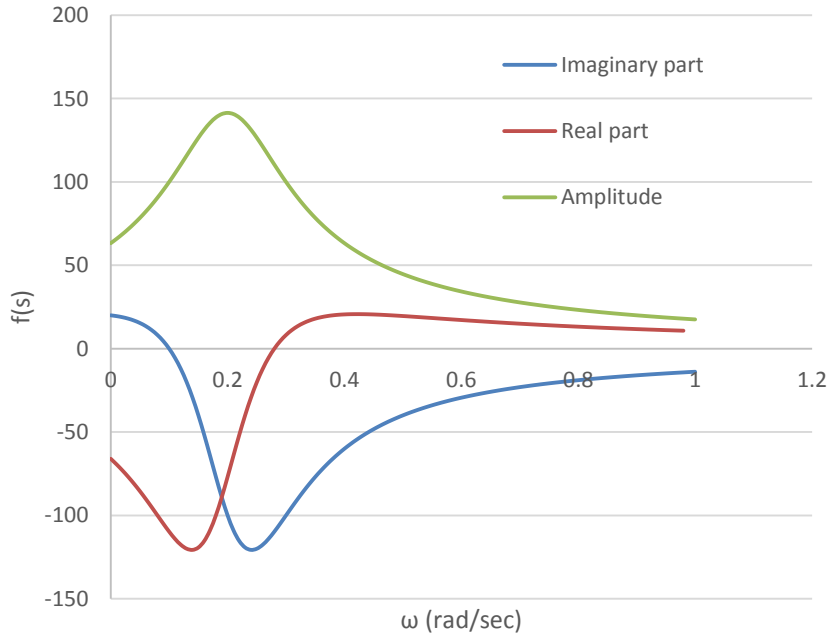

Figure 17: Examination of real part of pole, case 3

For case 3, we increase the value of the real part of the pole, from 10^{-3} to 10^{-1}. The peak for this case is smoother than in the previous plots. Therefore, the real part of the poles influences the sharpness of the peak.

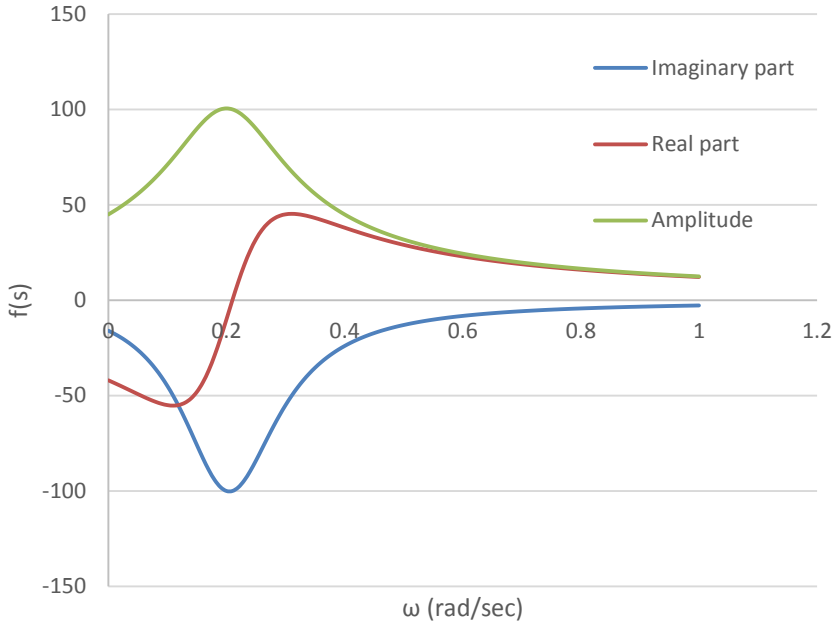

Figure 18: Examination of real part of residue, case 4

For case 4, the real part of the residue is reduced from 10 to 1. The values for the real and imaginary parts of the pole are the same with case 3. Because of changing the real part of the residue, the curve of the real part of the approximation function is modified. The imaginary part of the approximation function is slightly changed. Finally, the values of the amplitude of the approximation function are reduced.

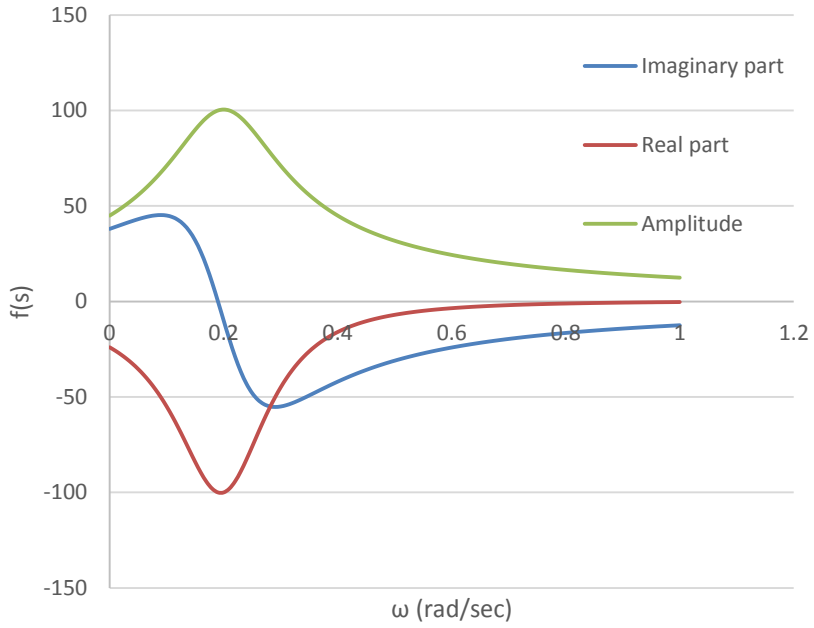

Figure 19: Examination of imaginary part of residue, case 5

For case 5, the real part of the residue is 10 (same with case 3) and the imaginary part of the residue is reduced from 10 to 1. In this case, the curve of the imaginary part of the approximation function is mainly influenced and the values of the amplitude are the same as in case 4.

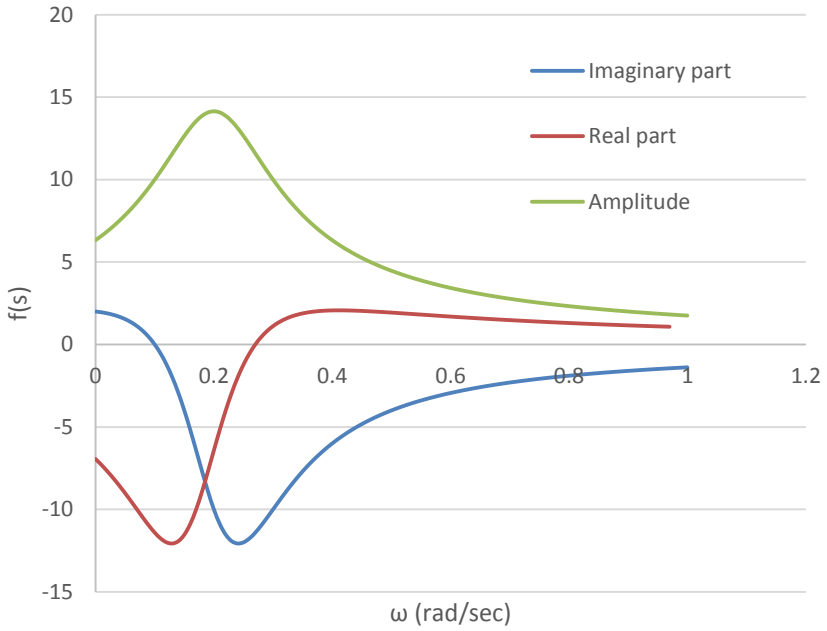

Figure 20: Examination of both imaginary and real parts of residue, case 6

With respect to case 6, both the real and imaginary parts of the residue are reduced from 10 to 1. Although the shape of the curves doesn't change, the approximation function is scaled for the entire frequency interval.

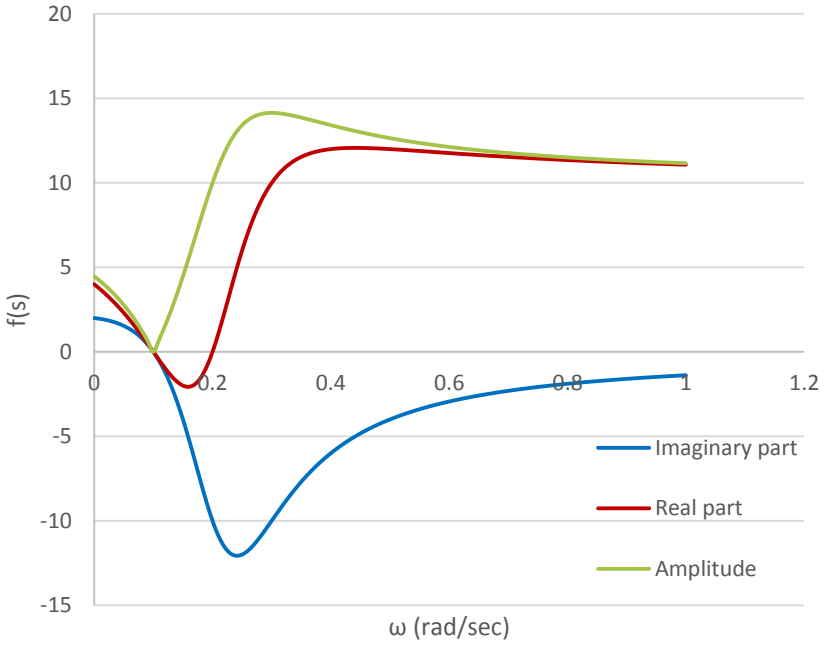

Figure 21: Examination of real quantity 'd', case 7

For case 7, the real quantity 'd' takes the value of 10. The values for the rest of the coefficients are the same as in case 6. As it can be seen in the figure above, the curves for the real part and the amplitude of the approximation function end up to a value of 10 units more than in case 6.

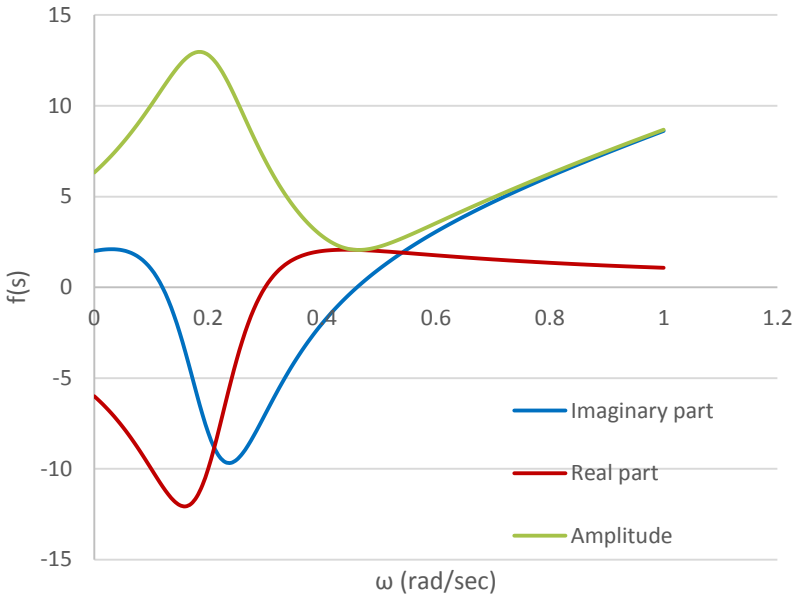

Figure 22: Examination of real quantity 'h', case 8

For case 8, the real quantity 'd' takes the value of 0 and the real quantity 'h' is increased from 0 to 10. The values for the rest of the coefficients are the same as in the previous case. The figure above indicates that the curves for the imaginary part and the amplitude of the approximation function end up to a value of 10 units more than in case 6. Also, these curves have a positive inclination. This means that the parameter h influences the inclination of the curves at higher frequencies. In general, the parameters, d and h, influence the final part of the curves. When d and h are zero (cases 1-6), the approximation function tends to approach 0 for the higher frequencies.

In conclusion, each parameter plays a certain role for the resulting approximation function. By selecting the appropriate values of these parameters, we can create a curve with specific resonant peaks, certain amplitude and defined limits at the high frequencies:

- The frequencies at which the curve indicates resonant peaks are specified by the imaginary part of the poles, p_I.
- The real parts of the poles create either sharp or smooth peaks. For example, if we want to create a curve with sharp peaks, the real parts of the poles should take very low values, p_R.
- The real and imaginary parts of the residues specify the amplitude of the curve.
- Finally, the parameters, d, h, define the behavior of the highest frequencies.

3.2 THEORY ABOUT THE VECTOR FITTING METHOD

As it was mentioned before, the hydrodynamic database is approximated by functions with several complex poles, residues and two real quantities. The determination of the approximation functions with more than one pole becomes more complicated. The method which is used to identify all the parameters of these functions is called vector fitting. The theory of vector fitting is extensively described in literature referred to the sources 12, 13, 14, 15, 16, 17. These sources provide the general methodology for the fitting of frequency domain responses with rational function approximations. In this section, the method of vector fitting is described according to the before mentioned sources.

The vector fitting method includes two stages: The first stage is carried out by the selection of the starting complex poles which should be distributed over the frequency range. Then, an unknown frequency dependent scaling parameter is introduced and leads to the approximation

function to be accurately fitted to a set of new poles. The second stage is carried out with the new poles from stage 1 and the determination of the rest of the parameters [12].

It should be noticed that the poles of the approximation function cannot be identified by a simple least squares solution of a linear matrix equality [13].

Given the following equation:

$$f(s) = \sum_{n=1}^{N} \left(\frac{c_n}{s-p_n}\right) + d + s \cdot h \qquad \text{Eq. 3-3}$$

The matrices for the over determined linear matrix equality, **Ax**=**b**, should be:

$$\boldsymbol{A} = \begin{bmatrix} \frac{1}{s_1-p_1} & \cdots & \frac{1}{s_1-p_N} & 1 & s_1 \\ \frac{1}{s_2-p_1} & \cdots & \frac{1}{s_2-p_N} & 1 & s_2 \\ & & \vdots & & \\ \frac{1}{s_k-p_1} & \cdots & \frac{1}{s_k-p_N} & 1 & s_k \end{bmatrix}, \boldsymbol{x} = \begin{bmatrix} c_1 \\ c_2 \\ \vdots \\ c_N \\ d \\ h \end{bmatrix}, \boldsymbol{b} = \begin{bmatrix} f(s_1) \\ f(s_2) \\ \cdot \\ \cdot \\ \cdot \\ f(s_k) \end{bmatrix}$$

The dimensions of matrix **A** are k X (N+2), where k is the number of frequencies of the given data and N is the number of residues. Matrix **x** contains the unknown coefficients (c_n, d, h) and matrix **b** contains the frequency domain data.

As can be seen, the poles are found at the denominator of the partial fractions of the approximation function. If we consider the poles as unknown coefficients, the resulting problem is badly scaled. In order to solve the before-mentioned equality, the poles should be known. Thus, the purpose of stage 1 of the vector fitting method is to determine the poles of the approximation function.

3.2.1 Stage 1

First, it is necessary to decide on a set of starting poles and multiply the frequency domain data, f(s), with a scaling function σ(s) [13]. The function σ(s) is indicated below:

$$\sigma(s) = \sum_{n=1}^{N} \frac{r_n}{s-p_n} + 1 \qquad \text{Eq. 3-4}$$

where r_n are the residues of σ(s), p_n are the poles and N is the total number of poles. It should be noticed that the final approximation function and the scaling function σ(s) share the same complex poles [13].

After multiplying the given data with the function σ(s), we obtain the following relation [13]:

$$\sum_{n=1}^{N} \frac{c_n}{s-p_n} + d + s \cdot h = \sigma(s) \cdot f(s) = \left(\sum_{n=1}^{N} \frac{r_n}{s-p_n} + 1\right) \cdot f(s) \qquad \text{Eq. 3-5}$$

where:

- f(s) contains the frequency domain data
- $\sum_{n=1}^{N} \frac{c_n}{s-p_n} + d + s \cdot h$ is the final approximation function
- $\sum_{n=1}^{N} \frac{r_n}{s-p_n} + 1$ is the scaling function

To understand the role of σ(s), each sum of partial fractions in Eq. 3-5 is written as follows [13]:

$$\sum_{n=1}^{N} \frac{c_n}{s-p_n} + d + s \cdot h = h \frac{\prod_{n=1}^{N+1}(s-z_n)}{\prod_{n=1}^{N}(s-p_n)} \quad \text{and} \quad \sigma(s) = \sum_{n=1}^{N} \frac{r_n}{s-p_n} + 1 = \frac{\prod_{n=1}^{N}(s-v_n)}{\prod_{n=1}^{N}(s-p_n)} \qquad \text{Eq. 3-6}$$

Then Eq. 3-5 becomes:

$$\sum_{n=1}^{N}\frac{c_n}{s-p_n}+d+s\cdot h=\left(\sum_{n=1}^{N}\frac{r_n}{s-p_n}+1\right)\cdot f(s) \Rightarrow h\frac{\prod_{n=1}^{N+1}(s-z_n)}{\prod_{n=1}^{N}(s-p_n)}=\frac{\prod_{n=1}^{N}(s-v_n)}{\prod_{n=1}^{N}(s-p_n)}\cdot f(s)$$

Thus: $f(s)=\frac{h\frac{\prod_{n=1}^{N+1}(s-z_n)}{\prod_{n=1}^{N}(s-p_n)}}{\frac{\prod_{n=1}^{N}(s-v_n)}{\prod_{n=1}^{N}(s-p_n)}}=h\frac{\prod_{n=1}^{N+1}(s-z_n)}{\prod_{n=1}^{N}(s-v_n)}$ Eq. 3-7

Given the equation above, the poles of f(s) can be found if we set $\prod_{n=1}^{N}(s-v_n)=0$. Therefore, the poles of f(s) become equal to the zeros of σ(s). A good set of poles should minimize the sum of the residues of σ(s) [13].

In order to understand the procedure of stage 1, the following steps are provided:

1. Selection of starting poles.
2. Identification of the coefficients of the approximation function and the scaling function: residues of σ(s), residues and real quantities of the approximation function.
3. Given the residues of σ(s) from step 2, we calculate the zeros of σ(s) and we get a new set of poles.
4. Given the new set of poles, we go back to step 2 and check if the sum of the new residues of σ(s) is close to zero.
5. If the sum of the residues of σ(s) is not close to zero, we go to step 3 and calculate another set of poles. We repeat this procedure until we find a set of poles that leads to a minimum value for the sum of residues of σ(s).

For step 2, Eq. 3-5 is written as [14]:

$$\sum_{n=1}^{N}\frac{c_n}{s-p_n}+d+s\cdot h-\left(\sum_{n=1}^{N}\frac{r_n}{s-p_n}\right)\cdot f(s)=f(s)$$ Eq. 3-8

Writing the above equation for all frequency points, gives the over determined linear matrix equality [14]: **Ax**=**b**. The matrices **A**, **b**, **x** are presented below:

$$\boldsymbol{A}=\begin{bmatrix}\frac{1}{s_1-p_1}&\cdots&\frac{1}{s_1-p_N}&1&s_1&\frac{-f(s_1)}{s_1-p_1}&\cdots&\frac{-f(s_1)}{s_1-p_N}\\ \frac{1}{s_2-p_1}&\cdots&\frac{1}{s_2-p_N}&1&s_2&\frac{-f(s_2)}{s_2-p_1}&\cdots&\frac{-f(s_2)}{s_2-p_N}\\ &&&&\vdots&&&\\ \frac{1}{s_k-p_1}&\cdots&\frac{1}{s_k-p_N}&1&s_k&\frac{-f(s_k)}{s_k-p_1}&\cdots&\frac{-f(s_k)}{s_k-p_N}\end{bmatrix},\ \boldsymbol{x}=\begin{bmatrix}c_1\\c_2\\\vdots\\c_N\\d\\h\\r_1\\r_2\\\vdots\\r_N\end{bmatrix},\ \boldsymbol{b}=\begin{bmatrix}f(s_1)\\f(s_2)\\\cdot\\\cdot\\\cdot\\f(s_k)\end{bmatrix}$$

Matrix **A** has as many rows as the number of frequencies of the given data and as many columns as the sum of: the number of residues of the approximation function + the number of residues of scaling function + 2. Thus, the dimensions of **A** are: k X (2N+2). Matrix **x** contains the unknown coefficients (c_n, r_n, d, h) and matrix b contains the frequency domain data. The dimensions of **x** are: (2N+2) X 1 and the dimensions of **b** are: k X 1.

To ensure that the residues come in conjugate pairs, a modification is recommended. For example, given a pole 'p_n', the next pole is: p_{n+1}=conjugate (p_n). Then, the resulting residues should be in the form of [14]:

$$c_n=\alpha_{cn}+i\beta_{cn}\ ,\quad c_{n+1}=\alpha_{cn}-i\beta_{cn}$$

where α_{cn} and β_{cn} are the real and imaginary parts of c_n (or c_{n+1}), respectively.

The row of matrix A, which corresponds to a frequency s_k, is modified as follows [14]:

$$\boldsymbol{A}_{k,j} = \left\{\frac{1}{s_k - p_j} + \frac{1}{s_k - \mathrm{conj}(p_j)}\right\}, \boldsymbol{A}_{k,j+1} = \left\{\frac{i}{s_k - p_j} - \frac{i}{s_k - \mathrm{conj}(p_j)}\right\} \quad \ldots \; \boldsymbol{A}_{k,N+1} = 1, \boldsymbol{A}_{k,N+2} = s_k, \ldots$$

$$\boldsymbol{A}_{k,N+2+j} = \left\{\frac{-f(s_k)}{s_k - p_j} + \frac{-f(s_k)}{s_k - \mathrm{conj}(p_j)}\right\}, \boldsymbol{A}_{k,N+2+j} = \left\{\frac{-f(s_k)\cdot i}{s_k - p_j} - \frac{-f(s_k)\cdot i}{s_k - \mathrm{conj}(p_j)}\right\}$$

where j takes values: 1, 3, 5,…, N-1 and $s_k = i\omega_k$.

Moreover, the matrix **x** becomes:

$$\boldsymbol{x} = \begin{bmatrix} \Re(c_1) \\ \Im(c_1) \\ \Re(c_3) \\ \Im(c_3) \\ \vdots \\ \Re(c_{N-1}) \\ \Im(c_{N-1}) \\ d \\ h \\ \Re(r_1) \\ \Im(r_1) \\ \Re(r_3) \\ \Im(r_3) \\ \vdots \\ \Re(r_{N-1}) \\ \Im(r_{N-1}) \end{bmatrix}$$

To improve the fitting process, we should express the linear matrix equation in terms of real quantities [14]:

$$\begin{bmatrix} \Re(\boldsymbol{A}) \\ \Im(\boldsymbol{A}) \end{bmatrix} \cdot x = \begin{bmatrix} \Re(\boldsymbol{b}) \\ \Im(\boldsymbol{b}) \end{bmatrix}$$

Finally, the least squares solution to this overdetermined problem is shown below:

$$\boldsymbol{x} = (\boldsymbol{A}^T \cdot \boldsymbol{A})^{-1} \cdot \boldsymbol{A}^T \cdot \boldsymbol{b} \qquad \text{Eq. 3-9}$$

In most cases, the solution based on the starting poles does not give a good approximation function. For this reason, we should follow step 3. According to this step, we calculate the zeros of σ(s) and get a new set of poles [13].

Given the residues of σ(s) from step 2 and the starting poles, the equation of σ(s) is written as the following input-output system [15]:

$$s \cdot \boldsymbol{x_{sigma}} = \boldsymbol{A}_{sigma} \cdot \boldsymbol{x_{sigma}} + \boldsymbol{b}_{sigma} \cdot u \qquad \text{Eq. 3-10}$$

$$y = \boldsymbol{r}_{sigma}{}^T \cdot \boldsymbol{x_{sigma}} + d_1 \cdot u \qquad \text{Eq. 3-11}$$

where $\mathbf{A}_{\mathrm{sigma}}$ is a diagonal matrix (N X N) which contains the starting poles [15]:

$$\mathbf{A}_{\mathrm{sigma}} = \begin{bmatrix} p_1 & 0 & 0 \\ 0 & \ddots & 0 \\ 0 & 0 & p_N \end{bmatrix}$$

$\mathbf{b}_{\mathrm{sigma}}$ is a column vector of ones [15]:

$$\mathbf{b}_{\mathrm{sigma}} = \begin{bmatrix} 1 \\ \vdots \\ 1 \end{bmatrix}$$

$\boldsymbol{r}_{sigma}{}^T$ is a row vector which contains the residues of σ(s) [15]:

$$\boldsymbol{r}_{sigma}{}^{T} = [r_1 \quad \dots \quad r_N]$$

d_1=1 and u=1.

If we solve equation Eq.3-10 for $\boldsymbol{x_{sigma}}$, we get:

$$\boldsymbol{x_{sigma}} = \begin{bmatrix} \frac{1}{s-p_1} \\ \vdots \\ \frac{1}{s-p_N} \end{bmatrix}$$

It should be mentioned that 'y' in Eq. 3-11 represents the output of the system and gives the values of σ(s):

$$y = \sum_{n=1}^{N} \frac{r_n}{s-p_n} + 1$$

If we solve Eq.3-11 for 'u' and implement the solution to Eq.3-10, the following relation is obtained [15]:

$$s \cdot \boldsymbol{x_{sigma}} = \{\boldsymbol{A}_{sigma} - \boldsymbol{b}_{sigma} \cdot (d_1)^{-1} \boldsymbol{r}_{sigma}{}^{T}\} \cdot \boldsymbol{x_{sigma}} + \boldsymbol{b}_{sigma} \cdot (d_1)^{-1} \cdot y$$

In order to find a set of poles that leads to the zeros of σ(s), we calculate the eigenvalues of the following matrix [16]:

$$\boldsymbol{H} = \{\boldsymbol{A}_{sigma} - \boldsymbol{b}_{sigma} \cdot \boldsymbol{r}_{sigma}{}^{T}\} \qquad \text{Eq. 3-12}$$

Furthermore, to obtain complex conjugate pairs of poles, the corresponding matrices should be modified via a similarity transformation as follows [16]:

$$\boldsymbol{A}_{sigma} = \begin{bmatrix} \Re(p_n) & \Im(p_n) \\ -\Im(p_n) & \Re(p_n) \end{bmatrix},$$

$$\boldsymbol{b}_{sigma} = \begin{bmatrix} 2 \\ 0 \end{bmatrix}, \quad \boldsymbol{r}_{sigma} = [\Re(r_n) \quad \Im(r_n)]$$

where p_n are the starting poles and r_n are the residues of σ(s).

The eigenvalues of matrix **H** are the new poles and the least squared problem of step 2 is solved again. The whole procedure is repeated until the sum of the residues of σ(s) approaches zero [13].

3.2.2 Stage 2

After getting a good set of poles from stage 1, the coefficients of the final approximation function are determined by the least square solution of a new over determined linear problem. The matrices for this problem are shown below [13]:

$$\boldsymbol{A} = \begin{bmatrix} \frac{1}{s_1-a_1} & \dots & \frac{1}{s_1-a_N} & 1 & s_1 \\ \frac{1}{s_2-a_1} & \dots & \frac{1}{s_2-a_N} & 1 & s_2 \\ & & \vdots & & \\ \frac{1}{s_k-a_1} & \dots & \frac{1}{s_k-a_N} & 1 & s_k \end{bmatrix}, \boldsymbol{x} = \begin{bmatrix} c_1 \\ c_2 \\ \vdots \\ c_N \\ d \\ h \end{bmatrix}, \boldsymbol{b} = \begin{bmatrix} f(s_1) \\ f(s_2) \\ \cdot \\ \cdot \\ \cdot \\ f(s_k) \end{bmatrix}$$

As it can be seen, only the residues and the quantities d, h of the final approximation function are included in matrix **x**. The scaling function σ(s) is used only in stage 1.

3.2.3 Starting poles

The selection of the starting poles plays an important role for the method of vector fitting. Thus a sensible location of the starting poles should be decided.

The starting poles should be complex conjugate pairs distributed over the frequency range. They should have the following form [17]:

$$p_n = -\alpha_{pn} + i\beta_{pn} \ , \ \ p_{n+1} = -\alpha_{pn} - i\beta_{pn}$$

According to paragraph 3.1, the imaginary part of the poles is related to the frequencies at which the data indicate resonant peaks. Therefore, the imaginary part of the starting poles is equal to the peak frequencies of the data. Also, it is assumed that the real part of the starting poles is [17]: $\alpha_{pn} = \frac{\beta_{pn}}{100}$

3.3 VECTOR FITTING: ADDED MASS AND DAMPING

In this section, the vector fitting method is applied to approximate the frequency domain elements of the added mass and damping. As mentioned in CHAPTER 2, the added mass and damping should not be treated separately. Based on potential theory, added mass and damping belong to the same complex quantity. Therefore, the fitting process is accomplished for the following relation:

$$ab_{ij}(\omega) = a_{ij}(\omega) - \frac{b_{ij}(\omega)}{\omega} \cdot i \qquad \text{Eq. 3-13}$$

where a_{ij} is an element of the added mass matrix, b_{ij} is an element of the damping matrix and ω is the wave frequency.

In total, 36 approximation functions should be constructed for each frequency depended element of the added mass and damping matrices. The real part of these functions stands for the approximation of the added mass. The imaginary part, multiplied by ω, stands for the approximation of damping.

Furthermore, some of the vessels such as the Thialf and the Balder, have a vertical-longitudinal plane of symmetry. Thus, their motions can be split into symmetric and anti-symmetric components. Surge, heave and pitch are coupled symmetric motions and sway, roll and yaw are coupled anti-symmetric motions. Taking advantage of symmetry-anti symmetry conditions, the number of approximation functions can be reduced significantly. For example the added mass and damping coefficients which correspond to the uncoupled motions are zero. In addition, the symmetric elements with respect to the main diagonal of the matrices have the same values. The number of the fitting functions can thus be reduced from 36 to 12.

The matrices of the hydrodynamic added mass and damping for the symmetric SSCV Thialf are shown below:

$$A(\omega)= \begin{vmatrix} a_{11}(\omega) & 0 & a_{13}(\omega) & 0 & a_{15}(\omega) & 0 \\ 0 & a_{22}(\omega) & 0 & a_{24}(\omega) & 0 & a_{26}(\omega) \\ a_{31}(\omega) & 0 & a_{33}(\omega) & 0 & a_{35}(\omega) & 0 \\ 0 & a_{42}(\omega) & 0 & a_{44}(\omega) & 0 & a_{46}(\omega) \\ a_{51}(\omega) & 0 & a_{53}(\omega) & 0 & a_{55}(\omega) & 0 \\ 0 & a_{62}(\omega) & 0 & a_{64}(\omega) & 0 & a_{66}(\omega) \end{vmatrix} \quad B(\omega)= \begin{vmatrix} b_{11}(\omega) & 0 & b_{13}(\omega) & 0 & b_{15}(\omega) & 0 \\ 0 & b_{22}(\omega) & 0 & b_{24}(\omega) & 0 & b_{26}(\omega) \\ b_{31}(\omega) & 0 & b_{33}(\omega) & 0 & b_{35}(\omega) & 0 \\ 0 & b_{42}(\omega) & 0 & b_{44}(\omega) & 0 & b_{46}(\omega) \\ b_{51}(\omega) & 0 & b_{53}(\omega) & 0 & b_{55}(\omega) & 0 \\ 0 & b_{62}(\omega) & 0 & b_{64}(\omega) & 0 & b_{66}(\omega) \end{vmatrix}$$

where $a_{ij}=a_{ji}$ and $b_{ij}=b_{ji}$.

Each element of these matrices is replaced by a fitting function as it is shown below:

$$A(s)=\begin{vmatrix} \Re\{f_{ab_{11}}(s)\} & 0 & \Re\{f_{ab_{13}}(s)\} & 0 & \Re\{f_{ab_{15}}(s)\} & 0 \\ 0 & \Re\{f_{ab_{22}}(s)\} & 0 & \Re\{f_{ab_{24}}(s)\} & 0 & \Re\{f_{ab_{26}}(s)\} \\ \Re\{f_{ab_{31}}(s)\} & 0 & \Re\{f_{ab_{33}}(s)\} & 0 & \Re\{f_{ab_{35}}(s)\} & 0 \\ 0 & \Re\{f_{ab_{42}}(s)\} & 0 & \Re\{f_{ab_{44}}(s)\} & 0 & \Re\{f_{ab_{46}}(s)\} \\ \Re\{f_{ab_{51}}(s)\} & 0 & \Re\{f_{ab_{53}}(s)\} & 0 & \Re\{f_{ab_{55}}(s)\} & 0 \\ 0 & \Re\{f_{ab_{62}}(s)\} & 0 & \Re\{f_{ab_{64}}(s)\} & 0 & \Re\{f_{ab_{66}}(s)\} \end{vmatrix}$$

$$B(s)=\begin{vmatrix} \Im\{f_{ab_{11}}(s)\}\omega & 0 & \Im\{f_{ab_{13}}(s)\}\omega & 0 & \Im\{f_{ab_{15}}(s)\}\omega & 0 \\ 0 & \Im\{f_{ab_{22}}(s)\}\omega & 0 & \Im\{f_{ab_{24}}(s)\}\omega & 0 & \Im\{f_{ab_{26}}(s)\}\omega \\ \Im\{f_{ab_{31}}(s)\}\omega & 0 & \Im\{f_{ab_{33}}(s)\}\omega & 0 & \Im\{f_{ab_{35}}(s)\}\omega & 0 \\ 0 & \Im\{f_{ab_{42}}(s)\}\omega & 0 & \Im\{f_{ab_{44}}(s)\}\omega & 0 & \Im\{f_{ab_{46}}(s)\}\omega \\ \Im\{f_{ab_{51}}(s)\}\omega & 0 & \Im\{f_{ab_{53}}(s)\}\omega & 0 & \Im\{f_{ab_{55}}(s)\}\omega & 0 \\ 0 & \Im\{f_{ab_{62}}(s)\}\omega & 0 & \Im\{f_{ab_{64}}(s)\}\omega & 0 & \Im\{f_{ab_{66}}(s)\}\omega \end{vmatrix}$$

where:

$$f_{ab11}(s) = \sum_{n=1}^{N} \frac{c_{n,ab11}}{s-p_{n,ab11}} + d_{ab11} + s \cdot h_{ab11}$$

$$f_{ab12}(s) = \sum_{n=1}^{N} \frac{c_{n,ab12}}{s-p_{n,ab12}} + d_{ab12} + s \cdot h_{ab12}\ ,\ldots,$$

$$f_{ab66}(s) = \sum_{n=1}^{N} \frac{c_{n,ab66}}{s-p_{n,ab66}} + d_{ab66} + s \cdot h_{ab66}$$

$s=i\omega$, N=number of poles, $c_{n,abij}$, $p_{n,abij}$, d_{abij}, h_{abij}= sets of residues, poles and the real quantities for the approximation function of element 'ij'

As mentioned before, fitting functions are developed for the symmetrical SSCV Thialf at a draft of 22m. Therefore, the next paragraphs describes the approximation functions for only 12 elements of the added mass and damping matrices.

3.3.1 Added mass and Damping-Stage 1

Regarding stage 1, a set of starting poles should be defined. For the selection of the starting poles, it is suggested to use the resonant peaks of the frequency domain data. The peak selection for element ab_{33} is shown in the following figure.

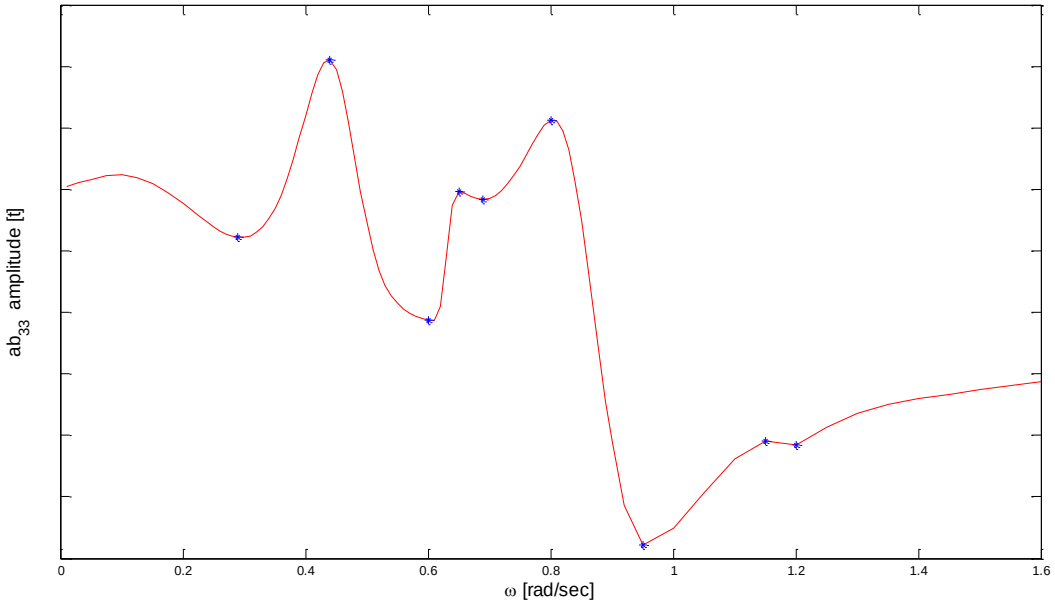

Figure 23: Peak Selection, ab_{33}

As shown in the above figure, we selected the local minima and maxima of the amplitude of ab_{33}. The wave frequencies that correspond to these minima and maxima are used as the imaginary part of the starting poles. Then the real part of the starting poles is calculated by dividing the imaginary part by 100. Due to the fact that the motions of the vessels are mainly influenced by wind sea and swell (section 2.6), the curve fitting should be done within the frequency range of 0.15-1.6 rad/sec. Thus, we avoid the selection of a pole at frequencies outside that range. The algorithm for the selection of the starting poles is provided in Appendix A1.

Furthermore, several repetitions should be accomplished to calculate the zeros of σ(s) and get a better set of poles. The repetitions stop when σ(s) reaches a minimum value. The number of iterations is also limited to 1000. The algorithm for the identification of poles is given in Appendix A2.

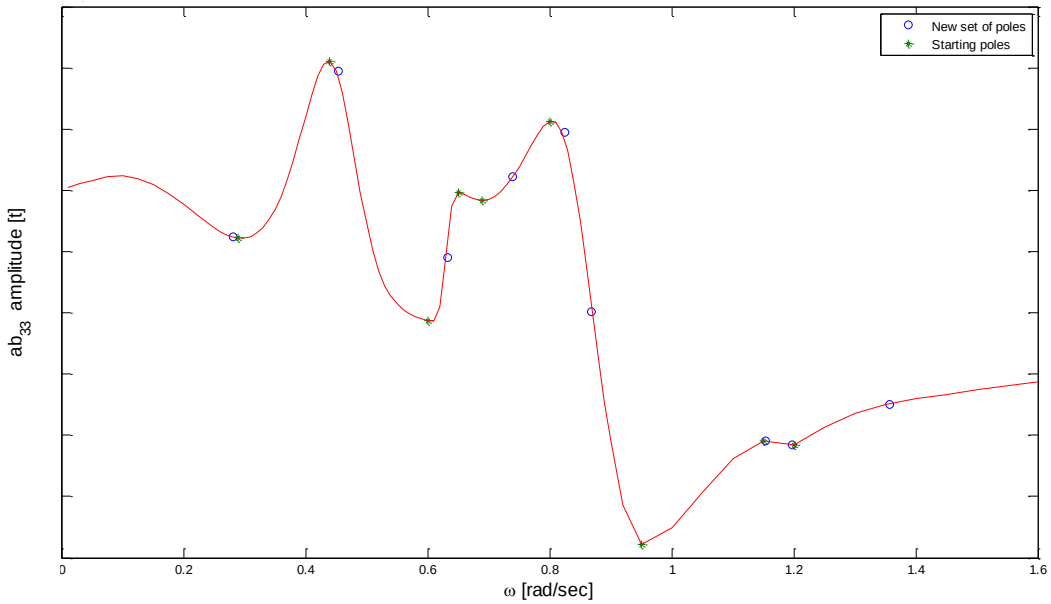

Figure 24: New set of poles, ab_{33}

In some cases, the new set of poles includes pairs with zero imaginary parts. This could lead to an inaccurate curve fitting. For this reason, the imaginary parts of these pairs are forced to take the minimum value of 0.0001.

3.3.2 Added mass and Damping-Stage 2

With respect to the second stage of vector fitting, the residues and the real quantities of the final approximation function are identified. The algorithm for this stage is indicated in Appendix A3.

To evaluate the accuracy of the fitting process, we calculate the Normalized Root Mean Square Error [18].

The NRMSE is calculated as follows:

$$NRMSE_{ab33} = 1 - \frac{\sqrt{\frac{1}{k}\cdot\sum_{i=1}^{k}\left(ab_{33,VF}(\omega_i) - ab_{33,OR}(\omega_i)\right)^2}}{\sqrt{\frac{1}{k}\cdot\sum_{i=1}^{k}\left(ab_{33,OR}(\omega_i) - mean(ab_{33,OR})\right)^2}} \qquad \text{Eq. 3-14}$$

where $ab_{33,VF}$ represents the approximated values of ab_{33}, $ab_{33,OR}$ contains the original values of element ab_{33}, ω_i is the wave frequency and k is the total number of wave frequencies. The denominator: $\sqrt{\frac{1}{k}\cdot\sum_{i=1}^{k}\left(ab_{33,OR}(\omega_i) - mean(ab_{33,OR})\right)^2}$ indicates the standard deviation of the original values of element ab_{33}.

The NRMSE varies between $-\infty$ (bad fit) to 1 (perfect fit). For the element ab_{33}, the NRMSE is 0.984. This means that the fitting function approximates the data with great accuracy. The figure below shows the fitted and the original curves of the elements a_{33} and b_{33}.

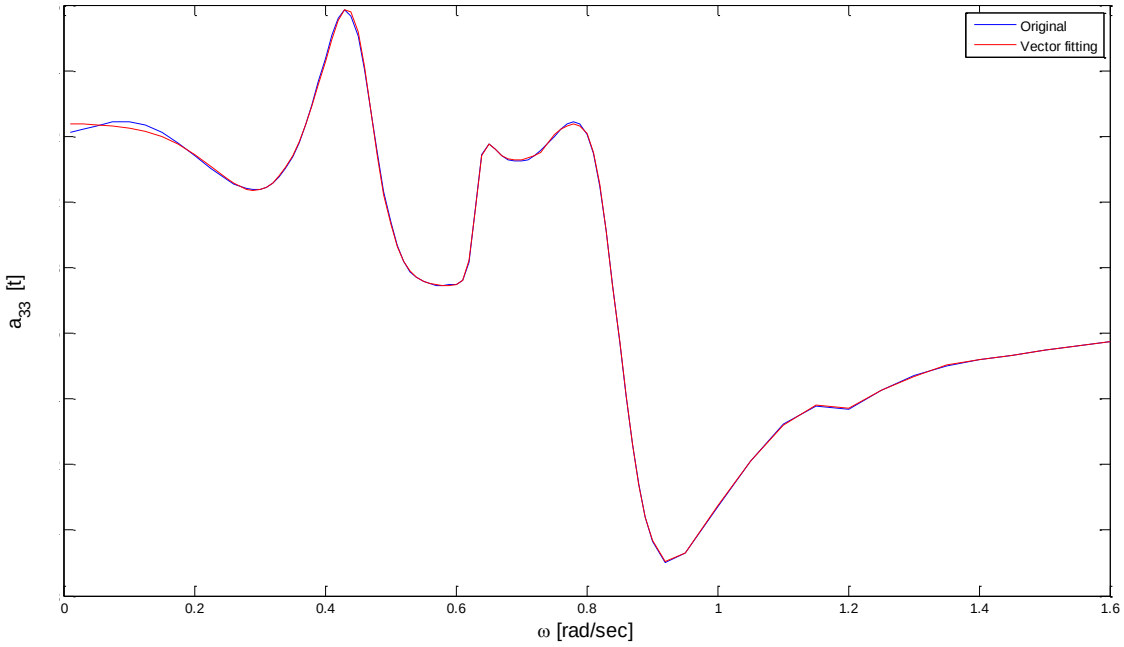

Figure 25: Vector fitting for hydrodynamic added mass a_{33}

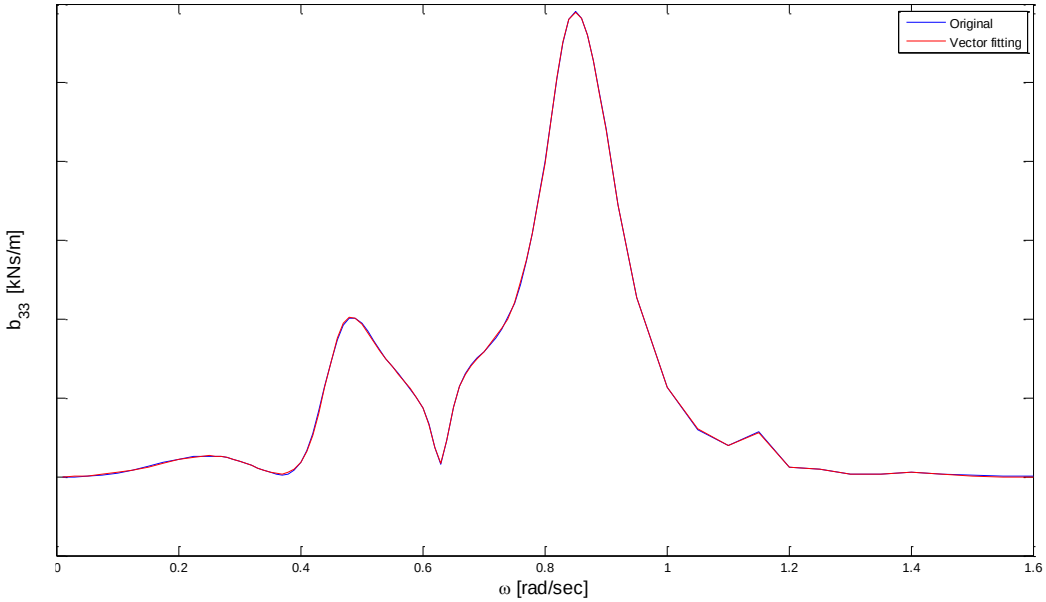

Figure 26: Vector fitting for hydrodynamic damping b_{33}

With respect to the rest of the elements of the added mass and damping matrices, the NRMSEs are provided in the following table:

Table 2: Normalized Root Mean Square Error: Hydrodynamic added mass and damping

ab_{11}	ab_{22}	ab_{31}	ab_{33}	ab_{42}	ab_{44}	ab_{51}	ab_{53}	ab_{55}	ab_{62}	ab_{64}	ab_{66}
0.996	0.996	0.991	0.984	0.967	0.997	0.982	0.996	0.989	0.998	0.992	0.947

According to the above table, the element ab_{66} indicates the highest inaccuracies. If the resulting response spectra do not fit the original response spectra (next chapter), we may need to find a better approximation for this element. The plots of the fitted and the original curves of this element are shown below.

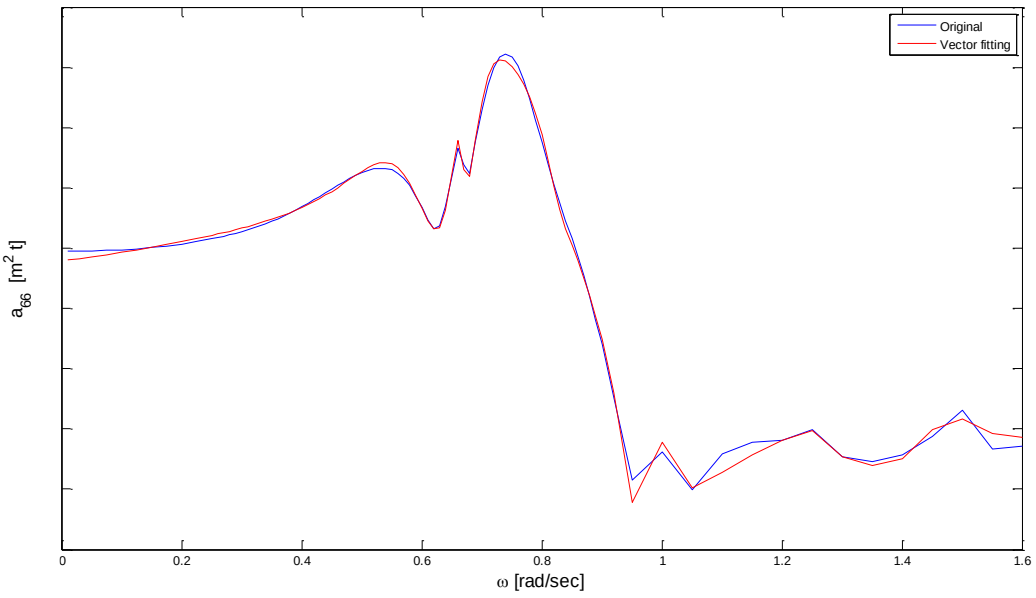

Figure 27: Vector fitting for hydrodynamic added mass a_{66}

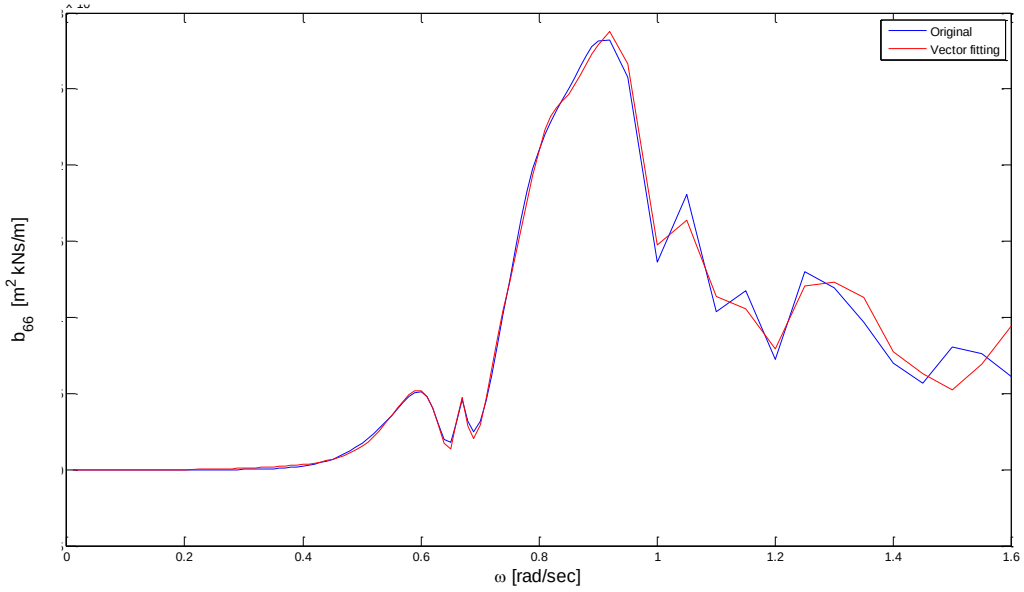

Figure 28: Vector fitting for hydrodynamic damping b_{66}

3.4 VECTOR FITTING –WAVE FORCES AND MOMENTS

With respect to the hydrodynamic wave forces and moments, the output of the diffraction software gives the frequency domain forces for 6 DOFs and 24 wave directions. For every wave direction, there is a set of 3 hydrodynamic forces and 3 hydrodynamic moments which correspond to the 6 vessel motions. The wave directions start at 0 degrees, increase by 15 degrees and reaches 345 degrees of wave heading. As a result, 144 (24*6) approximation functions should be found for the wave forces and moments.

However, this number of fitting functions can be reduced based on the symmetry-anti symmetry conditions. The forces and moments which are related with the symmetric motions have the same amplitude and phase for symmetrical angles of wave heading with respect to x axis of the vessel. However the forces and moments, which are related with the anti-symmetric motions have the same amplitude and opposite phases for those wave headings. As a result, we only need to find the approximation functions corresponding to the range of 0 to 180 degrees of wave headings.

The matrices for the wave forces and moments are defined below:

$$\boldsymbol{F}(\omega,0^\circ)=\begin{bmatrix}F_1(\omega_1,0^\circ) & \cdots & F_1(\omega_k,0^\circ)\\ \vdots & \ddots & \vdots\\ M_6(\omega_1,0^\circ) & \cdots & M_6(\omega_k,0^\circ)\end{bmatrix}\ldots\ \boldsymbol{F}(\omega,345^\circ)=\begin{bmatrix}F_1(\omega_1,345^\circ) & \cdots & F_1(\omega_k,345^\circ)\\ \vdots & \ddots & \vdots\\ M_6(\omega_1,345^\circ) & \cdots & M_6(\omega_k,345^\circ)\end{bmatrix}$$

where k is the number of the wave frequencies.

After applying the fitting functions, the matrices become:

$$\boldsymbol{F}(\omega,0^\circ)=\begin{bmatrix}f_1(s_1,0^\circ)\ldots f_1(s_k,0^\circ)\\ f_2(s_1,0^\circ)\ldots f_2(s_k,0^\circ)\\ \vdots\\ f_6(s_1,0^\circ)\ldots f_6(s_k,0^\circ)\end{bmatrix},\quad \boldsymbol{F}(\omega,15^\circ)=\begin{bmatrix}f_1(s_1,15^\circ)\ldots f_1(s_k,15^\circ)\\ f_2(s_1,15^\circ)\ldots f_2(s_k,15^\circ)\\ \vdots\\ f_6(s_1,15^\circ)\ldots f_6(s_k,15^\circ)\end{bmatrix}\ldots\ldots$$

$$\ldots\ldots\ \boldsymbol{F}(\omega,345^\circ)=\begin{bmatrix}f_1(s_1,345^\circ)\ldots f_1(s_k,345^\circ)\\ f_2(s_1,345^\circ)\ldots f_2(s_k,345^\circ)\\ \vdots\\ f_6(s_1,345^\circ)\ldots f_6(s_k,345^\circ)\end{bmatrix}$$

where:

$$f_1(s,0^\circ)=\sum_{n=1}^{N}\frac{c_{n,F_1\_0^\circ}}{s-\mathrm{p}_{n,F_1\_0^\circ}},\quad f_2(s,0^\circ)=\sum_{n=1}^{N}\frac{c_{n,F_2\_0^\circ}}{s-\mathrm{p}_{n,F_2\_0^\circ}},\ldots..,$$

$$f_1(s,345^\circ)=\sum_{n=1}^{N}\frac{c_{n,F_1\_15^\circ}}{s-\mathrm{p}_{n,F_1\_15^\circ}},\ldots\ldots,\quad f_6(s,345^\circ)=-\left\{\sum_{n=1}^{N}\frac{c_{n,F_6\_15^\circ}}{s-\mathrm{p}_{n,F_6\_15^\circ}}\right\}$$

As it is shown from the equations above, we use the same fitting functions for symmetrical wave headings:

$$f_1(s,345^\circ)=f_1(s,15^\circ),\quad f_3(s,345^\circ)=f_3(s,15^\circ),\quad f_5(s,345^\circ)=f_5(s,15^\circ)$$

and

$$f_2(s,345^\circ)=-f_2(s,15^\circ),\qquad f_4(s,345^\circ)=-f_4(s,15^\circ),\quad f_6(s,345^\circ)=-f_6(s,15^\circ)$$

In addition, for the approximation functions of the wave forces and moments, we don't need to use the real quantities d, h.

3.4.1 Wave forces and moments-Stage 1

For each of the 6 wave forces and moments, it is suggested to use the same poles for the entire range of 0 to 180 degrees of wave headings. First, we identify a set of poles for the force or moment that corresponds to the wave direction with the highest number of peaks. Then this set of poles is applied for the approximation functions of all of the wave directions. For the directions with less resonant peaks, the residues related to the extra poles can get low values. In this way, the extra poles do not create any extra peak.

The curves of the amplitude of F_3 for 0º-180º wave headings, are indicated below:

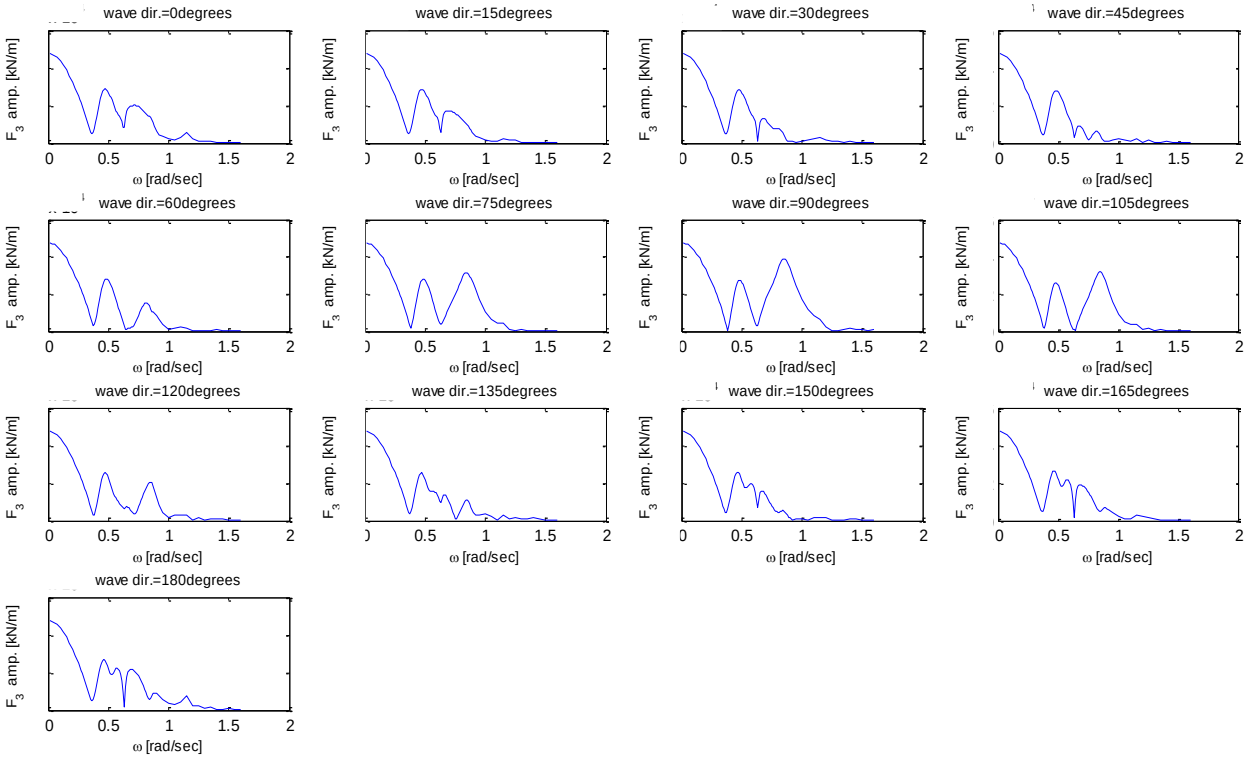

Figure 29: Amplitude of F_3, wave directions = 0º -180º

As it can be seen, the curve for the wave direction 180º indicates the maximum number of peaks. The method to determine the starting poles was described in paragraph 3.3.1. The same

algorithm (Appendix A1) is used for the starting poles of $F_3(\omega, 180^\circ)$. The following figure shows the local minima and maxima of $F_3(\omega, 180^\circ)$.

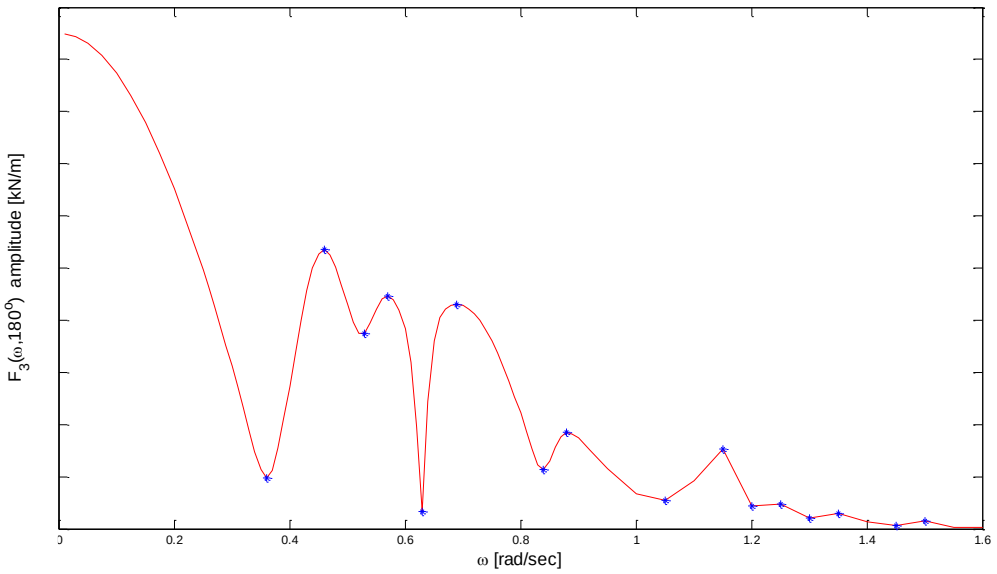

Figure 30: Peak selection, amplitude of $F_3(\omega, 180^\circ)$

To get the final set of poles, we use a similar algorithm as in section 3.3.1 (Appendix B1). If the imaginary part of the poles is zero, it is forced to take the value of 0.001.

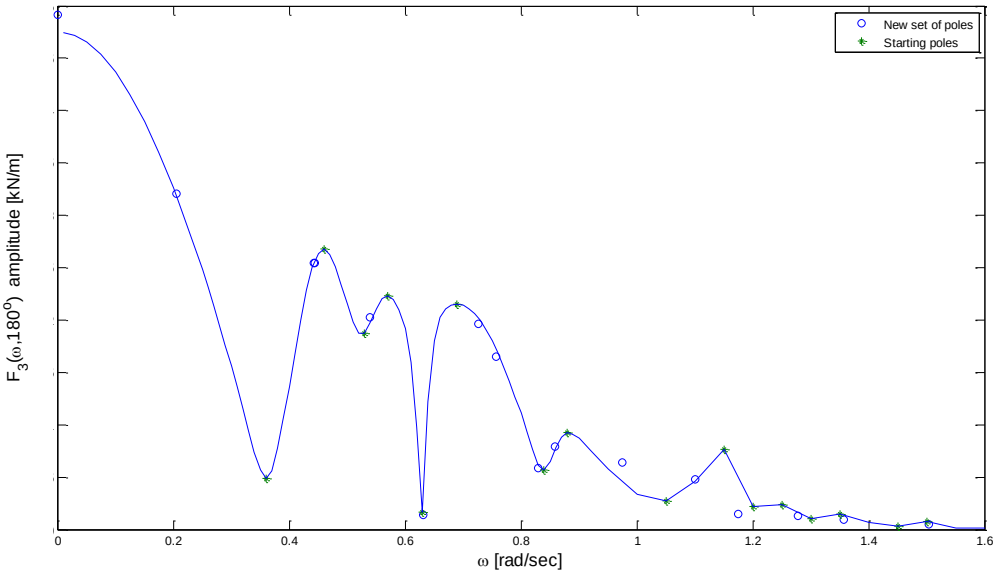

Figure 31: New set of poles, $F_3(\omega, 180^\circ)$

3.4.2 Wave forces and moments-Stage 2

For the second stage of vector fitting, the residues for all wave directions are identified. The residues of $F_3(\omega, 180^\circ)$ are calculated according to the algorithm in Appendix B2.

The figure below shows the results of the fitting process of $F_3(\omega, 180^\circ)$.

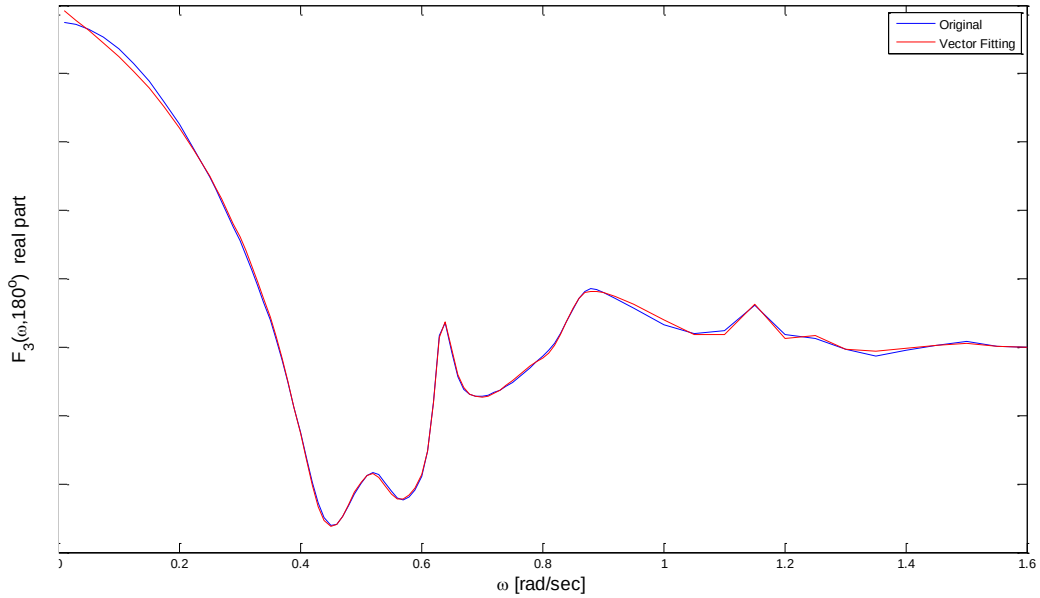

Figure 32: Vector fitting for $F_3(\omega, 180^\circ)$, real part

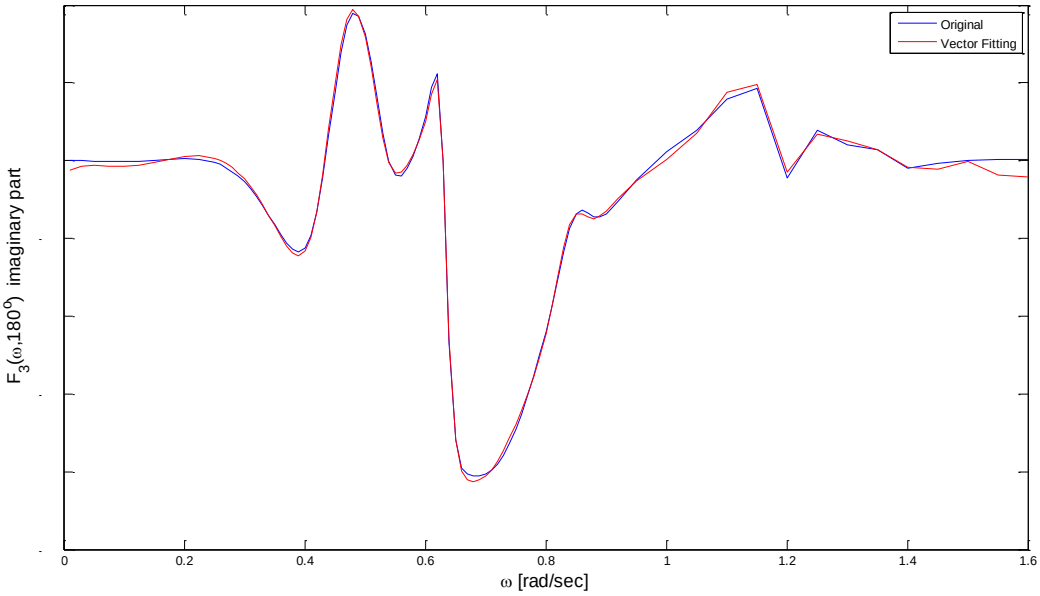

Figure 33: Vector fitting for $F_3(\omega, 180^\circ)$, imaginary part

As mentioned in the previous paragraphs, to find the fitting functions of F3 for the other wave directions, we use the poles of 180º. For example, the overdetermined problem for the identification of the residues of $F_3(\omega, 15^\circ)$ becomes:

$$\boldsymbol{A} = \begin{bmatrix} \frac{1}{s_1 - \mathrm{p}_{1,F_3\_180^\circ}} & \cdots & \frac{1}{s_1 - \mathrm{p}_{N,F_3\_180^\circ}} \\ \frac{1}{s_2 - \mathrm{p}_{1,F_3\_180^\circ}} & \cdots & \frac{1}{s_2 - \mathrm{p}_{N,F_3\_180^\circ}} \\ & \vdots & \\ \frac{1}{s_k - \mathrm{p}_{1,F_3\_180^\circ}} & \cdots & \frac{1}{s_k - \mathrm{p}_{N,F_3\_180^\circ}} \end{bmatrix}$$

$$\boldsymbol{x} = \begin{bmatrix} c_{1,F_3\_15^\circ} \\ c_{2,F_3\_15^\circ} \\ \vdots \\ c_{N,F_3\_15^\circ} \end{bmatrix}, \boldsymbol{b} = \begin{bmatrix} F_3(\omega_1, 15^\circ) \\ F_3(\omega_2, 15^\circ) \\ \vdots \\ F_3(\omega_k, 15^\circ) \end{bmatrix}$$

where $c_{n,F_3\_15^\circ}$ are the residues of the fitting function of $F_3(\omega, 15^\circ)$, $\mathrm{p}_{n,F_3\_180^\circ}$ is the set of poles of the approximation function of $F_3(\omega, 180^\circ)$, N is the total amount of poles and k is the number of wave frequencies.

Thus, matrix **A** remains the same for every wave direction. The following figures show the results of the fitting process of the wave force F_3 for all wave headings.

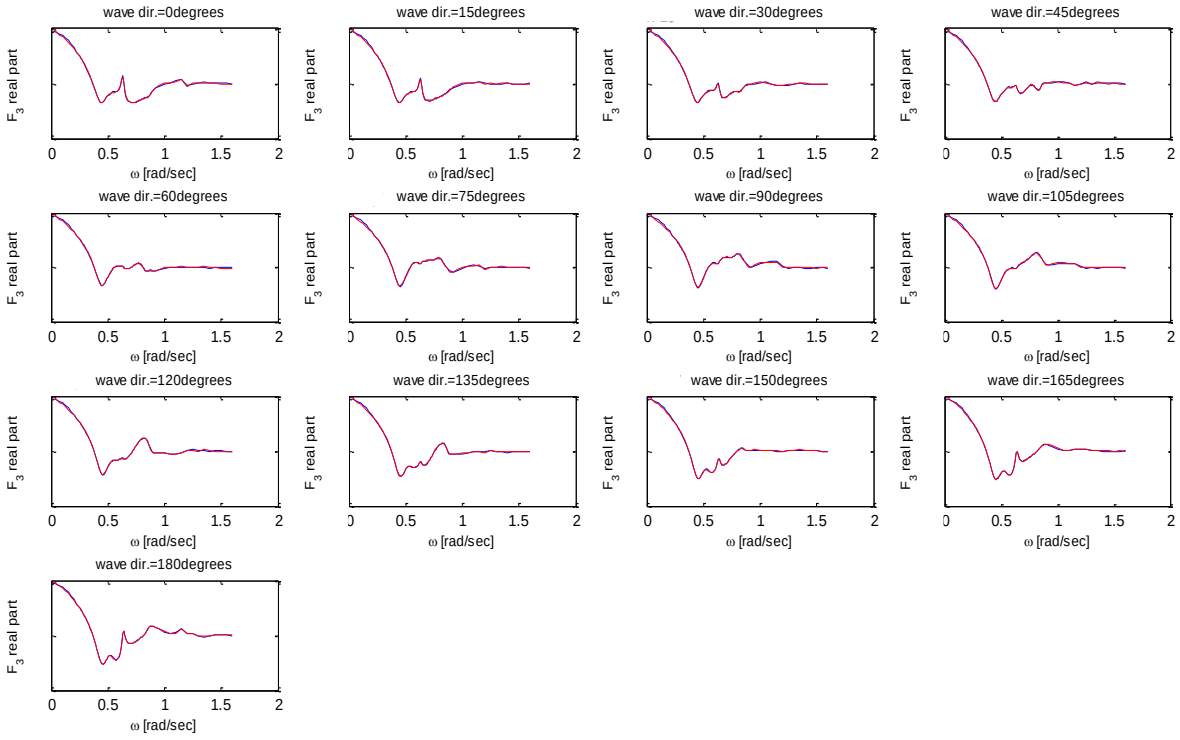

Figure 34: Real part of F_3, directions=0º-180º, fitted curve=red color, original curve=blue color

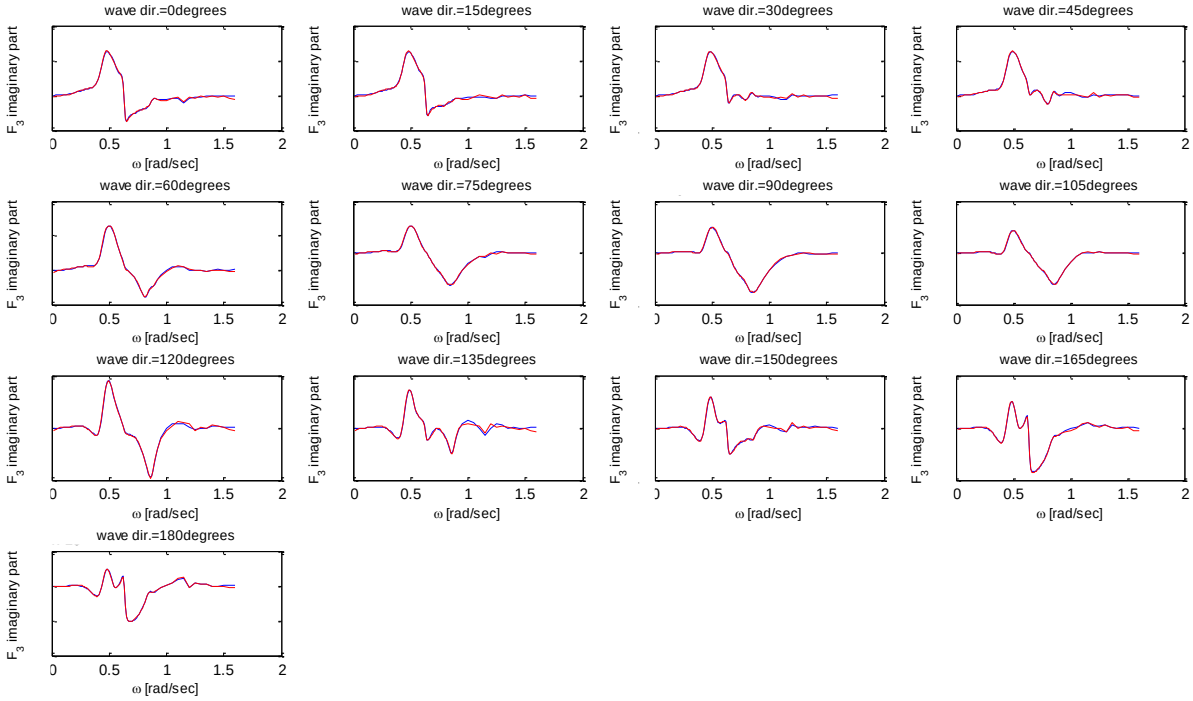

Figure 35: Imaginary part of F_3, directions=0º-180º, fitted curve=red color, original curve=blue color

The following table shows the Normalized Root Mean Square Error of the fitted wave forces and moments:

Table 3: Normalized Root Mean Square Error: Wave forces and moments

NRMSE	F1	F1	F3	M4	M5	M6
0º	0.841	-	0.961	-	0.993	-
15º	0.898	0.839	0.958	0.972	0.986	0.995
30º	0.863	0.899	0.959	0.993	0.967	0.889
45º	0.958	0.879	0.960	0.968	0.951	0.835
60º	0.905	0.905	0.962	0.967	0.927	0.898
75º	0.859	0.919	0.962	0.960	0.885	0.929
90º	0.733	0.903	0.962	0.948	0.920	0.810
105º	0.885	0.933	0.964	0.951	0.888	0.883
120º	0.869	0.922	0.963	0.965	0.869	0.846
135º	0.773	0.944	0.959	0.952	0.859	0.888
150º	0.811	0.846	0.967	0.931	0.879	0.845
165º	0.849	0.895	0.972	0.903	0.889	0.863
180º	0.839	-	0.973	-	0.888	-

According to Table 3, the vector fitting of the wave forces and moments produces higher inaccuracies than the vector fitting of the added mass and damping. However, the next figures show that the results are reasonable. This can also be justified by the response spectra which will be determined in the next chapters. The next figures display the curve fitting of $F_1(\omega, 90^\circ)$, which has the largest error (NRMSE=0.733).

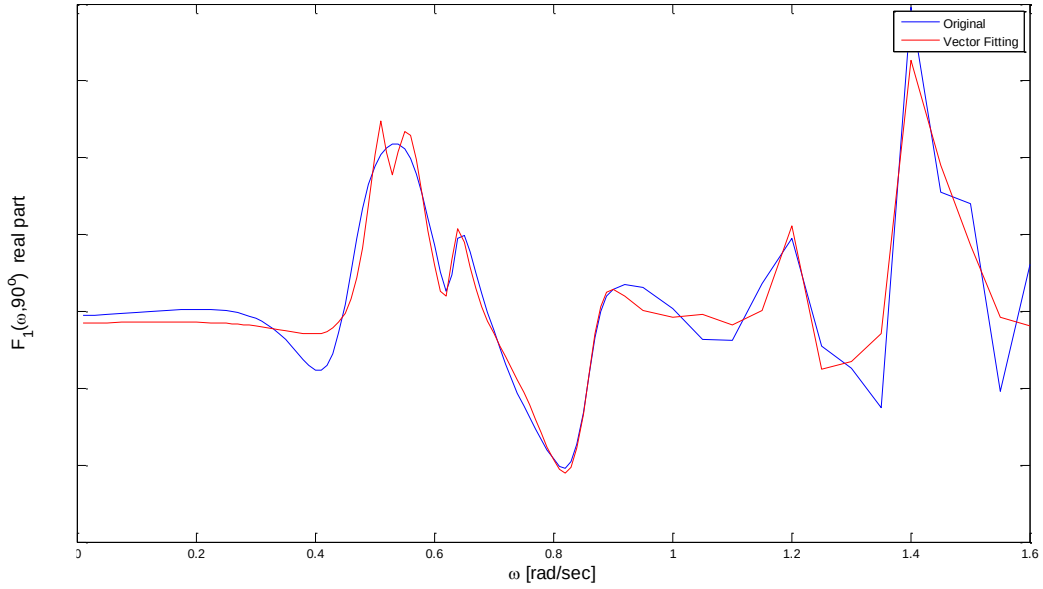

Figure 36: Vector fitting for $F_1(\omega, 90^\circ)$, real part

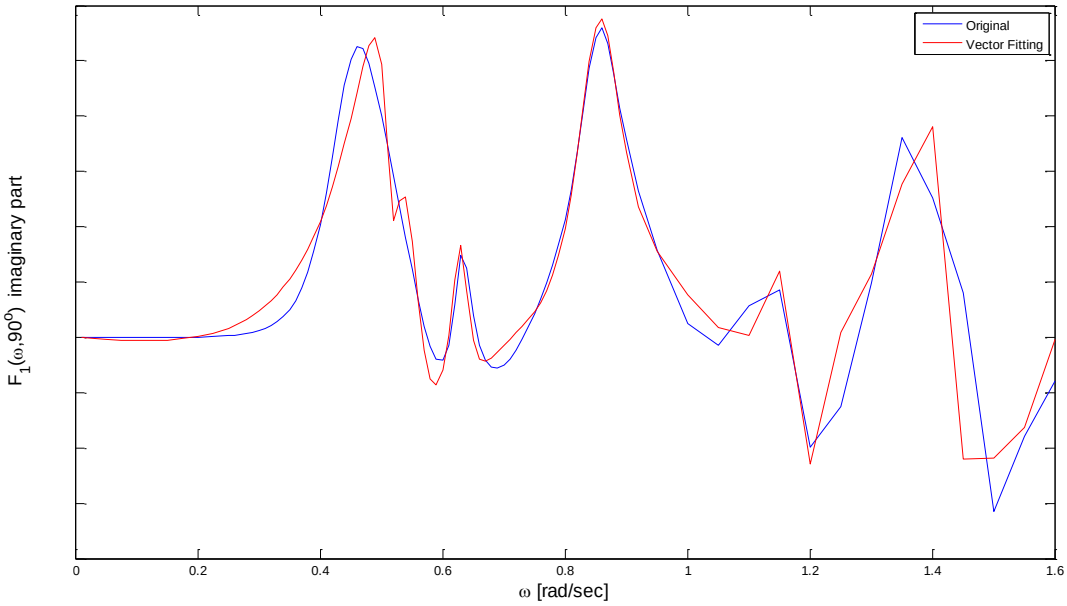

Figure 37: Vector fitting for $F_1(\omega, 90^\circ)$, imaginary part

3.4.3 Interpolation of wave forces and moments

The hydrodynamic forces are given for the range of 0° to 345° of wave heading with a step of 15°. To get more information about the RAOs, we interpolate the wave forces and moments within the ranges of 15°.

Instead of interpolating the data for each frequency over the wave directions, we interpolate only the residues of the approximation functions. With the same poles and the interpolated

residues, we can construct the functions of the interpolated hydrodynamic forces. To explain this, we give the following example.

We assume that the forces along the z axis for 0º and 15º of wave heading are approximated by the following functions:

$$f_3(s,0^\circ) = \frac{c_{1,F_3\_0^\circ}}{s-\mathrm{p}_{1,F_3\_180^\circ}} + \frac{conj(c_{1,F_3\_0^\circ})}{s-conj(\mathrm{p}_{1,F_3\_180^\circ})} + \cdots + \frac{c_{N,F_3\_0^\circ}}{s-\mathrm{p}_{N,F_3\_180^\circ}} + \frac{conj(c_{N,F_3\_0^\circ})}{s-conj(\mathrm{p}_{N,F_3\_180^\circ})} \quad \text{Eq. 3-15}$$

$$f_3(s,15^\circ) = \frac{c_{1,F_3\_15^\circ}}{s-\mathrm{p}_{1,F_3\_180^\circ}} + \frac{conj(c_{1,F_3\_15^\circ})}{s-conj(\mathrm{p}_{1,F_3\_180^\circ})} + \cdots + \frac{c_{N,F_3\_15^\circ}}{s-\mathrm{p}_{N,F_3\_180^\circ}} + \frac{conj(c_{N,F_3\_15^\circ})}{s-conj(\mathrm{p}_{N,F_3\_180^\circ})} \quad \text{Eq. 3-16}$$

Each of these functions has exactly the same poles and as a consequence the same number of residues. First, it is important to ensure that the residues and the poles are in the correct order. For instance, the first conjugate pair should correspond to the low wave frequencies for both wave headings. The residues and the poles are forced to be in the correct order according to the imaginary part of the poles. As mentioned before, the imaginary part of the poles relates to the frequency of the resonant peaks. Thus, the first pole (p_1) has the lowest imaginary part and the last pole (p_N) has the highest imaginary part. The algorithm for this process is indicated in appendix B3.

The following figures show the real and imaginary parts of residues, c_{1,F_3}, c_{3,F_3} over the wave directions.

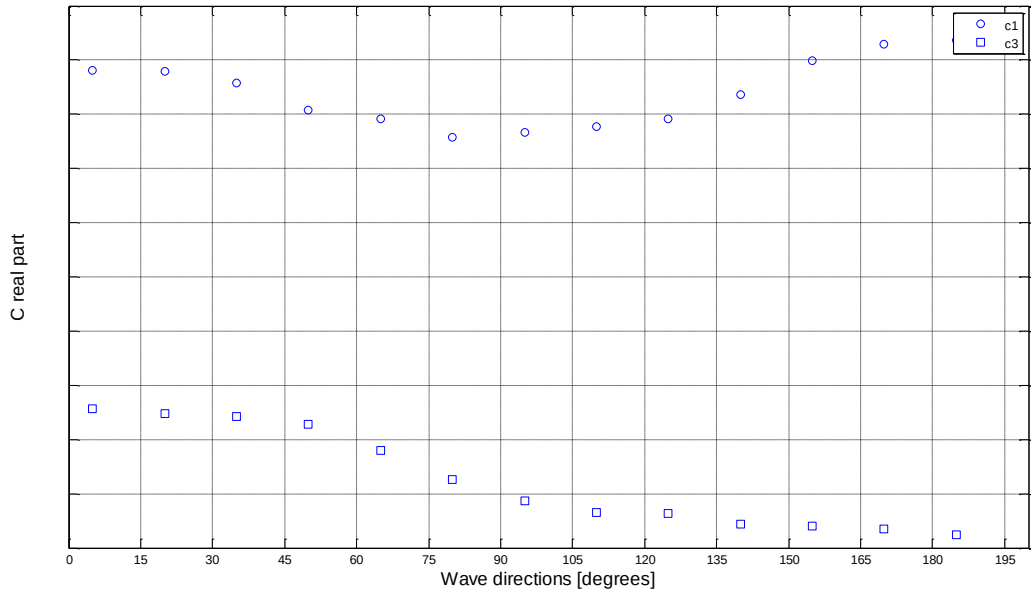

Figure 38: Real part of residues of F_3 over the wave directions

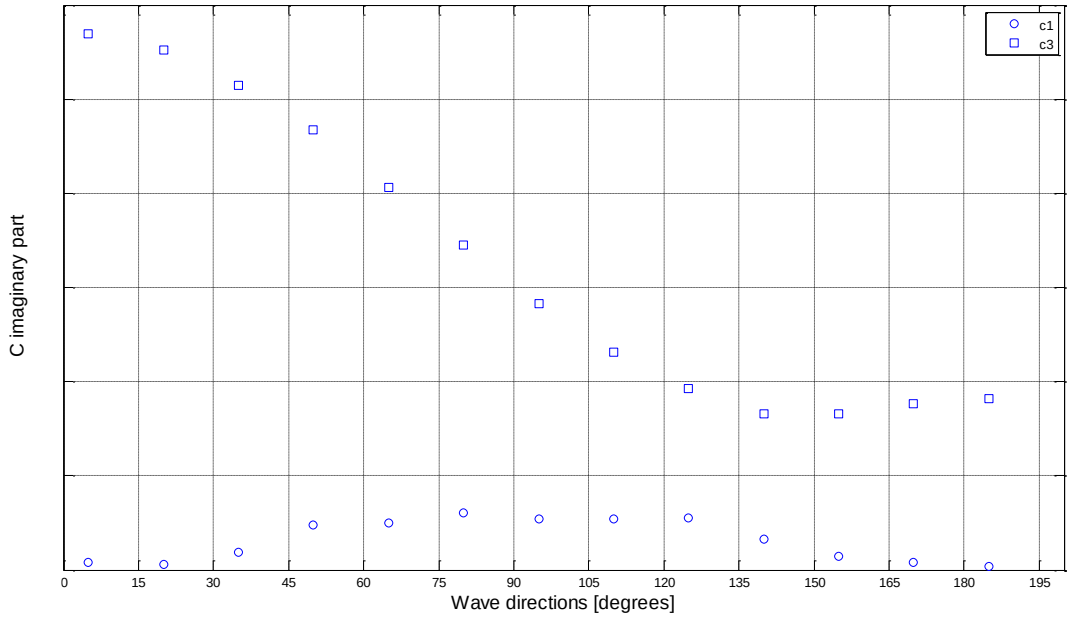

Figure 39: Imaginary part of residues of F3 over the wave directions

To find the wave forces with respect to the wave directions 5° and 10°, we introduce the residues $c_{1,F_3\_5^\circ}$, $c_{1,F_3\_10^\circ}$ among the residues $c_{1,F_3\_0^\circ}$, $c_{1,F_3\_15^\circ}$ by a simple linear interpolation of the real and imaginary parts. The same should be done for all the residues. The algorithm to interpolate the residues is shown in appendix B4. The following figure shows the real and imaginary parts of the interpolated residues over the wave directions.

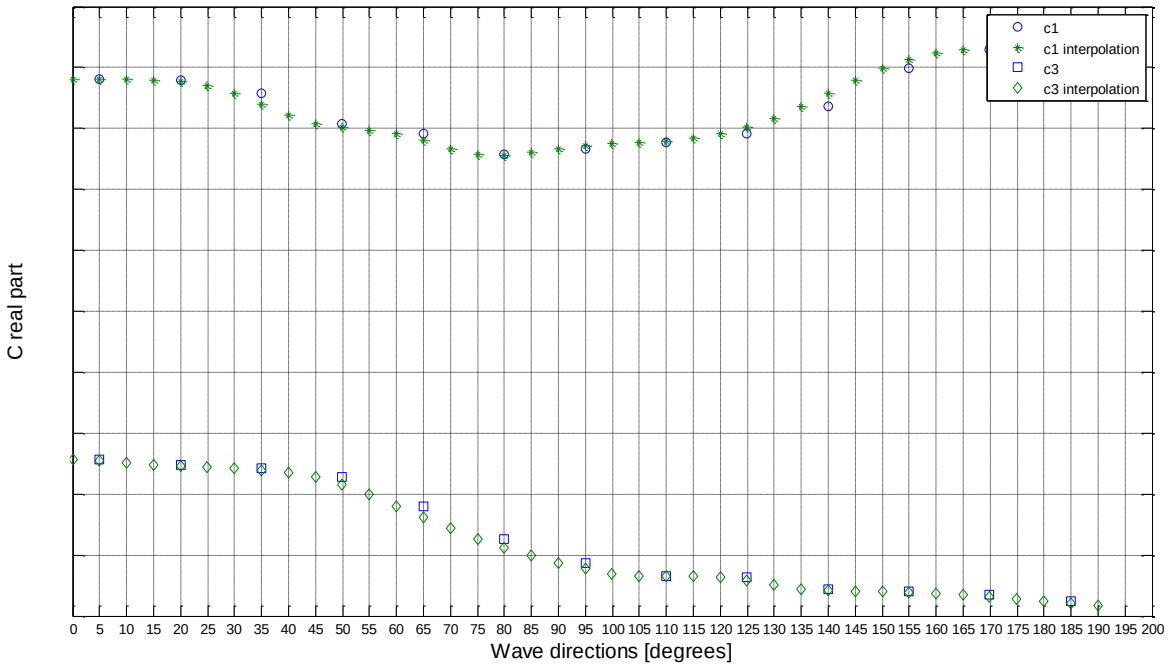

Figure 40: Interpolated real part of residues of F_3

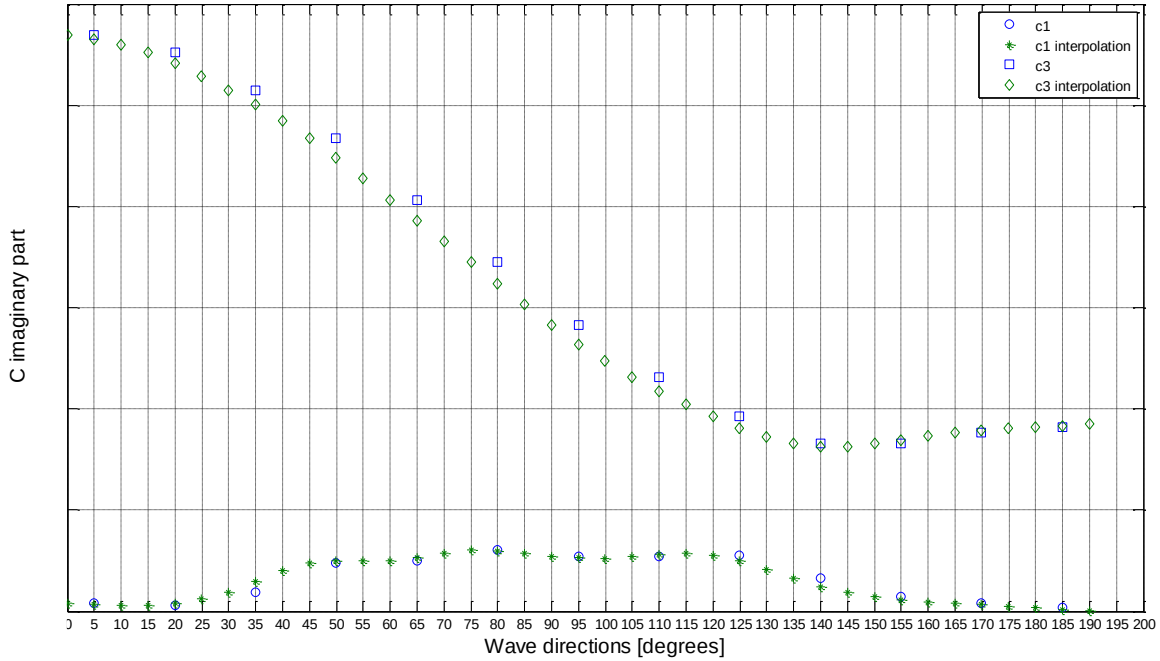

Figure 41: Interpolated imaginary part of residues of F_3

The following figure shows the curves of the amplitude of F_3 for 0º, 5º, 10º and 15º wave heading.

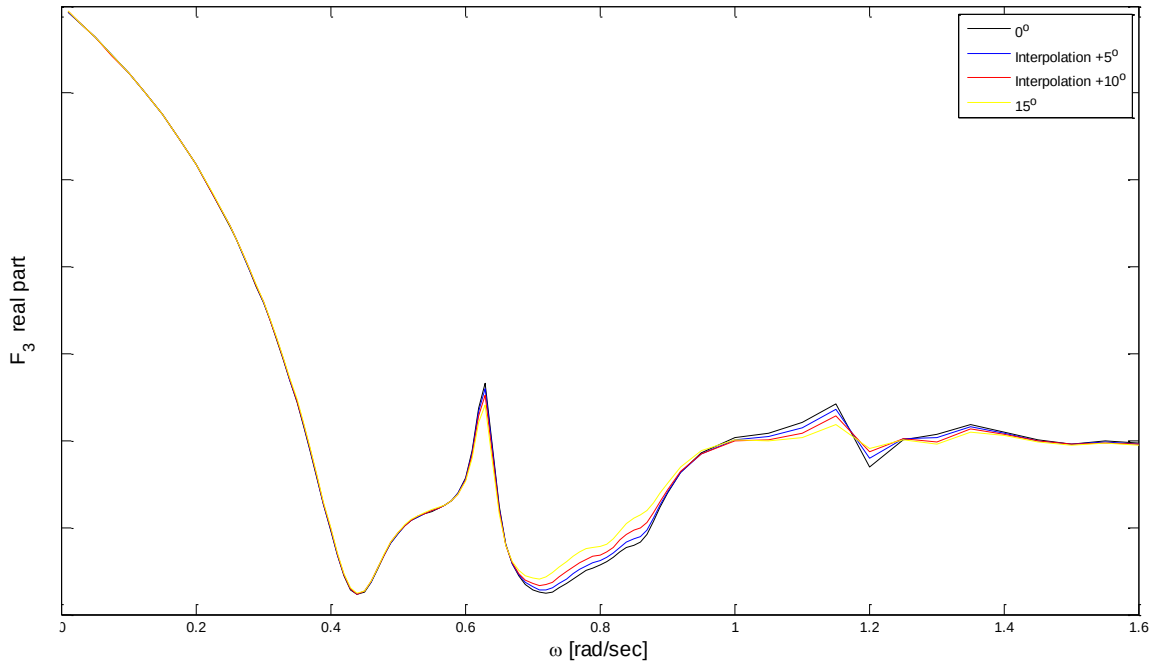

Figure 42: Interpolation of F_3, real part

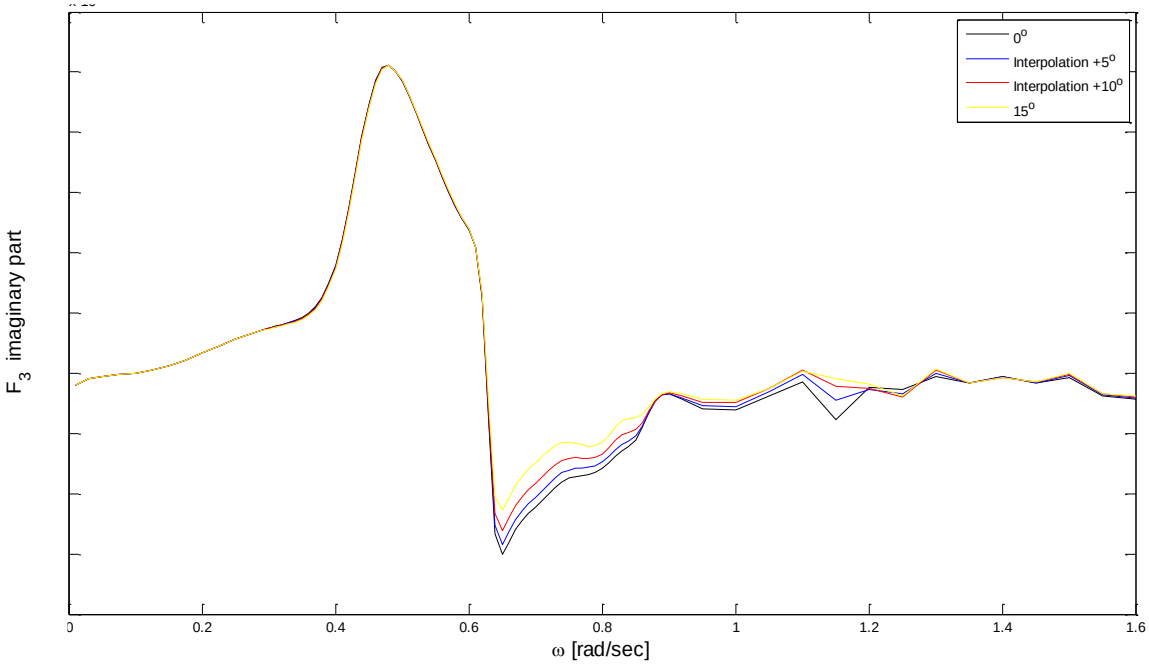

Figure 43: Interpolation of F_3, imaginary part

To verify that the resulting interpolated forces are correct, we set a step of 5° of wave heading and we recalculate the hydrodynamic forces by the diffraction software. Then the output of the diffraction software is compared with the interpolated forces.

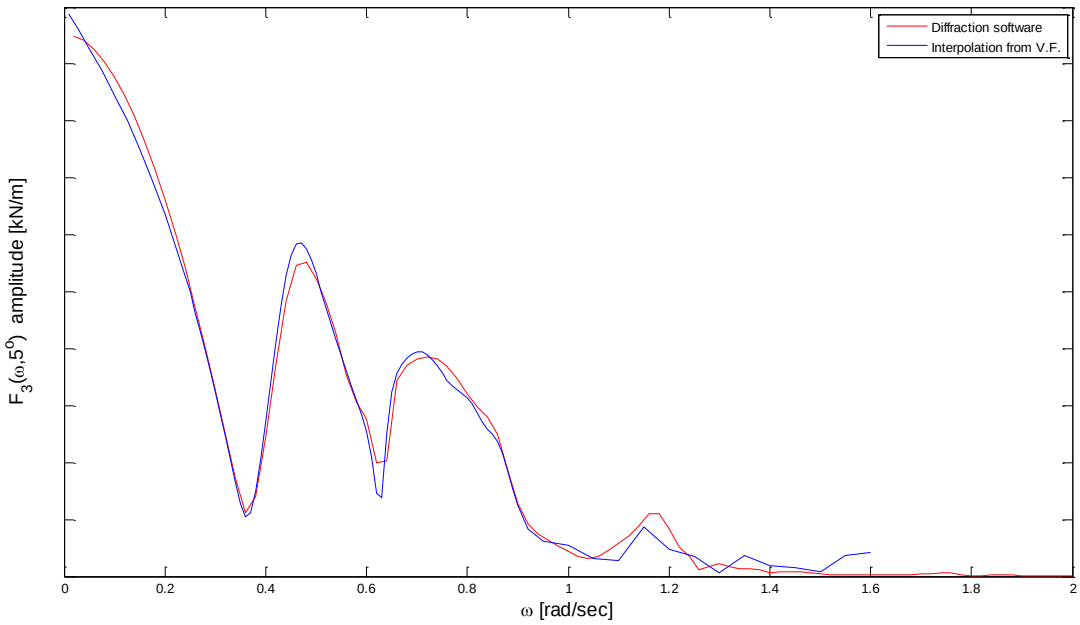

Figure 44: Amplitude of $F_3(\omega, 5^\circ)$, verification of interpolated forces

According to the above figure, the results of the interpolation of the wave forces and moments are satisfying.

3.5 REMARKS FOR THE VECTOR FITTING METHOD

To conclude this chapter, the vector fitting method proved to be suitable to express the hydrodynamic properties of the vessel using only limited number of parameters. Regarding the added mass and damping, the approximation functions are constructed by a set of poles, residues and two real quantities, d, h. However, for the approximation functions of the hydrodynamic forces and moments, we only used sets of poles and residues. The added mass and damping showed a good correspondence between the fitted curve and the original one. Regarding the wave forces and moments, the highest inaccuracies were indicated for F_1, F_2 and M_6. Moreover, the implementation of the same poles for all wave directions was a great advantage for the interpolation over the wave directions. Only by interpolating the residues, we could determine the forces and moments for the in-between wave directions. Therefore, the residues are of great importance for the fitted curves. This also means that the modification of the residues can remarkably change the curves of the hydrodynamic database. For instance, if we want to lower a peak of a curve, we can reduce the values of the corresponding residues. Also, if we want to create an extra peak, we can increase the related pair of residues. As a result, during the identification procedure, it is suggested to modify the residues and keep constant the other coefficients.

CHAPTER 4. CoG transformations

In order to calculate the RAOs, all the matrices should be expressed with respect to the global axes system and the CoG of the vessel. However, the axis system of the hydrodynamic data base is assumed to be at the sea surface in line, vertically, with the center of buoyancy of the vessel (different than CoF). This chapter shows the method to transfer the hydrodynamic properties from the hydrodynamic origin to the CoG of the vessel. The following figures indicate the CoG and the hydrodynamic origin of the SSCV Thialf (without the two cranes).

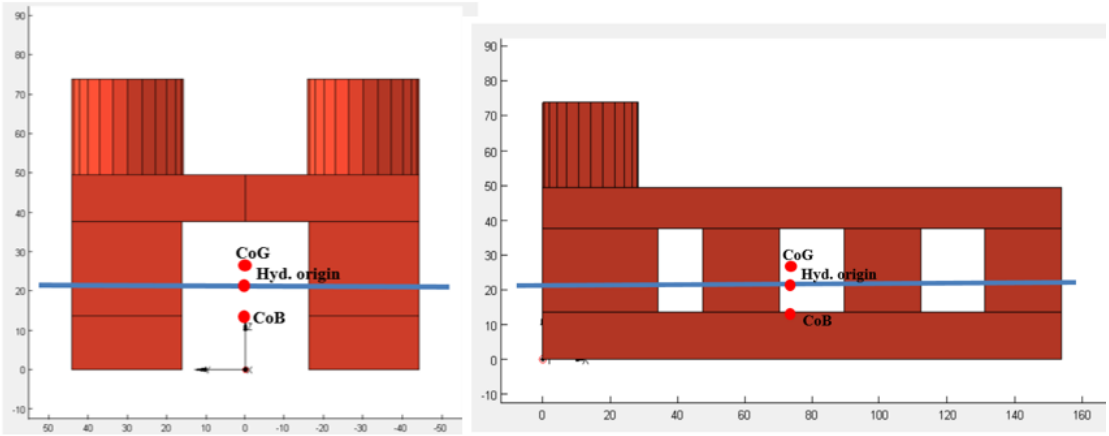

Figure 45: CoG, Hyd.Origin, CoB for SSCV Thialf

4.1 TRANSFORMATION MATRICES

In order to transfer the hydrodynamic database from the hydrodynamic origin to the CoG of the vessel, several transformations matrices should be constructed. These matrices are categorized as follows [19]:

- motion translations
- motion rotations
- force and moment translations
- force and moment rotations

The transformation matrix for the translation of motions at point 'a' to motions at point 'b' is indicated below [20]:

$$\boldsymbol{T_{M\_Shift}}(b-a) = \begin{bmatrix} 1 & 0 & 0 & 0 & b_z - a_z & -(b_y - a_y) \\ 0 & 1 & 0 & -(b_z - a_z) & 0 & b_x - a_x \\ 0 & 0 & 1 & b_y - a_y & -(b_x - a_x) & 0 \\ 0 & 0 & 0 & 1 & 0 & 0 \\ 0 & 0 & 0 & 0 & 1 & 0 \\ 0 & 0 & 0 & 0 & 0 & 1 \end{bmatrix}$$

Points 'a' and 'b' are defined by three coordinates with respect to the global axes system: a=(a_x, a_y, a_z) and b=(b_x, b_y, b_z).

Given the matrix T_{M_Shift}, the equation for the translation of motions becomes:

$$\boldsymbol{X_b} = \boldsymbol{T_{M_{Shift}}}(b-a) \cdot \boldsymbol{X_a} \qquad \text{Eq. 4-1}$$

where $\mathbf{X_b}$ and $\mathbf{X_a}$ are the matrices for motions at point 'b' and 'a' respectively.

With respect to the motion rotations, the following matrix is constructed [21]:

$$\boldsymbol{T_{Rot}}(\beta,\gamma) = \begin{bmatrix} \cos\beta\, cos\gamma & sin\,\beta\, cos\gamma & sin\gamma & 0 & 0 & 0 \\ -\sin\beta & \cos\beta & 0 & 0 & 0 & 0 \\ -\cos\beta\, sin\gamma & -\sin\beta\, sin\gamma & cos\gamma & 0 & 0 & 0 \\ 0 & 0 & 0 & \cos\beta\, cos\gamma & sin\,\beta\, cos\gamma & sin\gamma \\ 0 & 0 & 0 & -\sin\beta & \cos\beta & 0 \\ 0 & 0 & 0 & -\cos\beta\, sin\gamma & -\sin\beta\, sin\gamma & cos\gamma \end{bmatrix}$$

where β is the azimuth angle in the horizontal plane between the y-axes and γ is the elevation angle between the x- axes.

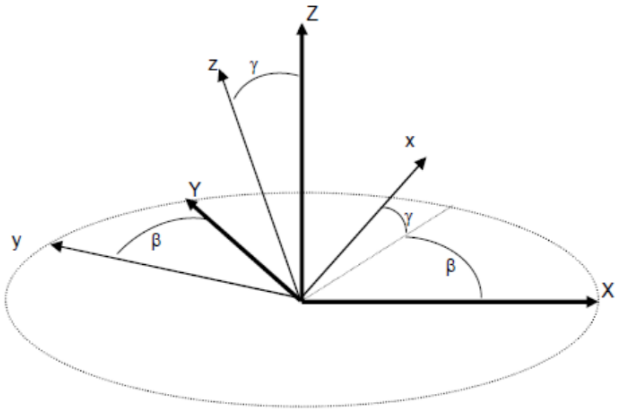

Figure 46: Azimuth angle β and elevation angle γ

The equation for the rotation of motions is as follows:

$$\boldsymbol{X_{local}} = \boldsymbol{T_{Rot}}(\beta,\gamma) \cdot \boldsymbol{X_{global}} \qquad \text{Eq. 4-2}$$

For the inverse rotation of motions, the equation becomes:

$$\boldsymbol{X_{global}} = \boldsymbol{T_{Rot}}(\beta,\gamma)^{-1} \cdot \boldsymbol{X_{local}} \qquad \text{Eq. 4-3}$$

where

$$\boldsymbol{T_{Rot}}(\beta,\gamma)^{-1} = \begin{bmatrix} \cos\beta\, cos\gamma & -sin\,\beta & -\cos\beta\, sin\gamma & 0 & 0 & 0 \\ \sin\beta\, cos\gamma & \cos\beta & -\sin\beta\, sin\gamma & 0 & 0 & 0 \\ sin\gamma & 0 & cos\gamma & 0 & 0 & 0 \\ 0 & 0 & 0 & \cos\beta\, cos\gamma & -sin\,\beta & -\cos\beta\, sin\gamma \\ 0 & 0 & 0 & \sin\beta\, cos\gamma & \cos\beta & -\sin\beta\, sin\gamma \\ 0 & 0 & 0 & sin\gamma & 0 & cos\gamma \end{bmatrix}$$

With respect to the translation of forces, the following matrix is created [22]:

$$\boldsymbol{T_{F\_Shift}}(b-a) = \begin{bmatrix} 1 & 0 & 0 & 0 & 0 & 0 \\ 0 & 1 & 0 & 0 & 0 & 0 \\ 0 & 0 & 1 & 0 & 0 & 0 \\ 0 & b_z - a_z & -(b_y - a_y) & 1 & 0 & 0 \\ -(b_z - a_z) & 0 & b_x - a_x & 0 & 1 & 0 \\ b_y - a_y & -(b_x - a_x) & 0 & 0 & 0 & 1 \end{bmatrix}$$

The equation for the translation of forces then becomes:

$$\boldsymbol{F_b} = \boldsymbol{T_{F\_Shift}}(b-a) \cdot \boldsymbol{F_a} \qquad \text{Eq. 4-4}$$

Regarding the rotation of forces, the same rotation matrices can be used as for the motion. The equations for the rotation of forces are shown below:

$$\boldsymbol{F_{local}} = \boldsymbol{T_{Rot}}(\beta, \gamma) \cdot \boldsymbol{F_{global}} \quad \text{Eq. 4-5}$$

$$\boldsymbol{F_{global}} = \boldsymbol{T_{Rot}}(\beta, \gamma)^{-1} \cdot \boldsymbol{F_{local}} \quad \text{Eq. 4-6}$$

4.2 TRANSFORMATION OF THE HYDRODYNAMIC DATA BASE

The axis system of the hydrodynamic data base is assumed to be equal to the local axes system of the submerged body [23]. However, if the z-axis of the hydrodynamic data base points downwards, it should be rotated and be equal to the local z-axis. Thus, the azimuth angle β is zero and the elevation angle γ is either 0º or 180º. The next step is to shift the local axes system of the submerged body to the CoG of the vessel.

The relation between the accelerations of the hydrodynamic origin and the added inertia forces at the hydrodynamic origin is expressed by the following equation [23]:

$$\boldsymbol{A_{hyd}} \cdot \ddot{\boldsymbol{X}}_{\boldsymbol{hyd}} = \boldsymbol{F_{a,hyd}} \quad \text{Eq. 4-7}$$

where $\mathbf{A_{hyd}}$ is the added mass matrix given by the diffraction software, $\ddot{\boldsymbol{X}}_{\boldsymbol{hyd}}$ is the matrix of the accelerations of the hydrodynamic origin and $\boldsymbol{F_{a,hyd}}$ is the matrix of the added inertia forces at the hydrodynamic origin.

The accelerations of the hydrodynamic origin in local body axes are indicated by the equation below:

$$\ddot{\boldsymbol{X}}_{\boldsymbol{hyd}} = \boldsymbol{T_{rot}}(0, \gamma)^{-1} \cdot \ddot{\boldsymbol{X}}_{\boldsymbol{local}} \quad \text{Eq. 4-8}$$

Thus, equation 4-7 becomes*:*

$$\boldsymbol{A_{hyd}} \cdot \boldsymbol{T_{rot}}(0, \gamma)^{-1} \cdot \ddot{\boldsymbol{X}}_{\boldsymbol{local}} = \boldsymbol{F_{a,hyd}} \quad \text{Eq. 4-9}$$

If we multiply both sides with $\boldsymbol{T_{rot}}(0, \gamma)$, we have:

$$\boldsymbol{T_{rot}}(0, \gamma) \cdot \boldsymbol{A_{hyd}} \cdot \boldsymbol{T_{rot}}(0, \gamma)^{-1} \cdot \ddot{\boldsymbol{X}}_{\boldsymbol{local}} = \boldsymbol{T_{rot}}(0, \gamma) \cdot \boldsymbol{F_{a,hyd}} \quad \text{Eq. 4-10}$$

Therefore, the added mass matrix and the added inertia forces are expressed in the local axes system of the submerged hull by the following equations:

$$\boldsymbol{A_{local}} = \boldsymbol{T_{rot}}(0, \gamma) \cdot \boldsymbol{A_{hyd}} \cdot \boldsymbol{T_{rot}}(0, \gamma)^{-1} \quad \text{Eq. 4-11}$$

$$\boldsymbol{F_{a,local}} = \boldsymbol{T_{rot}}(0, \gamma) \cdot \boldsymbol{F_{a,hyd}} \quad \text{Eq. 4-12}$$

To determine the accelerations of the CoG of the vessel, we use the following relation:

$$\boldsymbol{A_{local}} \cdot \ddot{\boldsymbol{X}}_{\boldsymbol{local}} = \boldsymbol{F_{a,local}} \quad \text{Eq. 4-13}$$

The accelerations of the CoG of the ship are indicated by the equation below:

$$\ddot{\boldsymbol{X}}_{\boldsymbol{local}} = \boldsymbol{T_{M\_Shift}}(Hyd.Origin - CoG) \cdot \ddot{\boldsymbol{X}}_{\boldsymbol{CoG}} \quad \text{Eq. 4-14}$$

where 'CoG' and 'Hyd.Origin' contain the three coordinates of the CoG and the hydrodynamic origin respectively. These coordinates are expressed according to the global coordinate system.

Thus, equation 4-13 becomes*:*

$$\boldsymbol{A_{local}} \cdot \boldsymbol{T_{M\_Shift}}(Hyd.Origin - CoG) \cdot \ddot{\boldsymbol{X}}_{\boldsymbol{CoG}} = \boldsymbol{F_{a,local}} \quad \text{Eq. 4-15}$$

If we multiply both sides of the equation with $\boldsymbol{T_{F\_Shift}}(CoG - Hyd.Origin)$, we have:

$$\boldsymbol{T_{F\_Shift}}(CoG - Hyd.Origin) \cdot \boldsymbol{A_{local}} \cdot \boldsymbol{T_{M\_Shift}}(Hyd.Origin - CoG) \cdot \ddot{\boldsymbol{X}}_{\boldsymbol{CoG}} = \boldsymbol{T_{F\_Shift}}(CoG - Hyd.Origin) \cdot \boldsymbol{F_{a,local}}$$

Therefore, the added mass matrix and the added inertia forces which correspond to the CoG of the vessel are indicated below:

$$\boldsymbol{A_{CoG}} = \boldsymbol{T_{F\_Shift}}(CoG - Hyd.Origin) \cdot \boldsymbol{A_{local}} \cdot \boldsymbol{T_{M\_Shift}}(Hyd.Origin - CoG) \quad \text{Eq. 4-16}$$

$$\boldsymbol{F_{a,CoG}} = \boldsymbol{T_{F\_Shift}}(CoG - Hyd.Origin) \cdot \boldsymbol{F_{a,local}} \quad \text{Eq. 4-17}$$

where

$$\boldsymbol{A_{local}} = \boldsymbol{T_{rot}}(0,\gamma) \cdot \boldsymbol{A_{hyd}} \cdot \boldsymbol{T_{rot}}(0,\gamma)^{-1} \quad \text{Eq. 4-18}$$

$$\boldsymbol{F_{a,local}} = \boldsymbol{T_{rot}}(0,\gamma) \cdot \boldsymbol{F_{a,hyd}} \quad \text{Eq. 4-19}$$

Similar equations are applied for the transformation of the damping matrix. Given the relations between the velocities of the hydrodynamic origin and the forces required to achieve these velocities, the final equations are shown below [24]:

$$\boldsymbol{B_{CoG}} = \boldsymbol{T_{F\_Shift}}(CoG - Hyd.Origin) \cdot \boldsymbol{B_{local}} \cdot \boldsymbol{T_{M\_Shift}}(Hyd.Origin - CoG) \quad \text{Eq. 4-20}$$

$$\boldsymbol{F_{v,CoG}} = \boldsymbol{T_{F\_Shift}}(CoG - Hyd.Origin) \cdot \boldsymbol{F_{v,local}} \quad \text{Eq. 4-21}$$

where

$$\boldsymbol{B_{local}} = \boldsymbol{T_{rot}}(0,\gamma) \cdot \boldsymbol{B_{hyd}} \cdot \boldsymbol{T_{rot}}(0,\gamma)^{-1} \quad \text{Eq. 4-22}$$

$$\boldsymbol{F_{v,local}} = \boldsymbol{T_{rot}}(0,\gamma) \cdot \boldsymbol{F_{v,hyd}} \quad \text{Eq. 4-23}$$

The hydrodynamic forces need to be translated and rotated to global forces at the CoG of the vessel as well. According to the before mentioned analysis, we apply the equations below [25]:

$$\boldsymbol{F_{local}} = \boldsymbol{T_{rot}}(0,\gamma) \cdot \boldsymbol{F_{hyd}} \quad \text{Eq. 4-24}$$

$$\boldsymbol{F_{CoG}} = \boldsymbol{T_{M\_Shift}}(CoG - Hyd.Origin) \cdot \boldsymbol{F_{local}} \quad \text{Eq. 4-25}$$

When the mass distribution of the vessel is modified, the hydrodynamic database, given by the diffraction software, should only be shifted to the new CoG. According to the previous paragraph, the transformation matrices, $\boldsymbol{T_{M\_Shift}}$ and $\boldsymbol{T_{F\_Shift}}$, are determined by the three coordinates of the CoG. Based on those transformation matrices, the hydrodynamic data base is shifted automatically to the CoG according to the algorithm in Appendix C1.

Changing the CoG of the vessel influences the hydrostatic spring matrix as well. According to CHAPTER 2, the values of GM_T and GM_L should be modified by changing the distance KG. This parameter is the vertical distance of the keel point of the hull to the CoG of the vessel. Therefore, only the z coordinate of the CoG influences he hydrostatic spring matrix. The transformation of the spring matrix is accomplished by the algorithm presented in Appendix C2.

CHAPTER 5. Motion Response Spectra

This chapter shows the final response spectra which are obtained with the fitted vessel properties of the Thialf at 22m draft in deep water. Apart from the response spectra, this chapter also provides the final fitted RAOs.

5.1 MOTION RAOS

The RAOs, given by the original vessel matrices, are compared with the RAOs given by the approximation functions of the vector fitting method. The results are indicated in the following figures:

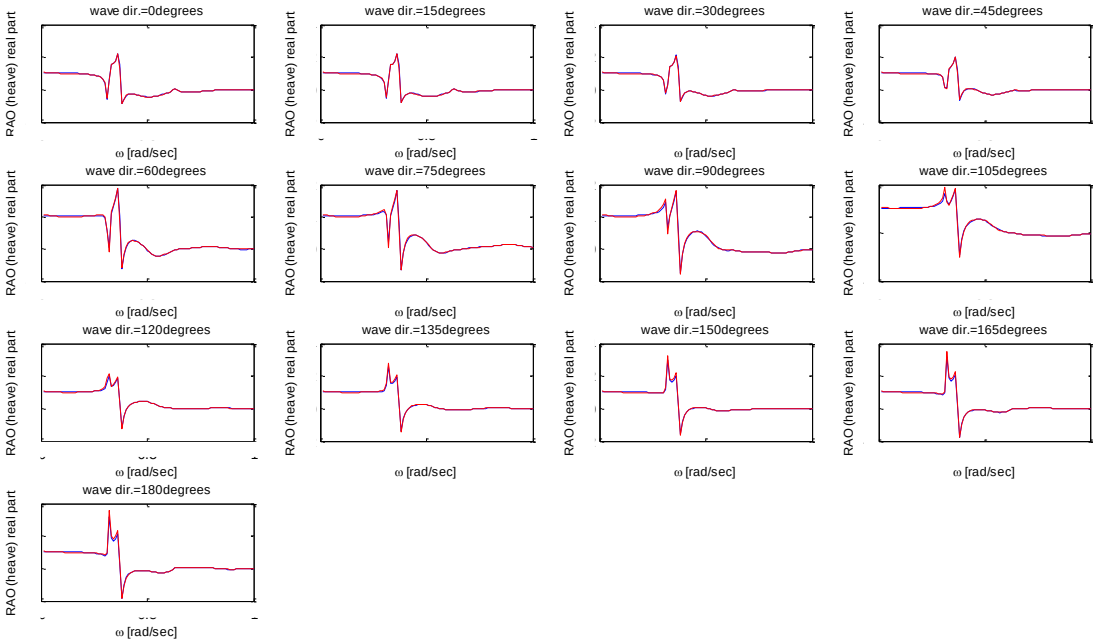

Figure 47: Heave RAO, real part, fitted curve=red color, original curve=blue color

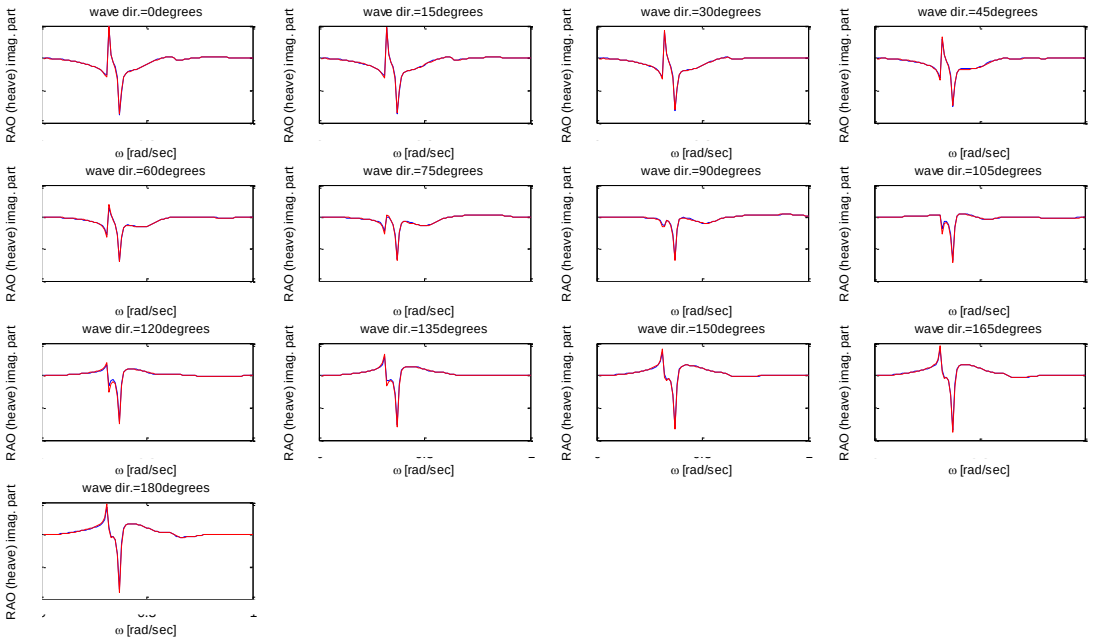

Figure 48: Heave RAO, imaginary part, fitted curve=red color, original curve=blue color

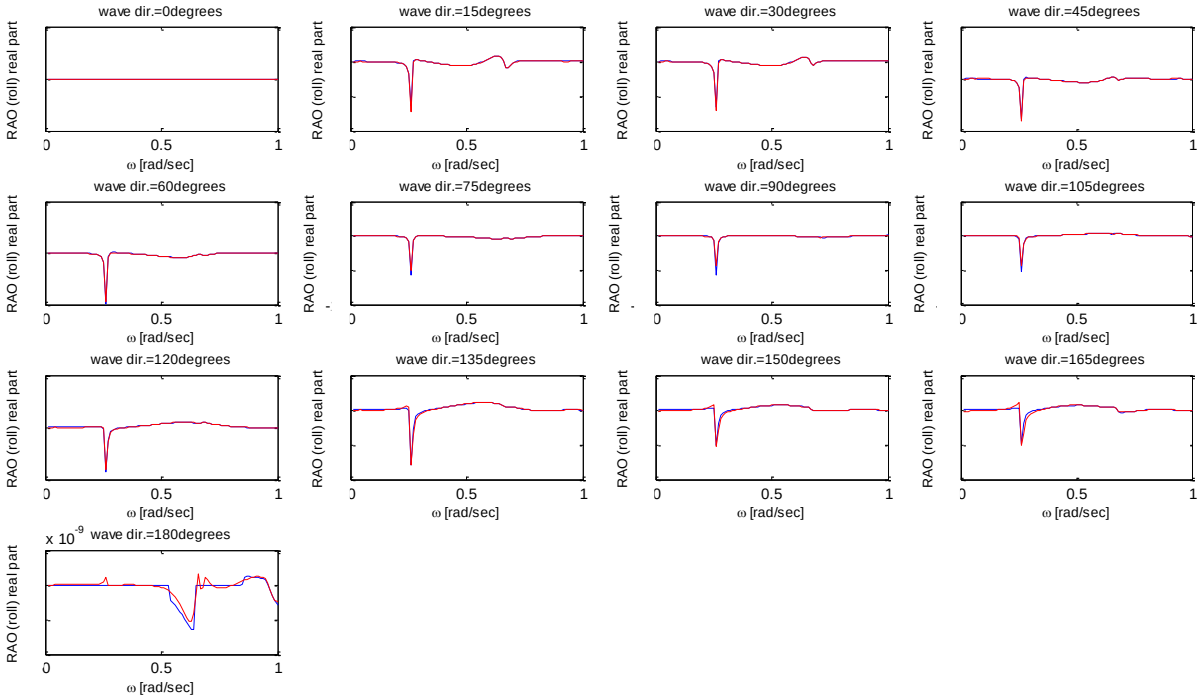

Figure 49: Roll RAO, real part, fitted curve=red color, original curve=blue color

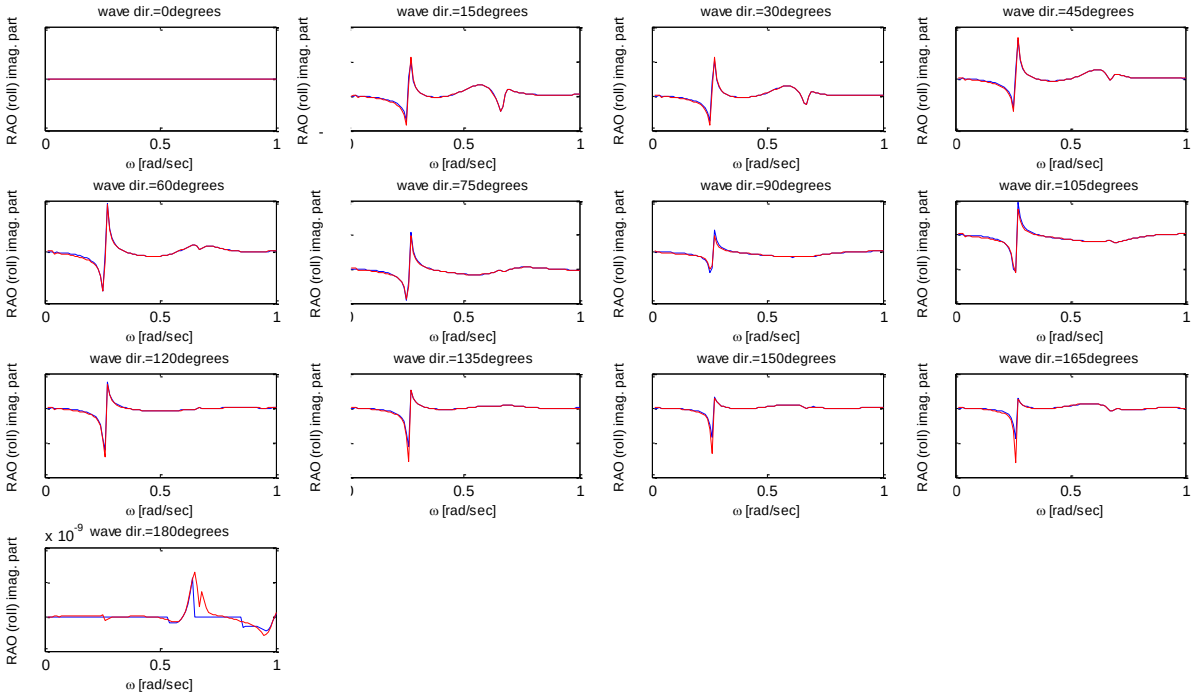

Figure 50: Roll RAO, imaginary part, fitted curve=red color, original curve=blue color

It should be mentioned that the motion RAOs for surge, sway and yaw indicate poor fitting results at low frequencies. This is shown in the following figures.

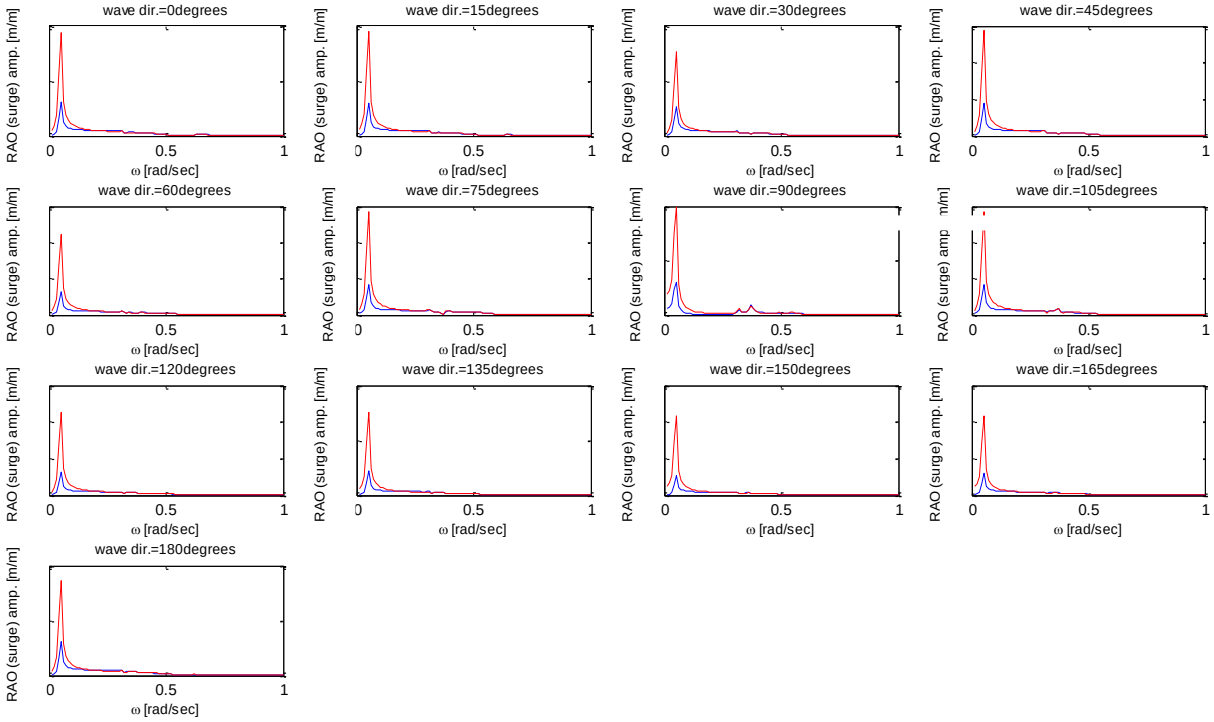

Figure 51: Surge RAO, amplitude, fitted curve=red color, original curve=blue color

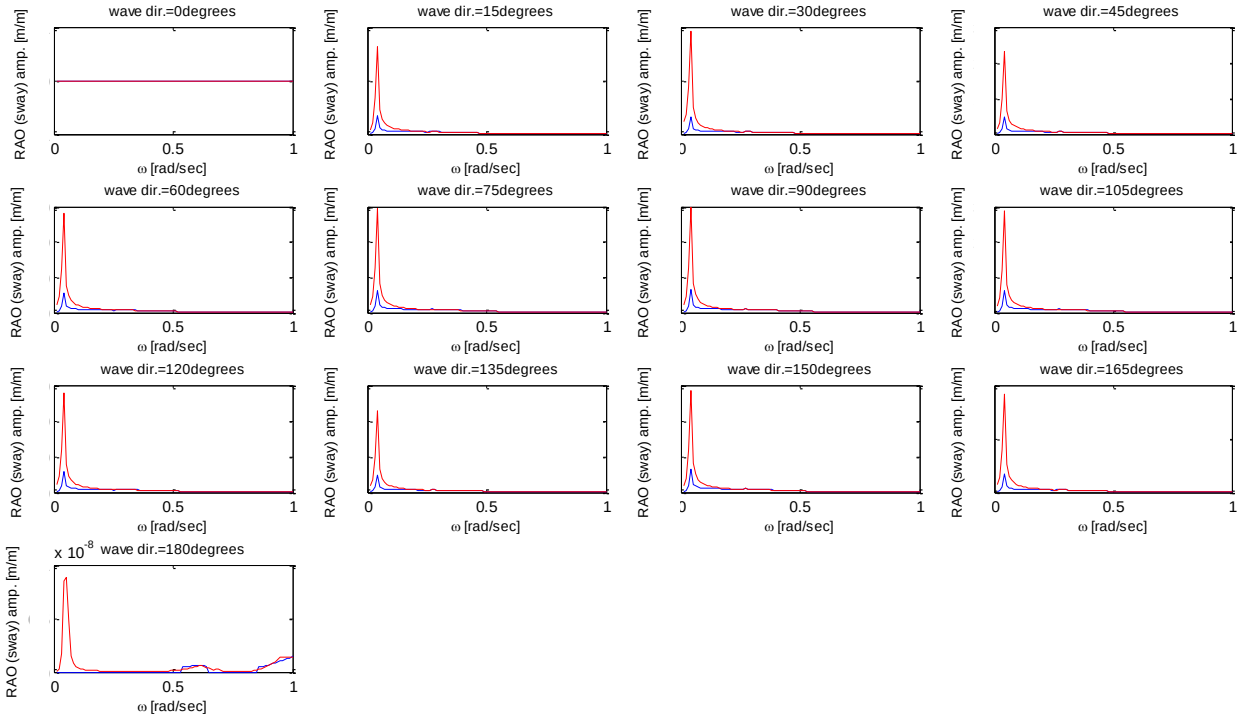

Figure 52: Sway RAO, amplitude, fitted curve=red color, original curve=blue color

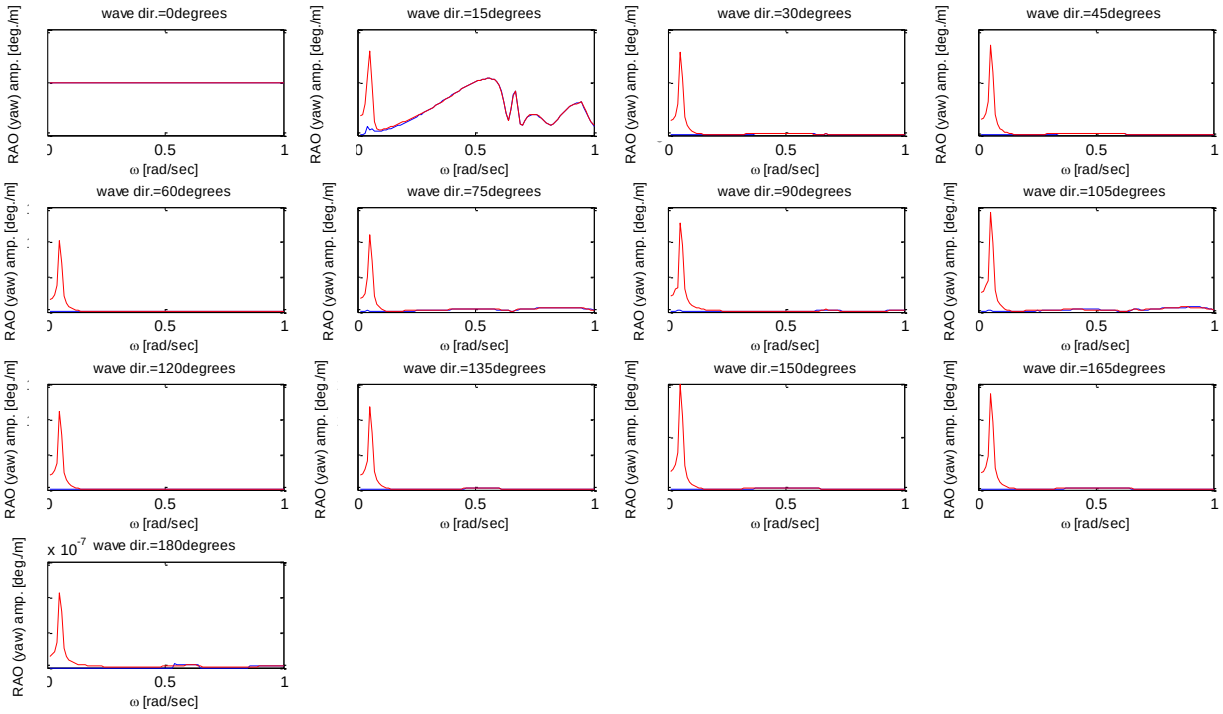

Figure 53: Yaw RAO, amplitude, fitted curve=red color, original curve=blue color

The fitted RAOs for surge, sway and yaw show high peaks at low wave frequencies. However, these peaks have a low impact on the final response spectra. The wave frequencies of swell and wind sea are higher than 0.2rad/sec (section 2.6). As a result, the peaks of the fitted RAOs which correspond to wave frequencies less than 0.2rad/sec will not influence the final response spectra. Also, as mentioned in section 2.3, the additional spring matrix is such that the resonances for those motions are outside the wave spectrum.

The normalized root mean square errors for the motion RAOs are shown in the following table. The NRMSEs are calculated for the frequencies of 0.2-1.6 rad/sec.

Table 4: NRMSE of the vector fitting of motion RAOs

Wave dir.\Motion	SURGE	SWAY	HEAVE	ROLL	PITCH	YAW
0º	0.922	-	0.951	-	0.9424	-
15º	0.927	0.893	0.953	0.870	0.940	0.983
30º	0.928	0.892	0.956	0.881	0.931	0.873
45º	0.962	0.891	0.948	0.910	0.910	0.822
60º	0.944	0.915	0.938	0.933	0.870	0.803
75º	0.917	0.925	0.929	0.891	0.823	0.884
90º	0.707	0.924	0.932	0.780	0.821	0.574
105º	0.886	0.930	0.908	0.848	0.760	0.860
120º	0.915	0.925	0.902	0.899	0.759	0.803
135º	0.894	0.917	0.918	0.789	0.825	0.853

150º	0.888	0.906	0.930	0.668	0.875	0.851
165º	0.881	0.882	0.924	0.519	0.876	0.850
180º	0.8761	-	0.918	-	0.871	-

As shown in the above table, the roll-RAO of 165º wave heading and the yaw-RAO of 90º wave heading indicate the lowest NRMSEs. The curves of the amplitude of those RAOs are shown below:

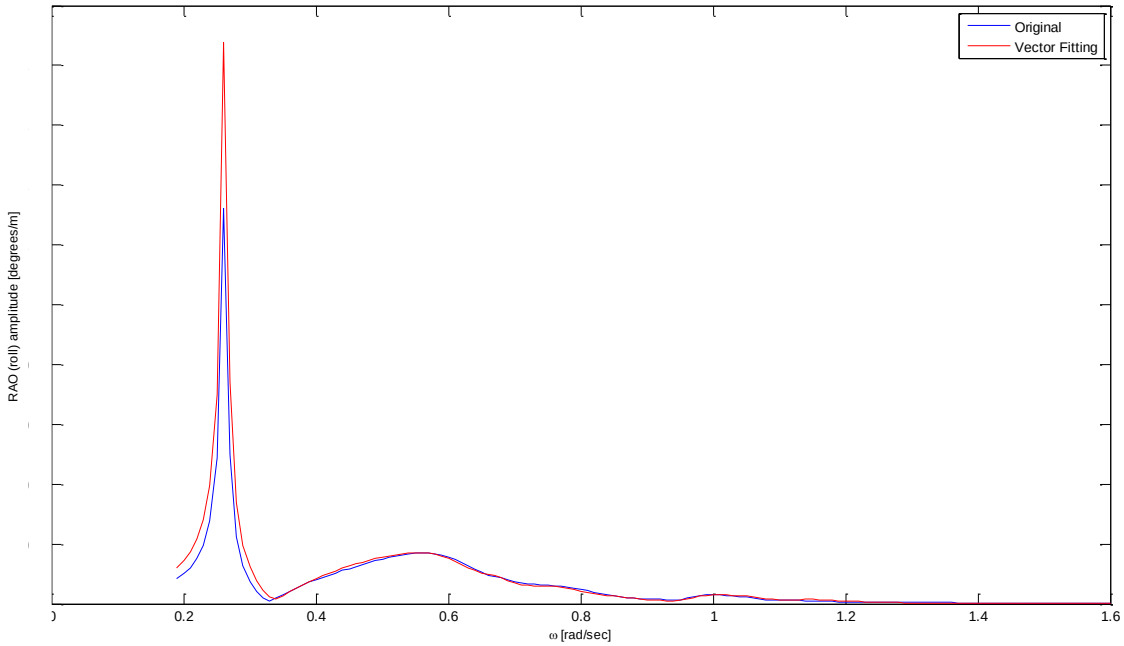

Figure 54: Roll-RAO, amplitude, 165º wave heading

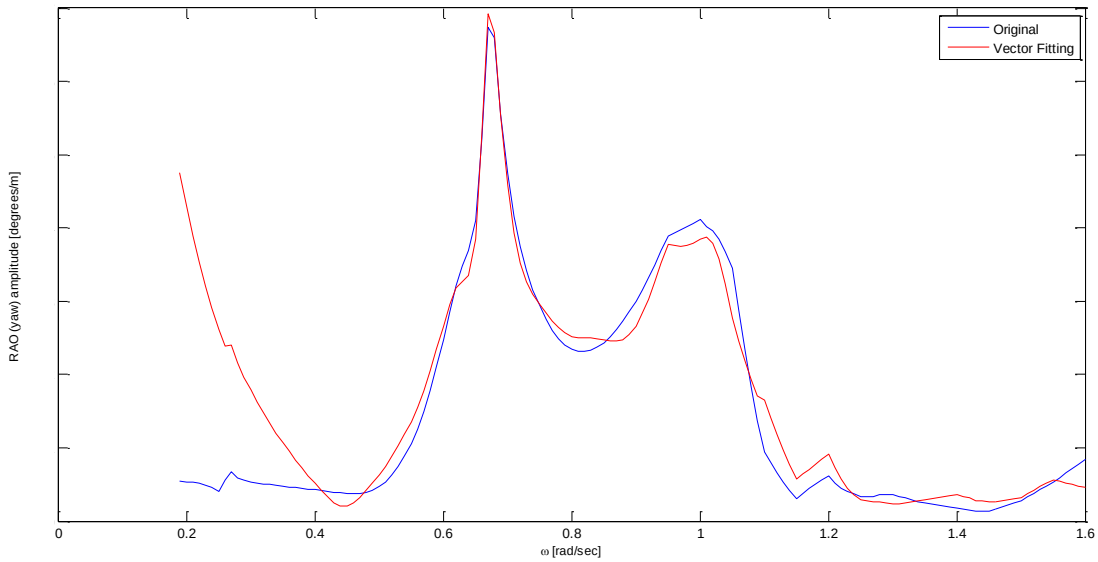

Figure 55: Yaw-RAO, amplitude, 90º wave heading

Regarding the roll-RAO, the fitted curve overestimates the peak at the frequency of 0.26 rad/sec. With respect to the yaw-RAO, the amplitude of the fitted RAO at the frequency of 0.2

rad/sec is higher than the original value. If the peak of the wave spectrum is at the above mentioned wave frequencies, the inaccuracies of the fitting process will affect the final response spectra. Therefore, the fitting process is not accurate enough to approximate the wave frequencies at around 0.2 rad/sec.

5.2 MOTION RESPONSE SPECTRA

In order to calculate the motion response spectra, we use the fitted RAOs and a Jonswap wave spectrum. The Jonswap wave spectrum has the following characteristics: Hs=5m, Tp=8.5sec, main wave direction=30°. The 1D and 2D wave spectra are shown in the following figures.

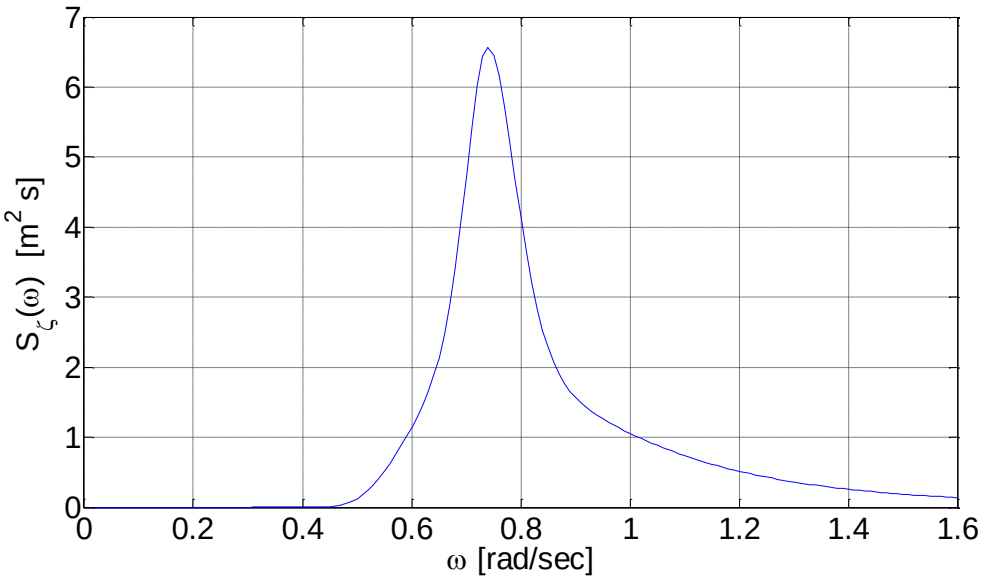

Figure 56: 1D Jonswap Spectrum, T_p=8.5s, H_s=5m

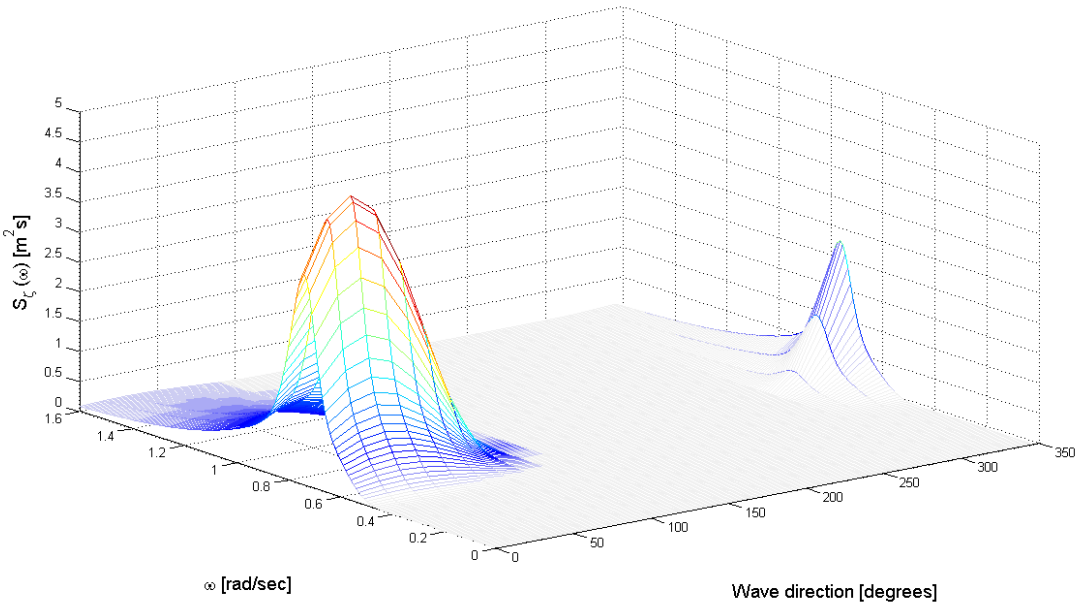

Figure 57: 2D Jonswap Spectrum, main wave direction=30°

The equation to determine the final response spectra is shown below:

$$S_i(\omega) = \int_{-\pi}^{\pi} S_\zeta(\omega, dir) * RAO_i(\omega, dir)^2 \, d(dir)$$

The plots of the fitted and original response spectra are indicated in the following figure:

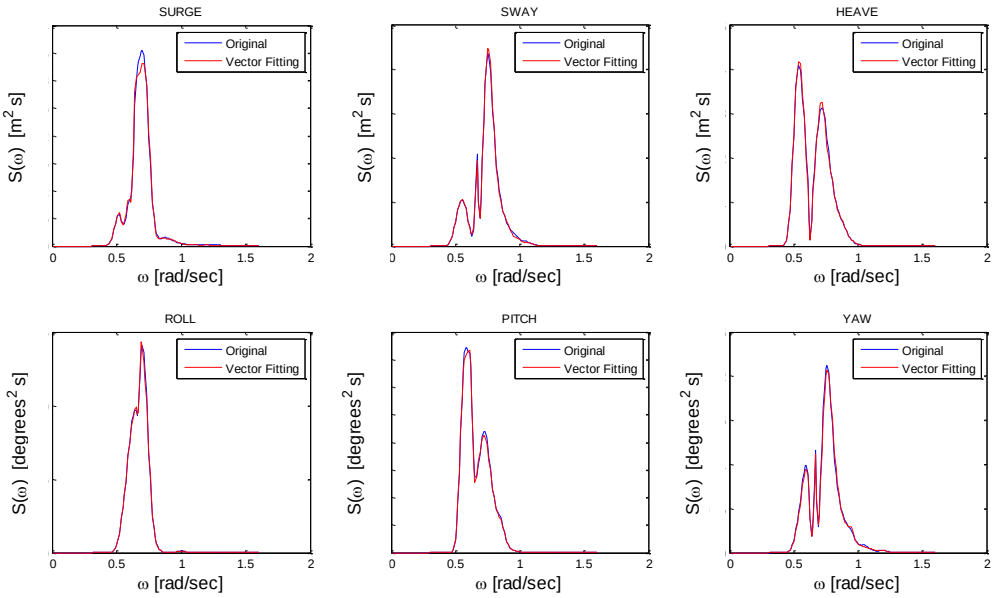

Figure 58: Motion Response Spectra

The significant value of the fitted and original response spectra for the 6 vessel motions is also calculated using the following equation:

$$X_{s,i} = 4 \cdot \sqrt{\int_0^\infty S_i(\omega) \cdot d\omega} \qquad \text{Eq. 5-1}$$

where i stands for the 6 vessel motions and S_i is the frequency domain response spectra.

The significant values of the vessel responses are shown in the following table:

Table 5: Significant responses: Fitted and original response spectra

Motions \ X_s	Original	Deviations of fitting process (% Orig.)
SURGE (m)		-0.39
SWAY (m)		-0.19
HEAVE (m)		-0.11
ROLL (degrees)		-0.10
PITCH (degrees)		-0.60
YAW (degrees)		-0.82

As it can be seen, the inaccuracies of the RAOs at low wave frequencies do not influence the final response spectra. However, if the wave spectrum has a peak period of 25-30 seconds (0.2-0.25 rad/sec), the inaccuracies mentioned in the previous section will affect the resulting response spectra. In case of swell, the lowest possible peak frequency is approximately 0.3 rad/sec, thus the wave energy in the range of 0.2-0.25 rad/sec is not significant. It is expected

that the inaccuracies of the fitted RAOs at 0.2-0.25 rad/sec is unlikely to cause inaccurate response spectra.

CHAPTER 6. Sensitivity analysis

In order to calibrate the RAOs based on the measurement data, a sensitivity analysis should first be performed. As mentioned before, the components that are going to be adjusted are the CoG of the vessel, the radius of gyration, the viscous damping and the hydrodynamic properties. The hydrodynamic properties are calibrated by modifying the residues of the approximation functions. By performing a sensitivity analysis, we can predict which vessel motions are affected by these components and to which degree. Also, we are able to eliminate the parameters that do not influence the motions with the highest inaccuracies. To show the effects of each parameter on the final responses, the following cases are analyzed:

1. Investigation of influence of the coordinates of the CoG. Several values are applied for each of the three coordinates and the resulting response spectra are then analyzed.
2. Modification of the mass matrix. Similar to the CoG of the vessel, each of the radii of gyration is modified and the resulting responses are calculated.
3. Examination of viscous damping. The influence of each element of the viscous damping matrix is examined.
4. Investigation of hydrodynamic added mass and damping. Only the residues of the approximation functions of the added mass and damping elements are modified. For each modification, the corresponding response spectra are calculated.
5. Analysis of the impact of the wave forces. The residues of the approximation function of each force corresponding to a certain wave heading is modified. It should be noticed that the main wave direction plays an important role in the sensitivity analysis.

The motion response spectra are calculated by using a 'Jonswap' wave spectrum of: T_p=8.5sec, H_s=5m and main wave direction=30°.

It should also be mentioned that the difference between the new value and the original value of each coordinate of the CoG (except 'y' coordinate) is calculated as follows:

$$dv = \frac{v_{new} - v_{original}}{v_{original}} \cdot 100\% \qquad \text{Eq. 6-1}$$

where dv is the relative difference between the new and the original values, v_{new} is the new value of the coordinate and $v_{original}$ is the original value of the coordinate.

The same equation is used to calculate the relative differences between the new and the original values of the radii of gyration.

6.1 SENSITIVITY ANALYSIS FOR COG

The original coordinates of the CoG of the SSCV Thialf with respect to the global axis system are: x=[redacted], y=[redacted], z=[redacted].

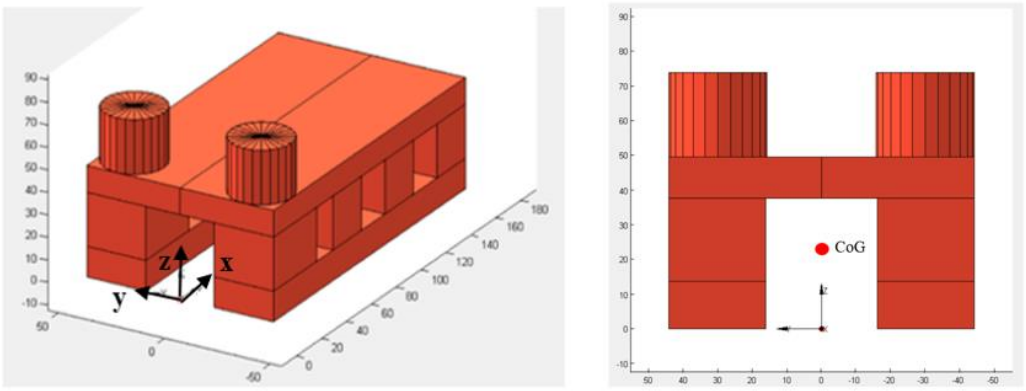

Figure 59: CoG of the SSCV Thialf

The following cases are examined:

- $x_{original}$ = [redacted], x_1= [redacted] (dx_1= -13.7%), x_2= [redacted] (dx_2=+13.7%).
- $y_{original}$ = [redacted], y_1= [redacted] (dy_1= -22% of total width), y_2= [redacted] (dy_1= +22% of total width).
- $z_{original}$ = [redacted], z_1= [redacted] (dz_1= -42.9%), z_2= [redacted] (dz_2= +42.9%).

For each case, only one coordinate is modified while the other two coordinates are kept fixed.

The following figures show the results of the above mentioned cases.

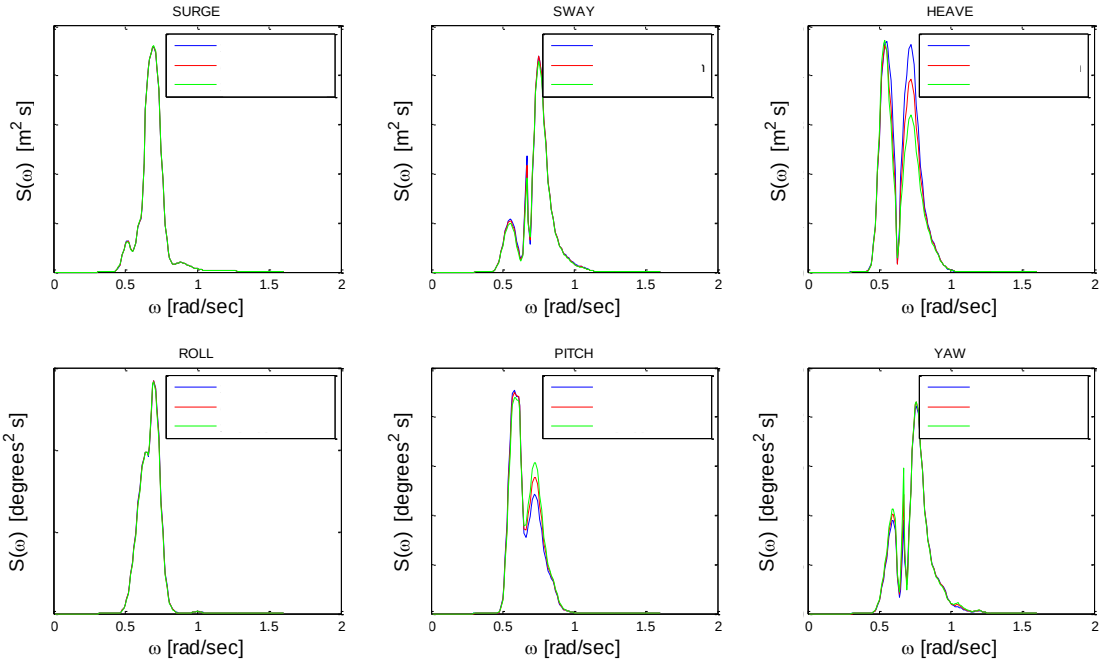

Figure 60: Sensitivity analysis for the 'x' coordinate of the CoG, x_1=blue, orig=red, x_2=green

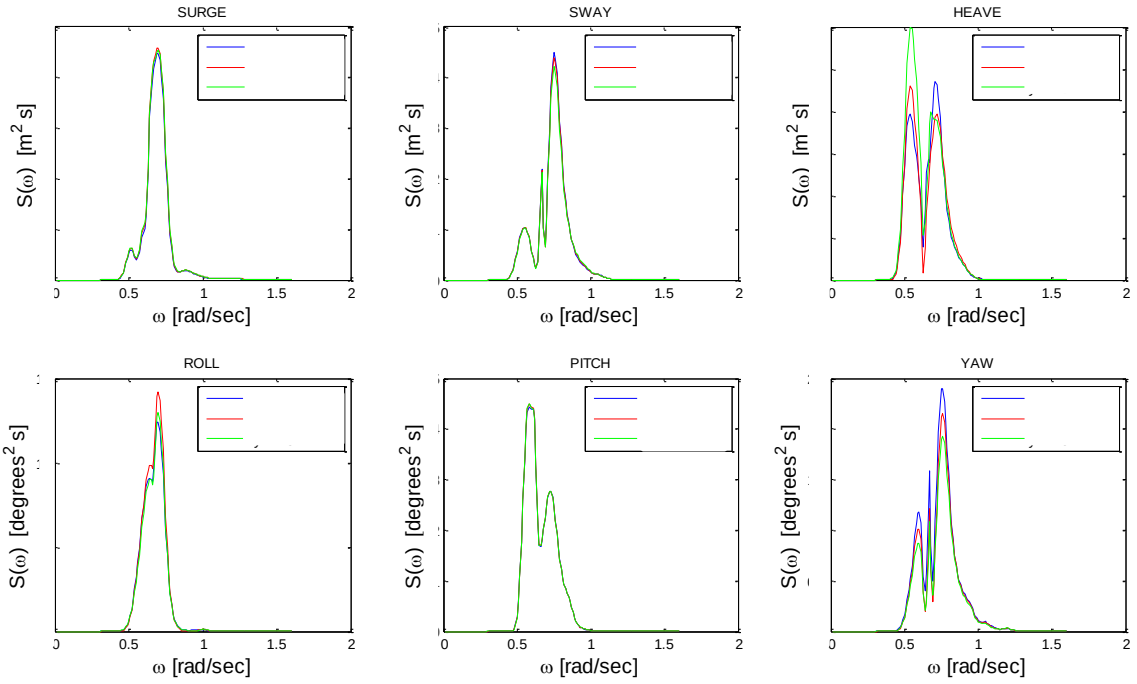

Figure 61: Sensitivity analysis for the 'y' coordinate of the CoG, , y_1=blue, orig=red, y_2=green

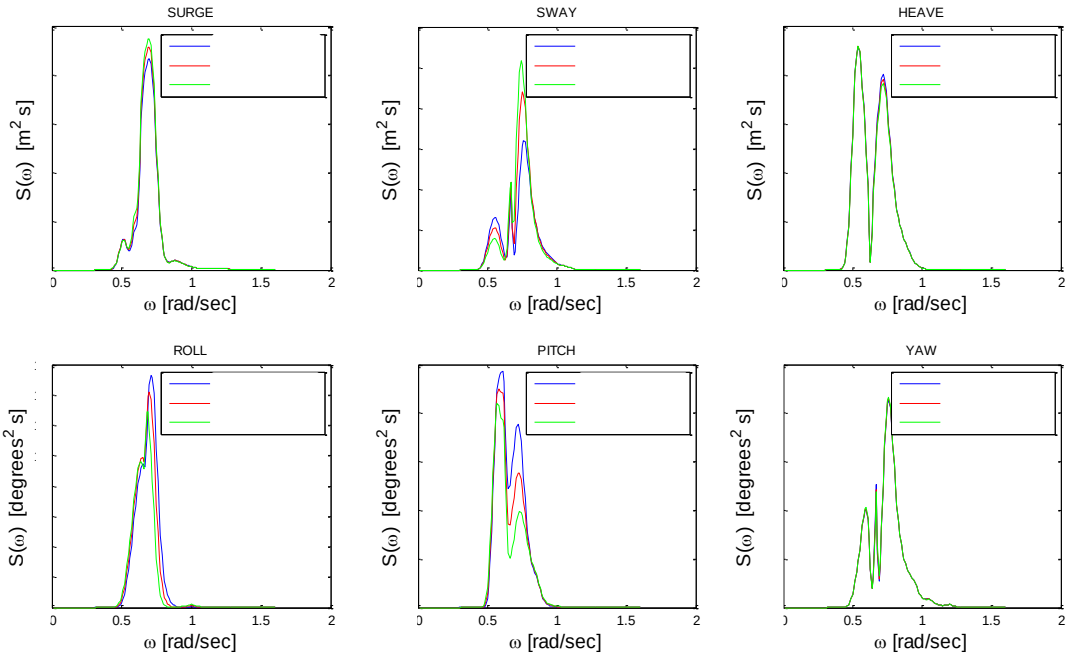

Figure 62: Sensitivity analysis for the 'z' coordinate of the CoG, , z_1=blue, orig=red, z_2=green

As can be seen from the figures above, a change in one coordinate of the CoG modifies, almost all 6 vessel motions. If we change the 'x' coordinate, the heave motion is mostly affected. Also, the sway, pitch and yaw motions are slightly modified. Surge and roll do not show any change. The variations in 'y' coordinate influence mainly the heave and yaw. The roll motion also shows some small changes. However, the rest of the vessel motions remained almost the same. Finally, regarding the modifications of the 'z' coordinate, pitch and sway were mostly affected. In addition, the modification of 'z' coordinate had a slight impact on surge and roll. Heave and yaw remained the same.

During projects, the semi-submersible vessels is preferred to be ballasted on even keel. Therefore, the coordinates 'x' and 'y' do not show great variation during projects. Only the z coordinate can get a large range of values because of the lifting operations of the cranes of the vessels.

6.2 SENSITIVITY ANALYSIS FOR THE RADIUS OF GYRATION

The original values of the radii of gyration of the Thialf are the following: r_{xx}=[redacted] r_{yy}=[redacted] r_{zz}=[redacted]. Similar to the sensitivity analysis of the coordinates of the CoG, three cases are examined:

- r_{xx}: $r_{xx,original}$ =[redacted] $r_{xx,1}$ =[redacted] ($dr_{xx,1}$= -26.3%), $r_{xx,2}$ =[redacted] ($dr_{xx,2}$= +26.3%).
- r_{yy}: $r_{yy,original}$ =[redacted] $r_{yy,1}$ =[redacted] ($dr_{yy,1}$= -16.9%), $r_{yy,2}$ =[redacted] ($dr_{yy,2}$= +16.9%).
- r_{zz}: $r_{zz,original}$[redacted], $r_{zz,1}$ =[redacted] ($dr_{zz,1}$= -15.4%), $r_{zz,2}$ =[redacted] ($dr_{zz,2}$= +15.4%).

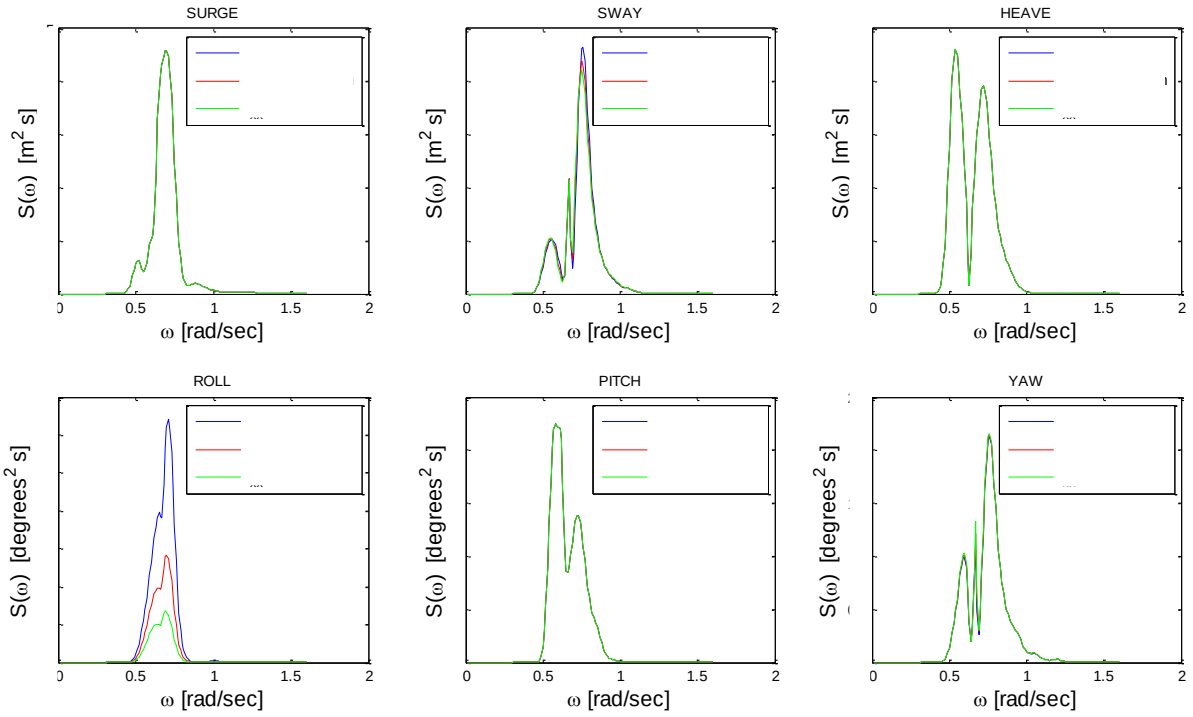

Figure 63: Sensitivity analysis for the radius of gyration 'r_{xx}' , $r_{xx,1}$ =blue, orig=red, $r_{xx,2}$ =green

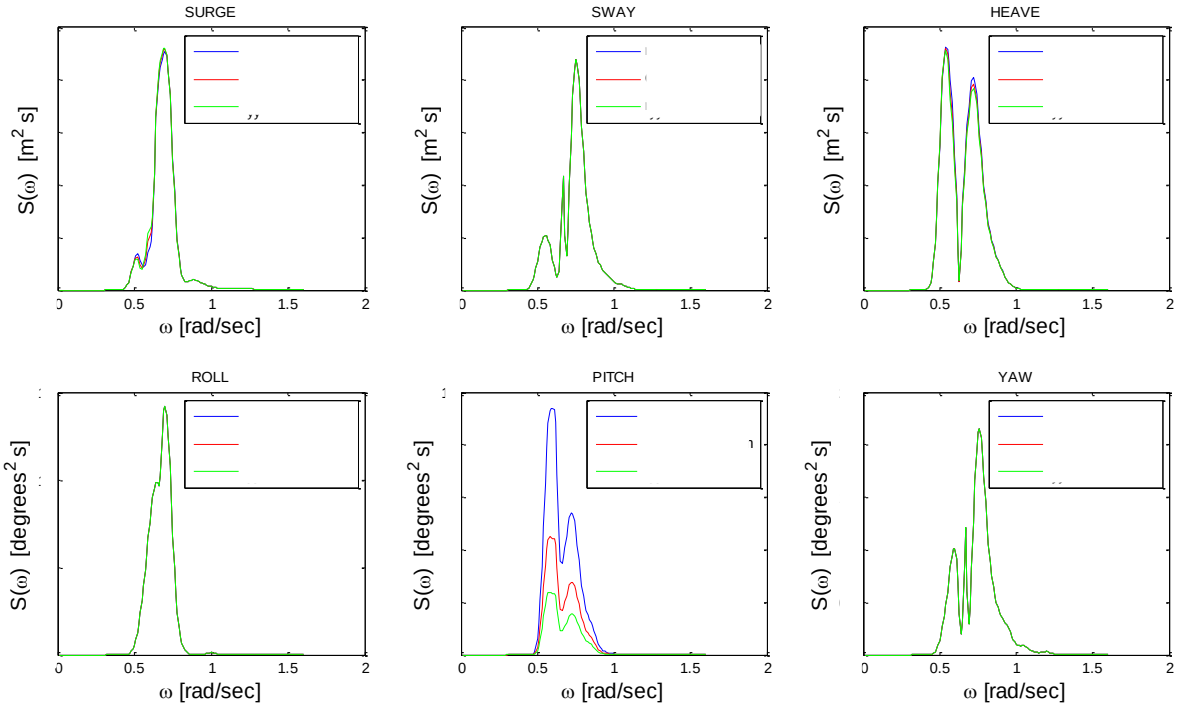

Figure 64: Sensitivity analysis for the radius of gyration 'r_{yy}', $r_{yy,1}$ =blue, orig=red, $r_{yy,2}$ =green

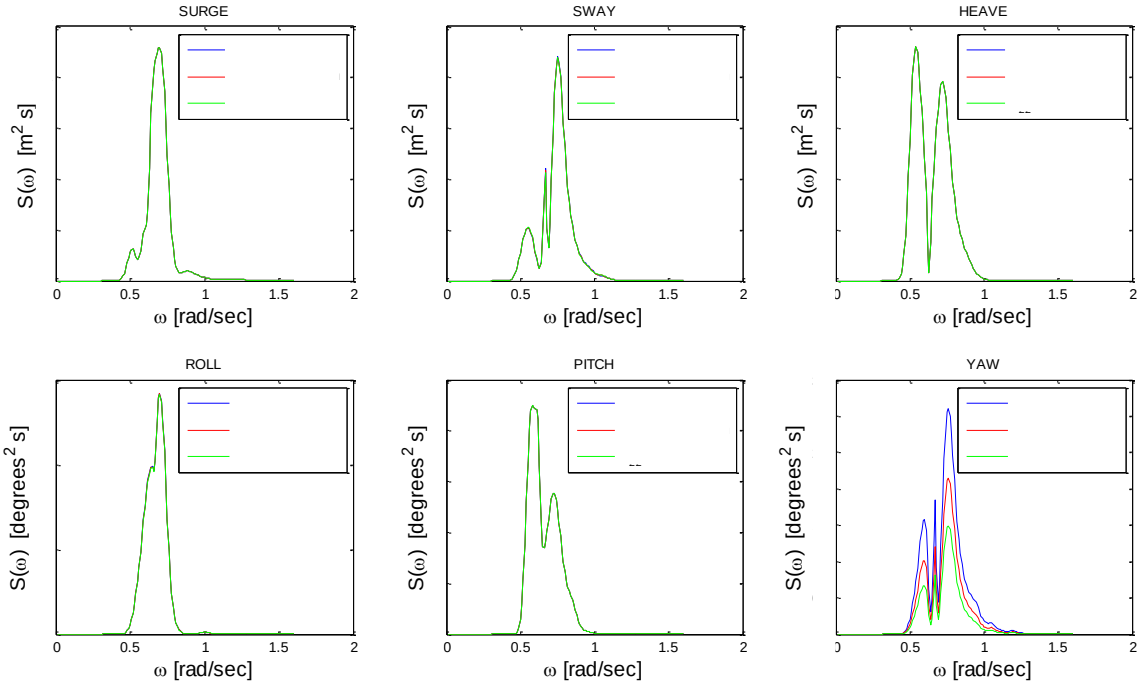

Figure 65: Sensitivity analysis for the radius of gyration 'r_{zz}', $r_{zz,1}$ =blue, orig=red, $r_{zz,2}$ =green

Given the above figures, the radius of gyration with respect to x axis has a great impact on roll motion and less on sway and yaw. It doesn't influence the surge, heave and pitch motions. The radius of gyration r_{yy} influences the pitch motion and less the surge and heave motions. Finally, the radius of gyration r_{zz} affects the yaw motion and less the sway and roll motions. The modification of each radius of gyration mainly affects a specific motion.

6.3 SENSITIVITY ANALYSIS OF VISCOUS DAMPING

The matrix of the additional viscous damping is indicated below:

$$\boldsymbol{Original\_B_{ad}} = \begin{bmatrix} \blacksquare\,[\frac{kNs}{m}] & 0 & 0 & 0 & 0 & 0 \\ 0 & \blacksquare\,[\frac{kNs}{m}] & 0 & 0 & 0 & 0 \\ 0 & 0 & \blacksquare\,[\frac{kNs}{m}] & 0 & 0 & 0 \\ 0 & 0 & 0 & \blacksquare\,[\frac{kNsm^2}{m}] & 0 & 0 \\ 0 & 0 & 0 & 0 & \blacksquare\,[\frac{kNsm^2}{m}] & 0 \\ 0 & 0 & 0 & 0 & 0 & \blacksquare\,[\frac{kNsm^2}{m}] \end{bmatrix}$$

The sensitivity analysis for the viscous damping is similar to the sensitivity analysis performed for the radius of gyration. Each element of the diagonal of the viscous damping matrix affects the corresponding degree of freedom. For example, after modifying the element $\mathbf{B_{ad}}(1,1)$, the surge motion is highly influenced. To achieve the sensitivity analysis of the viscous damping, the following relations were applied to each element:

- $\boldsymbol{B_{ad}}(1,1)$: $0.2 \cdot \boldsymbol{Original\_B_{ad}}(1,1)$, $\boldsymbol{Original\_B_{ad}}(1,1)$, $50 \cdot \boldsymbol{Original\_B_{ad}}(1,1)$
- $\boldsymbol{B_{ad}}(2,2)$: $0.2 \cdot \boldsymbol{Original\_B_{ad}}(2,2)$, $\boldsymbol{Original\_B_{ad}}(2,2)$, $50 \cdot \boldsymbol{Original\_B_{ad}}(2,2)$
- $\boldsymbol{B_{ad}}(3,3)$: $0.2 \cdot \boldsymbol{Original\_B_{ad}}(3,3)$, $\boldsymbol{Original\_B_{ad}}(3,3)$, $10 \cdot \boldsymbol{Original\_B_{ad}}(3,3)$
- $\boldsymbol{B_{ad}}(4,4)$: $0.2 \cdot \boldsymbol{Original\_B_{ad}}(4,4)$, $\boldsymbol{Original\_B_{ad}}(4,4)$, $20 \cdot \boldsymbol{Original\_B_{ad}}(4,4)$

- $\boldsymbol{B_{ad}}(5,5)$: $0.2 \cdot \boldsymbol{Original\_B_{ad}}(5,5)$,$\boldsymbol{Original\_B_{ad}}(5,5)$, $20 \cdot \boldsymbol{Original\_B_{ad}}(5,5)$
- $\boldsymbol{B_{ad}}(6,6)$: $0.2 \cdot \boldsymbol{Original\_B_{ad}}(6,6)$,$\boldsymbol{Original\_B_{ad}}(6,6)$, $50 \cdot \boldsymbol{Original\_B_{ad}}(6,6)$

The following figures show the vessel motion which is mostly affected by each of the diagonal elements.

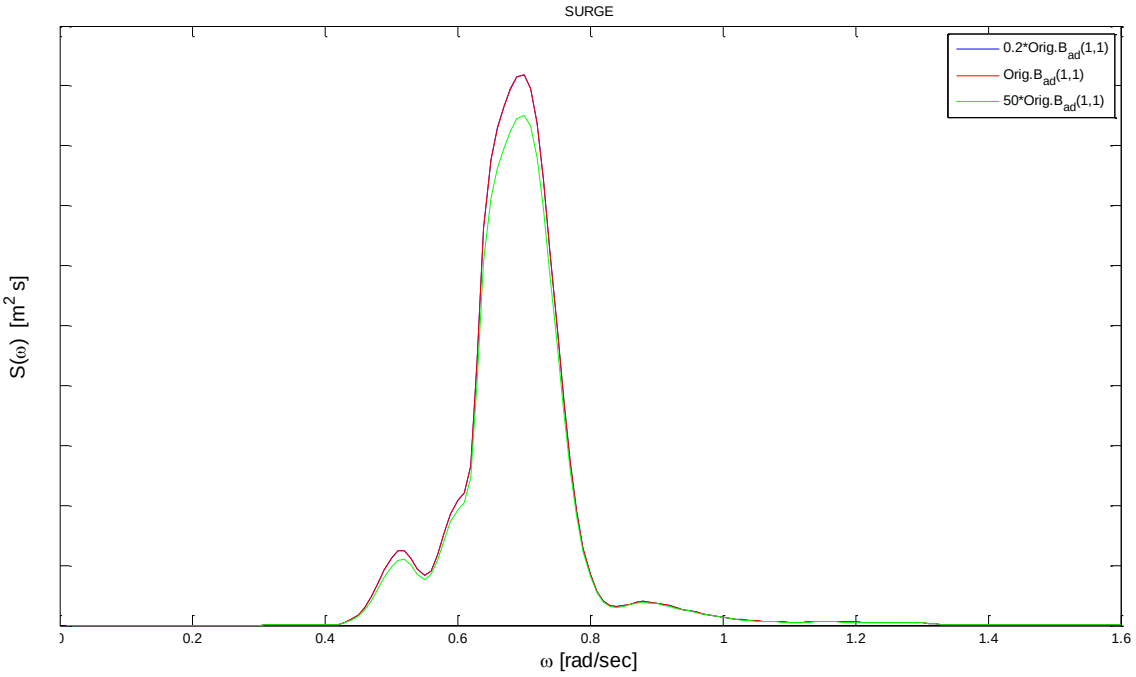

Figure 66: Sensitivity analysis for viscous damping element $B_{ad}(1,1)$

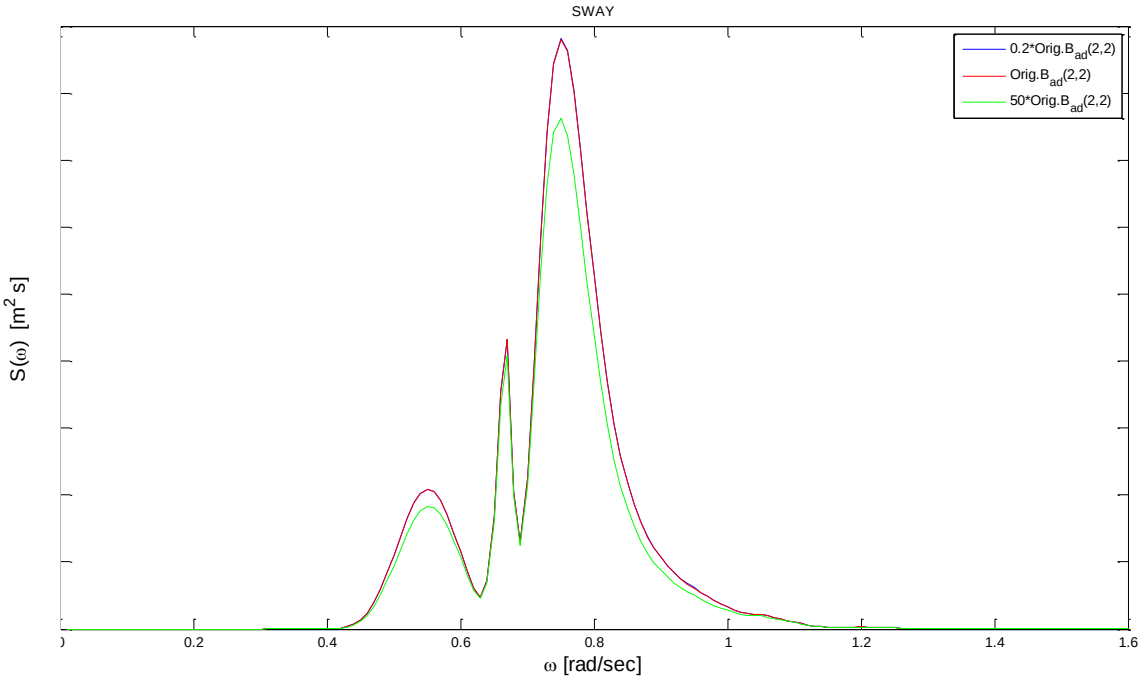

Figure 67: Sensitivity analysis for viscous damping element $B_{ad}(2,2)$

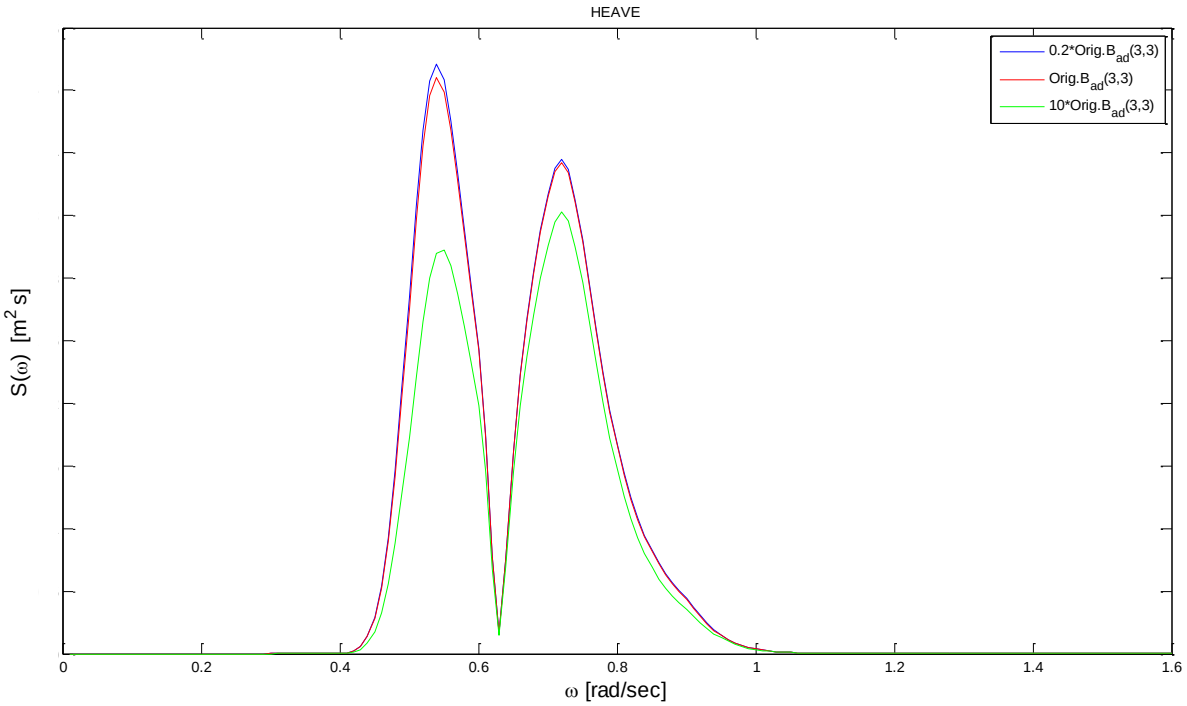

Figure 68: Sensitivity analysis for viscous damping element $B_{ad}(3,3)$

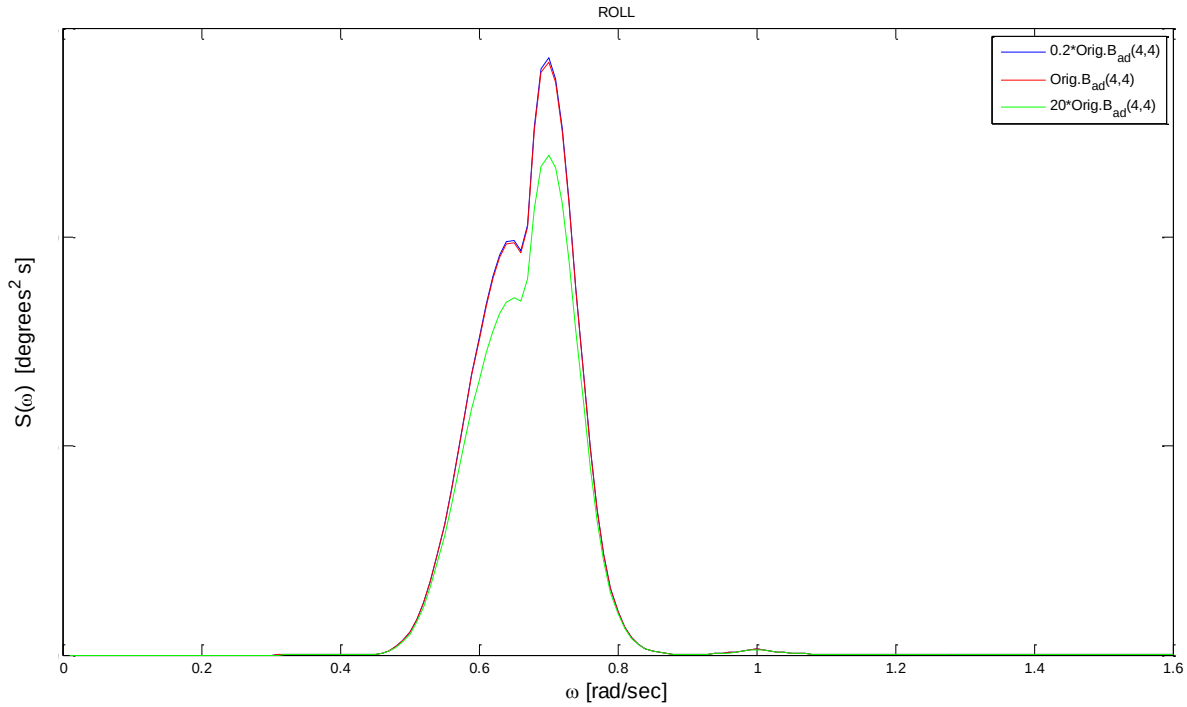

Figure 69: Sensitivity analysis for viscous damping element $B_{ad}(4,4)$

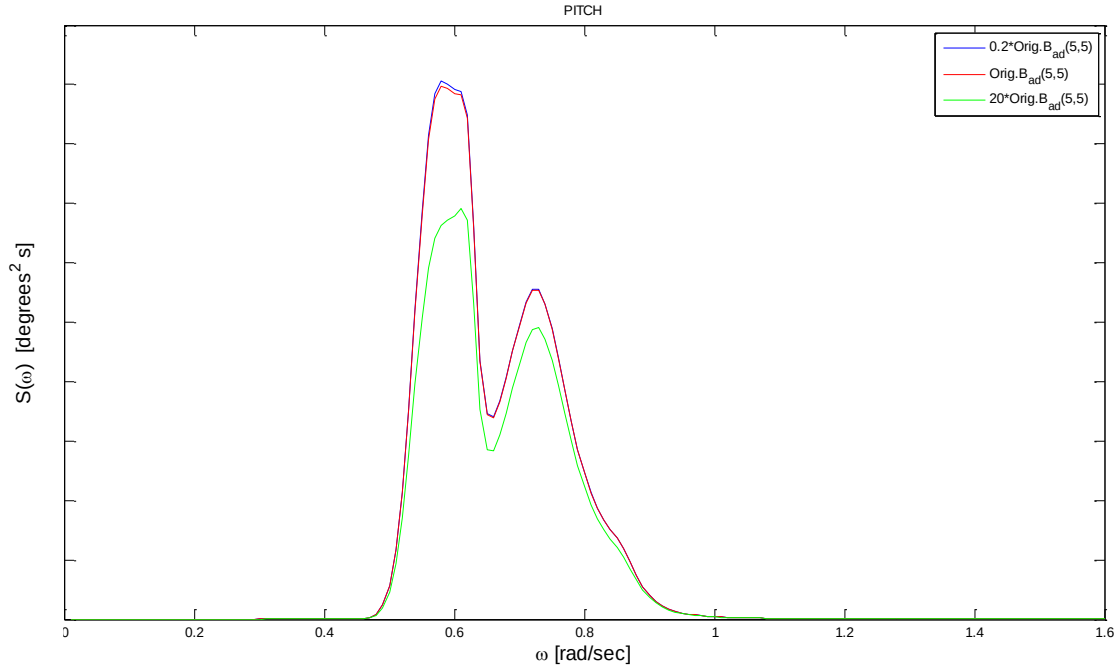

Figure 70: Sensitivity analysis for viscous damping element $B_{ad}(5,5)$

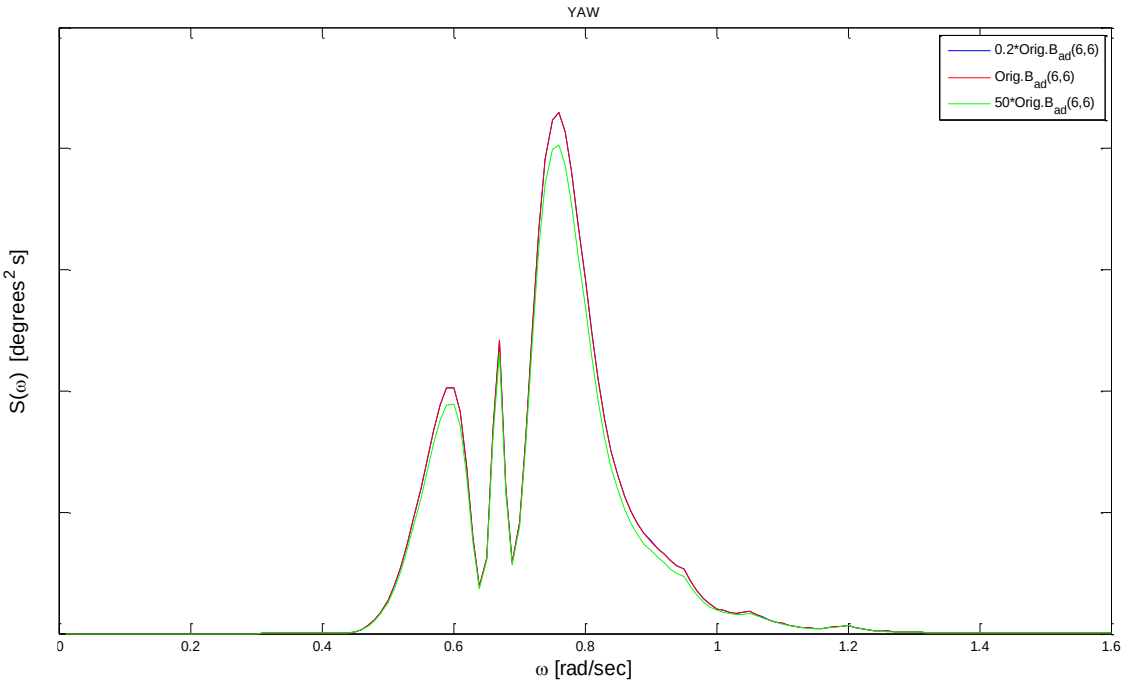

Figure 71: Sensitivity analysis for viscous damping element $B_{ad}(6,6)$

According to the above figures, the viscous damping has a negligible influence on the vessel responses. Only when the viscous damping is drastically increased, the vessel motions are affected. The elements $\mathbf{B_{ad}}(1,1)$, $\mathbf{B_{ad}}(2,2)$ $\mathbf{B_{ad}}(6,6)$ had to be increased by a factor of 50 in order to cause noticeable changes to surge, heave and yaw motions, respectively. The elements $\mathbf{B_{ad}}(3,3)$, $\mathbf{B_{ad}}(4,4)$ and $\mathbf{B_{ad}}(5,5)$, were increased slightly less than the previous elements: 10 to 20 times their original values. To explain the results of this sensitivity analysis, we should mention that the values of the original viscous damping matrix are much lower than the magnitude of the hydrodynamic damping. Thus, the viscous damping has a minor impact on

the final vessel responses. However, the viscous damping can be significant for rolling ships. For example, the vessel Aegir has low hydrodynamic damping for roll, thus the changes in the added damping matrix can cause considerable modifications to the roll motion.

6.4 SENSITIVITY ANALYSIS: ADDED MASS AND DAMPING

The sensitivity analysis for the added mass and damping is accomplished by using the approximation functions (CHAPTER 3). After changing the residues of the approximation function of each element, the vessel responses are determined. Before starting the sensitivity analysis of each element, we should mention the following:

- Each diagonal element of the added mass and damping matrices influences only the motion related to the corresponding degree of freedom. For example, the element a_{33} is important for the modification of the heave motion.
- The elements with indices 1,3,5 influence the symmetric motions (surge, heave, pitch). Also, the elements with indices 2,4,6, influence the antisymmetric motions (sway, roll, and yaw).

Because of the large number of elements, only two examples are given for this sensitivity analysis. It is suggested to examine the following cases: the influences of a diagonal element and the impact of a random element on the corresponding coupled motions. Thus, the chosen elements are: ab_{33} and ab_{35}.

The residues $c_{7,ab33}$ and $c_{8,ab33}$ of the approximation function of the element ab_{33} are modified. The original complex quantities of these residues are as follows: $c_{7,ab33}$=-10.15+31.62i, $c_{8,ab33}$=-10.15-31.62i. The related poles are: $p_{7,ab33}$=-0.012+0.739i, $p_{8,ab33}$=-0.012-0.739i. Thus, the curve of ab_{33} is expected to be changed at the frequency of 0.74 rad/sec (according to the imaginary part of poles). The following cases are examined:

- $c_{7,case1}=-50\cdot c_{7,ab33}$ and $c_{8,case1}=-50\cdot c_{8,ab33}$
- $c_{7,original}=c_{7,ab33}$ and $c_{8,original}=c_{8,ab33}$
- $c_{7,case2}=+50\cdot c_{7,ab33}$ and $c_{8,case2}=+50\cdot c_{8,ab33}$

The following figures show the modified element ab_{33} and the resulting vessel motions.

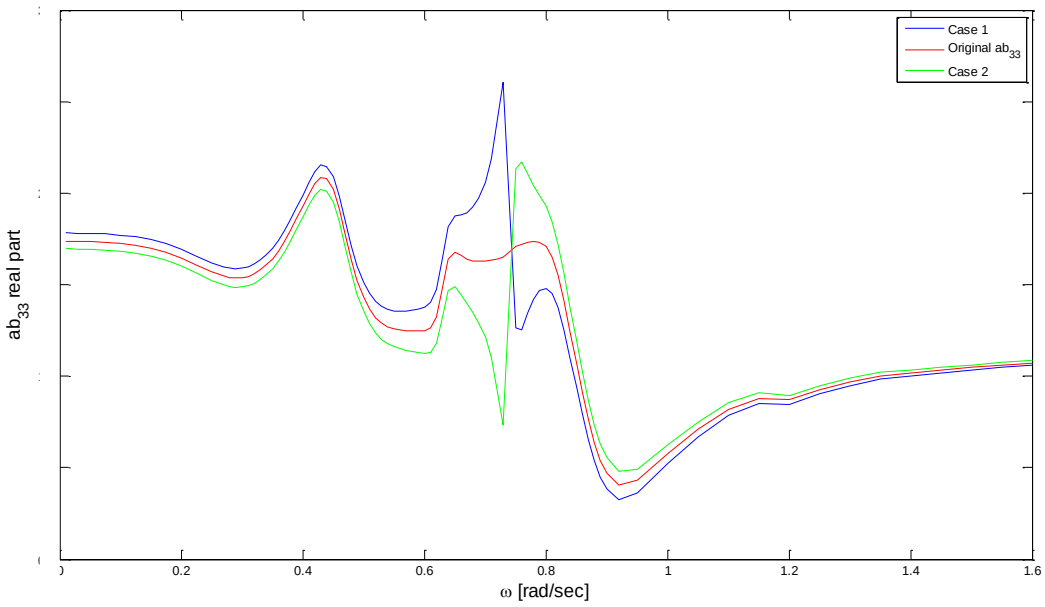

Figure 72: Modification of ab_{33}, real part

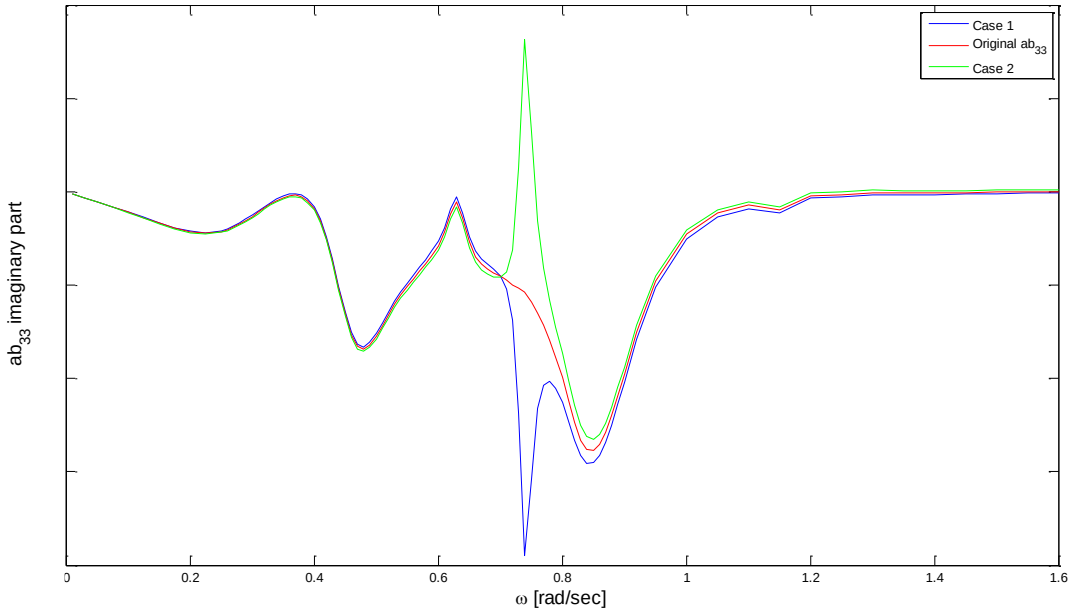

Figure 73: Modification of ab_{33}, imaginary part

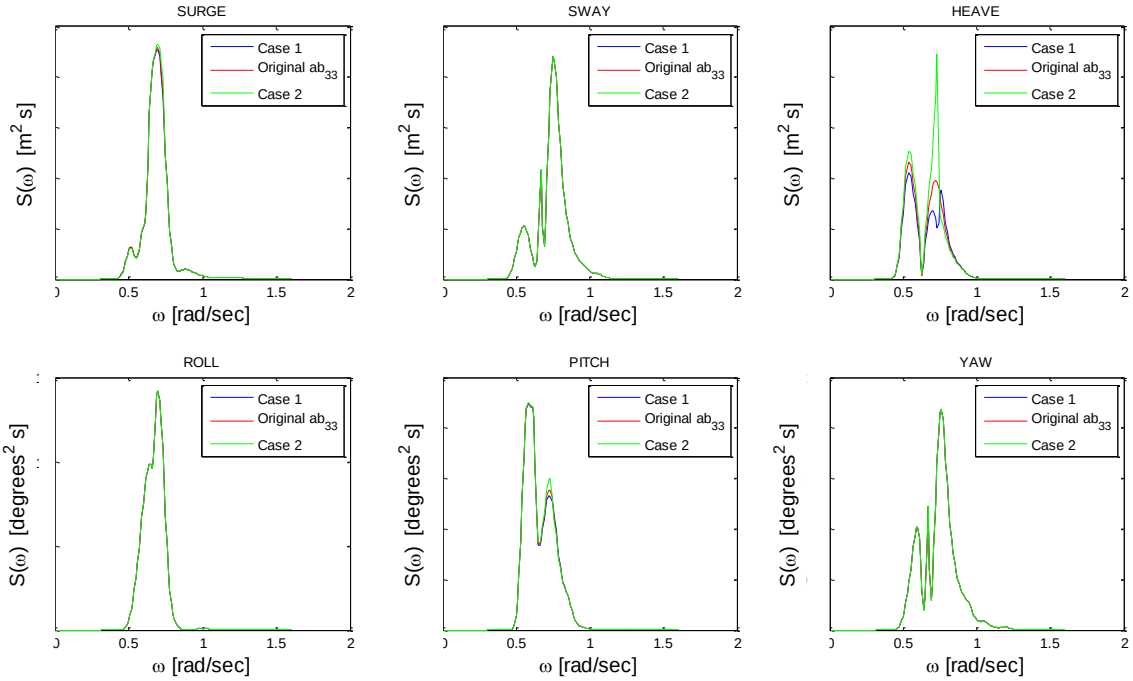

Figure 74: Response spectra, sensitivity analysis, ab_{33}

With respect to the element ab_{35}, the following residues are modified: $c_{7,ab35}$=-10E03-4.81E03i, $c_{8,ab35}$=-10E03+4.81E03i. The corresponding poles are: $p_{7,ab35}$=-0.018+0.63i, $p_{8,ab35}$-0.018-0.63i. The following cases are examined:

- $c_{7,case1}=-50\cdot c_{7,ab35}$ and $c_{8,case1}=-50\cdot c_{8,ab35}$
- $c_{7,original}=c_{7,ab35}$ and $c_{8,original}=c_{8,ab35}$
- $c_{7,case2}=+50\cdot c_{7,ab35}$ and $c_{8,case2}=+50\cdot c_{8,ab35}$

The following figures show the modified element ab_{35} and the resulting vessel motions.

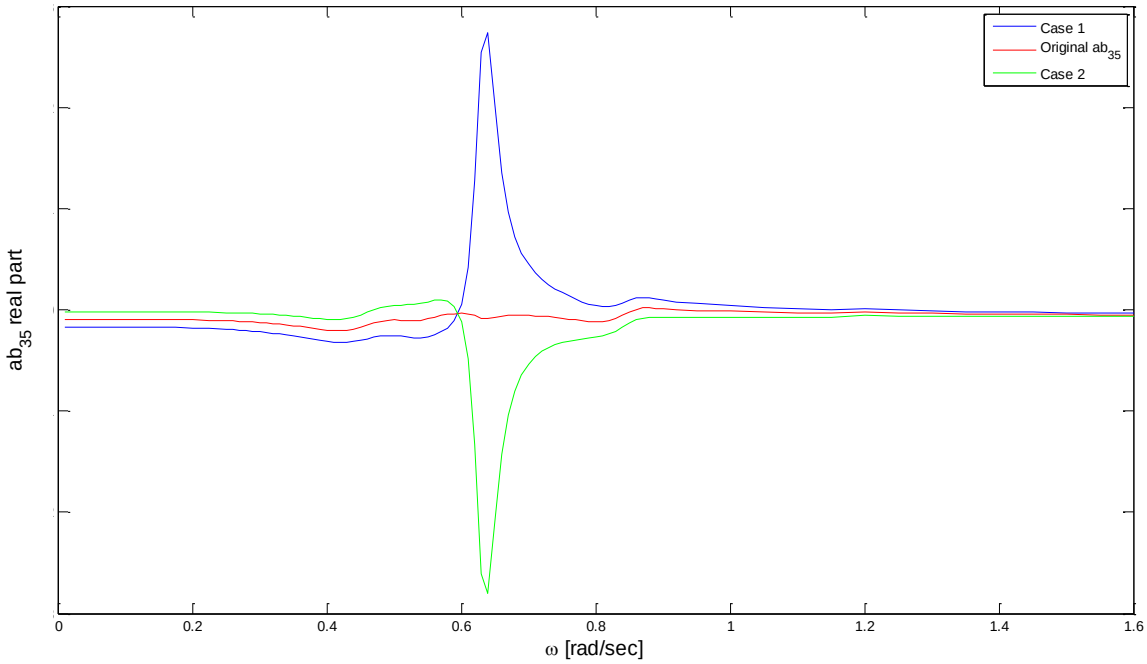

Figure 75: Modification of ab_{35}, real part

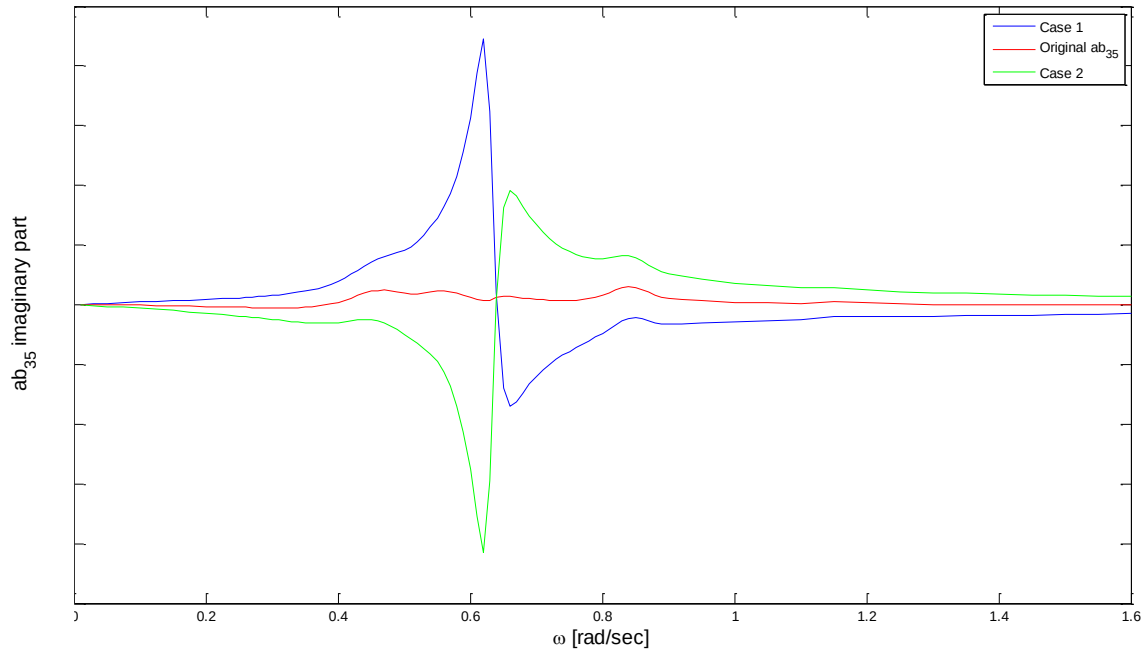

Figure 76: Modification of ab_{35}, imaginary part

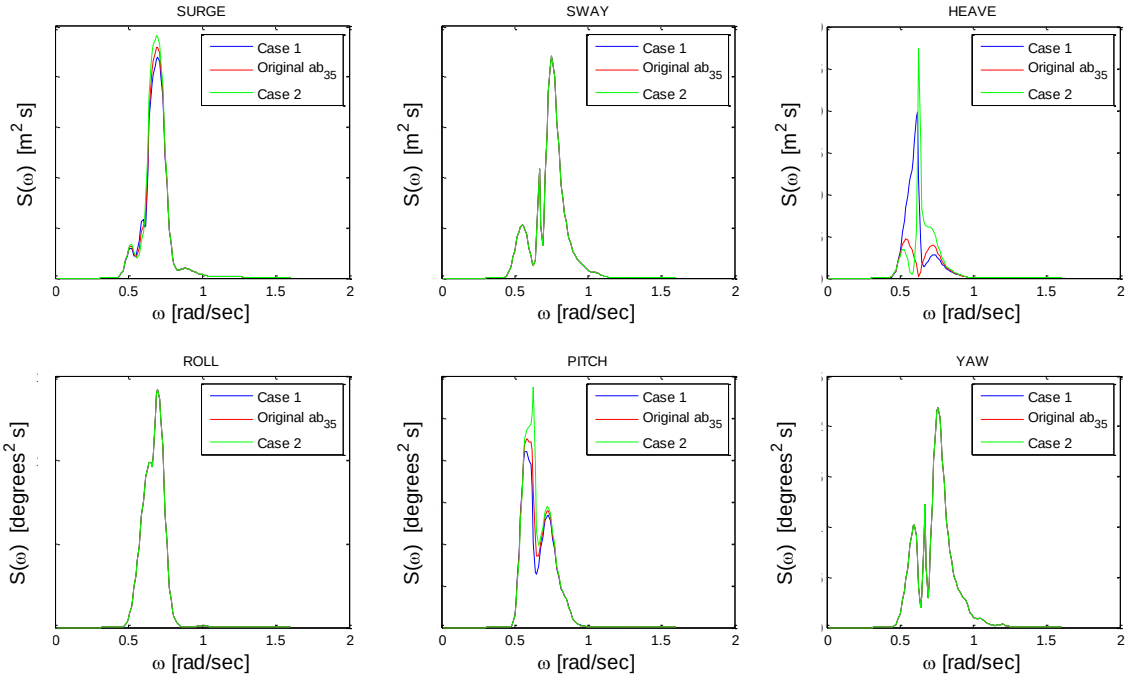

Figure 77: Response spectra, sensitivity analysis, ab_{35}

As expected, when we change the elements ab_{35}, the coupled motions of surge, heave and pitch are modified, whereas, only the heave motion is influenced by the element ab_{33}.

6.5 SENSITIVITY ANALYSIS: WAVE FORCES AND MOMENTS

The sensitivity analysis of the hydrodynamic forces and moments is similar to the analysis of the hydrodynamic added mass and damping. After modifying the residues of a function which approximates one wave force in a certain wave direction, the vessel responses are determined. Also, we should mention the following:

- The forces F_1, F_3 and the moment M_5 influence the surge, heave and pitch motions. The force F_2 and the moments M_4, M_6 influence the sway, roll and yaw motions.
- The forces within the range of -45° to +45° with respect to the main wave direction indicate the highest impact on the vessel motions.

Two examples are shown for the sensitivity analysis of the wave forces: 1) The impact of a wave force coming from the same directions as the waves. 2) The influence of the same force coming from a direction of +60 degrees from the main wave direction. Therefore, the selected forces are: $F_3(\omega, 30^o)$ and $F_3(\omega, 90^o)$.

The residues which are modified for $F_3(\omega, 30^o)$ are the following: $c_{7,F3\_30}$=-5.34E03-1.79E04i, $c_{8,F3\_30}$=-5.34E03+1.79E04i. The corresponding poles are: $p_{7,F3\_30}$ =0.41+0.44i, $p_{8,F3\_30}$ =0.41-0.44i. The following cases are examined:

- $c_{7,case1}$=-2·$c_{7,F3\_30}$ and $c_{8,case1}$=-2·$c_{8,F3\_30}$
- $c_{7,original}$= $c_{7,F3\_30}$ and $c_{8,original}$= $c_{8,F3\_30}$
- $c_{7,case2}$=+2· $c_{7,F3\_30}$ and $c_{8,case2}$=+2·$c_{8,F3\_30}$

The modified $F_3(\omega,30^o)$ and the corresponding vessel response spectra are shown below:

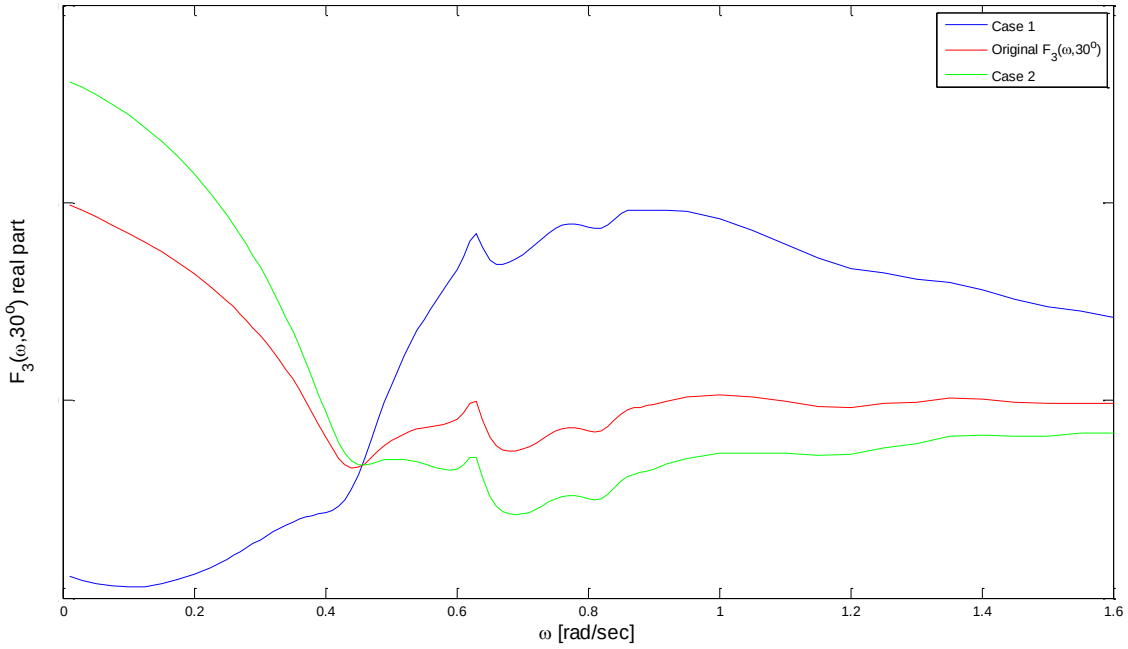

Figure 78: Modification of $F_3(\omega,30^o)$, real part

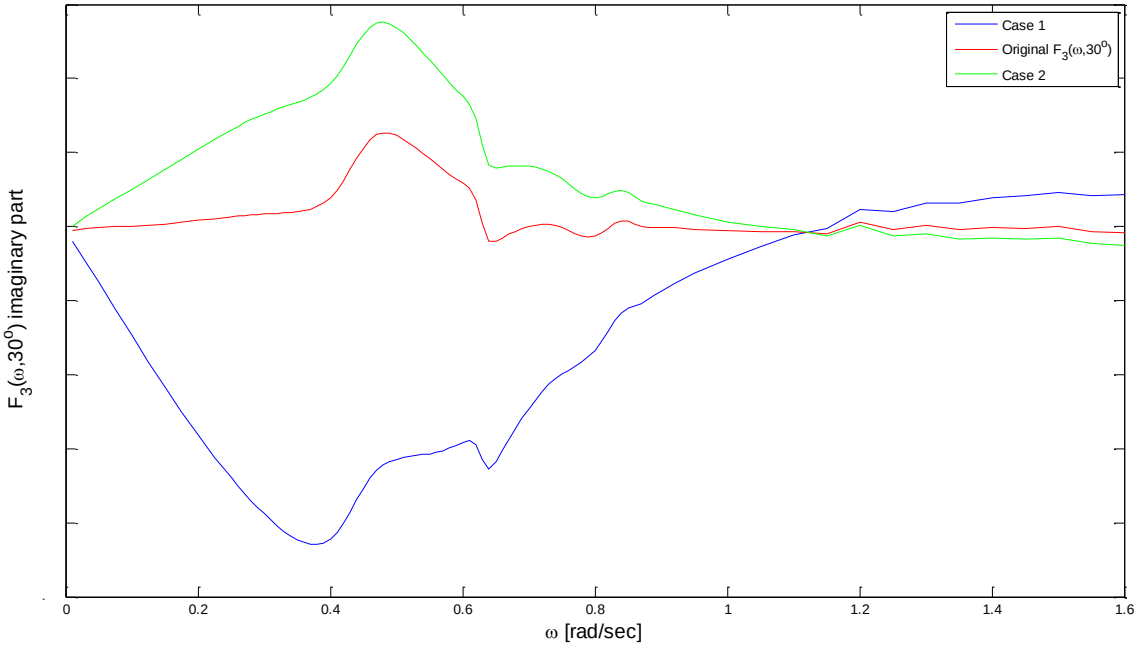

Figure 79: Modification of $F_3(\omega,30^o)$, imaginary part

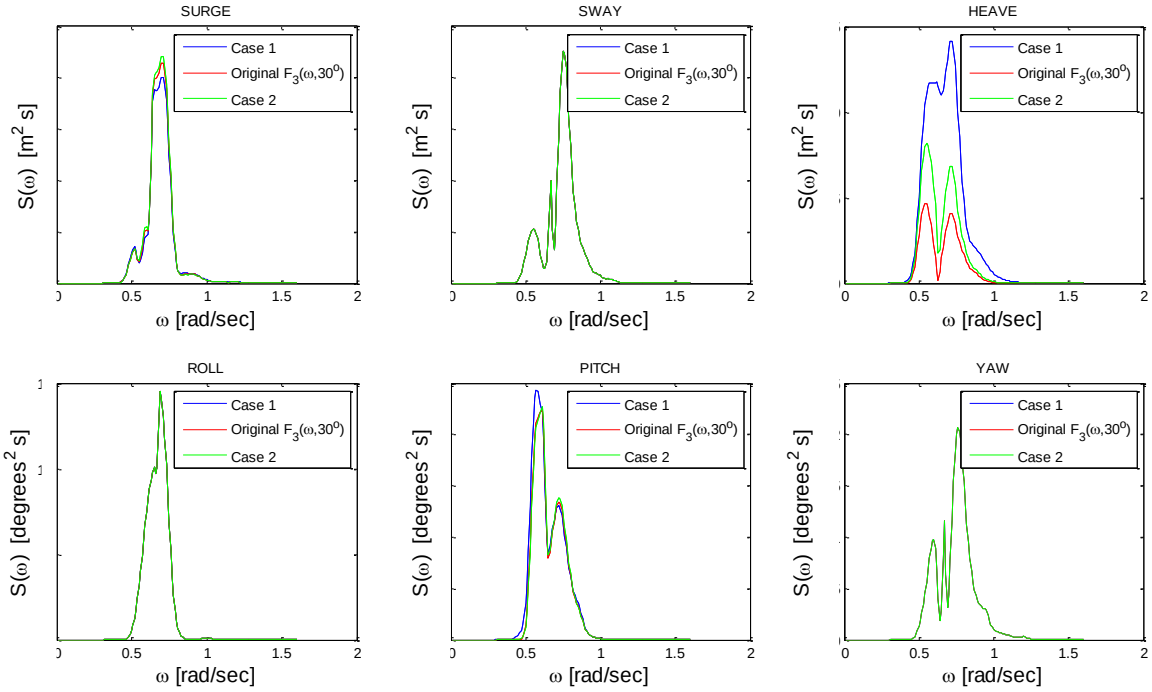

Figure 80: Response spectra, sensitivity analysis, $F_3(\omega,30^o)$

The residues which are modified for $F_3(\omega, 90^o)$ are the following: $c_{7,F3\_90}$=-4.43E03-1.66E04i, $c_{8,F3\_90}$=--4.43E03+1.66E04i. The corresponding poles are: $p_{7,F3\_90}$ =0.41+0.44i, $p_{8,F3\_90}$ =0.41-0.44i. The following cases are examined:

- $c_{7,case1}$=-2·$c_{7,F3\_90}$ and $c_{8,case1}$=-2· $c_{8,F3\_90}$
- $c_{7,original}$= $c_{7,F3\_90}$ and $c_{8,original}$= $c_{8,F3\_90}$
- $c_{7,case2}$=+2· $c_{7,F3\_90}$ and $c_{8,case2}$=+2· $c_{8,F3\_90}$

The real and imaginary parts of $F_3(\omega,90^o)$ and the corresponding vessel response spectra are shown below:

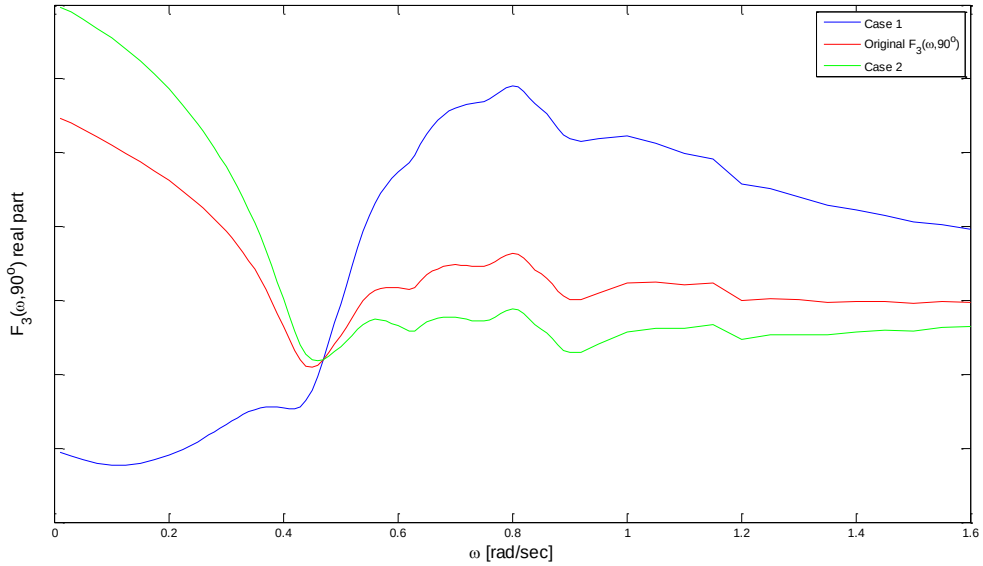

Figure 81: Modification of $F_3(\omega,90^o)$, real part

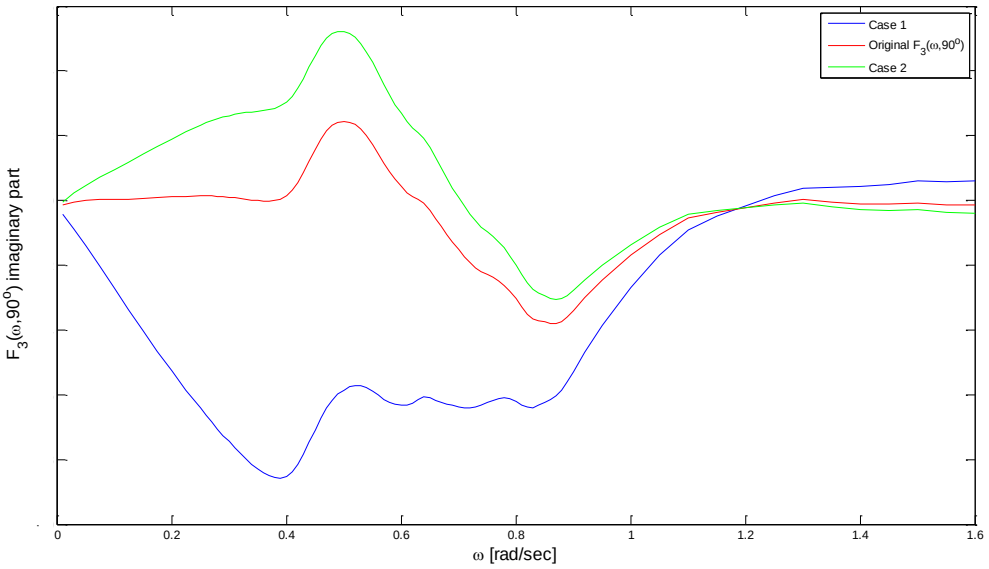

Figure 82: Modification of $F_3(\omega,90^o)$, imaginary part

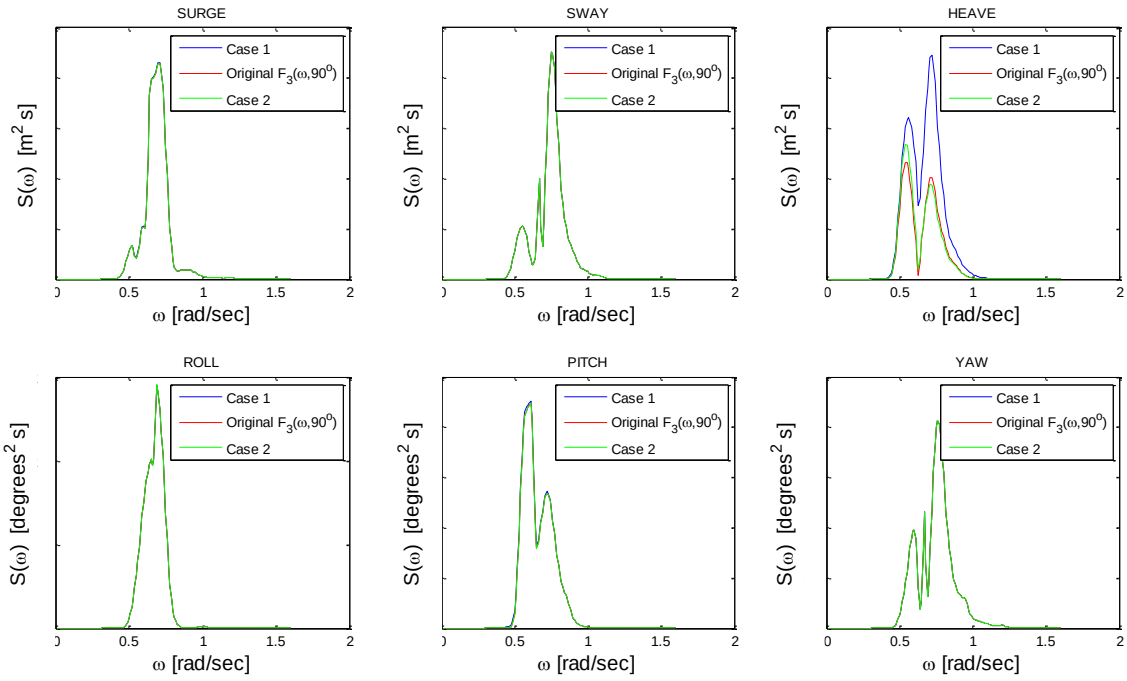

Figure 83: Response spectra, sensitivity analysis, $F_3(\omega,90^o)$

When we change the wave force $F_3(\omega,30^o)$ and $F_3(\omega,90^o)$, the heave motion is affected. However the modifications of $F_3(\omega,90^o)$ have lower impact on the vessel responses than the modifications of $F_3(\omega, 30^o)$. During the identification procedure, it is suggested to calibrate the wave forces closer to the main wave direction (main wave direction $\pm$ 45°). If the calibrated forces for those directions cannot further improve the response spectra, the rest of wave directions should also be investigated. The reason why some wave directions are excluded is to make the identification process faster.

The results of the sensitivity analysis are summarized in the following table. The empty cells indicate that there is no influence of the parameter on the corresponding motion.

Table 6: Results of sensitivity analysis

Vessel Properties	Vessel Motions					
COG	Surge	Sway	Heave	Roll	Pitch	Yaw
x	+	++	++	+	++	++
y	++	+	++	++	+	++
z	++	++	+	++	++	+
Radius of gyration	Surge	Sway	Heave	Roll	Pitch	Yaw
r_{xx}		+		++		+
r_{yy}	+		+		++	
r_{zz}		+		+		++
Viscous damping	Surge	Sway	Heave	Roll	Pitch	Yaw
$\mathbf{B_{ad}}(1,1)$	++		+		+	
$\mathbf{B_{ad}}(2,2)$		++		+		+
$\mathbf{B_{ad}}(3,3)$	+		++		+	
$\mathbf{B_{ad}}(4,4)$		+		++		+
$\mathbf{B_{ad}}(5,5)$	+		+		++	
$\mathbf{B_{ad}}(6,6)$		+		+		++
Added mass and Damping	Surge	Sway	Heave	Roll	Pitch	Yaw
ab_{11}	++		+		+	
ab_{22}		++		+		+
ab_{31}	+		+		+	
ab_{33}	+		++		+	
ab_{42}		+		+		+
ab_{44}		+		++		+
ab_{51}	+		+		+	
ab_{53}	+		+		+	
ab_{55}	+		+		++	
ab_{62}		+		+		+
ab_{64}		+		+		+
ab_{66}		+		+		++
Hydrodynamic forces (mdir-45º<dir<45º+mdir)	Surge	Sway	Heave	Roll	Pitch	Yaw
F_1	++		+		+	
F_2		++		+		+
F_3	+		++		+	
M_4		+		++		+
M_5	+		+		++	
M_6		+		+		++

CHAPTER 7. Identification of RAOs

The procedure for the identification of the RAOs is tested by several cases. For each test case, we use a set of simulated data which gives information about the motions of the vessel and the environmental conditions. The set of the simulated data contains the wave spectrum, the direction of the vessel and simulated response spectra. The simulated response spectra are determined on the basis of the wave spectrum and modified RAOs. The modified RAOs are obtained by changing several parameters. The purpose of the test cases is to examine whether the identification procedure can find the modified parameters based on the wave spectrum and the response spectra of the simulated data. Each of the following parameters are investigated: the coordinates of CoG, the radii of gyration, the viscous damping and the residues of the approximation functions of the hydrodynamic database. Each parameter is tested for multiple values until the resulting response spectra approximate the responses given in the data set.

7.1 IDENTIFICATION PROCCEDURE

In order to calibrate the RAOs based on the response spectra of the data set, five algorithms are created. Each algorithm corresponds to the calibration of the CoG, the radius of gyration, the viscous damping, the hydrodynamic added mass-damping and the hydrodynamic forces, respectively. All of the algorithms are based on the following steps:

1. The vessel motions are calculated based on the original vessel properties. Then the resulting response spectra are compared with the response spectra given in the data set. This comparison is accomplished by calculating the normalized root mean square error of each vessel motion. Therefore, 6 NRMSEs are obtained in total. Then the average of these 6 values is determined.
2. For the parameter to be calibrated, a wide interval of possible values is selected.
3. By using the ‘golden section method’, we choose a value within the before mentioned interval. The ‘golden section method’ is described in the next paragraph.
4. The motion response spectra are calculated based on the new value of the parameter.
5. Similar to step 1, we compare the new response spectra with the response spectra of the data set. Again, the average value of the 6 NRMSEs is determined.
6. By comparing the two averages of the NRMSEs, of step 1 and step 5, we can obtain a smaller interval of values for the parameter. More details about the determination of the new interval of values, are provided in the description of the ‘golden section method’.
7. The process is repeated until the interval of values is acceptably small or the NRMSE cannot further be improved.

7.1.1 Golden section method

As mentioned before, the golden section method is applied to minimize the interval of values for each parameter. To understand this method, we give as example the identification of the radius of gyration, r_{xx}. The maximum NRMSE for roll motion is bracketed by a triplet of values of r_{xx}. The three different values of r_{xx} ($\alpha<\beta<\gamma$) are such that the NRMSE of the response spectrum for $r_{xx}=\beta$ is larger than the NRMSEs for $r_{xx}=\alpha$ and $r_{xx}=\gamma$. Therefore, we know that the NRMSE has a maximum within the interval $[\alpha,\gamma]$. The next step is to choose a new point χ, either between α and β or between β and γ. Suppose that we make the latter choice and then we evaluate the NRMSE for $r_{xx}=\chi$. If the NRMSE for $r_{xx}=\beta$ is larger than the NRMSE for $r_{xx}=\chi$, then the new bracketing triplet of points is $[\alpha, \beta, \chi]$. For the opposite case, the new bracketing triplet is $[\beta, \chi, \gamma]$. In all cases the middle point of the new triplet is the best maximum achieved so far. For each stage, the point χ has a fractional distance 0.61803 into the larger of the two intervals, $[\alpha,\beta]$ or $[\beta,\gamma]$ (measuring from the central point of the triplet). This fractional distance is the so called golden section or golden mean [26].

It should be clear that the limits of the NRMSE is $-\infty$, for poor approximations, and 1, for perfect approximations. Thus, we search for the appropriate modifications that lead to NRMSEs close to 1.

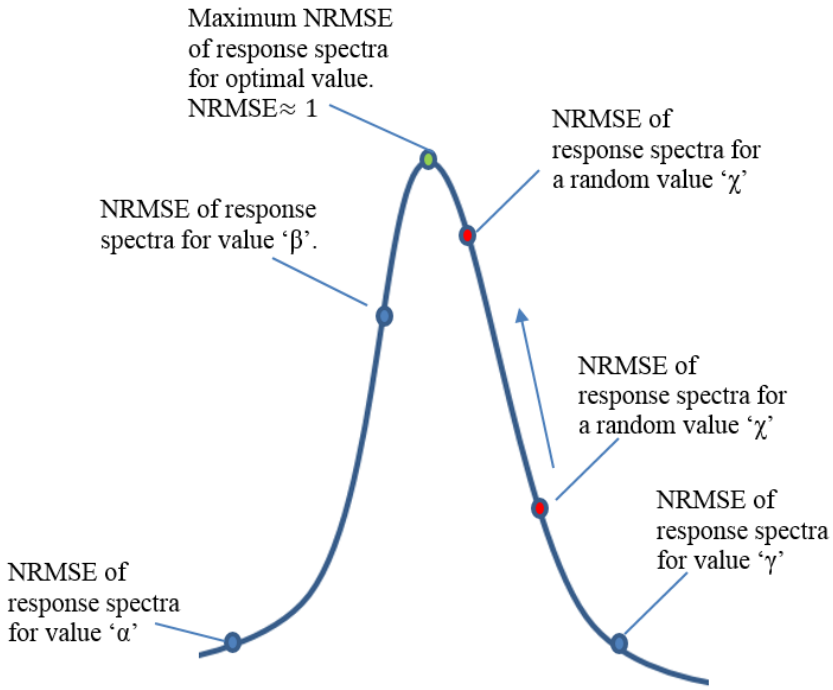

Figure 84: Golden section method

To stop the repetitions of the golden section method, the following conditions should be defined:

1. Minimum distance between the limits of the final bracketing interval.
2. Minimum difference between the resulting NRMSEs of the triplet. For example if the NMRSE for $r_{xx}=\chi$ differs from the NMRSE for $r_{xx}=\beta$ less than 0.0001, the repetitions stop.

Regarding the calibration of the CoG and the radius of gyration, we create two similar algorithms. Each coordinate of the CoG and each radius of gyration are investigated separately. As mentioned in the previous chapter, each radius of gyration mainly influences one specific motion. Thus, to calibrate the roll motion, only the radius of gyration, r_{xx}, is investigated. Also, we should only consider the NRMSE for roll motion. This is not valid for the identification of the CoG. Each coordinate influences more than one motion and as a consequence we should consider the average error of all vessel motions.

Regarding the calibration of the viscous damping, the procedure is the same as the identification of the radius of gyration. Each of the 6 elements of the viscous damping are calibrated by focusing on the corresponding motion. The sensitivity analysis showed that only extremely increased values of the viscous damping can cause considerable changes to the response spectra. As a result, the expected calibrated values are much different than the original ones. These values cannot be realistic and it is suggested to examine the viscous damping matrix at the end of the identification process.

With respect to the identification of the hydrodynamic added mass and damping, we focus on the motions showing the maximum inaccuracies. We can, thus, reduce the amount of elements that are going to be investigated. For example, if the roll motion indicates the highest error, only the elements with indices 2,4,6 are calibrated. The identification procedure of the added

mass and damping is similar to the previously described procedures. However, instead of changing each element for the entire frequency interval, we modify a conjugate pair of residues of the approximation function. For each change, the NRMSEs between the calculated and the measured response spectra are determined. Only the NRMSEs of the corresponding three coupled motions should be considered. For instance, if we want to calibrate the element ab_{44}, it is not needed to take into account the inaccuracies of surge, heave and pitch motions. The algorithm for the identification of the added mass and damping is performed for one conjugate pair of residues of one matrix element. The procedure is repeated for all the residues and all the elements (related to the coupled motions). After testing all residues of all elements, we select one pair of residues of one element that caused the maximum NRMSE.

For the calibration of the wave forces and moments, we should consider the motions with the maximum inaccuracies as well. If the pitch motion indicates the highest error, only F_1, F_3 and F_5 are calibrated. In addition, the hydrodynamic forces with directions within the range of -45° to +45° from the main wave direction are investigated. The output of this algorithm gives a modified conjugate pair of residues of a specific force with a certain wave direction.

The following table shows the starting triplets and the conditions of applying the golden section method for each parameter. This table is created based on the sensitivity analysis (CHAPTER 6):

Table 7: Golden section method-Vessel properties

Vessel Properties	Starting triplet	Minimum distance of bracketing limits	Minimum difference of NRMSEs during repetitions
x	[[redacted]m,[redacted]m,[redacted]m]	0.2m	0.0001
y	[[redacted]m,[redacted]m[redacted]m]	0.2m	0.0001
z	[[redacted]m,[redacted]m,[redacted]m]	0.2m	0.0001
r_{xx}	[[redacted]m,[redacted]m,[redacted]m]	0.2m	0.0001
r_{yy}	[[redacted]m,[redacted]m,[redacted]m]	0.2m	0.0001
r_{zz}	[[redacted]m,[redacted]m,[redacted]m]	0.2m	0.0001
B_{ad}	[0.2*B_{ad_orig}, B_{ad_orig}, 50*B_{ad_orig}]	0.5*B_{ad_orig}	0.0001
residues f_{ab}	[-50*Orig.Res, Orig.Res, 50*Orig.Res]	0.1*Orig.Res	0.001
residues f_F	[-10*Orig.Res, Orig.Res, 10*Orig.Res]	0.1*Orig.Res	0.001

The following figures show the identification algorithms for the above mentioned vessel properties.

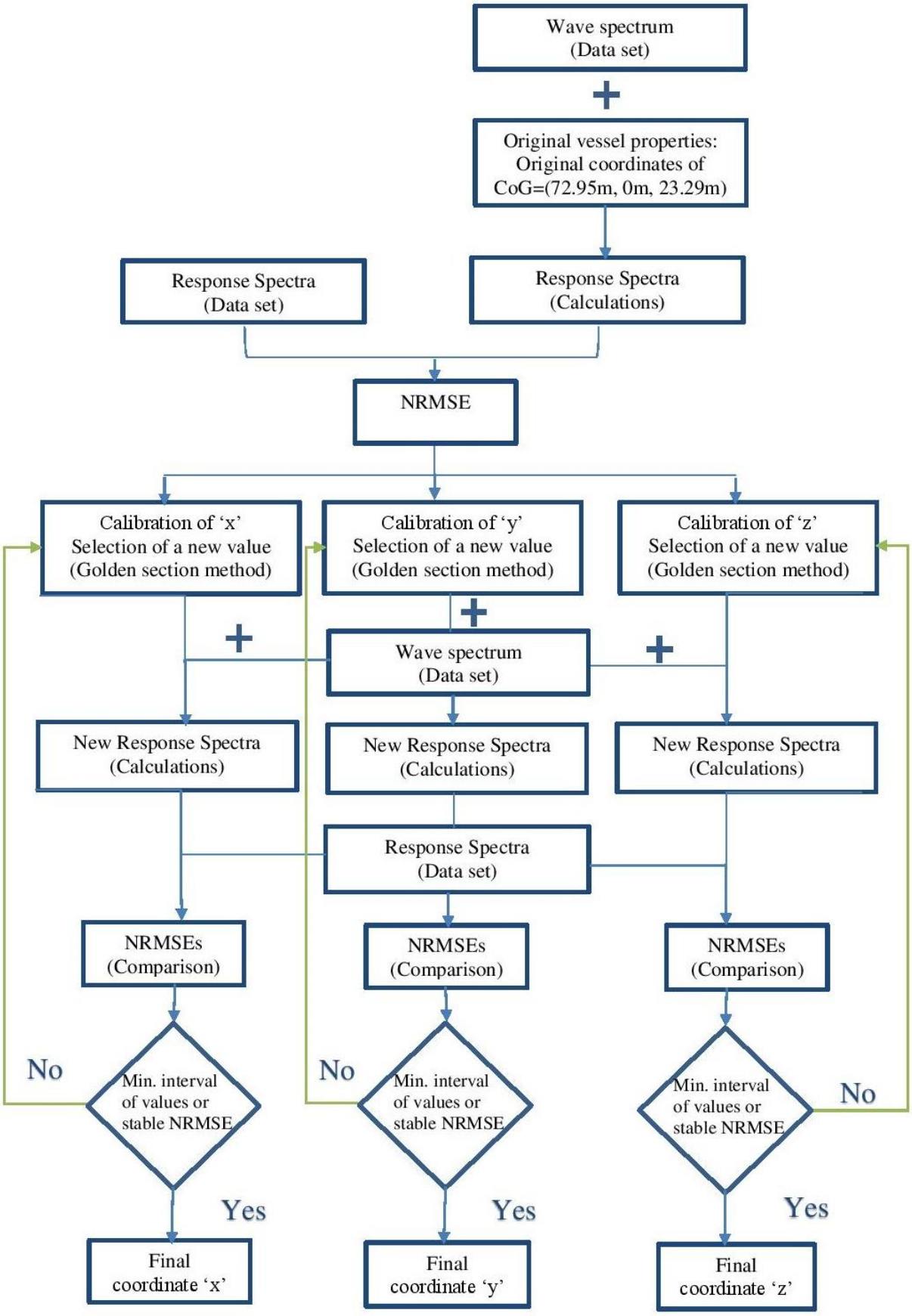

Figure 85: Identification of the CoG

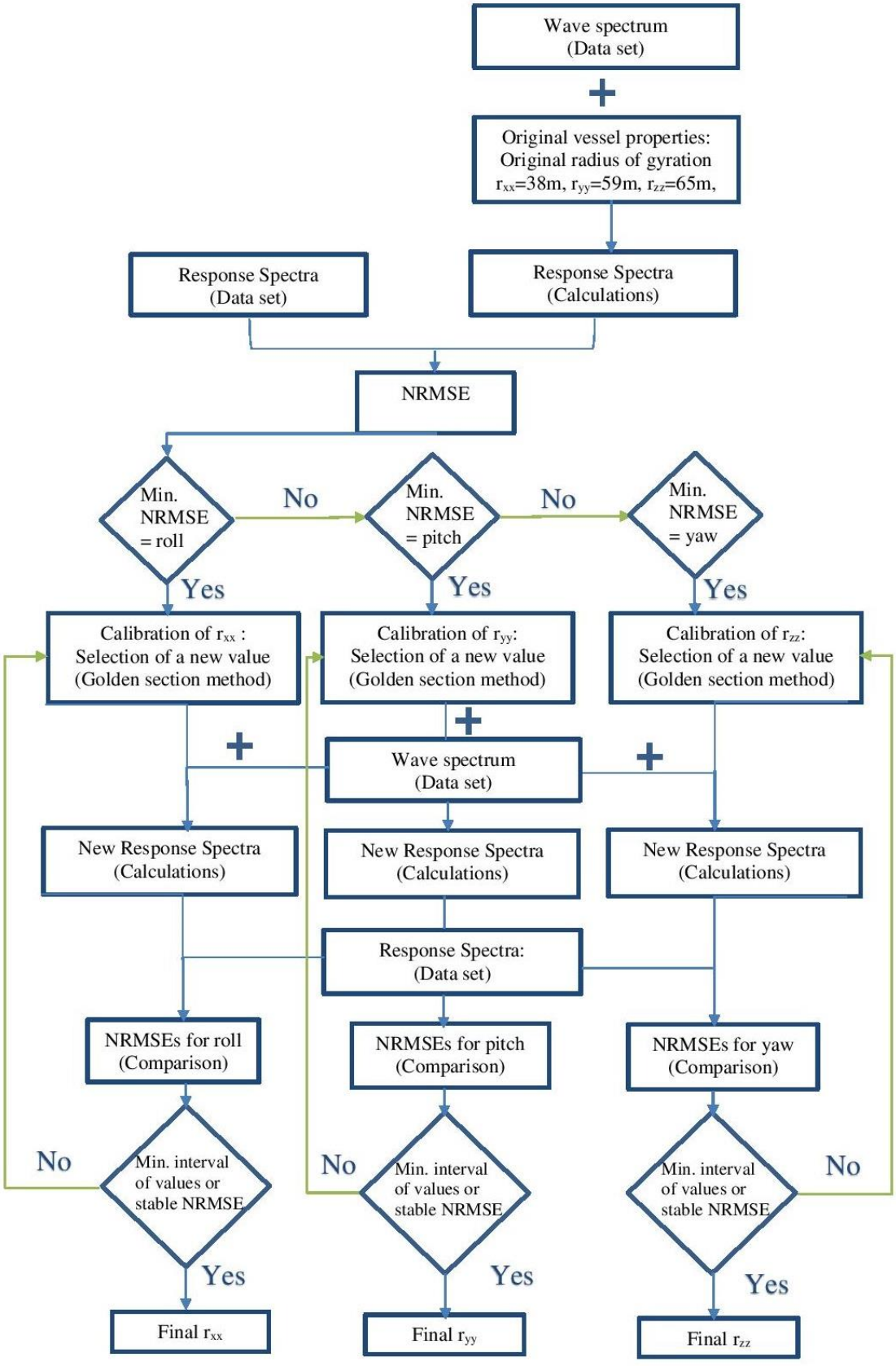

Figure 86: Identification of radius of gyration

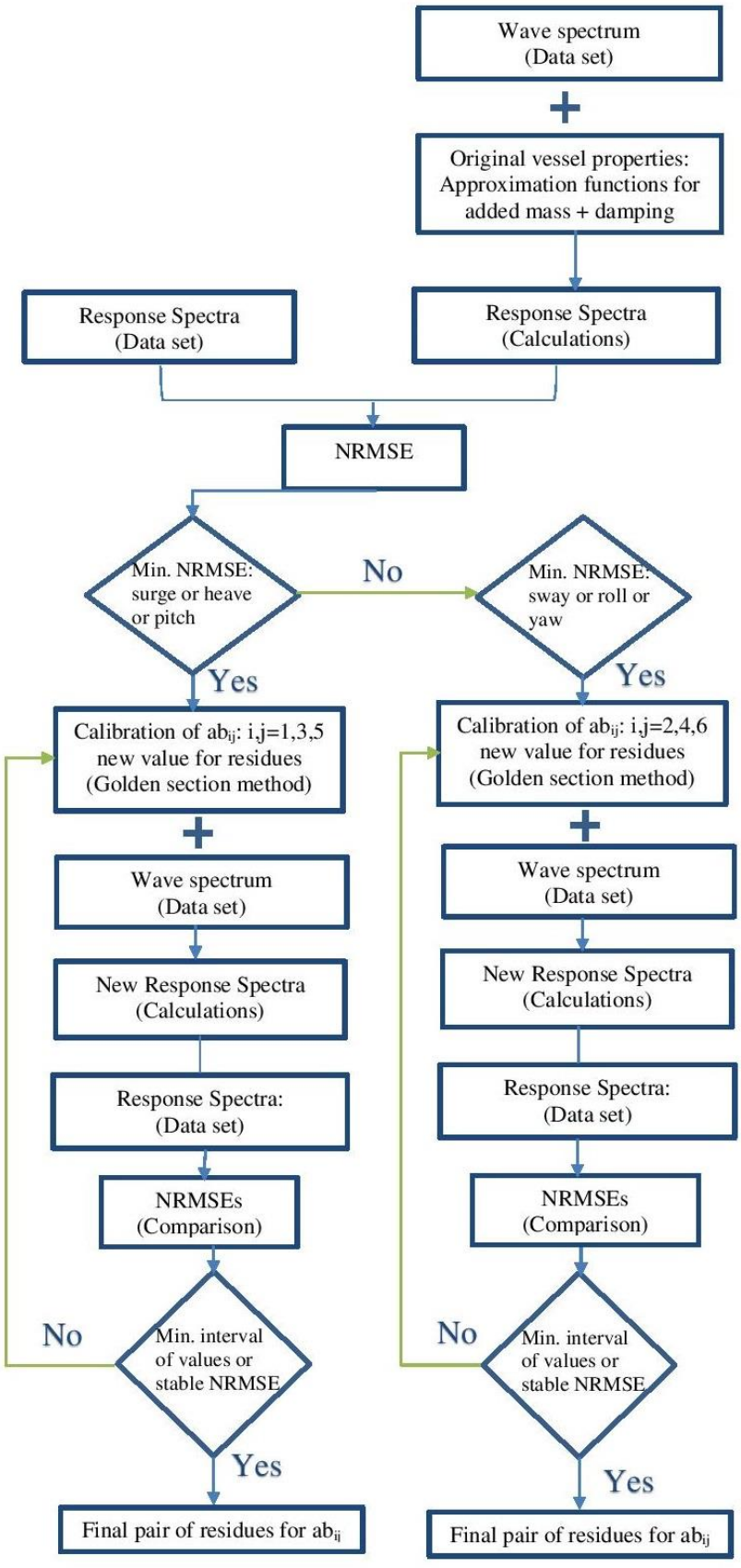

Figure 87: Identification of added mass and damping

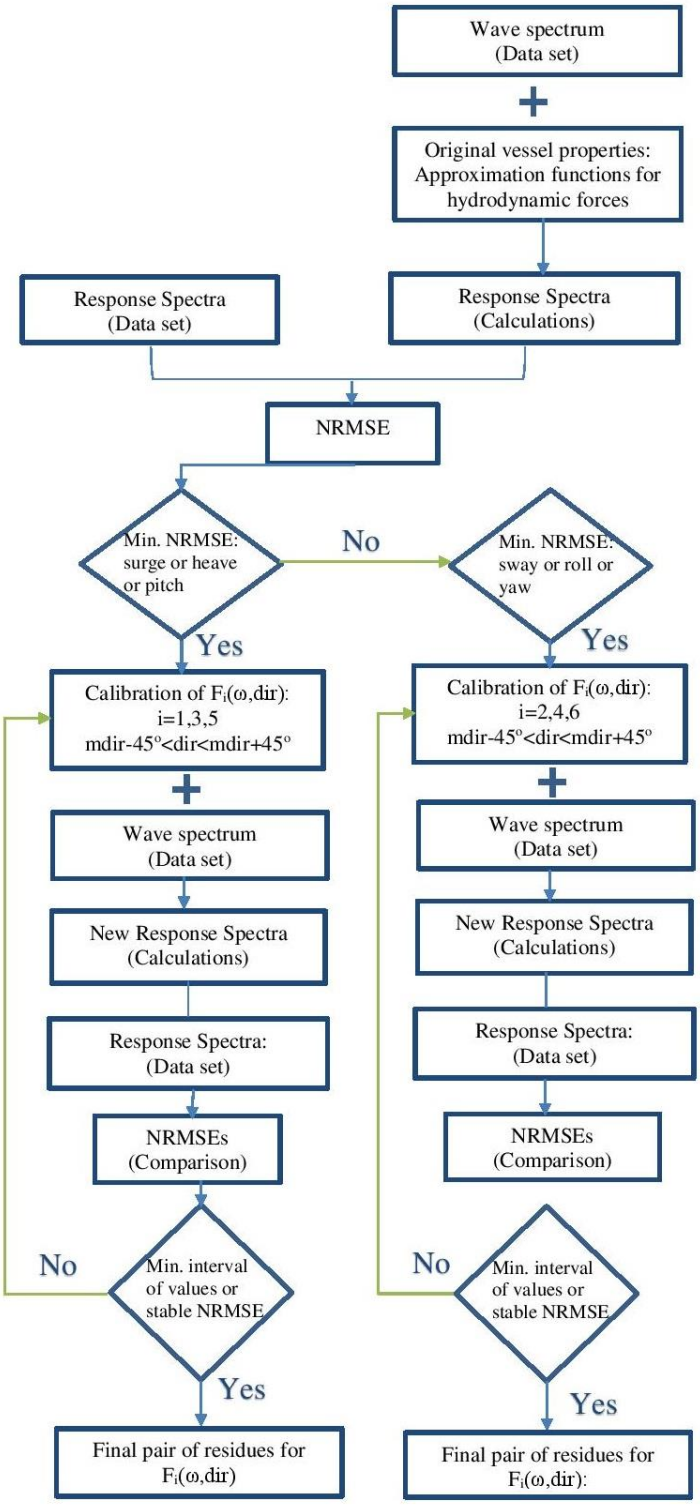

Figure 88: Identification of wave forces

In most cases, more than one parameter has to be modified. As described before, each algorithm gives one modified value of one parameter. Thus, we get 5 possible solutions (5 modified parameters). Among these 5 solutions, the parameter which leads to the maximum NRMSE is chosen. After modifying the parameter, all the algorithms are performed again. In the same way, another parameter is investigated and modified. After several repetitions the NRMSEs reach a certain limit. This means that all the possible parameters are already calibrated and any

additional change does not improve the accuracy of the calculated response spectra. The matlab scripts for the above mentioned algorithms are indicated in Appendix D.

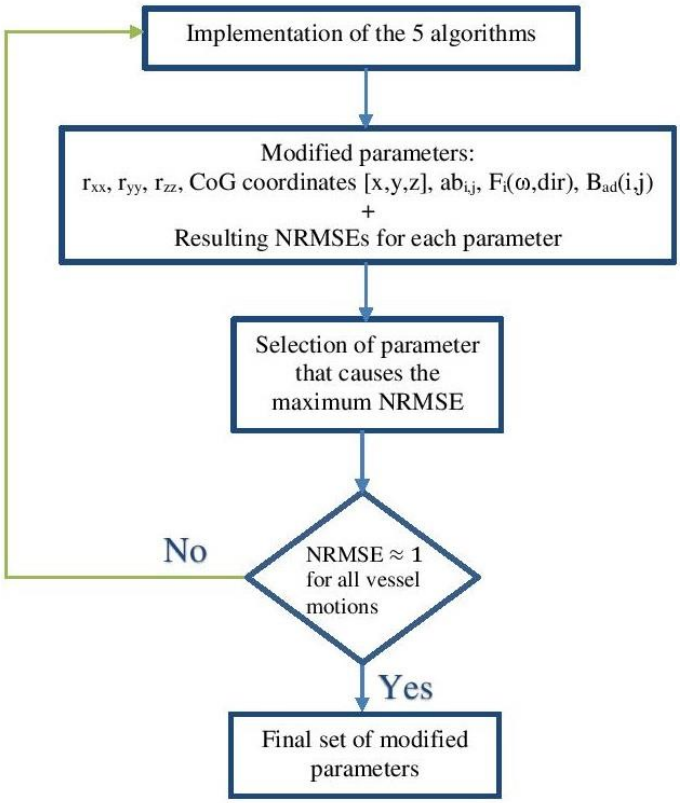

Figure 89: Final identification procedure

CHAPTER 8. Test cases

As mentioned in the previous section, the identification method is tested by several cases. For each test case, a set of simulated measurements is used. The data set of the simulated measurements consists of the following:

- The 2D wave spectrum
- The ship direction
- The response spectra. To obtain the simulated response spectra, several properties of the vessel are modified. These modifications are considered to be unknown.

Given the above mentioned data, the unknown modifications of the vessel properties should be identified by our method.

8.1 DATA PROCESSING

The procedure which is analyzed in the previous section is tested with 5 cases. For each test case, a specific set of data is received. Before starting the calibration of each vessel property, some data processing needs to be done. The data set (response spectra and wave spectrum) should be defined in the same frequency band as the calculated response spectra. The frequency interval is selected as follows: from 0.01 rad/sec to 1.7 rad/sec with a step of 0.01rad/sec. If the 2D wave spectrum and the response spectra, given in the data set, were not measured for all of the frequencies in the above mentioned interval, a frequency interpolation should be done. Also, the hydrodynamic database is not given for a frequency interval of a specific step. Thus, it is necessary to achieve a frequency interpolation for the added mass, damping and wave forces and moments.

Another important aspect of the measurement data is the axis system of the 2D wave spectrum. The reference point of the 2D wave spectrum is the North [27]. For example, the waves coming from the North have 0^o of heading [27]. However, in order to calculate the direction-dependent RAOs, we used the coordinate system of the ship (CHAPTER 4). Therefore, we should clarify the following:

- The headings of the calculated RAOs correspond to the local coordinate system of the ship.
- The wave directions are measured according to the coordinate system of the 2D wave spectrum.
- The heading of the vessel is calculated clockwise from the North.

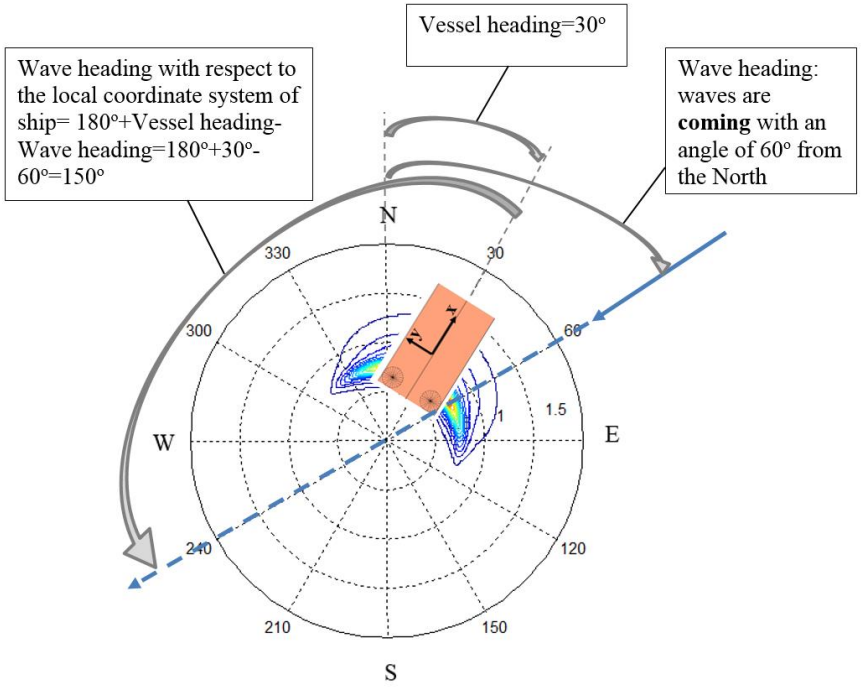

Figure 90: Coordinate system for the ship and the 2D wave spectrum

To calculate the response spectra by using the 2D wave spectrum of the data set, the directional RAOs are redefined by the following transformation:

$$\mathbf{RAO}_{\mathbf{final}}(\omega, dir_{waves}) = \mathbf{RAO}_{\mathbf{calculations}}(\omega, 180^{o}+\text{Vessel heading}-dir_{waves}) \quad \text{Eq. 8-1}$$

where dir_{waves} is the wave heading regarding the 2D wave spectrum and the quantity (180^{o}+Vessel heading-dir_{waves}) is the corresponding wave heading according to the local coordinate system of the vessel.

For all of the test cases, the 2D wave spectrum is measured for a larger number of wave directions (ex. step of 10^{o}) than the number of directions of the calculated RAOs. Therefore, a linear interpolation of the RAOs over the wave directions should be performed.

For each test case, the 1D and 2D wave spectra are shown. The 2D wave spectrum is also shown in a format in which the wave directions are calculated according to the local coordinate system of the ship.

8.1.1 Impact of data processing

It should be emphasized that the data set (response spectra and wave spectrum) should provide information about a range of frequencies comparable with the range of frequencies of the calculations. Suppose that the frequency step of the data set is much larger than the frequency step of the hydrodynamic database. The simulated response spectra will probably show a smaller number of resonant peaks than the calculated response spectra. Therefore, the inaccuracies are large and the results of the identification procedure is not valid.

Additional inaccuracies can also be caused by the interpolation of the RAOs over the wave directions. There are several methods to accomplish this interpolation. For example, we can make a linear interpolation of the wave forces over the wave directions and then calculate the corresponding RAOs. Instead of interpolating the wave forces, it is also possible to interpolate the amplitude of the RAOs. It was noticed that the different methods of interpolating over the wave directions influence the resulting response spectra. This effect will be illustrated by the results of the first test case.

8.2 TEST CASE 1

For the first test case, the response spectra of the data set are obtained without changing any of the standard vessel properties. Thus, the response spectra from our calculations should be the same as the response spectra from the data set. The 1D and 2D wave spectra are indicated in the following figures. The wave directions of the second depiction of the 2D wave spectrum correspond to the local coordinate system of the vessel. The heading of the Thialf is 45°.

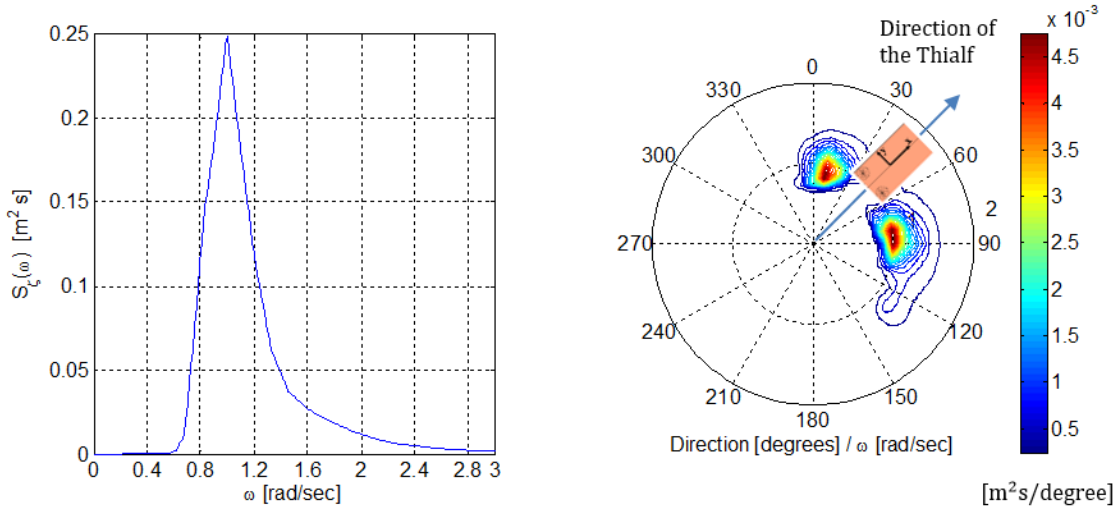

Figure 91: 1D and 2D wave spectra, test case 1

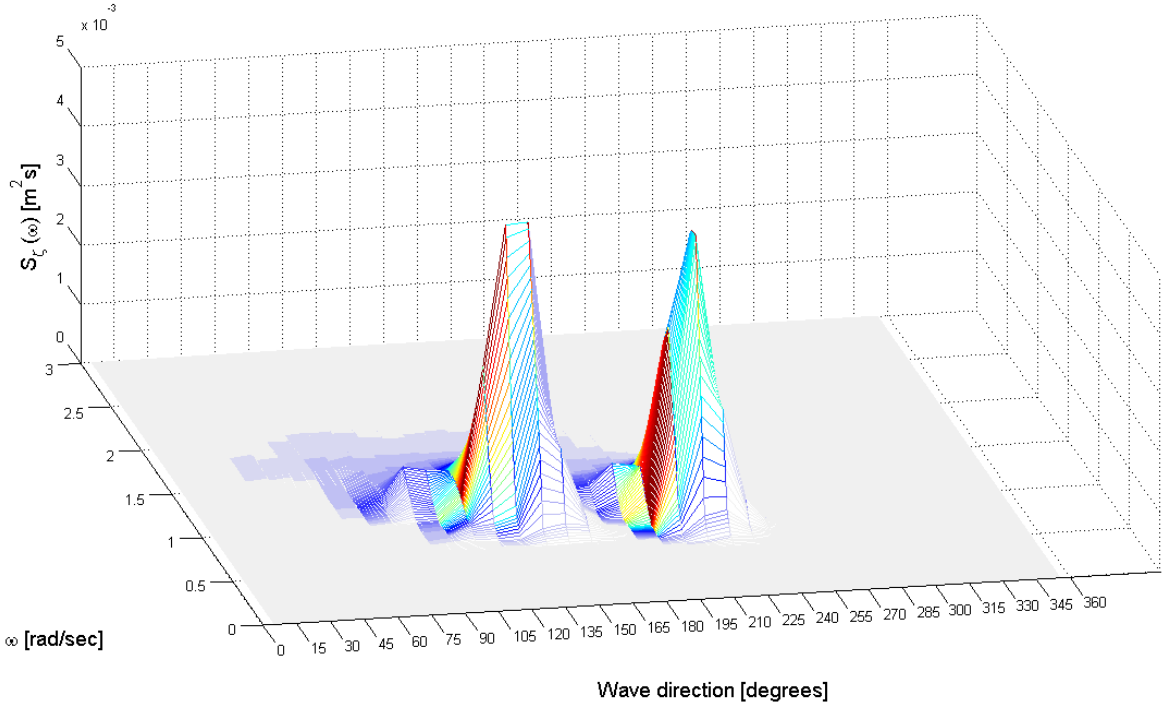

Figure 92: 2D wave spectrum, local coordinate system of the vessel, test case 1

The response spectra are first calculated by interpolating the wave forces and secondly by interpolating the amplitude of the RAOs. The resulting vessel motions of both interpolations are compared with the response spectra of the data set.

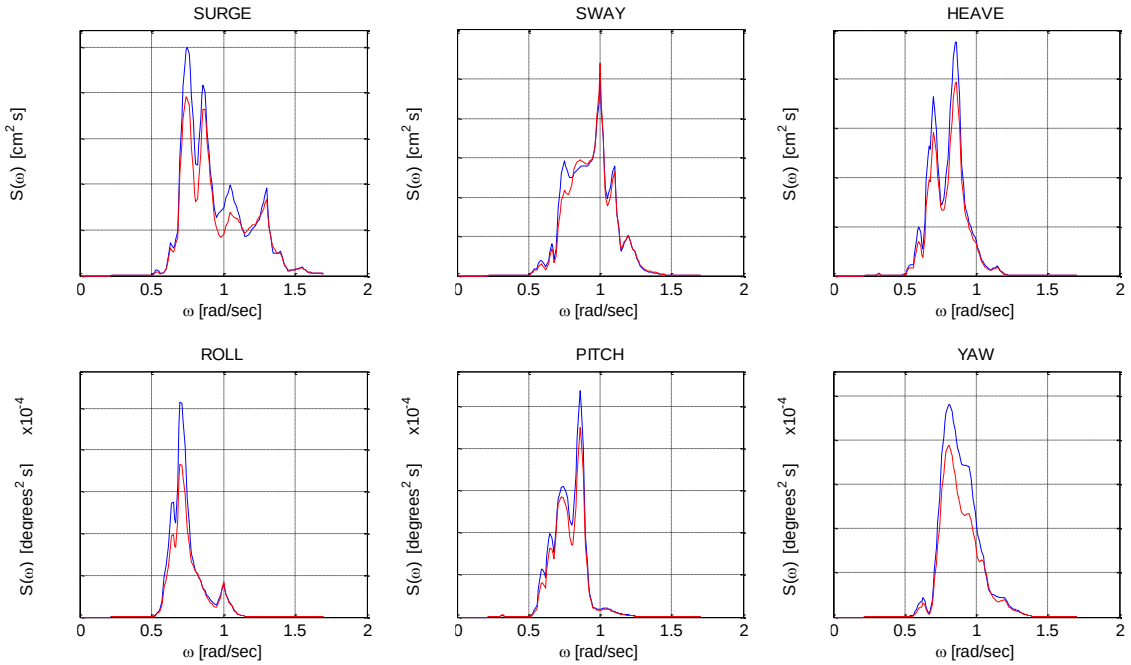

Figure 93: Comparison of motion response spectra, interpolation of wave forces, data set=blue, calculations=red

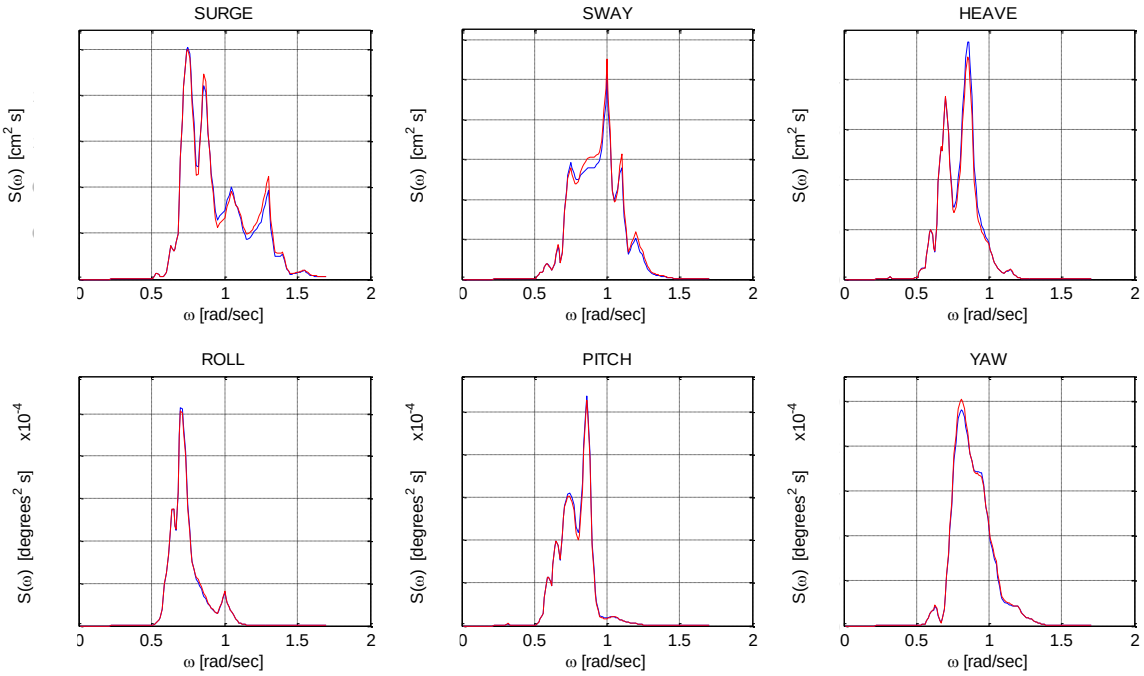

Figure 94: Comparison of motion response spectra, interpolation of RAOs, data set=blue, calculations=red

As can be seen, by interpolating the amplitude of the RAOs over the wave directions, the resulting response spectra approximate the response spectra of the data set with great accuracy. However, there are still some small variations which may influence the results of the identification procedure.

8.3 TEST CASE 2

The wave spectra for the second test case are indicated in the following figure. The heading of the Thialf is -30°.

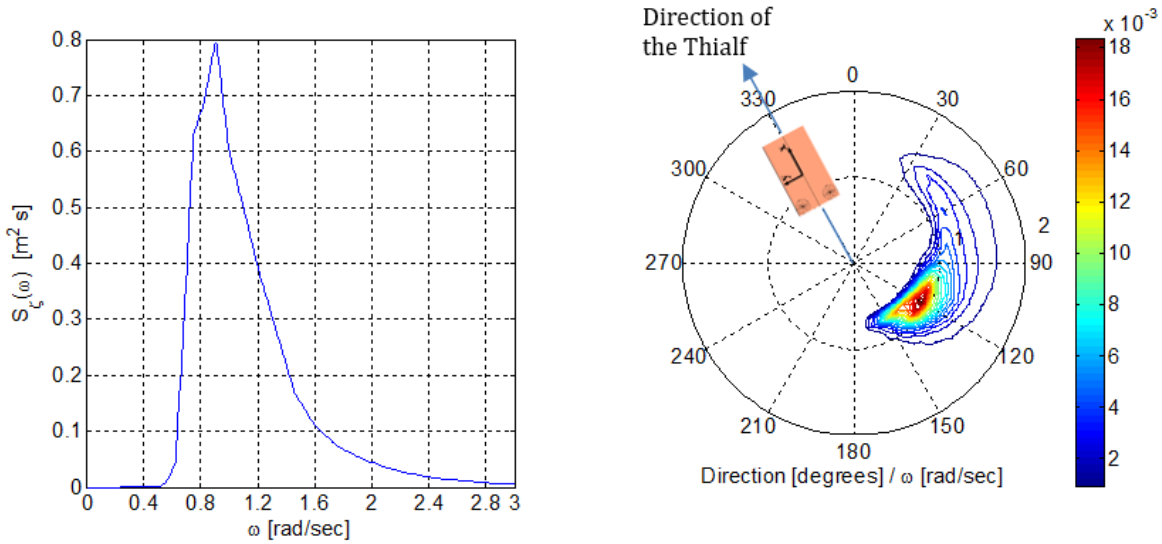

Figure 95: 1D and 2D wave spectra, test case 2

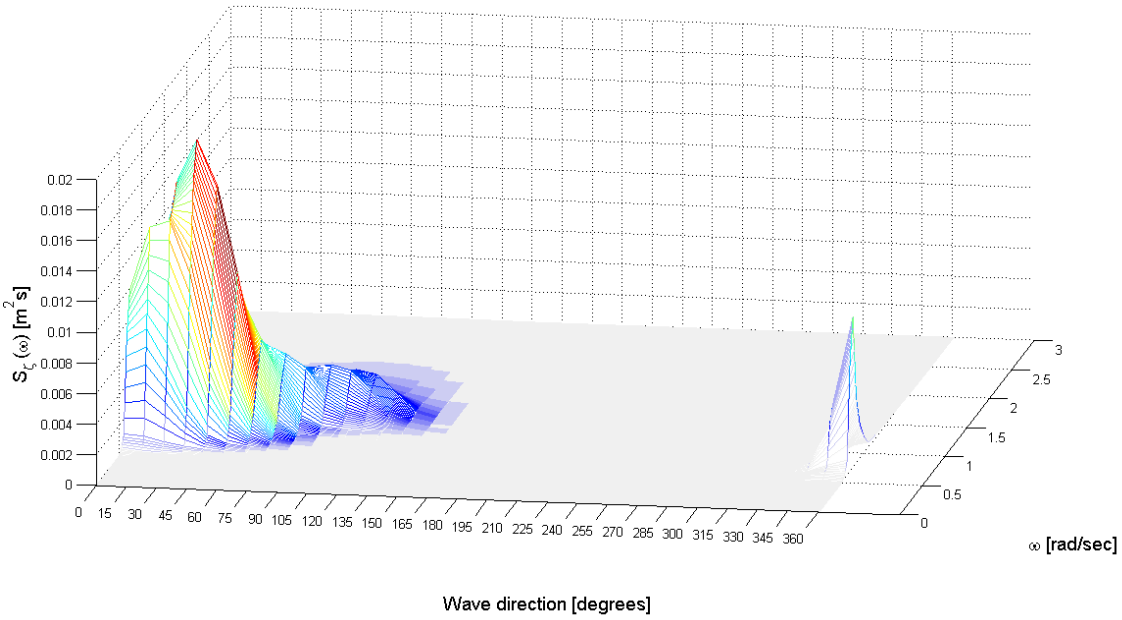

Figure 96: 2D wave spectrum, local coordinate system of the vessel, test case 2

The response spectra based on the original properties of the Thialf are compared with the response spectra of the data set. The resulting NRMSEs for each vessel motion are the following: surge=0.985, sway=0.906, heave=0.941, roll=0.739, pitch=0.142, yaw=0.787. In the next figure, the calculated response spectra are plotted together with the response spectra from the data set.

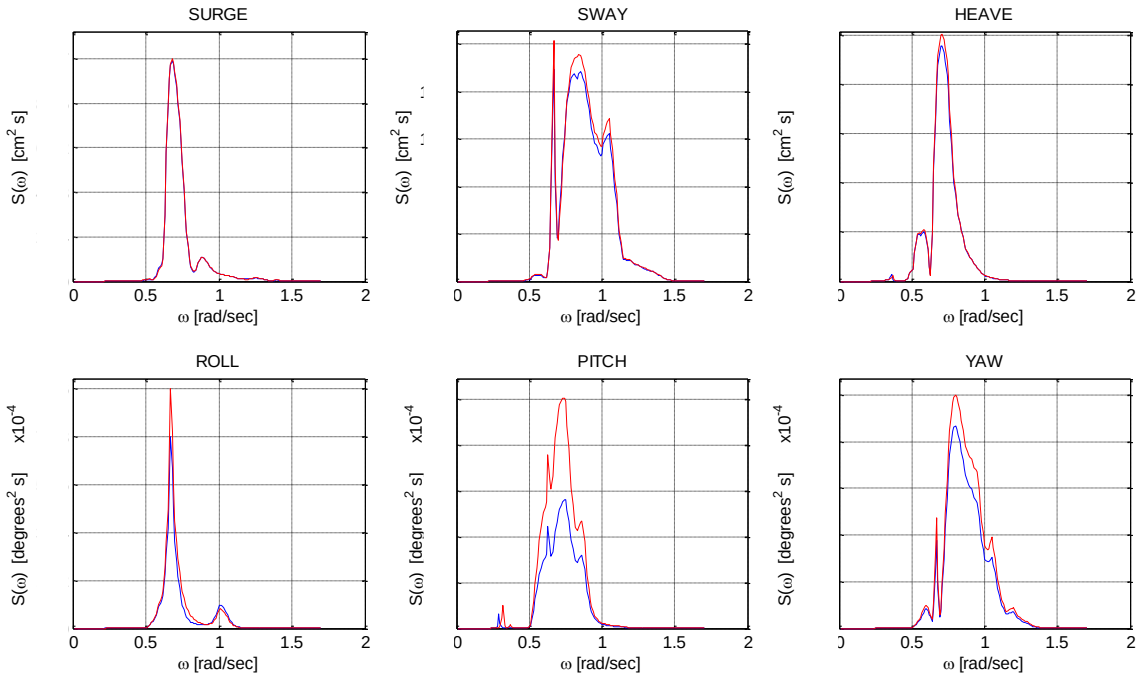

Figure 97: Comparison of response spectra, test case 2, data set=blue, calculations=red

The results from the first repetition of the identification procedure are given in the following tables (the parameters which cause considerable improvements on the response spectra are in bold and italic letters):

Table 8: Identification of CoG, x coordinate, test case 2

Coordinate	Original value	New value	Modification
x (m)	[redacted]	[redacted]	1.81
NRMSE	Before calibration	After calibration	Improvement
Surge	0.985	0.985	0.000
Sway	0.906	0.914	0.008
Heave	0.941	0.985	0.044
Roll	0.739	0.737	-0.003
Pitch	0.142	0.108	-0.034
Yaw	0.787	0.779	-0.008
Average (NRMSEs)	0.750	0.751	0.001

Table 9: Identification of CoG, y coordinate, test case 2

Coordinate	Original value	New value	Modification
y (m)	[redacted]	[redacted]	3.28
NRMSE	Before calibration	After calibration	Improvement
Surge	0.985	0.983	0.000
Sway	0.906	0.904	0.008
Heave	0.941	0.933	0.044
Roll	0.739	0.743	-0.003
Pitch	0.142	0.142	-0.034
Yaw	0.787	0.803	-0.008
Average (NRMSEs)	0.750	0.751	0.001

Table 10: Identification of CoG, z coordinate, test case 2

Coordinate	Original value	New value	Modification
z (m)	[redacted]	[redacted]	11.15
NRMSE	Before calibration	After calibration	Improvement
Surge	0.985	0.945	-0.040
Sway	0.906	0.899	-0.008
Heave	0.941	0.974	0.033
Roll	0.739	0.670	-0.070
Pitch	0.142	0.621	0.479
Yaw	0.787	0.794	0.006
Average (NRMSEs)	0.750	0.817	0.067

Table 11: Identification of radii of gyration, test case 2

Radii of gyration	Original value	New value	Modification
r_{xx} (m)	[redacted]	[redacted]	3
r_{yy} (m)	[redacted]	[redacted]	***9***
r_{zz} (m)	[redacted]	[redacted]	4
NRMSE	Before calibration	After calibration	Improvement
Roll motion (r_{xx})	0.739	0.929	0.190
Pitch motion (r_{yy})	***0.143***	***0.908***	***0.766***
Yaw motion (r_{zz})	0.787	0.978	0.191

Table 12: Identification of hydrodynamic added mass and damping, test case 2

Pair of residues	Original value (amp.)	New value (amp.)	Modification
c=1-2 for ab_{55}	***6.00E+06***	***4.51E+07***	***-7.52 · Orig.value***
NRMSE	Before calibration	After calibration	Improvement
Surge	0.985	0.991	0.006
Heave	0.941	0.963	0.021
Pitch	***0.142***	***0.827***	***0.685***

Table 13: Identification of hydrodynamic forces, test case 2

Pair of residues	Original value (amp.)	New value (amp.)	Modification
c=9-10 for $F_5(\omega,15^o)$	***2.64E+05***	***1.03E+05***	***0.39 · Orig.value***
NRMSE	Before calibration	After calibration	Improvement
Surge	0.985	0.934	-0.051
Heave	0.941	0.944	0.003
Pitch	***0.142***	***0.677***	***0.535***

Table 14: Identification of viscous damping, test case 2

Element	Original value	New value	Modification
$\mathbf{B_{ad}}(1,1)$ (kNs/m)	[redacted]	[redacted]	18.7 ·Orig.value
$\mathbf{B_{ad}}(2.2)$ (kNs/m)	[redacted]	[redacted]	19.1 ·Orig.value
$\mathbf{B_{ad}}(3.3)$ (kNs/m)	[redacted]	[redacted]	4.8 ·Orig.value
$\mathbf{B_{ad}}(4,4)$ (kNsm^2/m)	[redacted]	[redacted]	29.0 ·Orig.value
B_{ad}(5,5) (kNsm^2/m)	[redacted]	[redacted]	***47.3 ·Orig.value***
$\mathbf{B_{ad}}(6,6)$ (kNsm^2/m)	[redacted]	[redacted]	49.6 ·Orig.value
NRMSE	Before calibration	After calibration	Improvement
Surge motion-$\mathbf{B_{ad}}(1,1)$	0.985	0.991	0.006
Sway motion-$\mathbf{B_{ad}}(2,2)$	0.906	0.954	0.047
Heave motion-$\mathbf{B_{ad}}(3,3)$	0.941	0.975	0.033
Roll motion-$\mathbf{B_{ad}}(4,4)$	0.739	0.936	0.197
Pitch motion-B_{ad}(5,5)	***0.142***	***0.860***	***0.721***
Yaw motion-$\mathbf{B_{ad}}(6,6)$	0.787	0.899	0.111

According to the above tables, the pitch motion indicates the highest inaccuracies (NRMSE=0.142). The identification procedure showed that this motion is improved by the modification of several elements: r_{yy} or ab_{55} or $F_5(\omega,15^o)$ or $\mathbf{B_{ad}}(5,5)$. Among these elements we select to modify $r_{yy,}$ since that leads to the maximum NRMSE. By increasing the original value of r_{yy} (+9m), the NRMSE becomes 0.908.

Regarding the roll and yaw motions, the maximum NRMSE is accomplished by modifying r_{xx} and r_{zz}, respectively. For the radius of gyration, r_{xx}, it is suggested to keep the original value. In most cases, the mass distribution is symmetrical around the x axis of the vessel and r_{xx} doesn't show high deviations. It should be noticed that the element $\mathbf{B_{ad}}(4,4)$ improves the accuracy of roll motion as well. However the original value of $\mathbf{B_{ad}}(4,4)$ is highly increased (29.0*Original value). Thus, the modification of $\mathbf{B_{ad}}(4,4)$ is rejected. To sum up, after the first repetition of the identification procedure, we make the following changes: r_{yy}=[redacted]m, r_{zz}=[redacted]m. Then, the identification procedure is carried out again. For the second repetition, the calibration of the radius of gyration is excluded. Thus, the following tables are obtained:

Table 15: Identification of CoG, x coordinate, 2nd repetition, test case 2

Coordinate	Original value	New value	Modification
x (m)	[redacted]	[redacted]	0.89
NRMSE	Before calibration	After calibration	Improvement
Surge	0.985	0.985	0.000
Sway	0.903	0.906	0.004
Heave	0.970	0.985	0.015
Roll	0.740	0.738	-0.001
Pitch	0.908	0.906	-0.003
Yaw	0.978	0.977	-0.001
Average (NRMSEs)	0.914	0.916	0.002

Table 16: Identification of CoG, y coordinate, 2nd repetition, test case 2

Coordinate	Original value	New value	Modification
y (m)	[redacted]	[redacted]	-1.55
NRMSE	Before calibration	After calibration	Improvement
Surge	0.985	0.986	0.001
Sway	0.903	0.903	0.001
Heave	0.970	0.972	0.002
Roll	0.740	0.736	-0.004
Pitch	0.908	0.909	0.000
Yaw	0.978	0.978	0.000
Average (NRMSEs)	0.914	0.914	0.000

Table 17: Identification of CoG, z coordinate, 2nd repetition, test case 2

Coordinate	Original value	New value	Modification
z (m)	[redacted]	[redacted]	1.00
NRMSE	Before calibration	After calibration	Improvement
Surge	0.985	0.981	-0.003
Sway	0.903	0.908	0.005
Heave	0.970	0.972	0.002
Roll	0.740	0.738	-0.001
Pitch	0.908	0.917	0.008
Yaw	0.978	0.978	0.000
Average (NRMSEs)	0.914	0.916	0.002

Table 18: Identification of hydrodynamic added mass and damping, 2nd repetition, test case 2

Pair of residues	Original value (amp.)	New value (amp.)	Modification
c=7-8 for ab_{44}	***2.66E+07***	***2.24E+07***	***0.84 ·Orig.value***
NRMSE	Before calibration	After calibration	Improvement
Sway	0.903	0.907	0.004
Roll	***0.740***	***0.928***	***0.188***
Yaw	0.978	0.972	-0.006

Table 19: Identification of hydrodynamic forces, 2nd repetition, test case 2

Pair of residues	Original value (amp.)	New value (amp.)	Modification
c=11-12 for $F_4(\omega,30^o)$	***1.81E+04***	***1.12E+04***	***0.62 · Orig.value***
NRMSE	Before calibration	After calibration	Improvement
Sway	0.903	0.928	0.025
Roll	***0.740***	***0.897***	***0.157***
Yaw	0.978	0.967	-0.011

Table 20: Identification of viscous damping, 2nd repetition, test case 2

Element	Original value	New value	Modification
$\mathbf{B_{ad}}(1,1)$ (kNs/m)	[redacted]	[redacted]	15.3 ·Orig.value
$\mathbf{B_{ad}}(2.2)$ (kNs/m)	[redacted]	[redacted]	21.4 ·Orig.value
$\mathbf{B_{ad}}(3.3)$ (kNs/m)	[redacted]	[redacted]	3.09 ·Orig.value
B_{ad}(4,4) (kNsm²/m)	[redacted]	[redacted]	***27.9 ·Orig.value***
$\mathbf{B_{ad}}(5,5)$ (kNsm²/m)	[redacted]	[redacted]	0.51 ·Orig.value
$\mathbf{B_{ad}}(6,6)$ (kNsm²/m)	[redacted]	[redacted]	0.51 ·Orig.value
NRMSE	Before calibration	After calibration	Improvement
Surge motion-$\mathbf{B_{ad}}(1,1)$	0.985	0.997	0.012
Sway motion-$\mathbf{B_{ad}}(2,2)$	0.903	0.943	0.040
Heave motion-$\mathbf{B_{ad}}(3,3)$	0.970	0.980	0.010
Roll motion-B_{ad}(4,4)	***0.740***	***0.911***	***0.171***
Pitch motion-$\mathbf{B_{ad}}(5,5)$	0.908	0.909	0
Yaw motion-$\mathbf{B_{ad}}(6,6)$	0.978	0.978	0

The second repetition focuses on the improvement of the roll motion. The elements, which should be modified, are either ab_{44} or $F_4(\omega,30^o)$ or $\mathbf{B_{ad}}(4,4)$. The element $\mathbf{B_{ad}}(4,4)$ is rejected for the same reasons as explained in the previous paragraph. Between ab_{44} and $F_4(\omega,30^o)$, we select the parameter that gives the highest NRMSE: ab_{44}. The resulting NRMSE for roll motion is 0.928. The identification procedure is then repeated again for a 3rd time.

Table 21: Identification of CoG, x coordinate, 3rd repetition, test case 2

Coordinate	Original value	New value	Modification
x (m)	[redacted]	[redacted]	***1.45***
NRMSE	Before calibration	After calibration	Improvement
Surge	0.985	0.985	0.000
Sway	***0.903***	***0.913***	***0.010***
Heave	***0.970***	***0.990***	***0.019***
Roll	0.928	0.928	0.000
Pitch	0.908	0.908	-0.006
Yaw	0.972	0.970	-0.003
Average (NRMSEs)	0.944	0.948	0.003

Table 22: Identification of CoG, y coordinate, 3rd repetition, test case 2

Coordinate	Original value	New value	Modification
x (m)	[redacted]	[redacted]	-0.96
NRMSE	Before calibration	After calibration	Improvement
Surge	0.985	0.985	0.000
Sway	0.903	0.907	0.004
Heave	0.970	0.972	-0.001
Roll	0.928	0.927	0.000
Pitch	0.908	0.908	0.000
Yaw	0.972	0.972	0.000
Average (NRMSEs)	0.944	0.945	0.001

Table 23: Identification of CoG, z coordinate, 3rd repetition, test case 2

Coordinate	Original value	New value	Modification
z (m)	[redacted]	[redacted]	***1.40***
NRMSE	Before calibration	After calibration	Improvement
Surge	0.985	0.980	-0.005
Sway	***0.903***	***0.915***	***0.012***
Heave	0.970	0.973	0.003
Roll	***0.928***	***0.938***	***0.010***
Pitch	0.908	0.915	0.008
Yaw	0.972	0.973	0.001
Average (NRMSEs)	0.944	0.949	0.005

Table 24: Identification of hydrodynamic added mass and damping, 3rd repetition, test case 2

Pair of residues	Original value (amp.)	New value (amp.)	Modification
c=17-18 for ab_{22}	***1.34E+02***	***4.10E+03***	***30.52 ·Orig.value***
NRMSE	Before calibration	After calibration	Improvement
Sway	***0.907***	***0.953***	***0.046***
Roll	0.928	0.931	0.003
Yaw	0.972	0.973	0.001

Table 25: Identification of hydrodynamic forces, 2nd repetition, test case 2

Pair of residues	Original value (amp.)	New value (amp.)	Modification
c=25-26 for $F_2(\omega,30^o)$	***86.42***	***725.05***	***-8.39 ·Orig.value***
NRMSE	Before calibration	After calibration	Improvement
Sway	***0.903***	***0.938***	***0.035***
Roll	0.928	0.933	0.005
Yaw	0.972	0.971	-0.001

Table 26: Identification of viscous damping, 3rd repetition, test case 2

Element	Original value	New value	Modification
B_{ad}(1,1) (kNs/m)	[redacted]	[redacted]	***15.3 ·Orig.value***
B_{ad}(2.2) (kNs/m)	[redacted]	[redacted]	***19.7 ·Orig.value***
B_{ad}(3.3) (kNs/m)	[redacted]	[redacted]	3.09 ·Orig.value
B_{ad}(4,4) (kNsm^2/m)	[redacted]	[redacted]	2.69 ·Orig.value
B_{ad}(5,5) (kNsm^2/m)	[redacted]	[redacted]	0.51 ·Orig.value
B_{ad}(6,6) (kNsm^2/m)	[redacted]	[redacted]	1 ·Orig.value
NRMSE	Before calibration	After calibration	Improvement
Surge motion-B_{ad}(1,1)	***0.985***	***0.997***	***0.012***
Sway motion-B_{ad}(2,2)	***0.903***	***0.937***	***0.034***
Heave motion-**B_{ad}**(3,3)	0.970	0.975	0.005
Roll motion-**B_{ad}**(4,4)	0.928	0.930	0.002
Pitch motion-**B_{ad}**(5,5)	0.908	0.908	0
Yaw motion-**B_{ad}**(6,6)	0.978	0.978	0

After completing the third repetition, the NRMSEs were not improved significantly. However, it should be noticed that the modification of the element ab_{22} caused the highest improvement on the sway motion. The real and imaginary parts of the residues, 17-18, are increased 30.52 times. The resulting NRMSE of the response spectrum for sway becomes 0.953. The coordinates of the CoG also caused some improvements. The last repetition of the identification process will, therefore, be accomplished by only investigating the coordinates of the CoG.

Table 27: Identification of CoG, z coordinate, 4th repetition, test case 2

Coordinate	Original value	New value	Modification
z (m)	[redacted]	[redacted]	***1.80***
NRMSE	Before calibration	After calibration	Improvement
Surge	0.985	0.985	-0.000
Sway	0.953	0.957	0.004
Heave	0.970	0.970	0.000
Roll	0.931	0.938	0.007
Pitch	***0.908***	***0.918***	***0.010***
Yaw	0.973	0.973	0.000
Average (NRMSEs)	0.953	0.958	0.004

As mentioned before, the response spectra of the data set were obtained by making specific changes on the vessel properties. To validate the results of the identification procedure, these changes should now be revealed and compared with the identified modifications. The identified and the real changes are compared in the following table.

Table 28: Final results: Test case 2

Elements	Original values	Identified changes	Real changes	Comparison (real and identified changes)
r_{yy} (m)	[redacted]	[redacted] (+15 % ·Orig.value)	[redacted] (+10% ·Orig.value)	3 (5% ·Orig.value)
r_{zz} (m)	[redacted]	[redacted] (+6% ·Orig.value)	[redacted] (+5% ·Orig.value)	1 (1% ·Orig.value)
c=7-8 for ab_{44}	-2.60E07- 5.57E06i/ -2.60E07+5.57E06i	0.84·Orig.value	-	-
c=17-18 for ab_{22}	72.5 + 113.05i/ 72.5 - 113.05i	30.52·Orig.value	-	-
z coordinate (m)	[redacted]	[redacted] (+6 % ·Orig.value)	[redacted] (+20% ·Orig.value)	3.31 (14% ·Orig.value)

Table 29: Final NRMSEs: Test case 2

Motions	NRMSE-Identification	NRMSE-Solution
Surge	0.985	0.969
Sway	0.957	0.920
Heave	0.970	0.970
Roll	0.938	0.720
Pitch	0.918	0.904
Yaw	0.973	0.946
Average (NRMSEs)	0.957	0.905

The deviations between the identified and the real values of the parameters r_{yy}, r_{zz} and 'z' are 5%, 1% and 14% of the original values, respectively. The identified values of r_{yy} and r_{zz} are

satisfying. However, the identified value of the z coordinate is considerably smaller than the correct value. In addition, some extra parameters need to be modified during the identification procedure: the elements ab_{44} and ab_{22}.

As can be seen in Table 29, even if we calculate the response spectra based on the real changes of the standard vessel properties, there are still some inaccuracies. It should be noticed that the NRMSEs caused by the real changes are smaller than the NRMSEs caused by the identified changes. The inaccuracies due to the data processing are thus seen to affect the identification procedure.

The resulting response spectra based on the identified modifications and the response spectra based on the real changes of the standard vessel properties are shown in the following figures:

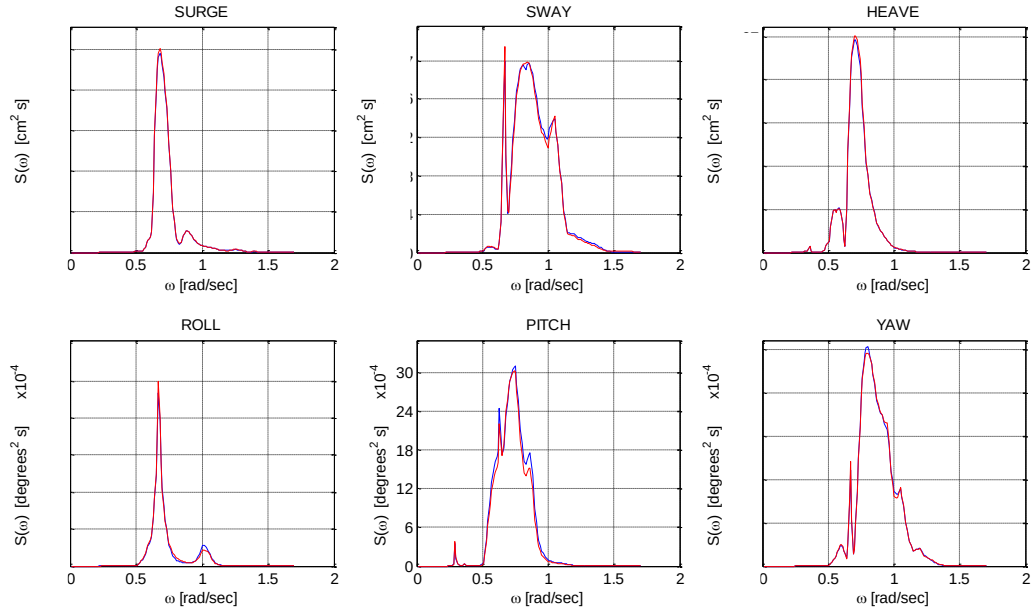

Figure 98: Motion response spectra, identification method, test case 2, data set=blue, calculations=red

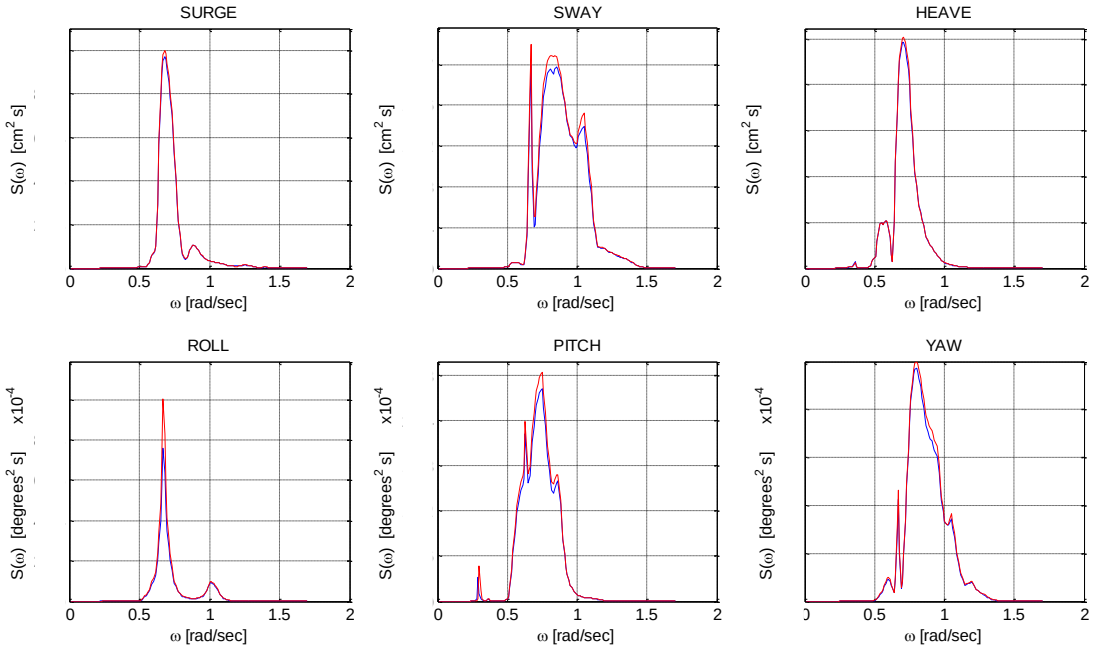

Figure 99: Motion response spectra, solution, test case 2, data set=blue, calculations=red

It is also important to calculate the significant value of each vessel motion based on the following response spectra:

- Response spectra given in the data set: Specified as 'Data'
- Calculated response spectra based on the original vessel properties: Specified as 'Original'
- Calculated response spectra based on the identified changes: Specified as 'Identification'
- Calculated response spectra based on the real changes: Specified as 'Solution'

The significant values of each motion for the above-mentioned cases are shown in the next table. The term 'dx' (next table) is the relative difference between the significant value of the calculated response spectrum ('Original' or 'Identification' or 'Solution') and the significant value of the response spectrum of the data set ('Data'). This term is calculated as follows:

$$dx = \frac{X_{s,calc.} - X_{s,data}}{X_{s,data}} \cdot 100\% \qquad \text{Eq. 8-2}$$

where $X_{s,calc.}$ is the significant value of each motion based on the calculated response spectrum and $X_{s,data}$ is the significant value of each motion based on the response spectrum given in the data set.

Table 30: Significant values of motions: Test case 2

Motions	Data	Original		Identification		Solution	
	Sign.value	Sign.value	dx (%)	Sign.value	dx (%)	Sign.value	dx (%)
Surge (m)	[redacted]	[redacted]	+0.53	[redacted]	+0.85	[redacted]	+1.33
Sway (m)	[redacted]	[redacted]	+3.21	[redacted]	-0.89	[redacted]	+2.94
Heave (m)	[redacted]	[redacted]	+2.18	[redacted]	+0.81	[redacted]	+0.86
Roll (degrees)	[redacted]	[redacted]	+9.70	[redacted]	+0.37	[redacted]	*+9.06*
Pitch (degrees)	[redacted]	[redacted]	+30.10	[redacted]	-3.39	[redacted]	+3.56
Yaw (degrees)	[redacted]	[redacted]	+9.19	[redacted]	-0.09	[redacted]	+2.26

According to the above table, the significant value for roll motion based on the response spectrum specified as 'Solution' is [redacted]. However, the significant value of roll motion according to the response spectrum of the data set is [redacted]. Therefore, the data processing increases the significant value of roll motion [redacted] (9%). The other vessel motions indicate less inaccuracies due to data processing. It can now be explained why the elements ab_{44} and ab_{22} need to be changed during the identification procedure. Also, the inaccuracies of the identified values of the other elements could be caused by the data processing.

The identification procedure is also validated by the comparison of the following RAOs:

- RAOs based on the identified modifications: Specified as 'Identification-Results'
- RAOs based on the original vessel properties: Specified as 'Original'
- RAOs based on the real changes: Specified as 'Solution'

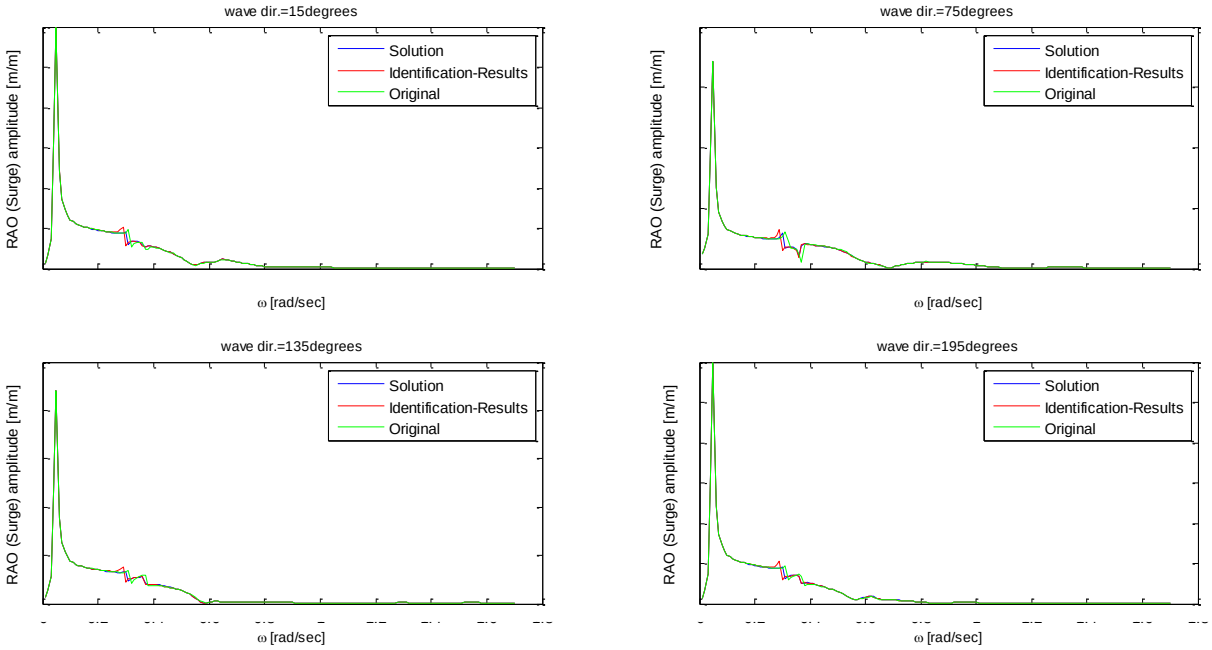

Figure 100: Comparison of RAOs, amplitude of Surge-RAO, test case 2

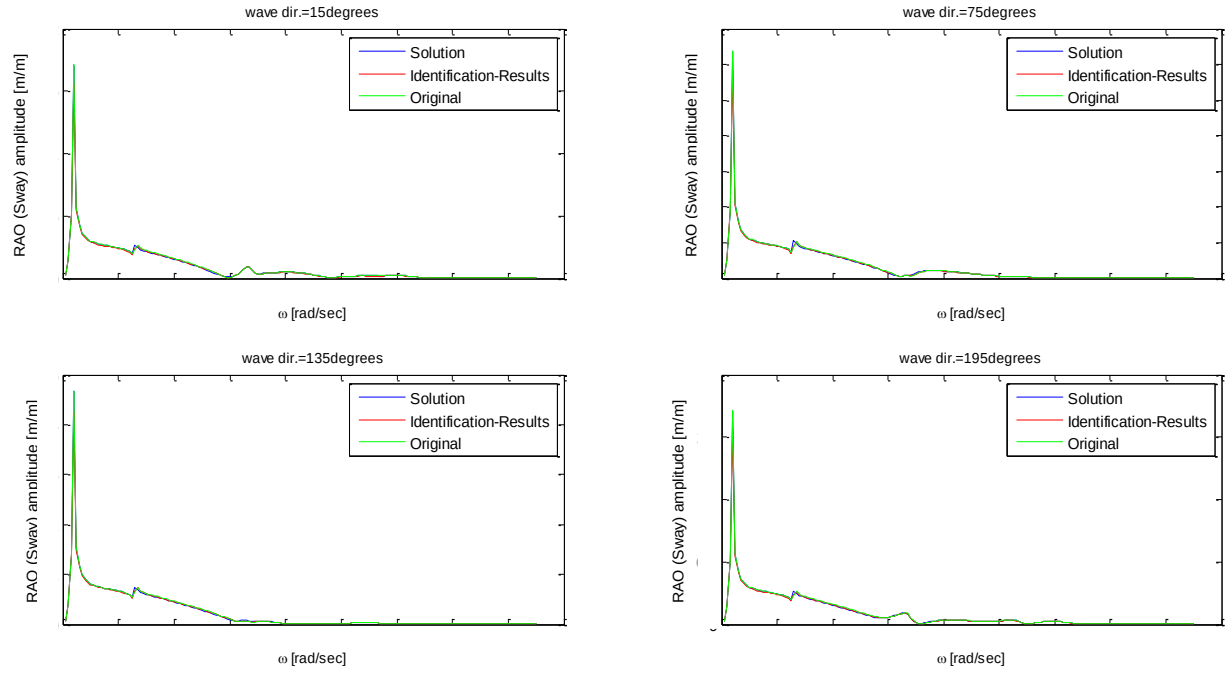

Figure 101: Comparison of RAOs, amplitude of Sway-RAO, test case 2

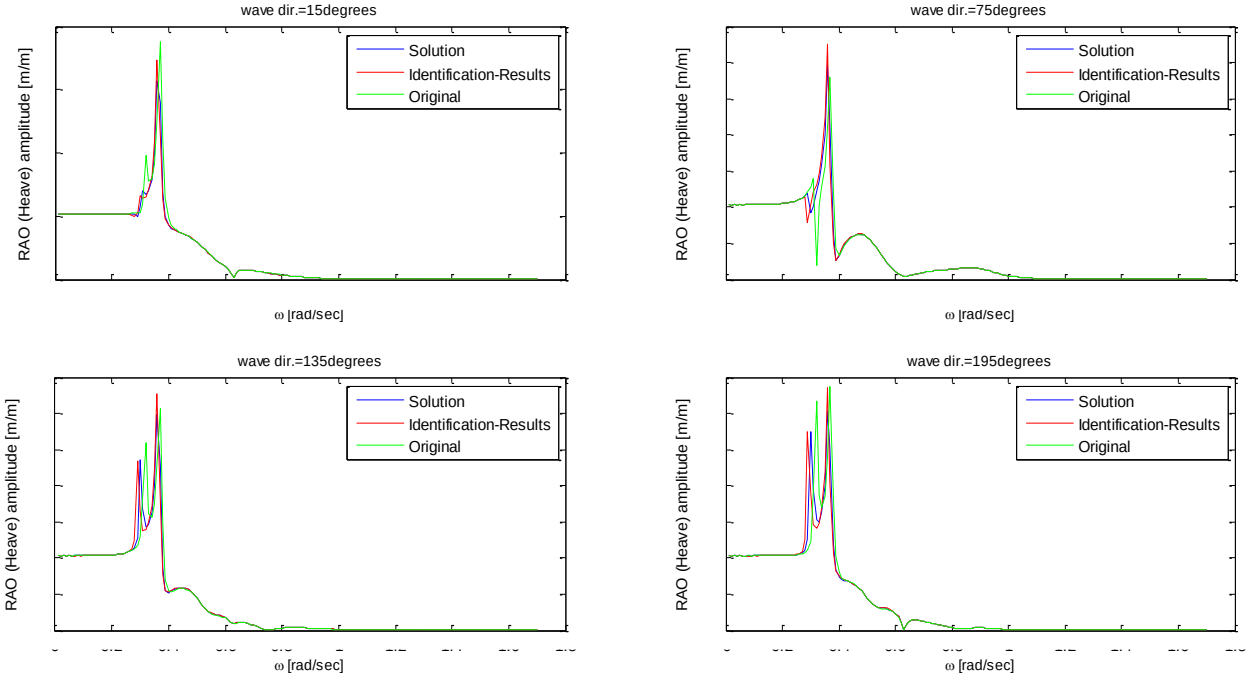

Figure 102: Comparison of RAOs, amplitude of Heave-RAO, test case 2

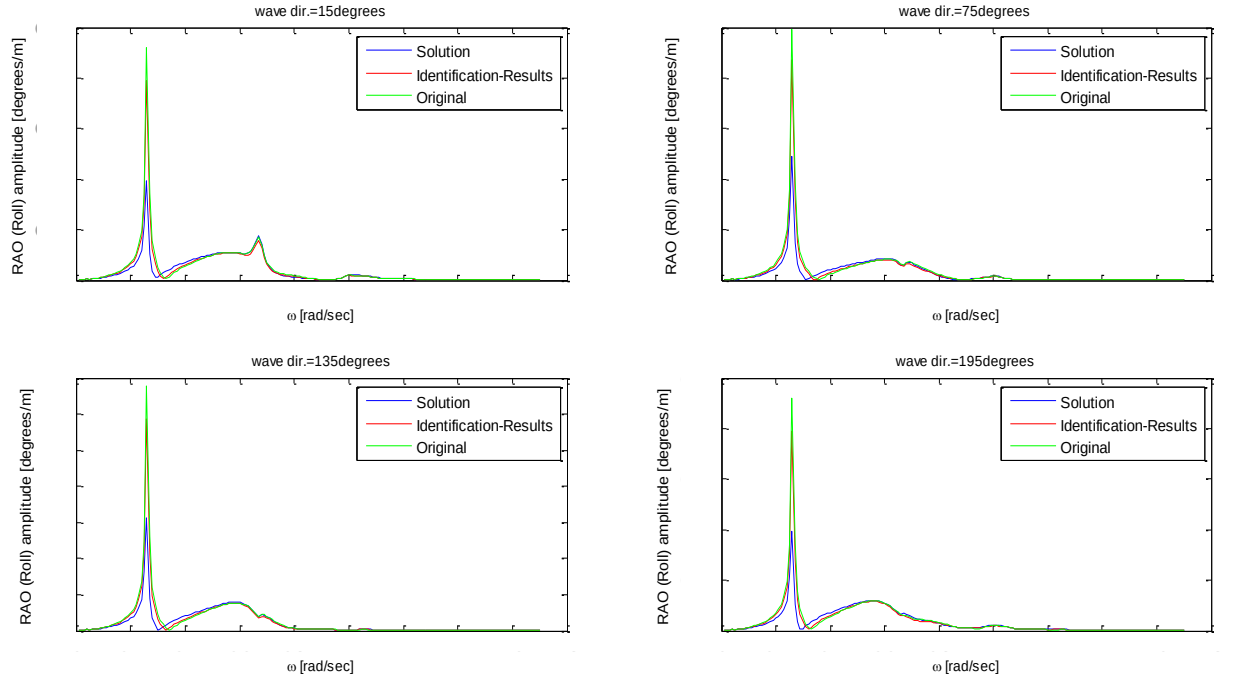

Figure 103: Comparison of RAOs, amplitude of Roll-RAO, test case 2

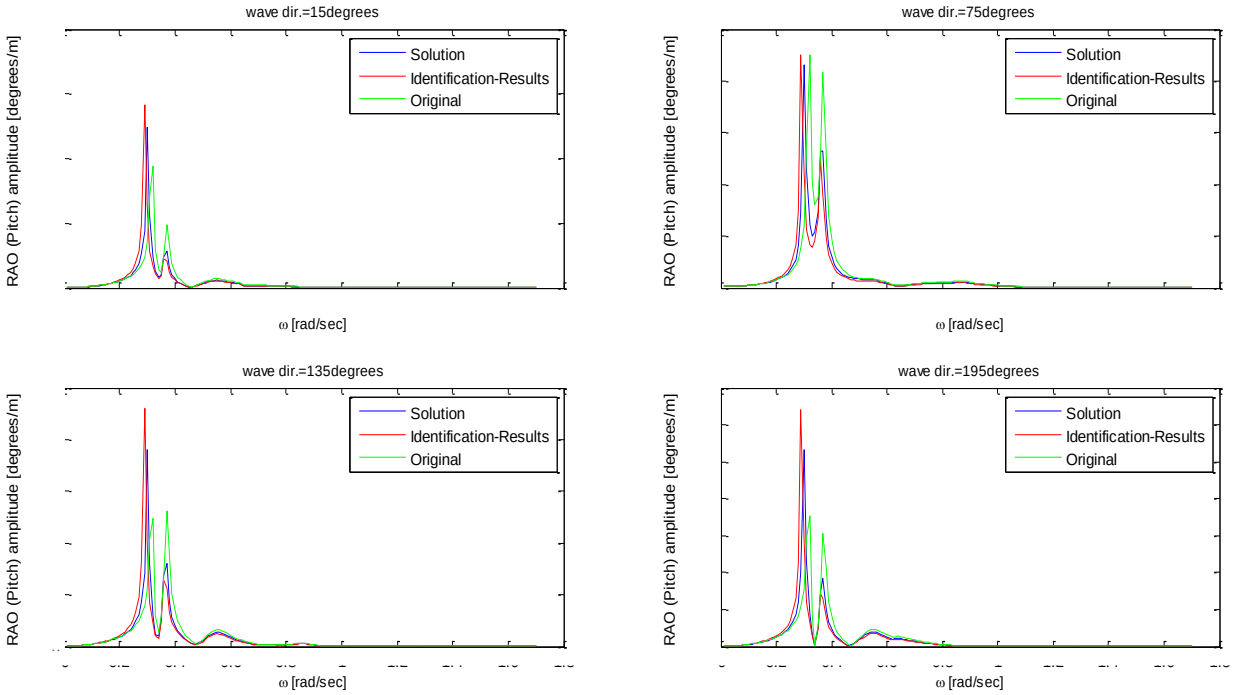

Figure 104: Comparison of RAOs, amplitude of Pitch-RAO, test case 2

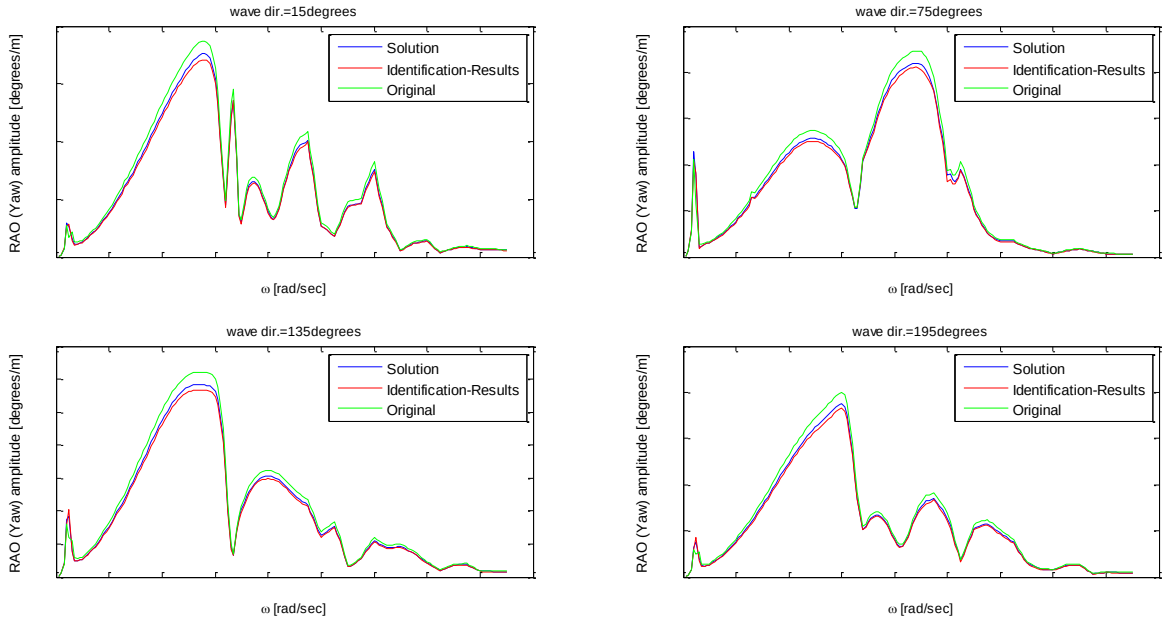

Figure 105: Comparison of RAOs, amplitude of Yaw-RAO, test case 2

The accuracy of the identification method is estimated by calculating the following NRMSEs:

- NRMSE between the identified RAOs and the correct RAOs (solution of the test case).
- NRMSE between the original RAOs and the correct RAOs.

For each degree of freedom, the average value of the NRMSEs over all wave directions is indicated in the following table. The minimum and maximum NRMSEs over the wave directions are also shown in the next table.

Table 31: Comparison of RAOs: Test case 2

Surge-RAO	Original RAOs-Correct RAOs	Identified RAOs-Correct RAOs
Average NRMSE (all wave dir.)	0.936	0.952
Minimum NRMSE	0.842 (directions: 90º, 270º)	0.932 (directions: 75º, 285º)
Maximum NRMSE	0.955 (directions:165º, 195º)	0.975 (directions:105º, 255º)
Sway-RAO	Original RAOs-Correct RAOs	Identified RAOs-Correct RAOs
Average NRMSE (all wave dir.)	0.971	0.979
Minimum NRMSE	0.970 (directions: 90º, 270º)	0.974 (directions: 90º, 270º)
Maximum NRMSE	0.973 (directions:180º)	0.983 (directions:135º, 225º)
Heave-RAO	Original RAOs-Correct RAOs	Identified RAOs-Correct RAOs
Average NRMSE (all wave dir.)	0.744	0.845
Minimum NRMSE	0.657 (directions:165º, 195º)	0.739 (directions:180º)
Maximum NRMSE	0.796 (directions:15º, 345º)	0.899 (directions:15º, 345º)
Roll-RAO	Original RAOs-Correct RAOs	Identified RAOs-Correct RAOs
Average NRMSE (all wave dir.)	0.464	0.546
Minimum NRMSE	0.434 (directions:165º, 195º)	0.520 (directions: 165º, 195º)
Maximum NRMSE	0.485 (directions: 90º, 270º)	0.564 (directions: 90º, 270º)
Pitch-RAO	Original RAOs-Correct RAOs	Identified RAOs-Correct RAOs
Average NRMSE (all wave dir.)	0.277	0.345
Minimum NRMSE	0.145 (directions: 0º)	0.291 (directions: 0º)
Maximum NRMSE	0.520 (directions: 90º, 270º)	0.560 (directions: 90º, 270º)
Yaw-RAO	Original RAOs-Correct RAOs	Identified RAOs-Correct RAOs
Average NRMSE (all wave dir.)	0.901	0.956
Minimum NRMSE	0.869 (directions:90º, 270º)	0.937 (directions: 90º, 270º)
Maximum NRMSE	0.910 (directions:165º, 195º)	0.960 (directions: 150º, 210º)

According to the above table, the identified RAOs corresponding to roll and pitch motions do not approximate the correct RAOs with great accuracy. However, there is an improvement compared to the original RAOs. For roll and pitch motions, the significant values of the response spectra of the 'Solution' indicate the highest deviations with respect to the responses of the data set. Therefore, it is assumed that results of the identification procedure were affected negatively by the data processing.

8.4 TEST CASE 3

The wave spectra of the data set for the third test case are indicated in the following figures. The heading of the Thialf is 75º.

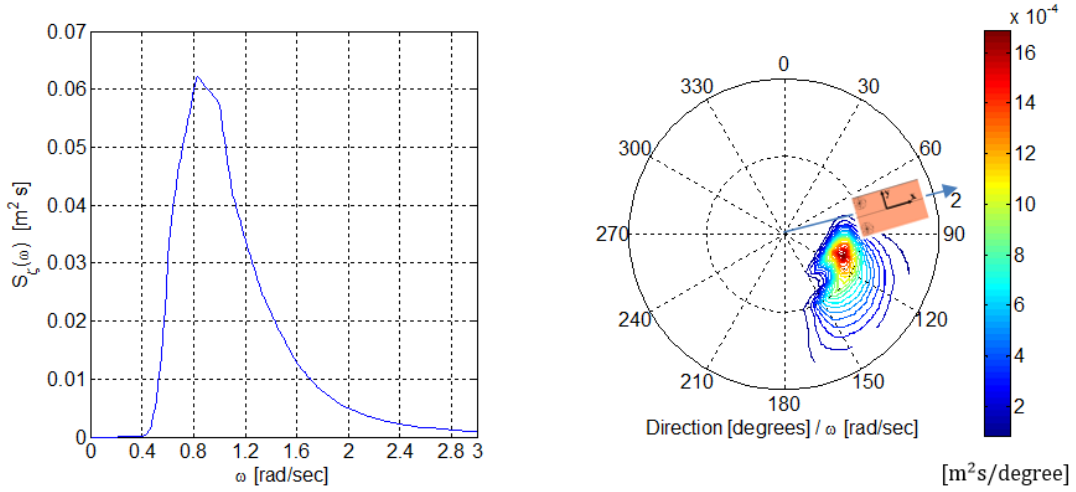

Figure 106: 1D and 2D wave spectra, test case 3

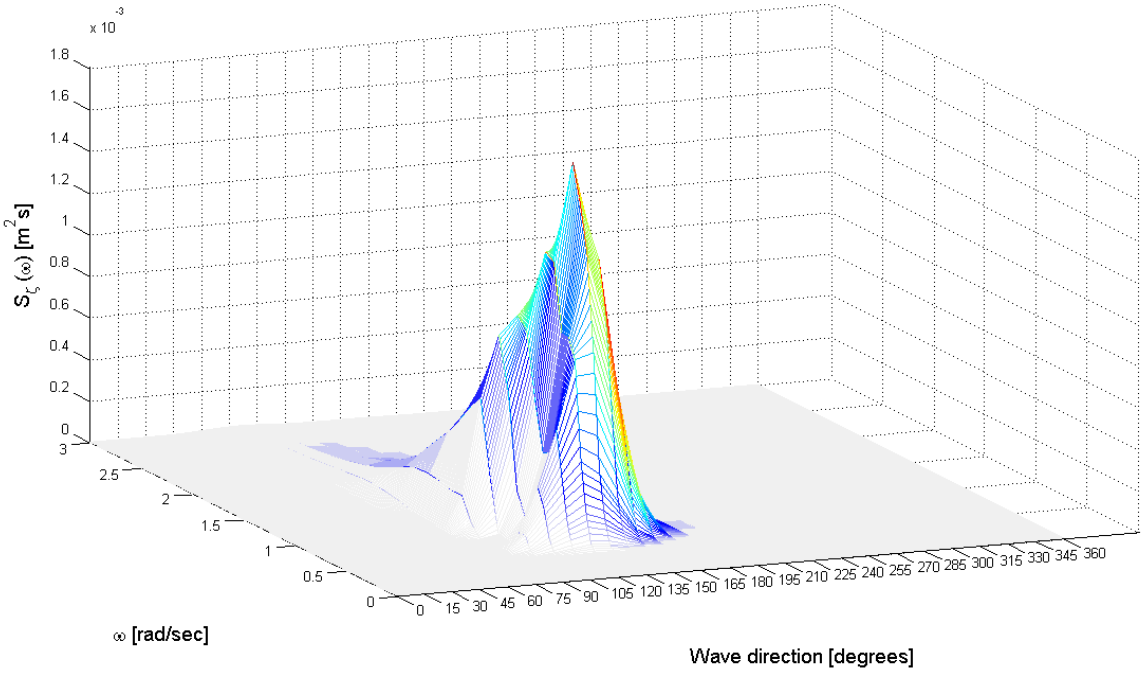

Figure 107: 2D wave spectrum, local coordinate system of the vessel, test case 3

The response spectra based on the original properties of the Thialf are compared with the response spectra of the data set. The NRMSEs for each vessel motion are the following: surge=0.869, sway=0.870, heave=0.849, roll=0.921, pitch=0.184, yaw=0.826. The next figure, shows the calculated response spectra and the response spectra from the data set.

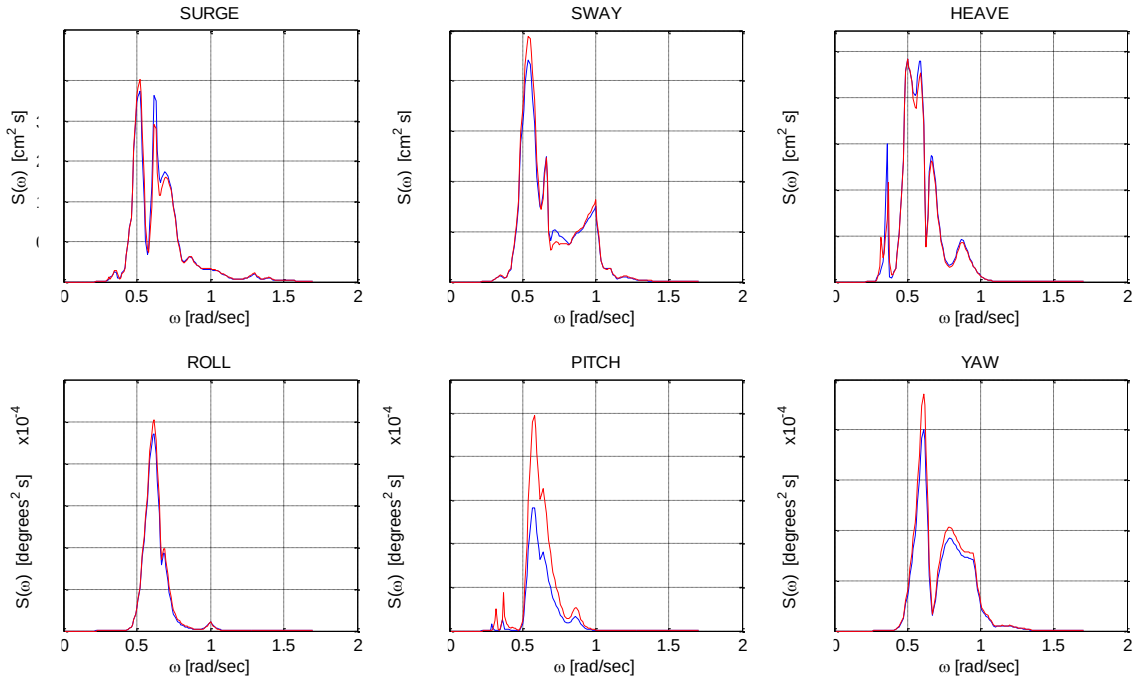

Figure 108: Comparison of motion response spectra, test case 3

The final results of the identification procedure are shown in the following table. Also the results are compared with the real modifications of test case 3.

Table 32: Final results: Test case 3

Elements	Original values	Identified changes	Real changes	Comparison (real and identified changes)
r_{yy} (m)	[redacted]	[redacted] (+15 % ·Orig.value)	[redacted] (+14% ·Orig.value)	1 (1% ·Orig.value)
r_{zz} (m)	[redacted]	[redacted] (+5% ·Orig.value)	[redacted] (+3% ·Orig.value)	1 (2% ·Orig.value)
c=9-10 for ab_{44}	-6.65E05- 2.51E06i/ -6.65E05+ 2.51E06i	3.09·Orig.value	-	-
$\mathbf{B_{ad}}(4,4)$	[redacted]	-	1.5·Orig.value	-
$\mathbf{B_{ad}}(5,5)$	[redacted]	-	0.8·Orig.value	-
z coordinate (m)	[redacted]	[redacted] (+13 % ·Orig.value)	[redacted] (+16% ·Orig.value)	0.7 (3% ·Orig.value)

Table 33: Final NRMSEs: Test case 3

Motions	NRMSE-Identification	NRMSE-Solution
Surge	0.973	0.976
Sway	0.955	0.957
Heave	0.980	0.975
Roll	0.974	0.897
Pitch	0.976	0.926
Yaw	0.964	0.932
Average (NRMSEs)	0.970	0.944

The identified values for r_{yy}, r_{zz} and 'z' match the real values sufficiently. However, the modifications of the elements, $\mathbf{B_{ad}}(4,4)$ and $\mathbf{B_{ad}}(5,5)$ could not be identified during the identification procedure. Due to the fact that the small changes of the viscous damping cause negligible variations in the final response spectra, the identification method cannot adjust the before-mentioned elements of the viscous damping. Also, an additional element was modified during the identification procedure: ab_{44}. Similar to the previous test case, the NRMSEs caused by the real changes are smaller than the NRMSEs caused by the identified changes. The resulting response spectra based on the identified modifications and the response spectra based on the real changes are shown in the following figures.

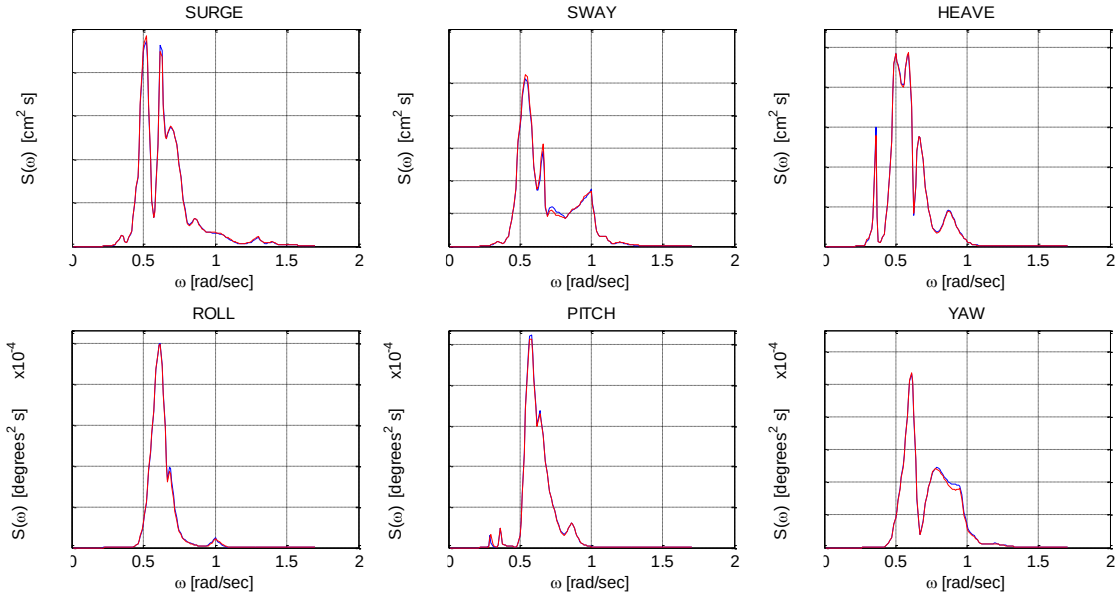

Figure 109: Motion response spectra, identification method, test case 3, data set=blue, calculations=red

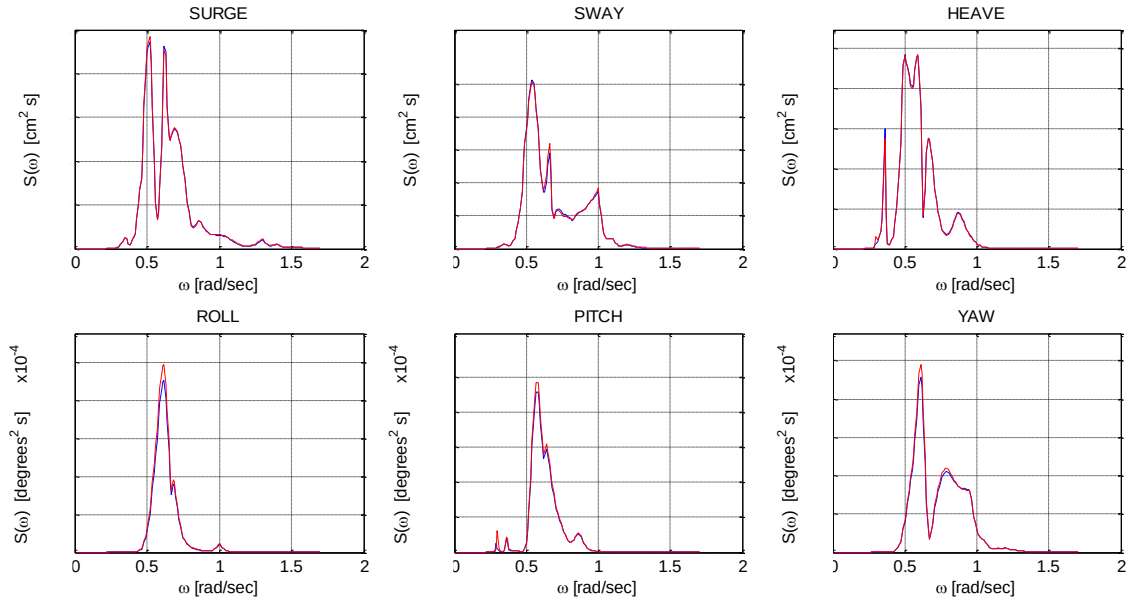

Figure 110: Motion response spectra, solution, test case 3, data set=blue, calculations=red

The significant values for each vessel motion are shown in the following table:

Table 34: Significant values of motions: Test case 3

Motions	Data	Original		Identification		Solution	
	Sign.value	Sign.value	dx (%)	Sign.value	dx (%)	Sign.value	dx (%)
Surge (m)	[redacted]	[redacted]	-0.96	[redacted]	0.21	[redacted]	0.36
Sway (m)	[redacted]	[redacted]	2.33	[redacted]	0.71	[redacted]	0.27
Heave (m)	[redacted]	[redacted]	-1.68	[redacted]	-0.23	[redacted]	-0.32
Roll (degrees)	[redacted]	[redacted]	3.50	[redacted]	-0.58	[redacted]	4.58
Pitch (degrees)	[redacted]	[redacted]	32.86	[redacted]	-0.65	[redacted]	2.94
Yaw (degrees)	[redacted]	[redacted]	6.41	[redacted]	-1.09	[redacted]	1.96

As in test case 2, the calculated response spectrum for roll motion based on the real changes shows inaccuracies (dx of 'Solution'=4.58%). Therefore, during the identification procedure, the element ab_{44} should be adjusted. Also, the significant value of pitch motion based on the correct modifications is 2.94% higher than the significant value according to the data set. The inaccuracies due to data processing for the other vessel motions are negligible. The identification procedure will also be validated by means of comparison of the RAOs:

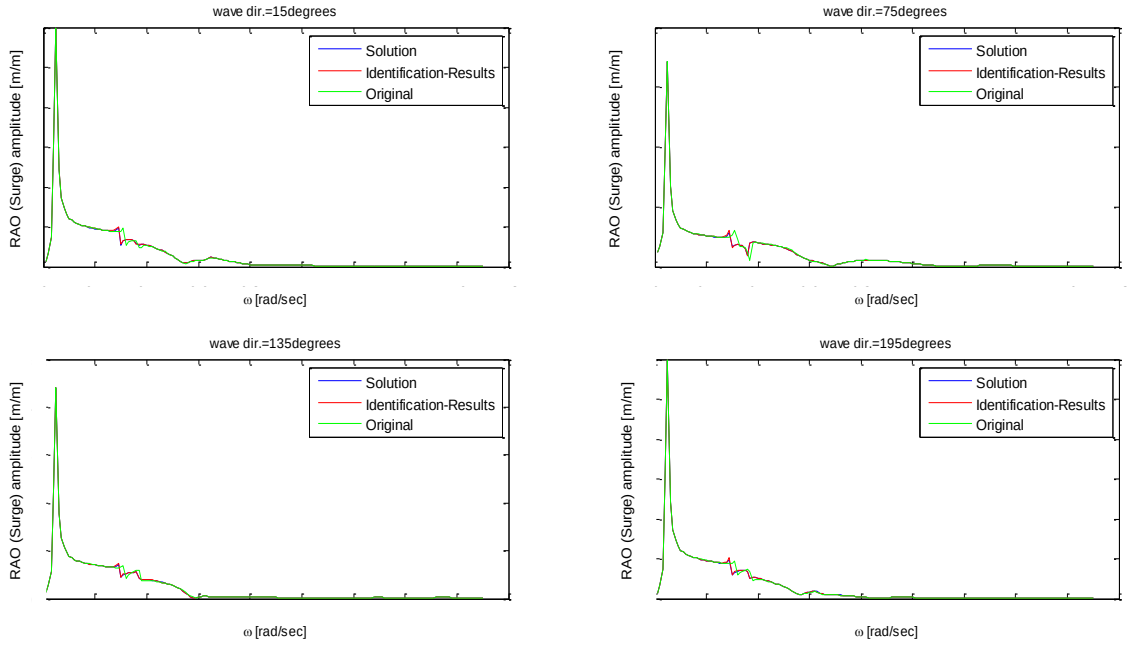

Figure 111: Comparison of RAOs: Amplitude of Surge-RAO, test case 3

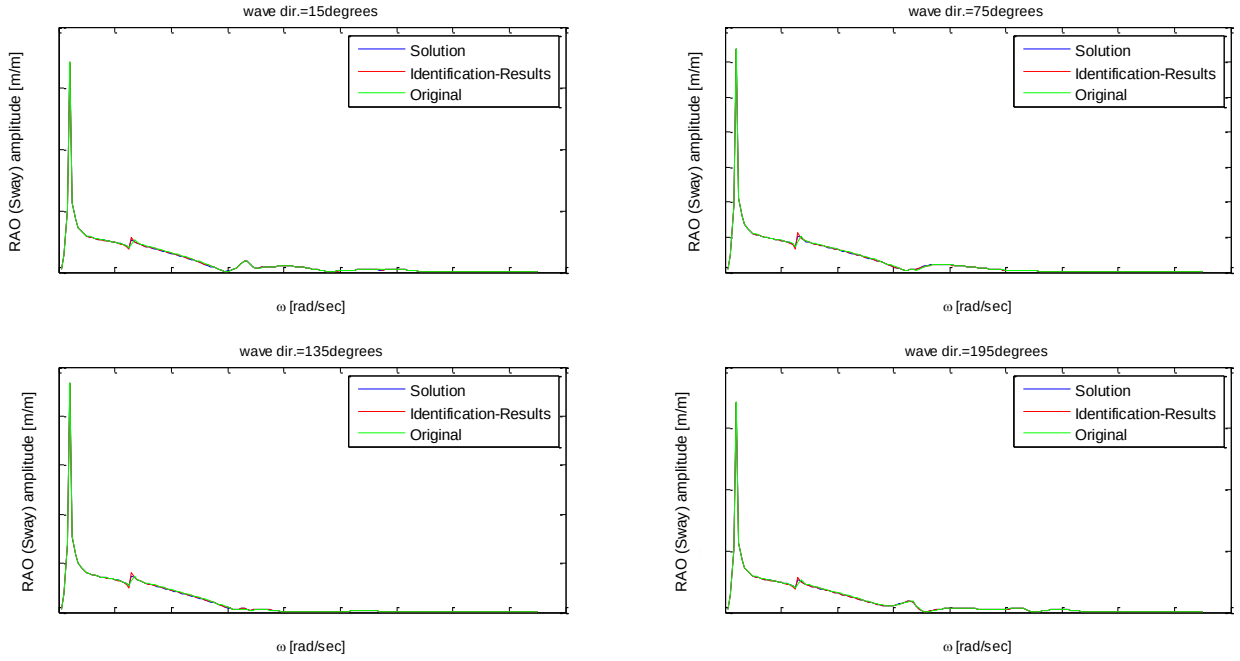

Figure 112: Comparison of RAOs: Amplitude of Sway-RAO, test case 3

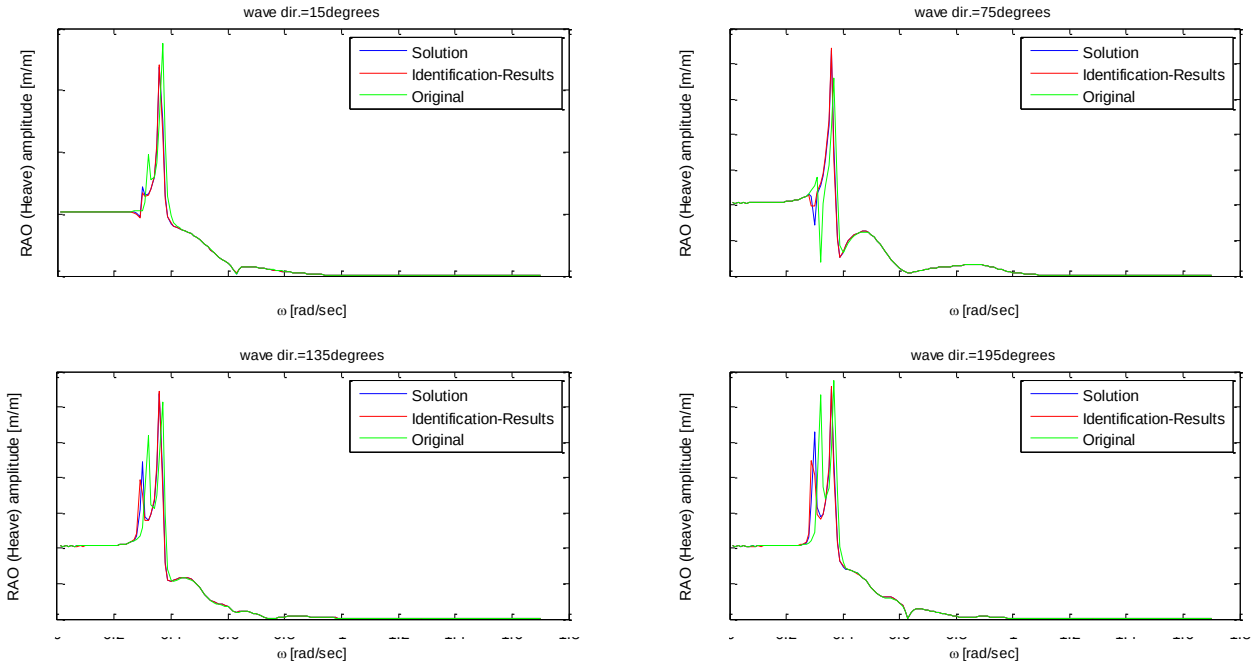

Figure 113: Comparison of RAOs: Amplitude of Heave-RAO, test case 3

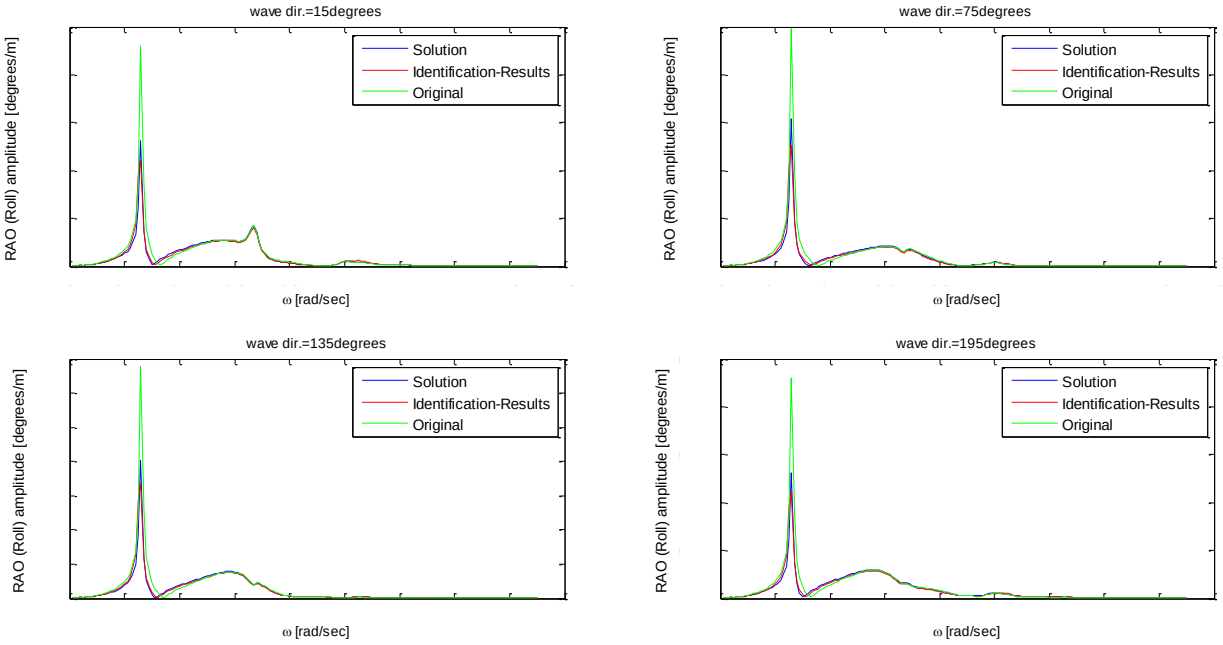

Figure 114: Comparison of RAOs: Amplitude of Roll-RAO, test case 3

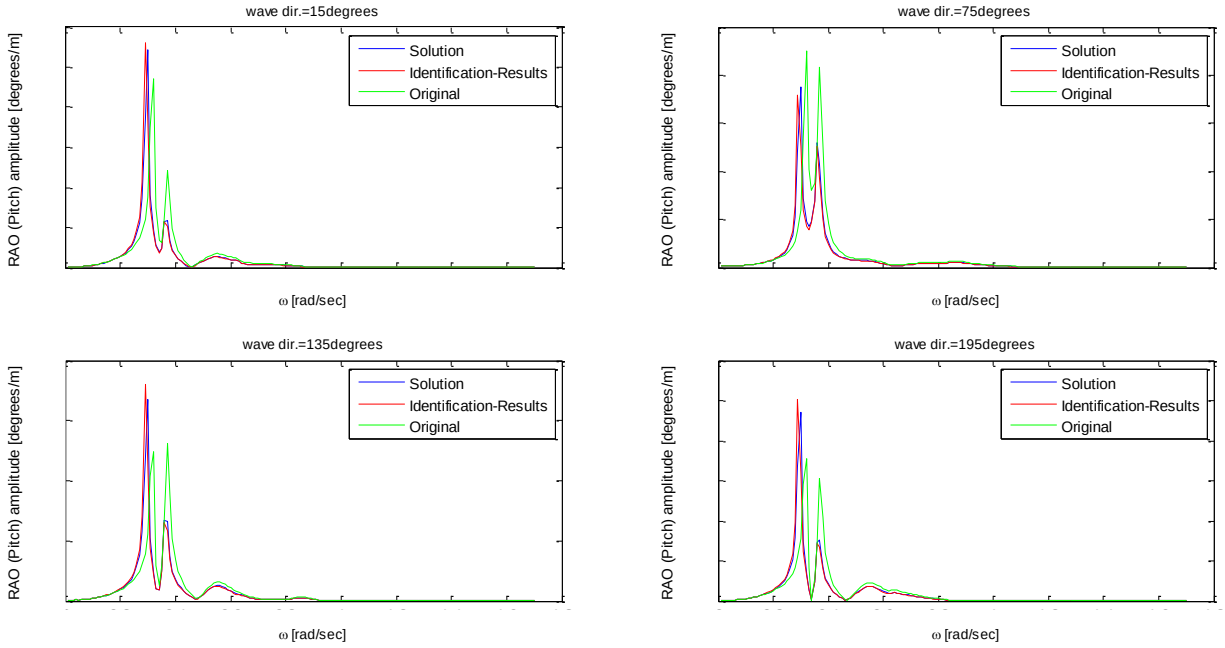

Figure 115: Comparison of RAOs: Amplitude of Pitch-RAO, test case 3

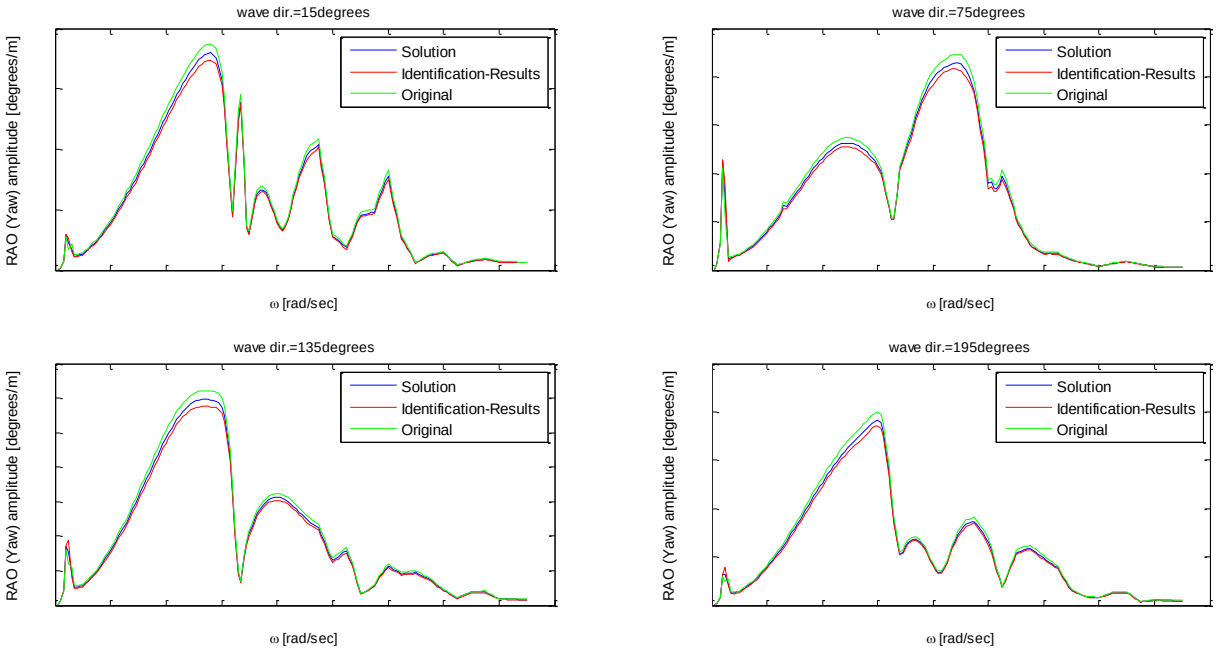

Figure 116: Comparison of RAOs: Amplitude of Yaw-RAO, test case 3

The NRMSEs of the RAOs for test case 3 are indicated in the following table

Table 35: Comparison of RAOs: test case 3

Comparison of Surge-RAO	Original RAOs-Correct RAOs	Identified RAOs-Correct RAOs
Average NRMSE (all wave dir.)	0.923	0.991
Minimum NRMSE	0.831 (directions: 90º, 270º)	0.980 (directions: 90º, 270º)
Maximum NRMSE	0.944 (directions: 165º, 195º)	0.993 (directions: 120º, 240º)
Comparison of Sway-RAO	Original RAOs-Correct RAOs	Identified RAOs-Correct RAOs
Average NRMSE (all wave dir.)	0.975	0.987
Minimum NRMSE	0.974 (directions: 90º, 270º)	0.987 (directions: 90º, 270º)
Maximum NRMSE	0.977 (directions: 15º, 345º)	0.988 (directions: 135º, 225º)
Comparison of Heave-RAO	Original RAOs-Correct RAOs	Identified RAOs-Correct RAOs
Average NRMSE (all wave dir.)	0.697	0.935
Minimum NRMSE	0.624 (directions: 180º)	0.875 (directions: 180º)
Maximum NRMSE	0.745 (directions: 30º, 330º)	0.966 (directions: 30º, 330º)
Comparison of Roll-RAO	Original RAOs-Correct RAOs	Identified RAOs-Correct RAOs
Average NRMSE (all wave dir.)	0.586	0.757
Minimum NRMSE	0.562 (directions: 165º, 195º)	0.745 (directions: 90º, 270º)
Maximum NRMSE	0.604 (directions: 90º, 270º)	0.774 (directions: 15º, 345º)
Comparison of Pitch-RAO	Original RAOs-Correct RAOs	Identified RAOs-Correct RAOs
Average NRMSE (all wave dir.)	0.213	0.686
Minimum NRMSE	0.089 (directions: 0º)	0.648 (directions: 0º)
Maximum NRMSE	0.447 (directions: 90º, 270º)	0.832 (directions: 90º, 270º)
Comparison of Yaw-RAO	Original RAOs-Correct RAOs	Identified RAOs-Correct RAOs
Average NRMSE (all wave dir.)	0.934	0.950
Minimum NRMSE	0.919 (directions: 90º, 270º)	0.930 (directions: 90º, 270º)
Maximum NRMSE	0.940 (directions: 165º, 195º)	0.954 (directions: 150º, 210º)

According to the above table, the RAOs with the maximum inaccuracies correspond to the motions that indicate the maximum inaccuracies due to data processing (roll and pitch). However, the inaccuracies caused by the data processing for test case 3 were lower than in test case 2. Thus, the results of the identification procedure for test case 3 were more accurate. The identified RAOs approximate the real RAOs with greater accuracy. Also it is clear that the original RAOs were remarkably improved after implementing the identified modifications.

8.5 TEST CASE 4

The wave spectra for the fourth test case are indicated in the following figure. The heading of the Thialf is 40°.

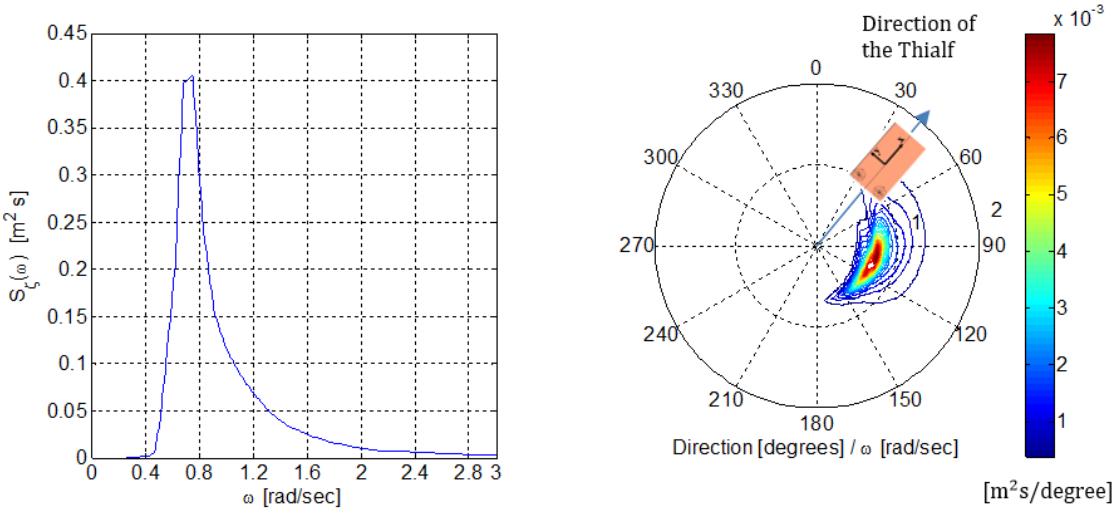

Figure 117: 1D and 2D wave spectra, test case 4

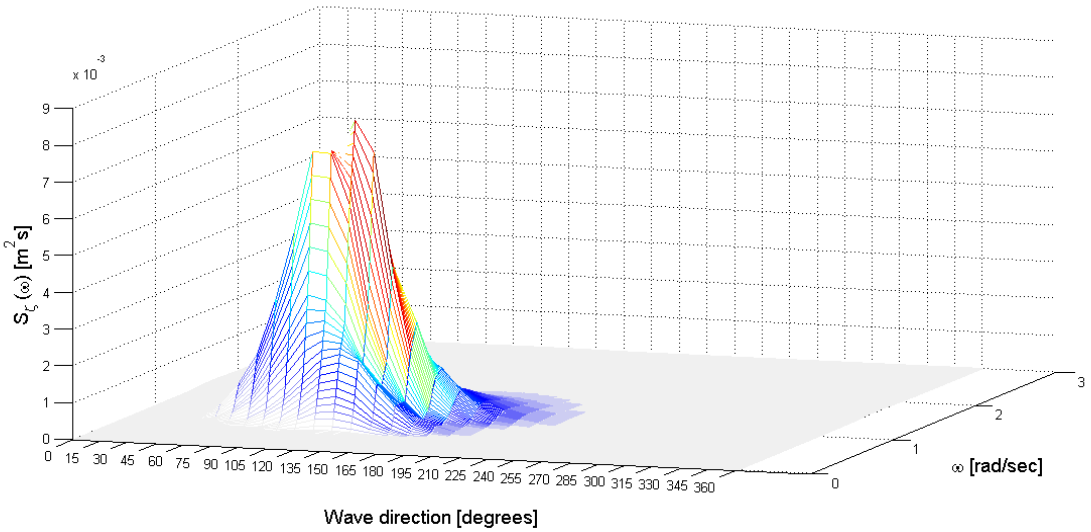

Figure 118: 2D wave spectrum, local coordinate system of the vessel, test case 4

The response spectra based on the original properties of the Thialf are compared with the response spectra of the data set. The NRMSEs for each vessel motion are the following: surge=0.882, sway=0.835, heave=0.598, roll=816, pitch=0.169, yaw=0.795. The next figure, shows the calculated response spectra and the response spectra from the data set.

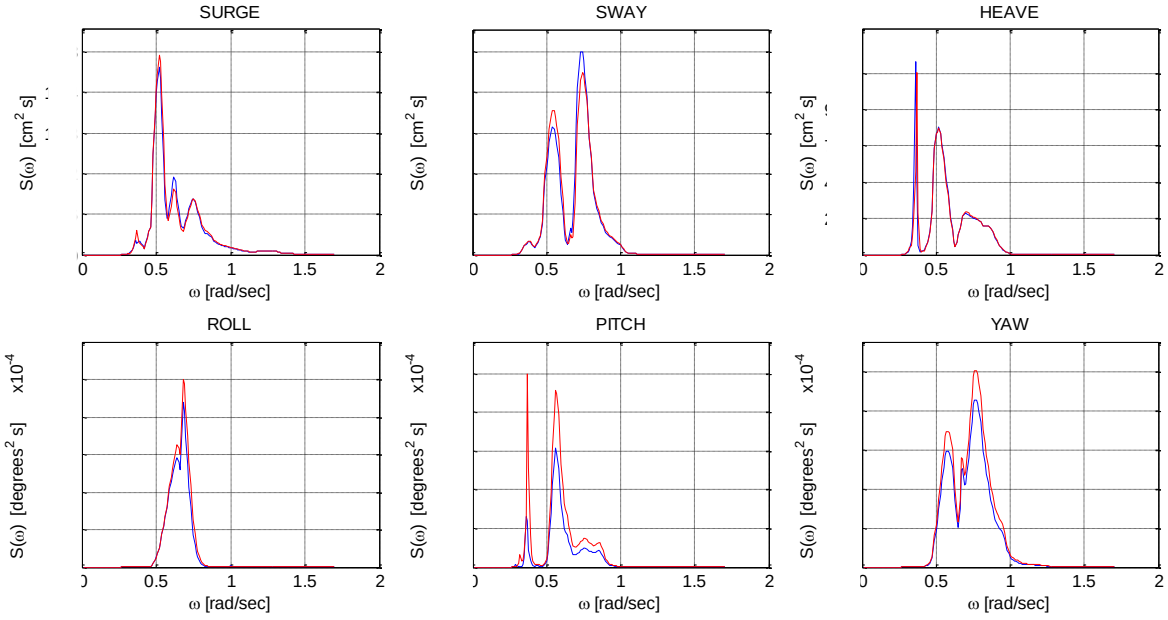

Figure 119: Comparison of motion response spectra, test case 4

The final results of the identification procedure and the real modifications of test case 4 are shown below.

Table 36: Final results: Test case 4

Elements	Original values	Identified changes	Real changes	Comparison (real and identified changes)
r_{yy} (m)	[redacted]	[redacted] (+12 % ·Orig.value)	[redacted] (+10% ·Orig.value)	1 (+2% ·Orig.value)
r_{zz} (m)	[redacted]	[redacted] (+6% ·Orig.value)	[redacted] (+4% ·Orig.value)	1 (+2% ·Orig.value)
c=9-10 for ab_{44}	-6.65E05- 2.51E06i/ -6.65E05+ 2.51E06i	2.69·Orig.value	-	-
$\mathbf{B_{ad}}(4,4)$	[redacted]	-	2.5·Orig.value	-
z coordinate (m)	[redacted]	[redacted] (+17 % ·Orig.value)	[redacted] (+20% ·Orig.value)	0.7 (+3% ·Orig.value)

Table 37: Final NRMSEs: Test case 4

Motions	NRMSE-Identification	NRMSE-Solution
Surge	0.968	0.970
Sway	0.977	0.970
Heave	0.936	0.886
Roll	0.965	0.868
Pitch	0.943	0.861
Yaw	0.977	0.948
Average (NRMSEs)	0.962	0.917

Similar to the previous test case, the identified values for r_{yy}, r_{zz} and 'z' approach the real values sufficiently. However, the elements $\mathbf{B_{ad}}(4,4)$ is not identified for the same reasons as in test case 3. The element ab_{44} has to be modified due to the variations resulting from the data processing. Furthermore, the NRMSEs caused by the real changes are smaller than the NRMSEs caused by

the identified changes. The resulting response spectra based on the identified modifications and the response spectra based on the real changes are shown in the following figures.

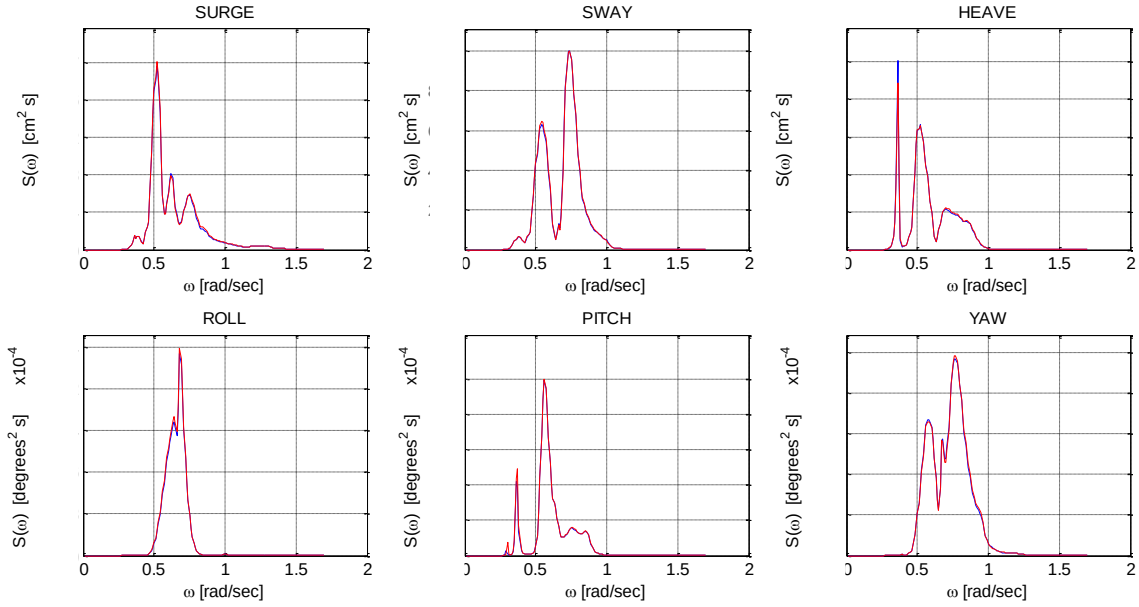

Figure 120: Motion response spectra, identification method, test case 4, data set=blue, calculations=red

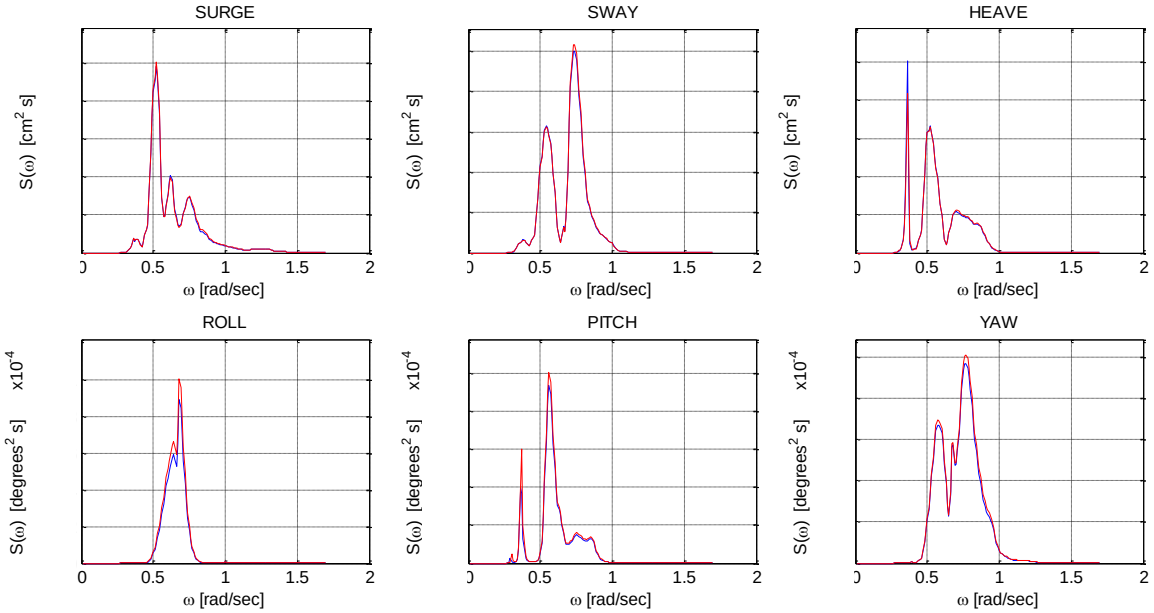

Figure 121: Motion response spectra, solution, test case 4, data set=blue, calculations=red

The significant values for each vessel motion are shown in the following table:

Table 38: Significant values of motions: Test case 4

Motions	Data	Original		Identification		Solution	
	Sign.value	Sign.value	dx (%)	Sign.value	dx (%)	Sign.value	dx (%)
Surge (m)	[redacted]	[redacted]	1.00	[redacted]	0.79	[redacted]	0.81
Sway (m)	[redacted]	[redacted]	0.32	[redacted]	0.51	[redacted]	0.72
Heave (m)	[redacted]	[redacted]	-0.54	[redacted]	-0.08	[redacted]	-0.07
Roll (degrees)	[redacted]	[redacted]	7.36	[redacted]	1.64	[redacted]	6.01
Pitch (degrees)	[redacted]	[redacted]	29.01	[redacted]	1.16	[redacted]	4.75
Yaw (degrees)	[redacted]	[redacted]	8.66	[redacted]	0.17	[redacted]	2.23

As in test case 3, the calculated response spectra for roll and pitch motions based on the real changes show inaccuracies: dx of 'Solution' equals to 6.01% and 4.75% respectively. The inaccuracies due to data processing for the other vessel motions are negligible.

The following figures show the comparison of the RAOs:

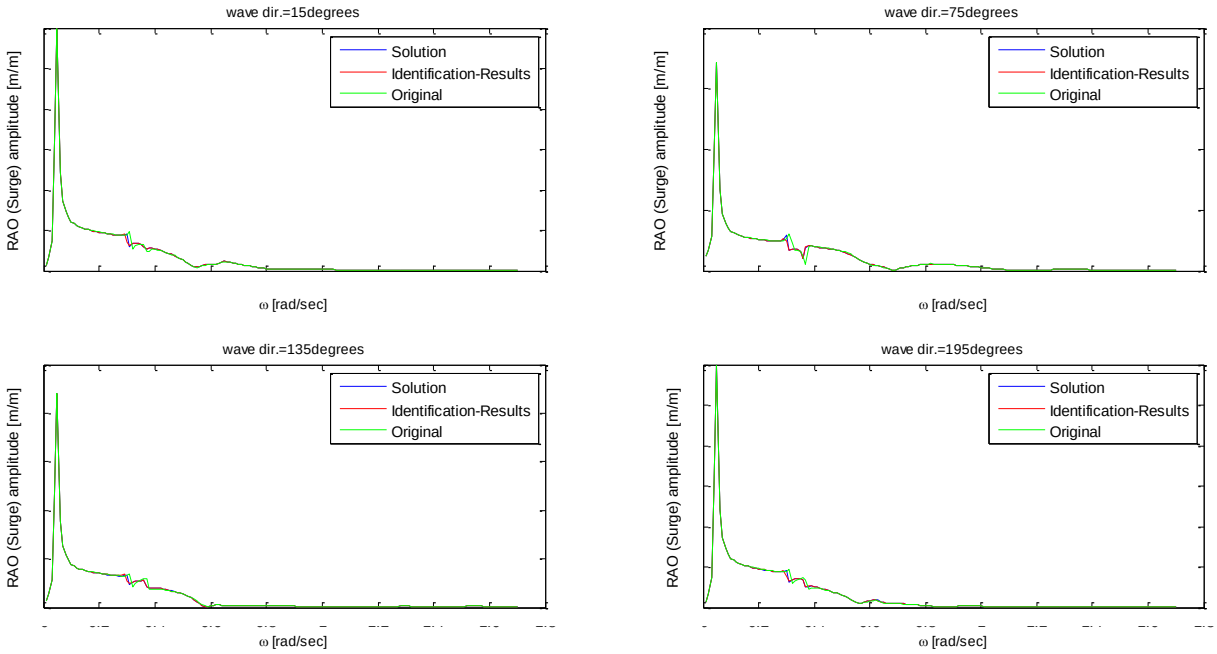

Figure 122: Comparison of RAOs: Amplitude of Surge-RAO, test case 4

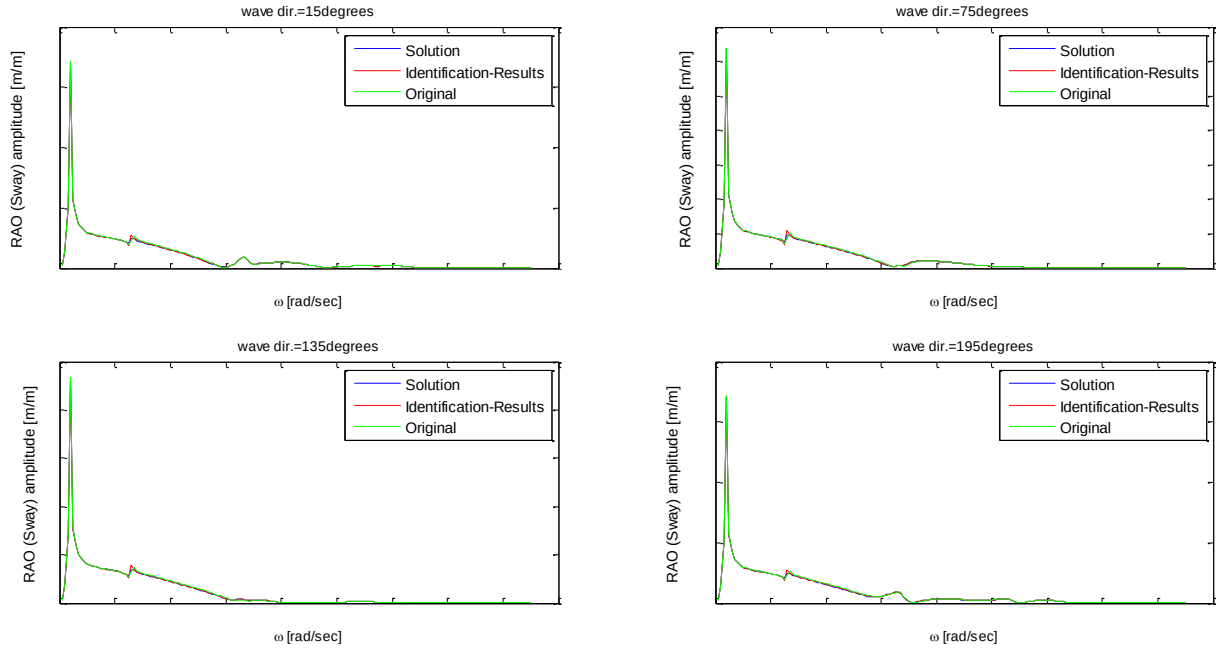

Figure 123: Comparison of RAOs: Amplitude of Sway-RAO, test case 4

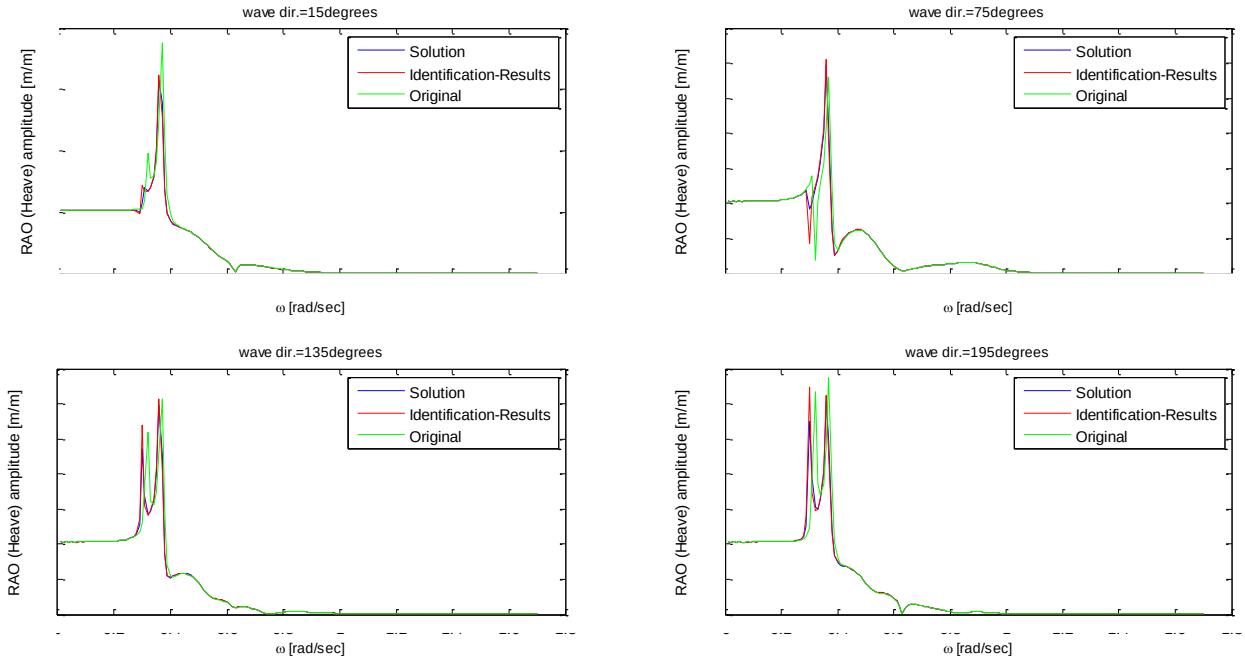

Figure 124: Comparison of RAOs: Amplitude of Heave-RAO, test case 4

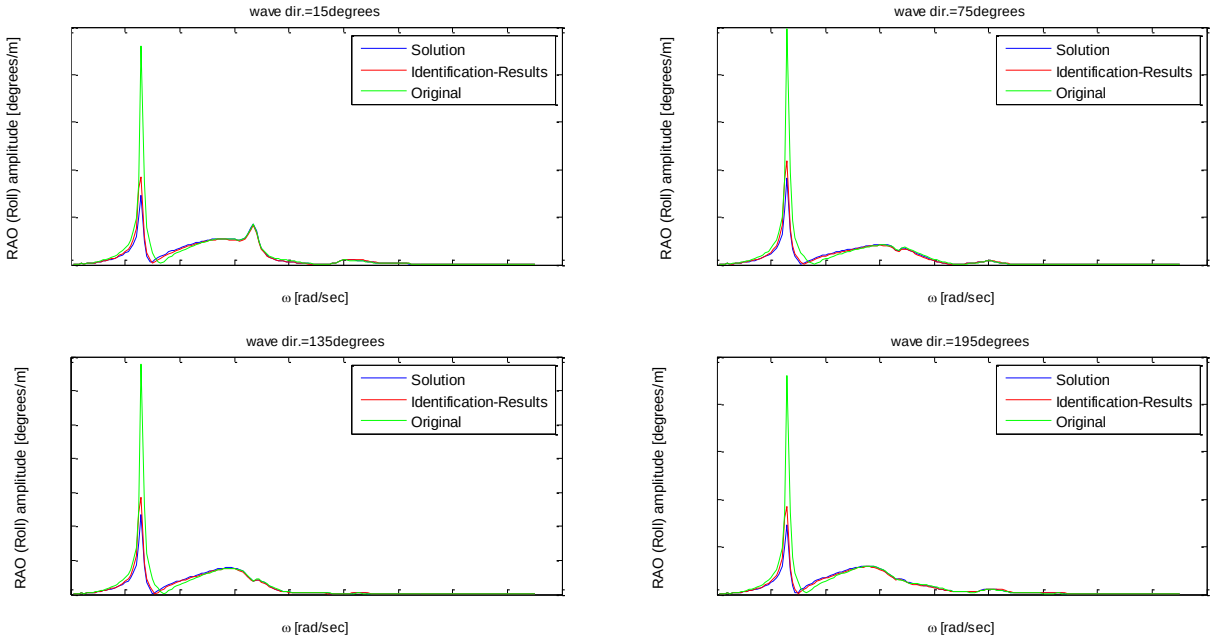

Figure 125: Comparison of RAOs: Amplitude of Roll-RAO, test case 4

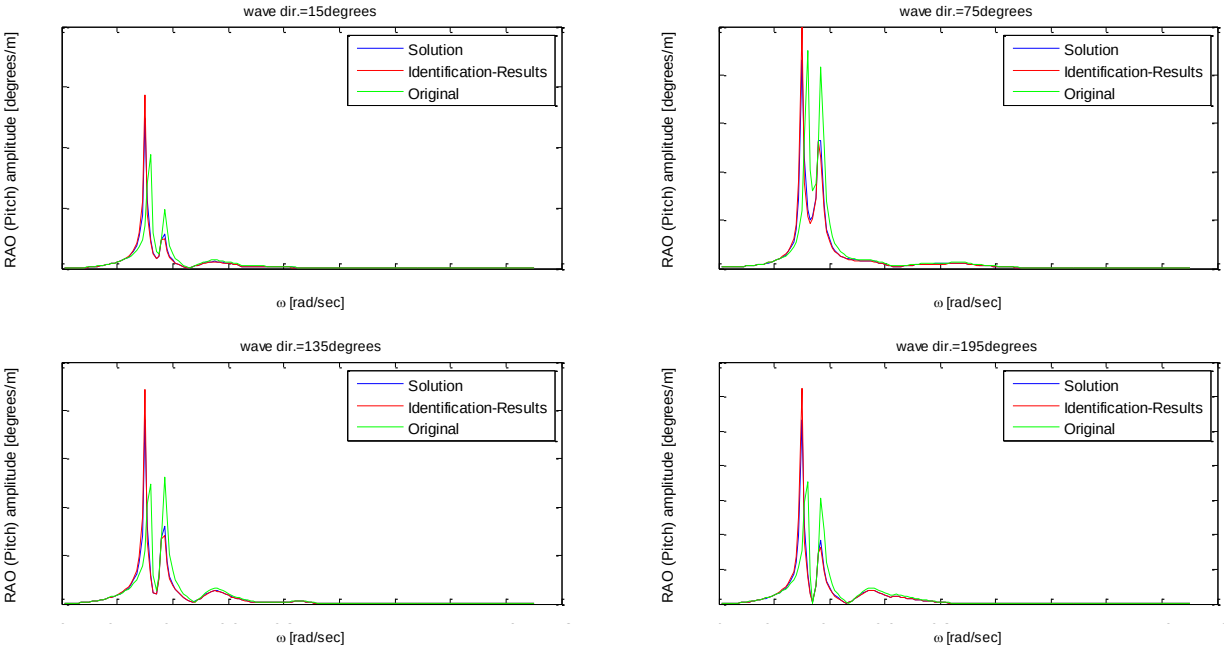

Figure 126: Comparison of RAOs: Amplitude of Pitch-RAO, test case 4

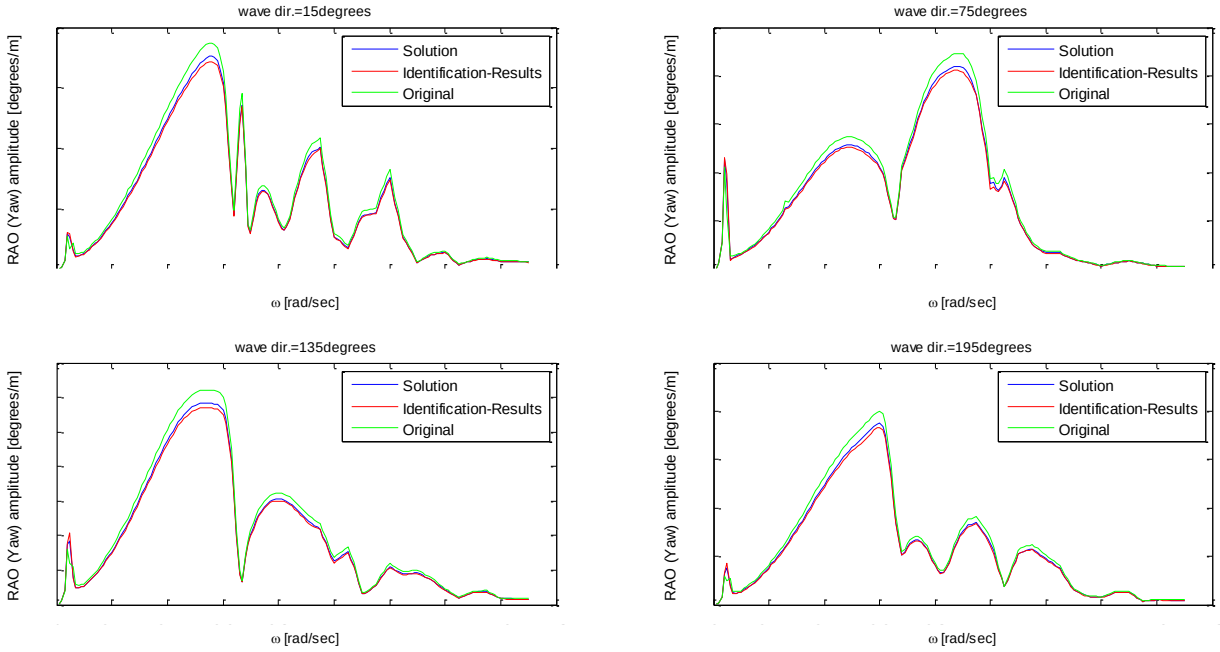

Figure 127: Comparison of RAOs: Amplitude of Yaw-RAO, test case 4

The NRMSEs of the RAOs for test case 4 are indicated in the following table

Table 39: Comparison of RAOs: Test case 4

Comparison of Surge-RAO	Original RAOs-Correct RAOs	Identified RAOs-Correct RAOs
Average NRMSE (all wave dir.)	0.936	0.978
Minimum NRMSE	0.842 (directions= 90º, 270º)	0.975 (directions= 0º)
Maximum NRMSE	0.955 (directions= 165º, 195º)	0.985 (directions= 90º, 270º)
Comparison of Sway-RAO	Original RAOs-Correct RAOs	Identified RAOs-Correct RAOs
Average NRMSE (all wave dir.)	0.976	0.983
Minimum NRMSE	0.975 (directions= 165º, 195º)	0.981 (directions= 90º, 270º)
Maximum NRMSE	0.977 (directions= 60º, 300º)	0.984 (directions= 165º, 195º)
Comparison of Heave-RAO	Original RAOs-Correct RAOs	Identified RAOs-Correct RAOs
Average NRMSE (all wave dir.)	0.744	0.938
Minimum NRMSE	0.657 (directions= 180º)	0.908 (directions= 60º, 300º)
Maximum NRMSE	0.796 (directions= 30º, 330º)	0.961 (directions= 105º, 255º)
Comparison of Roll-RAO	Original RAOs-Correct RAOs	Identified RAOs-Correct RAOs
Average NRMSE (all wave dir.)	0.374	0.765
Minimum NRMSE	0.351 (directions= 165º, 195º)	0.760 (directions= 165º, 195º)
Maximum NRMSE	0.389 (directions= 105º, 255º)	0.773 (directions= 15º, 345º)
Comparison of Pitch-RAO	Original RAOs-Correct RAOs	Identified RAOs-Correct RAOs
Average NRMSE (all wave dir.)	0.277	0.849
Minimum NRMSE	0.145 (directions= 0º)	0.840 (directions= 0º)
Maximum NRMSE	0.520 (directions= 90º, 270º)	0.883 (directions= 90º, 270º)
Comparison of Yaw-RAO	Original RAOs-Correct RAOs	Identified RAOs-Correct RAOs
Average NRMSE (all wave dir.)	0.901	0.965
Minimum NRMSE	0.868 (directions= 90º, 270º)	0.948 (directions= 90º, 270º)
Maximum NRMSE	0.910 (directions= 150º, 210º)	0.968 (directions= 30º, 330º)

The inaccuracies caused by the interpolation of the RAOs over the wave directions, were less than in the other test cases. Thus, the results of the identification procedure for test case 4, are the most accurate of all the other test cases. The identified RAOs approximate the real RAOs with NRMSEs larger than 0.7.

8.6 TEST CASE 5

The purpose of this test case is to show if it is possible to find the same results by calibrating either all the vessel properties or only the hydrodynamic database containing the added mass, damping and wave forces. As mentioned in CHAPTER 2, the hydrodynamic database should be investigated because of the awkward draught and the forward speed of the vessel. If those conditions do not occur, then the hydrodynamic properties of the vessel are defined properly. Based on these criteria, it is possible to choose either to calibrate the hydrodynamic database or the other vessel properties such as the radii of gyration, the CoG and the viscous damping. It is revealed that the response spectra of the data set for test case 5 are determined by using the hydrodynamic database corresponding to shallow water. Thus the identification procedure should calibrate the whole hydrodynamic database (original =deep water). The identification procedure is accomplished for two cases: 1) all the parameters are investigated 2) only the hydrodynamic database is examined. The wave spectra of the data set for the fifth test case are indicated in the following figure. The heading of the Thialf is 60°.

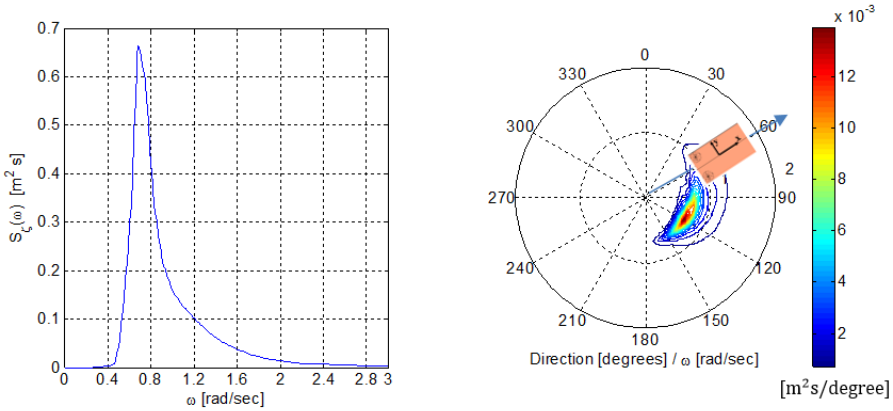

Figure 128: 1D and 2D wave spectra, test case 5

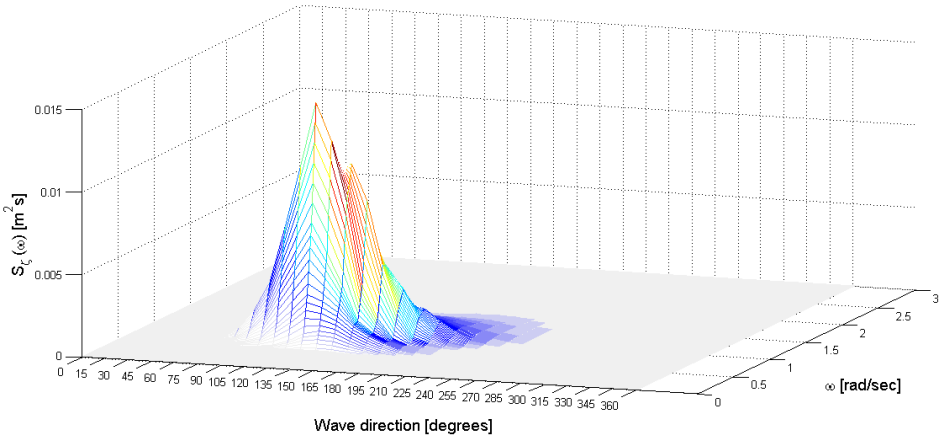

Figure 129: 2D wave spectrum, local coordinate system of the vessel, test case 5

Comparing the vessel motions on the basis of the original vessel properties with the motions of the vessel given in the data set, the following NRMSEs are obtained: surge=0.241, sway=0.807, heave=-1.810, roll=0.345, pitch=-0.842, yaw=0.855. The next figure shows the comparison of the calculated response spectra and the response spectra from the data set.

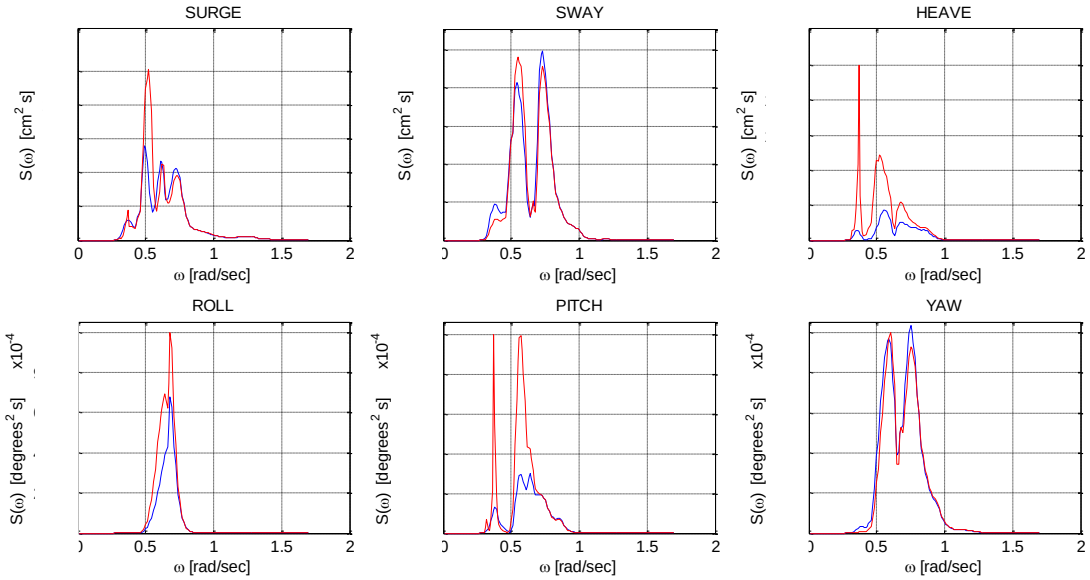

Figure 130: Comparison of motion response spectra, test case 5, data set=blue, calculations=red

As it can be seen, the differences between the calculations and the simulated data are higher than in the previous cases. The results of the two identification procedures are shown below: 1) all the parameters are investigated 2) only the hydrodynamic database is examined.

Table 40: Calibration of all the parameters

Elements	Modifications
r_{yy} (m)	74 (+25% Orig. value)
r_{zz} (m)	62 (-5% Orig. value)
z coordinate (m)	27.16 (+20% Orig. value)
c=1-2 for ab_{33}	-8.87*Orig.value
c=5-6 for ab_{44}	1.59*Orig.value
c=3-4 for ab_{31}	-7.53*Orig.value
c=7-8 for ab_{55}	31.28*Orig.value
c=3-4 for ab_{55}	1.4*Orig.value
c=1-2 for ab_{53}	-182*Orig.value
c=5-6 for ab_{11}	8.15*Orig.value
c=3-4 for ab_{51}	-0.09*Orig.value
c=21-22 for $F_5(\omega,120°)$	5.249*Orig.value
c=3-4 for $F_5(\omega,135°)$	4.44*Orig.value
c=15-16 for $F_3(\omega,165°)$	0.24*Orig.value
c=1-2 for $F_3(\omega,165°)$	4.44*Orig.value

Table 41: Calibration of the hyd. database

Elements	New values
c=5-6 for ab_{53}	26.87*Orig.value
c=5-6 for ab_{44}	1.59*Orig.value
c=1-2 for ab_{33}	-4.68*Orig.value
c=5-6 for ab_{11}	12.57*Orig.value
c=1-2 for ab_{53}	-42.56*Orig.value
c=5-6 for ab_{55}	5.42*Orig.value
c=3-4 for ab_{55}	1.4*Orig.value
c=5-6 for ab_{33}	3.73*Orig.value
c=7-8 for ab_{42}	2.44*Orig.value
c=23-24 for ab_{62}	31.28*Orig.value
c=1-2 for ab_{62}	-30.52*Orig.value
c=1-2 for $F_5(\omega,120°)$	0.298*Orig.value
c=3-4 for $F_1(\omega,120°)$	-0.605*Orig.value
c=3-4 for $F_1(\omega,135°)$	0.153*Orig.value
c=21-22 for $F_3(\omega,150°)$	-3.202*Orig.value
c=11-12 for $F_5(\omega,165°)$	-8.4*Orig.value
c=11-12 for $F_3(\omega,135°)$	-0.226*Orig.value
c=13-14 for $F_3(\omega,135°)$	0.0081*Orig.value
c=9-10 for $F_3(\omega,150°)$	4.44*Orig.value
c=9-10 for $F_4(\omega,135°)$	-1.22*Orig.value
c=5-6 for $F_4(\omega,135°)$	0.532*Orig.value
c=17-18 for $F_4(\omega,135°)$	-8.4*Orig.value
c=5-6 for $F_5(\omega,105°)$	0.387*Orig.value

The resulting NRMSEs are indicated in the following table.

Table 42: Final NRMSEs: Test case 5

Motions	NRMSE Identification1	NRMSE Identification2	NRMSE Solution
Surge	0.778	0.908	0.975
Sway	0.895	0.895	0.983
Heave	0.725	0.847	0.987
Roll	0.727	0.961	0.978
Pitch	0.752	0.77	0.989
Yaw	0.839	0.934	0.952
Average (NRMSEs)	0.786	0.886	0.977

The resulting response spectra of the two identification procedures and the response spectra based on the real changes are compared with the response spectra from the data set.

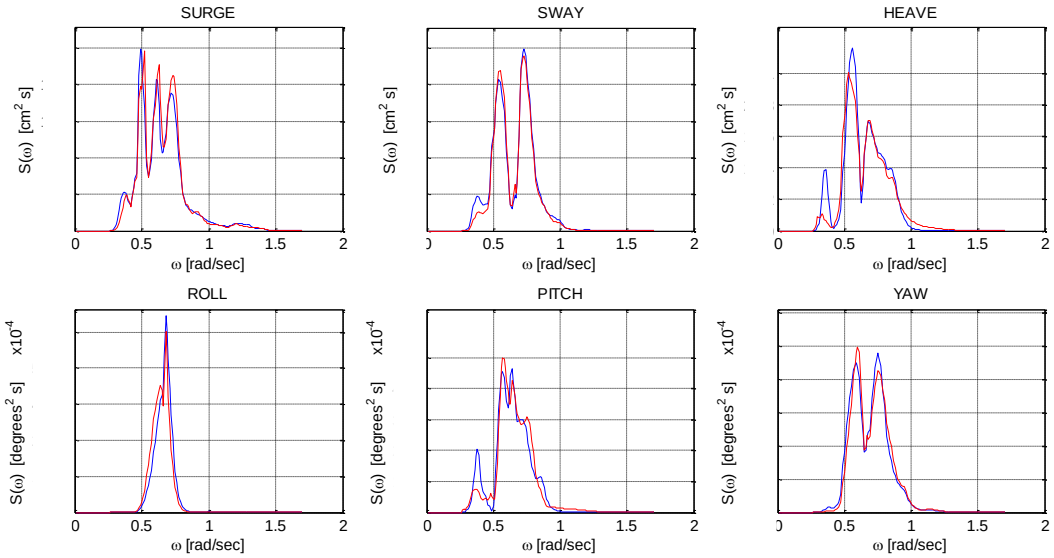

Figure 131: Motion response spectra, identification 1, test case 5, data set=blue, calculations=red

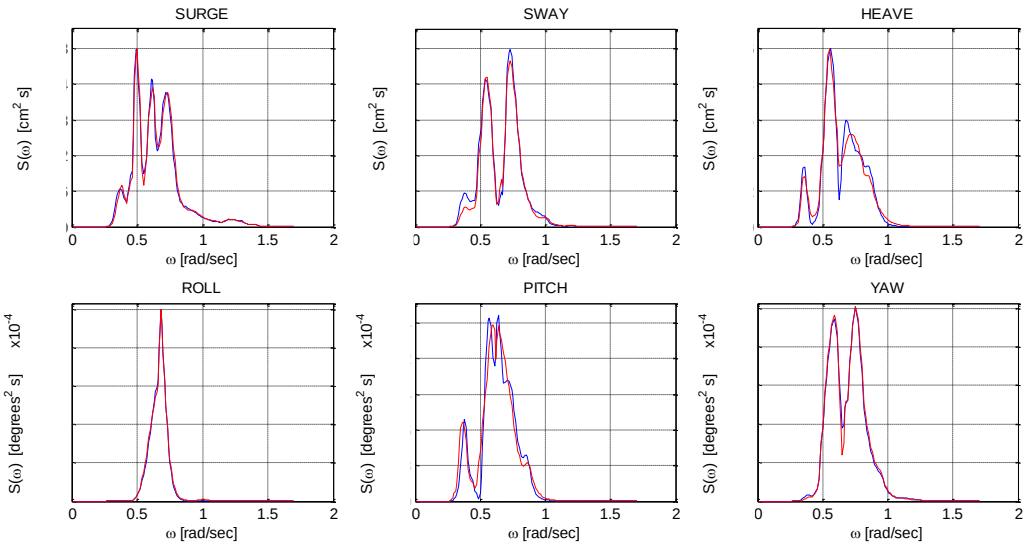

Figure 132: Motion response spectra, identification 2, test case 5, data set=blue, calculations=red

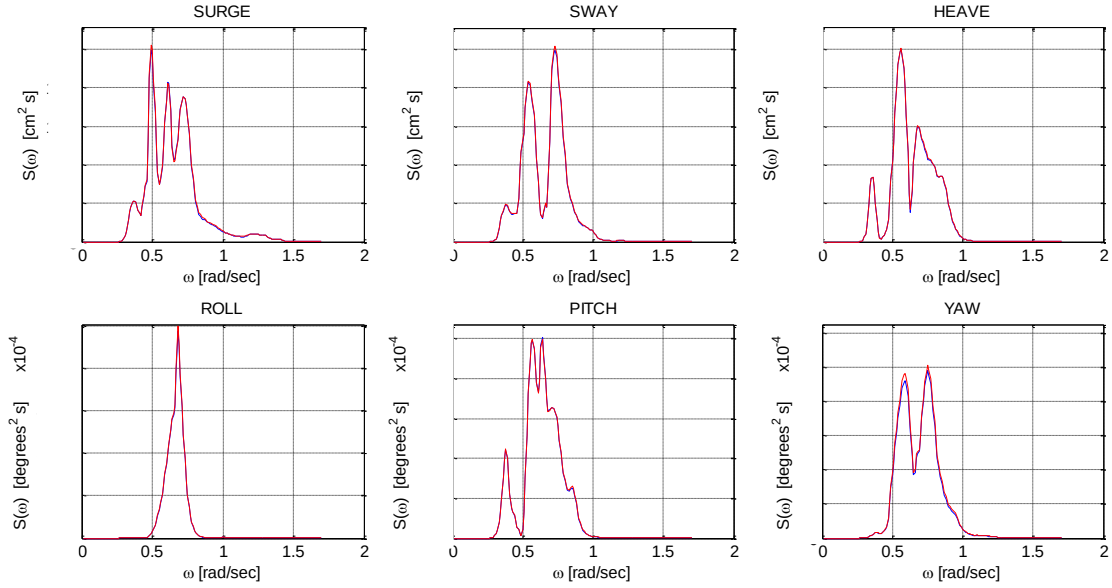

Figure 133: Motion response spectra, solution, test case 5, data set=blue, calculations=red

By only calibrating the hydrodynamic database, the resulting response spectra are slightly more accurate than in the case of calibrating all the vessel parameters.

The significant values for each vessel motion are shown in the following table:

Table 43: Significant values of motions: Test case 5

Motions	Data	Original		Identification1		Identification2		Solution	
	Sign.value	Sign.value	dx (%)	Sign.value	dx (%)	Sign.value	dx (%)	Sign.value	dx (%)
Surge (m)	[redacted]	[redacted]	8.10	[redacted]	1.15	[redacted]	-0.33	[redacted]	0.63
Sway (m)	[redacted]	[redacted]	-0.82	[redacted]	-1.99	[redacted]	-2.84	[redacted]	0.72
Heave (m)	[redacted]	[redacted]	65.43	[redacted]	-1.39	[redacted]	-0.18	[redacted]	0.42
Roll (degrees)	[redacted]	[redacted]	26.98	[redacted]	0.28	[redacted]	1.32	[redacted]	0.92
Pitch (degrees)	[redacted]	[redacted]	38.82	[redacted]	0.25	[redacted]	1.89	[redacted]	0.11
Yaw (degrees)	[redacted]	[redacted]	-3.77	[redacted]	-1.09	[redacted]	0.35	[redacted]	2.13

According to the above table, the inaccuracies due to data processing are less than in the other cases. For almost all motions, the term 'dx' of the 'Solution' is less than 1%. With respect to the results of the two identification procedures, the significant values of sway, roll and pitch are more accurate for the 1st identification process (calibration of all parameters). The significant values of surge, heave and yaw are more accurate for the 2nd identification process (calibration of hydrodynamic database). However, both identification procedures do not show large differences regarding the resulting significant values. This means that the changes of the elements of the hydrodynamic database can be confused with the changes of the other parameters. For instance, by changing either the element ab_{55} or the radius of gyration r_{yy}, we can obtain the same response spectra. It should also be mentioned that for the first identification procedure, the only element that improved the yaw motion was the radius of gyration r_{zz} (Table 40). However, to calibrate the yaw motion for the 2nd identification procedure, we change the element ab_{62} (Table 41). Finally, it is not clear which elements of the hydrodynamic data base of the 2nd identification procedure can replace the modification of the 'z' coordinate.

As shown in the previous table, the modifications found by both identification procedures lead to more accurate response spectra. The resulting significant values of motions are satisfying. However, it is also important to investigate the accuracy of the resulting RAOs. The following

figures show the comparison of the RAOs. The blue curve stands for the RAOs of the 'Solution', the red curve stands for the identified RAOs and green curve stands for the original RAOs.

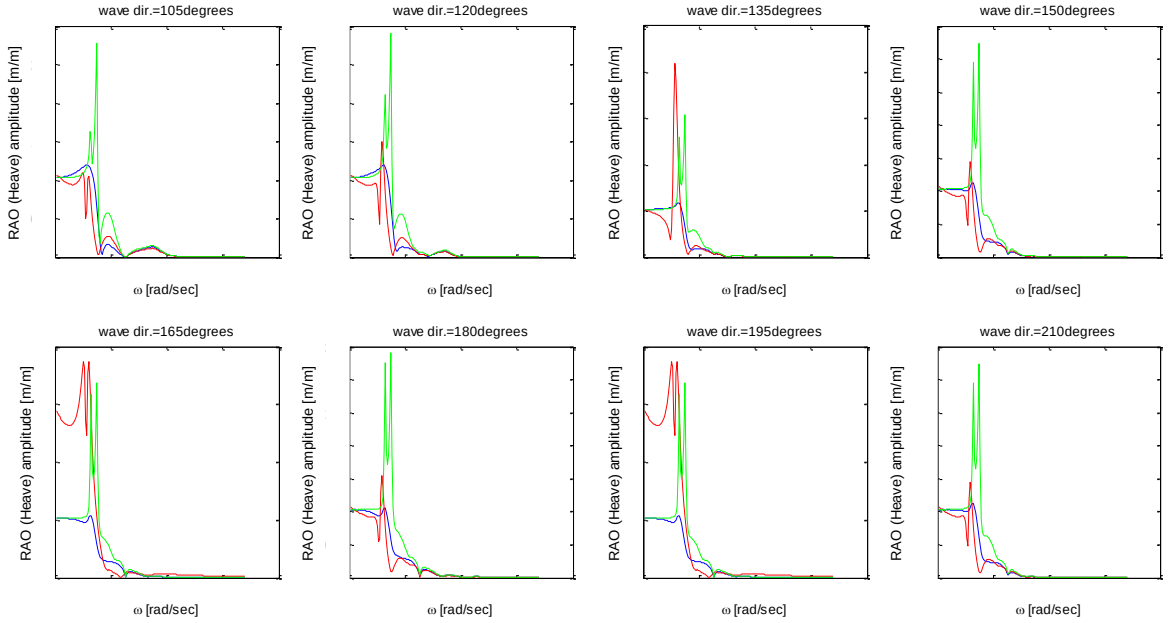

Figure 134: Comparison of RAOs, amplitude of Heave-RAO, identification 1, test case 5, blue=solution, red=identification-results, green=original

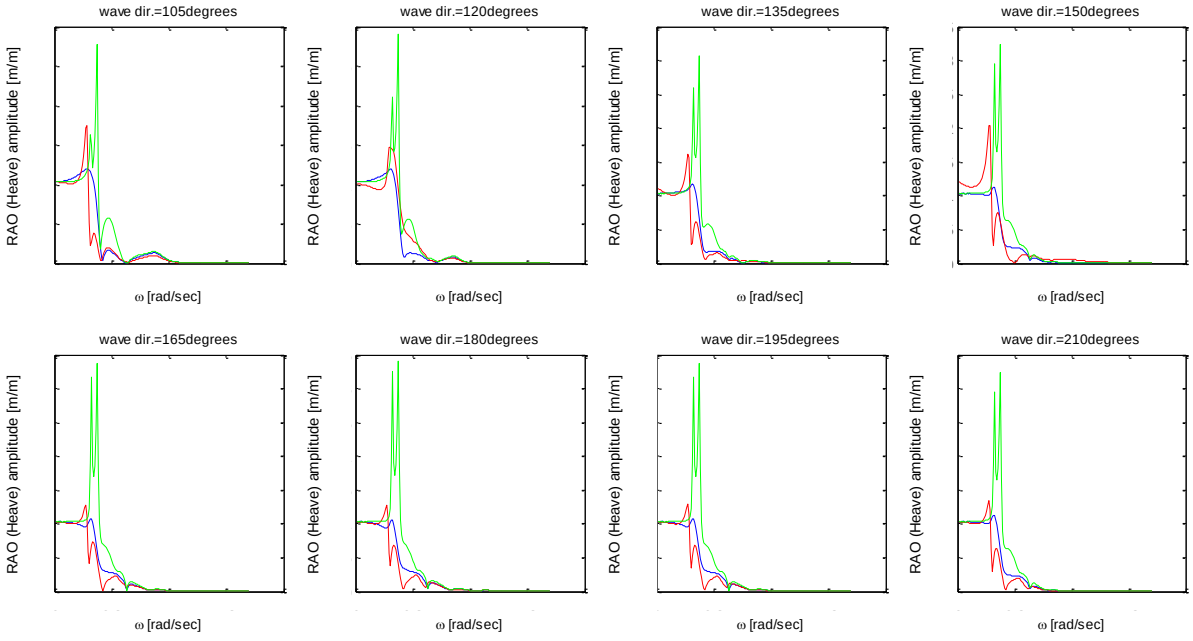

Figure 135: Comparison of RAOs, amplitude of Heave-RAO, identification 2, test case 5, blue=solution, red=identification-results, green=original

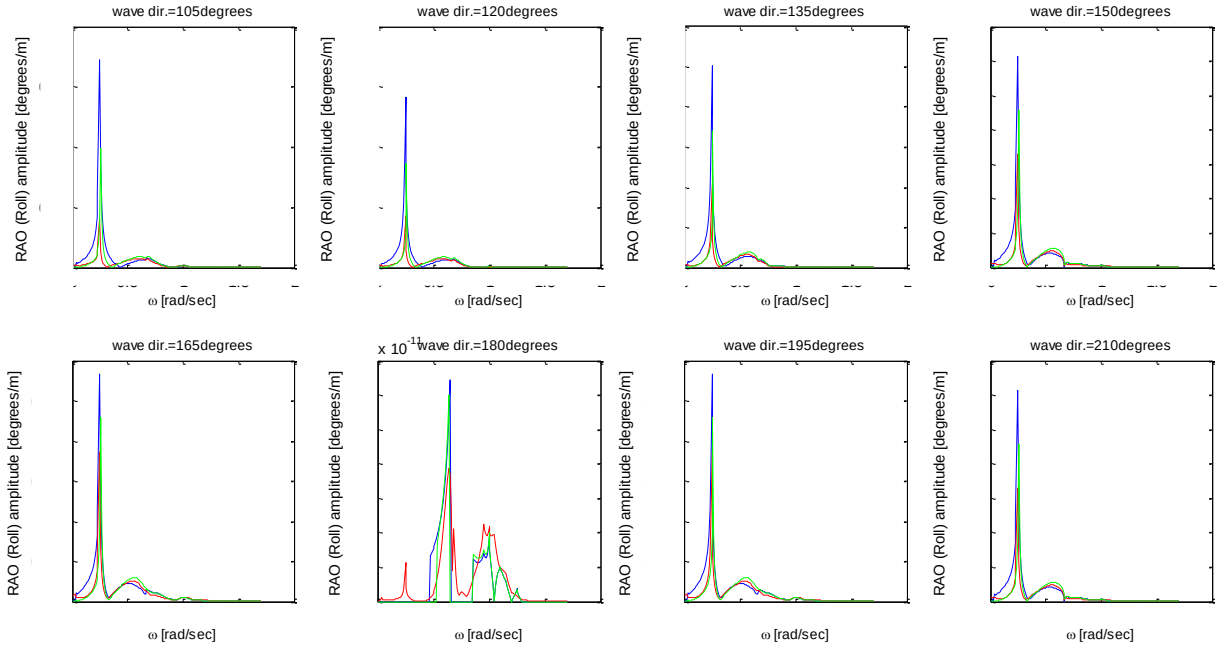

Figure 136: Comparison of RAOs, amplitude of Roll-RAO, identification 1, test case 5, blue=solution, red=identification-results, green=original

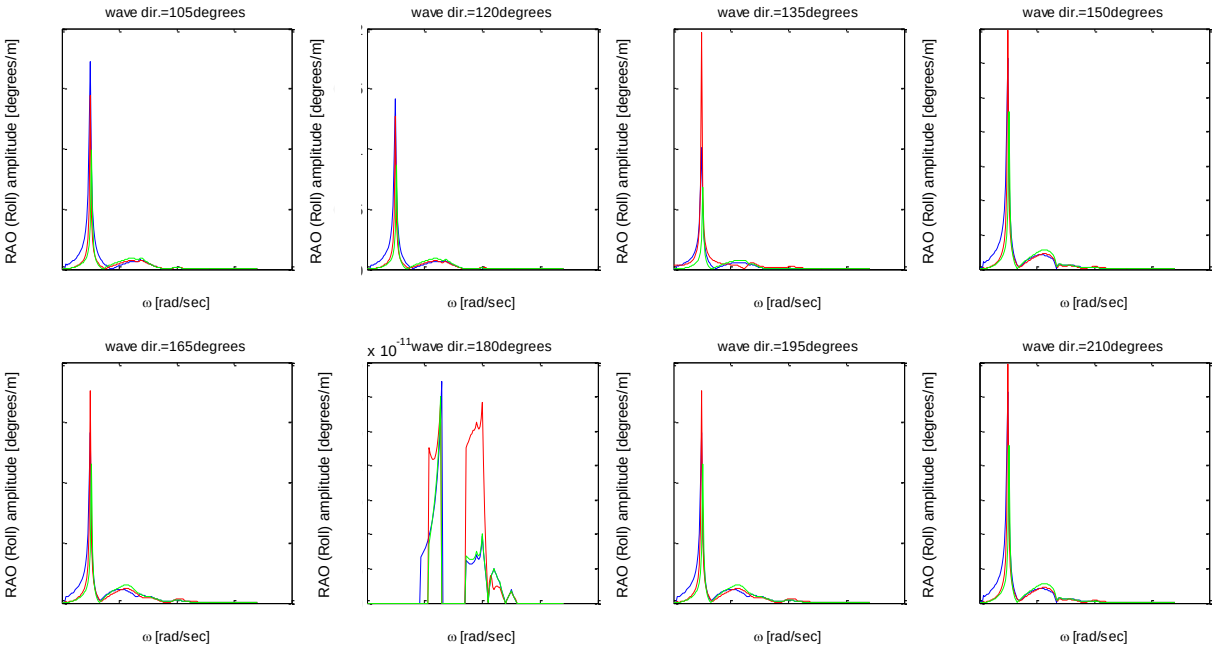

Figure 137: Comparison of RAOs, amplitude of Roll-RAO, identification 2, test case 5, blue=solution, red=identification-results, green=original

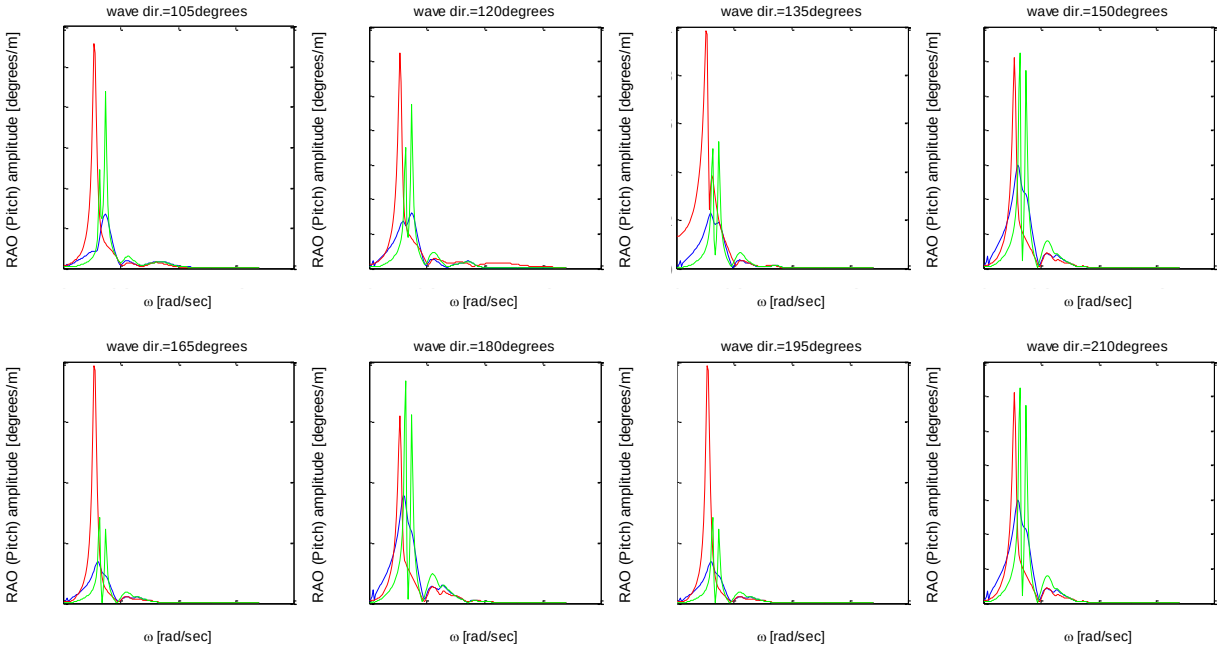

Figure 138: Comparison of RAOs, amplitude of Pitch-RAO, identification 1, test case 5, blue=solution, red=identification-results, green=original

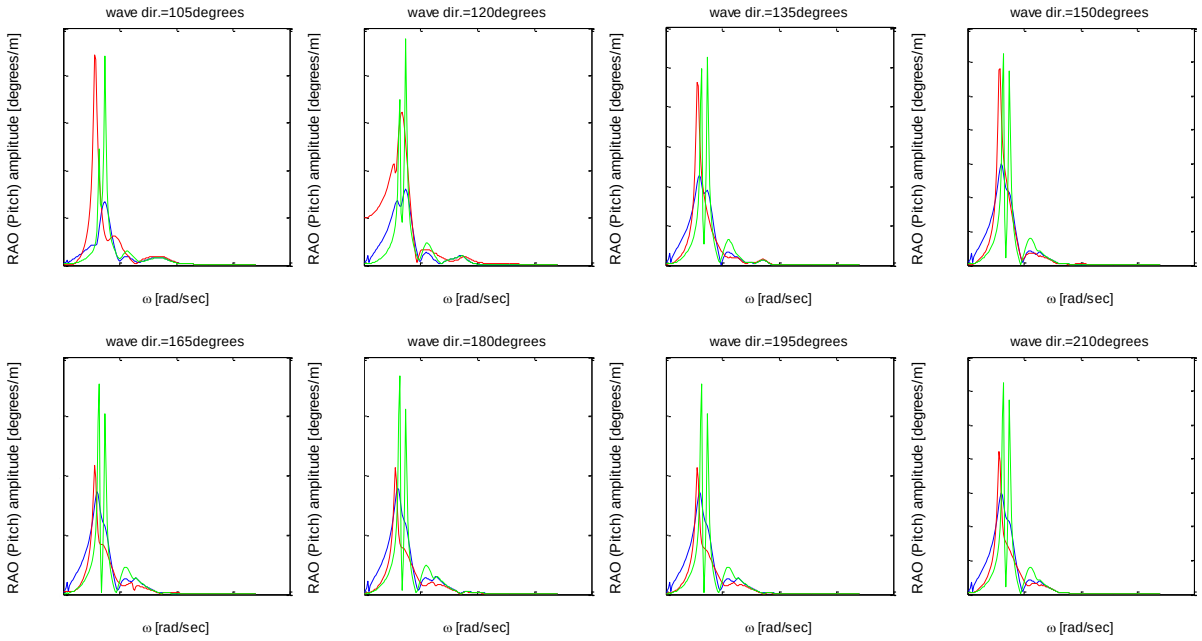

Figure 139: Comparison of RAOs, amplitude of Pitch-RAO, identification 2, test case 5, blue=solution, red=identification-results, green=original

The NRMSEs of the RAOs are shown in the following tables:

Table 44: Comparison of RAOs: Test case 5, Identification 1

Comparison of Surge-RAO	Original RAOs-Correct RAOs	Identified RAOs-Correct RAOs
Average NRMSE (all wave dir.)	-6.768	-1.013
Minimum NRMSE	-7.651 (directions=0º)	-1.818(directions=180º)
Maximum NRMSE	0.611 (directions=90º, 270º)	0.305(directions=90º, 270º)
Comparison of Sway-RAO	Original RAOs-Correct RAOs	Identified RAOs-Correct RAOs
Average NRMSE (all wave dir.)	-7.908	-0.364
Minimum NRMSE	-8.015 (directions=90º, 270º)	-0.625(directions=150º, 210º)
Maximum NRMSE	-7.808 (directions=135º, 225º)	0.021(directions=30º, 330º)
Comparison of Heave-RAO	Original RAOs-Correct RAOs	Identified RAOs-Correct RAOs
Average NRMSE (all wave dir.)	0.432	0.599
Minimum NRMSE	0.316 (directions=0º)	0.244(directions=165º, 195º)
Maximum NRMSE	0.534 (directions=105º, 255º)	0.754(directions=45º, 315º)
Comparison of Roll-RAO	Original RAOs-Correct RAOs	Identified RAOs-Correct RAOs
Average NRMSE (all wave dir.)	-0.344	-1.207
Minimum NRMSE	-0.615 (directions=90º, 270º)	-3.087(directions=90º, 270º)
Maximum NRMSE	-0.061 (directions=165º, 195º)	0.270(directions=165º, 195º)
Comparison of Pitch-RAO	Original RAOs-Correct RAOs	Identified RAOs-Correct RAOs
Average NRMSE (all wave dir.)	0.376	0.260
Minimum NRMSE	0.352 (directions=0º)	0.067(directions=105º, 255º)
Maximum NRMSE	0.408 (directions=90º, 270º)	0.462(directions=45º, 315º)
Comparison of Yaw-RAO	Original RAOs-Correct RAOs	Identified RAOs-Correct RAOs
Average NRMSE (all wave dir.)	-3.390	-0.033
Minimum NRMSE	-4.584 (directions=120º, 240º)	-2.402(directions=15º, 345º)
Maximum NRMSE	-2.226 (directions=75º, 285º)	0.392(directions=75º, 285º)

Table 45: Comparison of RAOs: Test case 5, Identification 2

Comparison of Surge-RAO	Original RAOs-Correct RAOs	Identified RAOs-Correct RAOs
Average NRMSE (all wave dir.)	-6.768	-6.344
Minimum NRMSE	-7.651 (directions=0º)	-7.887 (directions=0º)
Maximum NRMSE	0.611 (directions=90º, 270º)	0.504 (directions=90º, 270º)
Comparison of Sway-RAO	Original RAOs-Correct RAOs	Identified RAOs-Correct RAOs
Average NRMSE (all wave dir.)	-7.908	-7.875
Minimum NRMSE	-8.015 (directions=90º, 270º)	-8.010 (directions=165º, 195º)
Maximum NRMSE	-7.808 (directions=135º, 225º)	-7.507 (directions=135º, 225º)
Comparison of Heave-RAO	Original RAOs-Correct RAOs	Identified RAOs-Correct RAOs
Average NRMSE (all wave dir.)	0.432	0.640
Minimum NRMSE	0.316 (directions=0º)	0.500 (directions=0º)
Maximum NRMSE	0.534 (directions=105º, 255º)	0.741 (directions=120º, 240º)
Comparison of Roll-RAO	Original RAOs-Correct RAOs	Identified RAOs-Correct RAOs
Average NRMSE (all wave dir.)	-0.344	0.484
Minimum NRMSE	-0.615 (directions=90º, 27º)	0.299 (directions=90º, 270º)
Maximum NRMSE	-0.061 (directions=165º, 195º)	0.624 (directions=13º, 345º)
Comparison of Pitch-RAO	Original RAOs-Correct RAOs	Identified RAOs-Correct RAOs
Average NRMSE (all wave dir.)	0.376	0.315
Minimum NRMSE	0.352 (directions=0º)	-0.181 (directions=0º)
Maximum NRMSE	0.408 (directions=90º, 270º)	0.575 (directions=150º, 210º)
Comparison of Yaw-RAO	Original RAOs-Correct RAOs	Identified RAOs-Correct RAOs
Average NRMSE (all wave dir.)	-3.390	-2.618
Minimum NRMSE	-4.584 (directions=120º, 240º)	-4.210 (directions=60º, 300º)
Maximum NRMSE	-2.226 (directions=75º, 285º)	-0.603 (directions=90º, 270º)

The RAOs for surge, sway yaw and the RAOs for heave, roll pitch are more accurate for the 1st and the 2nd identification procedures, respectively. However, the NRMSEs are still very small for both identification procedures and thus, the identified RAOs do not approximate the correct RAOs. Although the identified response spectra match the response spectra of the data set, the resulting RAOs differ from the correct RAOs. Large number of combinations of modified elements can be found to adjust the final vessel responses. Therefore, it is not possible to find the correct combination that leads to accurate RAOs.

CHAPTER 9. Conclusions-Recommendations

9.1 CONCLUSIONS

As mentioned in the first chapter of this thesis, the main purpose of this graduation study was to develop a mathematical method which determines the RAOs from full-scale vessel motion measurements and available wave data. The main objective was to calibrate the following properties of the vessel that contribute to the calculation of the RAOs:

- Radii of gyration
- CoG coordinates
- Additional viscous damping
- Hydrodynamic potential added mass and damping
- Hydrodynamic potential forces and moments

After having developed and tested the proposed method in the previous chapters, the final conclusions are presented here.

9.1.1 Vector fitting

Fitting of frequency dependent vessel properties:

The vector fitting method can be used to express the frequency dependent elements of the added mass, the damping and the wave forces, with approximation functions of a limited number of parameters. The approximation functions are the sum of partial fractions of complex poles and related complex residues and in some cases they also include two real quantities. By applying the vector fitting method, we can fit an approximation function to each element of the following matrices: potential added mass, potential damping and potential wave forces.

Fitting of added mass and damping:

According to potential theory, the added mass and damping belong to the same complex number. Thus, the fitting process is accomplished for the following complex quantity: the real part is the added mass and the imaginary part is the damping divided by the wave frequency. The approximation of the hydrodynamic added mass and damping is performed with great accuracy.

Fitting of wave forces:

Regarding the wave forces, although the accuracy of the fitting process is lower than for the added mass and damping, the results are satisfying. The vector fitting method can also be used for the interpolation of the wave forces over the wave directions. The wave forces of the in-between wave directions can be determined by interpolating the residues of the approximation functions.

Use of fitted elements:

The calibration of the added mass, damping and wave forces can be accomplished by only modifying the residues of the approximation functions. If we want to lower a peak of a curve, we can reduce the values of the corresponding residues. Also, if we want to create an extra peak, we can increase the related pair of residues.

Accuracy of vector fitting:

The accuracy of the fitting process was also tested by calculating the response spectra and the RAOs using the approximated elements. The fitted response spectra match the original vessel responses with great accuracy. It is noticed that the fitted curves of the RAOs for surge, sway and yaw motions show high resonant peaks at very low wave frequencies. The swell and the wind sea occur at higher frequencies and thus, the before-mentioned resonant peaks do not influence the final response spectra of the vessel.

9.1.2 Sensitivity analysis

Radii of gyration

The sensitivity analysis shows that each radius of gyration mainly influences one specific motion. Thus the identification procedure for the radii of gyration can be simplified. The calibration of r_{xx} (around longitudinal axis of vessel), r_{yy} (around transversal axis of vessel) and r_{zz} (around vertical axis of vessel) influence the roll, pitch and yaw motions respectively. The identified values for r_{yy} and r_{zz}, are satisfying for all test cases. Regarding the radius of gyration r_{xx}, it is suggested to keep the original value. During projects, the mass distribution of the vessel is symmetrical with respect to x axis and does not show remarkable variations. Therefore, if we want to calibrate the roll motion, we should select an alternative parameter instead of r_{xx}. If it is necessary, we can make small changes to r_{xx} at the end of the identification procedure.

Coordinates of CoG

The fluctuations of each coordinate of the CoG affect more than one vessel motion. In order to adjust each coordinate, we should consider the average value of the normalized root mean square errors of the 6 vessel motions. The longitudinal, 'x', and transversal, 'y' coordinates do not show great variations during projects. However the vertical, 'z', coordinate can get several values during the lifting operations. Therefore, it is acceptable to change the 'z' coordinate as long as it leads to more accurate vessel motions. On the other hand, we should avoid the changes of the longitudinal and transversal coordinates and prefer the modifications of other alternative parameters.

Viscous damping

The magnitude of the additional viscous damping is much lower than the potential damping. This means that the variations of the viscous damping do not affect the final response spectra. This is the reason why the identification method cannot adjust small changes of the elements of the viscous damping matrix. However, for rolling ships, such as the Aegir, the hydrodynamic potential damping corresponding to the roll motion is low. Thus, it is possible to find a reasonable value for the element of the viscous damping corresponding to roll motion and obtain more accurate roll motion.

9.1.3 Identification procedure

Non unique solution

The main characteristic of the developed identification method is that each parameter of the RAOs is investigated, separately. For each repetition of the identification procedure, we get the best possible value for each parameter. For example, to calibrate the roll motion, several solutions are provided: to modify the radius of gyration, r_{xx}, or the element of the added mass-damping, ab_{44}, or the wave moment, M_4, or the diagonal element of the viscous damping related to roll motion, $\mathbf{B_{ad}}(4,4)$. The main criterion to select one of these modifications is to compare the resulting inaccuracies of the motion response spectra. These inaccuracies are determined by estimating the normalized mean square error between the calculated response spectra and the response spectra of the real measurements (data set). However, it is also important to make a choice based on logical criteria. For instance, if the viscous damping needs to take too high values to cause more accurate responses, then, it is more realistic to change the elements of the potential damping instead of the viscous damping.

Optimization of identification procedure by the golden section method

To find the best possible value for a parameter, the golden section method is applied. According to this method, a wide range of values are investigated until we find the value of the parameter that causes the most accurate response spectra. To apply this method, we assume that only one value for each parameter gives the most accurate response spectra. This assumption should further be investigated.

Data processing

The results of the identification method are affected by the quality of the measurements and the data processing. The measured response spectra should provide information about a great number of wave frequencies. If the frequency step is large, several resonant peaks will not be shown. Another cause of false results is the interpolation of the RAOs over the wave directions. If the directional wave spectrum is measured for a large number of wave directions, we need to interpolate the RAOs. The different methods of interpolation of the RAOs lead to slightly different response spectra. Also, if the distribution of the wave spectrum over the wave directions is not smooth, the inaccuracies due to the interpolation are higher.

Symmetry of the vessel and coupled motions

The identification procedure became much faster because of the symmetrical geometry of the semi-submersible crane vessel Thialf. If a vessel has a symmetrical geometry, limited number of motions are coupled and the matrices of the hydrodynamic database are symmetrical. Due to the fact that some elements of the hydrodynamic matrices are identical, the approximation functions are identical as well. During the identification procedure, we could also eliminate the modification of a great number of elements. For each repetition, the identification process focuses on the calibration of the motion with the maximum inaccuracies. Therefore, only the elements which are coupled with that motion are examined.

Accuracy of identified RAOs

If the number of the modifications needed for more accurate response spectra is large, then the resulting RAOs might not be accurate. This can be explained by the fact that there are many possible modifications that lead to accurate vessel responses but not to accurate RAOs. In case of small number of identified changes, the accuracy of the identified RAOs is satisfying.

9.2 RECOMMENDATIONS

After testing the identification method for several cases, the following recommendations can be proposed:

Selection of certain parameters to be investigated based on the causes of inaccuracies of vessel motions.

The potential added mass, damping and wave forces, calculated by the diffraction software, should be investigated only for the following cases:

- The awkward draught
- The forward speed of the vessel
- Change of vessel draft

Application of the identification method to the semi-submersible crane vessel Balder

The potential added mass, damping and wave forces should be investigated due to awkward draught. For the standard drafts that the pontoons are below the sea surface, only the radii of gyration and the CoG should be adjusted. After calibrating the before-mentioned properties, we can repeat the identification procedure to adjust the added mass, damping and wave forces for the awkward drafts. Finally, the identification procedure can also be accomplished when the J-lay tower is on the Balder. This means that the vessel will not have symmetrical geometry and the mass distribution will show high variations.

Application of the identification method to the deep water construction vessel Aegir

- **Non-symmetrical geometry.** The identification procedure should also be applied to the Aegir which is a non-symmetrical vessel. Because of the non-symmetrical geometry, the number of parameters to be examined will be increased and the identification procedure will be slower. In addition, the sensitivity analysis for this ship

will be more complicated. It might not be clear which parameters affect each motion. Thus, there will be many possible modifications to obtain accurate response spectra. This also means that the identified RAOs might not be accurate.

- **Viscous damping.** It would also be important to adjust the viscous damping matrix of the Aegir. For this ship, the hydrodynamic potential damping corresponding to roll motion is low and thus the deviations of viscous damping affects the roll motion. It would be interesting to examine if it is possible to identify the viscous damping for this vessel.

Use of real measurements

It is important to test the identification method using real measurements. In this case, the noise on the measurement data might have negative effects on the accuracy of the identification procedure.

Investigation of more wave directions

It is suggested to calibrate the RAOs for a large number of wave directions. The measured wave spectrum represents the wave energy that comes from different directions. Thus, it is preferred to calibrate the wave forces (used for the calculation of the RAOs) for wave directions with a step of 5 degrees instead of 15 degrees. By using a small step of wave directions, we can reduce the inaccuracies caused by the data processing. It should also be noted, that the range of wave directions which was examined is -45^{o} to +45^{o} with respect to the main wave direction. However, the wave forces outside that range can also affect the vessel motions. Therefore, it is suggested to examine a wider range of direction to obtain more accurate results.

References

1. J.M.J Journee, W.W.Massie, Offshore Hydromechanics, Delft University of Technology, January 2001, Chapter 6, pr. 6.2.3.

2. J.M.J Journee, W.W.Massie, Offshore Hydromechanics, Delft University of Technology, January 2001, Chapter 2, pr. 2.3.6.

3. J.M.J Journee, W.W.Massie, Offshore Hydromechanics, Delft University of Technology, January 2001, Chapter 6, pr. 6.3.2.

4. J.M.J Journee, W.W.Massie, Offshore Hydromechanics, Delft University of Technology, January 2001, Chapter 7, pr. 7.2.

5. J.M.J Journee, W.W.Massie, Offshore Hydromechanics, Delft University of Technology, January 2001, Chapter 7, pr. 7.2.2.

6. J.M.J Journee, W.W.Massie, Offshore Hydromechanics, Delft University of Technology, January 2001, Chapter 7, pr. 7.2.3.

7. J.M.J Journee, W.W.Massie, Offshore Hydromechanics, Delft University of Technology, January 2001, Chapter 7, pr. 7.2.4.

8. J.M.J Journee, W.W.Massie, Offshore Hydromechanics, Delft University of Technology, January 2001, Chapter 7, pr. 7.6.

9. LEO H. HOLTHUIJSEN. WAVES IN OCEANIC AND COASTAL WATERS. Delft University of Technology, UNESCO-IHE. First Published 2007. Chapter 3.

10. LEO H. HOLTHUIJSEN. WAVES IN OCEANIC AND COASTAL WATERS. Delft University of Technolog, UNESCO-IHE. First published 2007. Chapter 1.

11. HMC. Liftdyn Theory Manual. Version 1. pr. 7.3.1.

12. ‘Rational approximation of frequency domain responses by vector fitting’, Adam Semlyen & Bjorn Gustavsen, IEEE Transaction on Power Delivery, July 1999, Vol 14, p. 1052, No. 3. Section 1.

13. ‘Rational approximation of frequency domain responses by vector fitting’, Adam Semlyen & Bjorn Gustavsen, IEEE Transaction on Power Delivery, July 1999, Vol 14, p. 1052, No. 3. Section 2.

14. 'Rational approximation of frequency domain responses by vector fitting’, Adam Semlyen & Bjorn Gustavsen, IEEE Transaction on Power Delivery, July 1999, Vol 14. Appendix A, No 3.

15. ‘Simulation of transmission line transients using vector fitting and modal decomposition' , Bjorn Gustavsen & Adam Semlyen, IEEE Transaction on Power Delivery, April 1998, Vol. 13, Appendix C, No 3.

16. 'Rational approximation of frequency domain responses by vector fitting’, Adam Semlyen & Bjorn Gustavsen, IEEE Transaction on Power Delivery, July 1999, Vol 14, Appendix B, No 3.

17. ‘Rational approximation of frequency domain responses by vector fitting’, Adam Semlyen & Bjorn Gustavsen, IEEE Transaction on Power Delivery, July 1999, Vol 14, p. 1052, No. 3. Section 3.

18. 1994-2015 The MathWorks, Inc. Goodness of fit between test and reference data. http://nl.mathworks.com/help/ident/ref/goodnessoffit.html#zmw57dd0e33974.

19. HMC. Liftdyn Theory Manual. Version 1. pr. 4.1.

20. HMC. Liftdyn Theory Manual. Version 1. pr. 4.1.1.

21. HMC. Liftdyn Theory Manual. Version 1. pr. 4.1.2.

22. HMC. Liftdyn Theory Manual. Version 1. pr. 4.1.3.

23. HMC. Liftdyn Theory Manual. Version 1. pr. 4.3.

24. HMC. Liftdyn Theory Manual. Version 1. pr. 4.5.1.

25. HMC. Liftdyn Theory Manual. Version 1. pr. 4.6.

26. William H. Press, Saul A. Teukolsky, William T. Vetterling, Brian P. Flannery, Numerical Recipes in C, Second edition, Cambridge University Press, June 1992, Chapter 10, pr. 10.1.

27. Ruben de Bruin, hmc Spectral Body, HMC, June 2012

Appendix A1 Peak selection

```
%% For Added mass and Damping:
% fs=squeeze(AB(i,j,1:nfreq) ) for the local maxima
% fs_inv=squeeze(1/AB(i,j,1:nfreq)) for the local minima
% i: from 1 to 6 and j: from 1 to 6

%% For the wave forces:
% fs=squeeze(F(i,direction,1:nfreq) ) for the local maxima
% fs_inv=squeeze(1/F(i,direction,1:nfreq)) for the local minima
% i: values from 1 to 6

[pks_max,locs_max] = findpeaks(abs(fs(1,:)));
[pks_min,locs_min] = findpeaks(fs_inv(1,:));
nMax=size(locs_max,2);
nMin=size(locs_min,2);

p=0;
for i=1:nMax
    Max=locs_max(1,i);
    if (Omega(1,Max)>0.15)&&(Omega(1,Max)<1.6)
       p=p+1;
       PGuess(1,p)=Omega(1,Max);
       view_Om(1,p)=Omega(1,Max);
       view_fs(1,p)=fs(1,Max);
    end
end
for i=1:nMin
    Min=locs_min(1,i);
    if (Omega(1,Min)>0.15)&&(Omega(1,Min)<1.6)
        p=p+1;
        PGuess(1,p)=-Omega(1,Min);
        view_Om(1,p)=Omega(1,Min);
        view_fs(1,p)=fs(1,Min);
    end
end

npoles=size(PGuess,2);
t=1;
for i=1:npoles
    a(t,1)=PGuess(1,i)/100+PGuess(1,i)*1i;
    a(t+1,1)=conj(a(t,1));
    t=t+2;
end
```

Appendix A2 Stage1-Identification of poles

```
npoles=size(a,1);  %a is the matrix of the starting poles
step1=npoles;
step2=npoles+1;
step3=npoles+2;
step4=npoles+2+npoles;
%Find zeros of sigma by several repetitions(maxrep=1000)
%fs=squeeze(AB(i,j,1:nfreq) )
int=3;
RMS(1,1)=10^(50);
RMS(2,1)=10^(49);
while (RMS(int-1,1)<RMS(int-2,1))&&(int<maxrep)
        for i=1:nfrequencies
         for k=1:2:step1-1
             Asvd(i,k)=real((1/(s(1,i)-a(k,1)))+(1/(s(1,i)-
a(k+1,1))));
             Asvd(i,k+1)=real((1i/(s(1,i)-a(k,1)))-(1i/(s(1,i)-
a(k+1,1))));
             Asvd(i+nfrequencies,k)=imag((1/(s(1,i)-
a(k,1)))+(1/(s(1,i)-a(k+1,1))));
             Asvd(i+nfrequencies,k+1)=imag((1i/(s(1,i)-a(k,1)))-
(1i/(s(1,i)-a(k+1,1))));
         end
         Asvd(i,step2)=1;
         Asvd(i,step3)=real(s(1,i));
         Asvd(i+nfrequencies,step2)=imag(1);
         Asvd(i+nfrequencies,step3)=imag(s(1,i));
         for r=1+step3:2:step4-1
             Asvd(i,r)=real((-fs(1,i))/(s(1,i)-a(r-step3,1))+(-
fs(1,i))/(s(1,i)-a(r-step3+1,1)));
             Asvd(i,r+1)=real((-fs(1,i)*1i)/(s(1,i)-a(r-step3,1))-(-
fs(1,i)*1i)/(s(1,i)-a(r-step3+1,1)));
             Asvd(i+nfrequencies,r)=imag((-fs(1,i))/(s(1,i)-a(r-
step3,1))+(-fs(1,i))/(s(1,i)-a(r-step3+1,1)));
             Asvd(i+nfrequencies,r+1)=imag((-fs(1,i)*1i)/(s(1,i)-a(r-
step3,1))-(-fs(1,i)*1i)/(s(1,i)-a(r-step3+1,1)));
         end
        end
        %Least square solution
        for i=1:nfrequencies
         Refs(i,1)=real(fs(1,i));
         Imfs(i,1)=imag(fs(1,i));
        end
        flsq=[Refs;Imfs];
        Llsq=inv(Asvd'*Asvd)*Asvd'*flsq;
        %Calculation of residues of sigma for pole identification
        for k=1:2:npoles-1
        Csig(k,1)=Llsq(k+npoles+2,1);
        Csig(k+1,1)=Llsq(k+npoles+3,1);
        Csigma(k,1)=Csig(k,1)+1i*Csig(k+1,1);
        Csigma(k+1,1)=Csig(k,1)-1i*Csig(k+1,1);
        end
        %Calculation of sigma
        for i=1:nfrequencies
             sums(int,i)=0;
             for k=1:2:npoles-1
                sums(int,i)=sums(int,i)+Csigma(k,1)/(s(1,i)-
a(k,1))+Csigma(k+1,1)/(s(1,i)-a(k+1,1));
            end
```

```
            sigma(int,i)=sums(int,i)+1;
            Dsigma(int,i)=abs(sigma(int,i))-1;
        end
        sumRMS(int,1)=0;
        for r=1:size(Dsigma,2)
            sumRMS(int,1)=sumRMS(int,1)+Dsigma(int,r)^2;
        end

        RMS(int,1)=( sumRMS(int,1)/size(Dsigma,2))^0.5;
        if RMS(int,1)>RMS(int-1,1)
            FinalPoles=Holdpoles(:,int-1);
        else
            for h=1:npoles %Separate Real and Imaginary parts
             REpoles(h,1)=real(a(h,1));
             Impoles(h,1)=imag(a(h,1));
            end
            DiagRpoles=diag(REpoles);
            DiagImpoles=diag(Impoles);
            for h=1:2:npoles-1
             for d=1:2:npoles-1
                Apoles(h,d)=DiagRpoles(h,d);
                Apoles(h,d+1)=DiagImpoles(h,d);
                Apoles(h+1,d)=-DiagImpoles(h,d);
                Apoles(h+1,d+1)=DiagRpoles(h,d);
             end
            end
            for k=1:2:npoles-1
             b(k,1)=2;
             b(k+1,1)=0;
            end
            FinalPoles=eig(Apoles-b*Csig');%New poles=Zeros of sigma
            for p=1:npoles
                if imag(FinalPoles(p,1))==0
                    FinalPoles(p,1)=real(FinalPoles(p,1))+1i*0.0001;
                end
            end
% In case of sigma having higher value in the next repetition, we
hold the poles of current repetition.
            Holdpoles(:,int)=a(:,1);
            a=FinalPoles; %New poles for next interaction
        end
        int=int+1
end
```

Appendix A3 Stage 2-Vector fitting

```
%fs=squeeze(AB(i,j,1:nfreq) )
npoles=size(FinalPoles,1);
step1=npoles;
step2=npoles+1;
step3=npoles+2;
for i=1:nfrequencies
 for k=1:2:step1-1
     Asvd(i,k)=real((1/(s(1,i)-FinalPoles(k,1)))+(1/(s(1,i)-
FinalPoles(k+1,1))));
     Asvd(i,k+1)=real((1i/(s(1,i)-FinalPoles(k,1)))-(1i/(s(1,i)-
FinalPoles(k+1,1))));
     Asvd(i+nfrequencies,k)=imag((1/(s(1,i)-
FinalPoles(k,1)))+(1/(s(1,i)-FinalPoles(k+1,1))));
     Asvd(i+nfrequencies,k+1)=imag((1i/(s(1,i)-FinalPoles(k,1)))-
(1i/(s(1,i)-FinalPoles(k+1,1))));
 end
 Asvd(i,step2)=real(1);
 Asvd(i,step3)=real(s(1,i));
 Asvd(i+nfrequencies,step2)=imag(1);
 Asvd(i+nfrequencies,step3)=imag(s(1,i));
end
%Least square solution
for i=1:nfrequencies
 Refs(i,1)=real(fs(1,i));
 Imfs(i,1)=imag(fs(1,i));
end
flsq=[Refs;Imfs];
Llsq=inv(Asvd'*Asvd)*Asvd'*flsq;
%Final Calculation of fs
for i=1:nfrequencies
    sum(1,i)=0;
    for k=1:2:npoles-1
        Cres(k,1)=Llsq(k,1)+Llsq(k+1,1)*1i;
        Cres(k+1,1)=Llsq(k,1)-Llsq(k+1,1)*1i;
        sum(1,i)=sum(1,i)+(Cres(k,1)/(s(1,i)-
FinalPoles(k,1)))+(Cres(k+1,1)/(s(1,i)-FinalPoles(k+1,1)));
    end
    d=Llsq(step2);
    h=Llsq(step3);
    fVF(1,i)=sum(1,i)+d+h*s(1,i); %fVF=Approximation function
    DVF(1,i)=fVF(1,i)-fs(1,i);
    Deviation(1,i)=(real(fs(1,i))-mean(real(fs)))+(imag(fs(1,i))-
mean(imag(fs)))*1i;
    Element=squeeze(fVF(1,i));
    [Phase] = Calc_Phase(Element);
    fVF_phase(1,i)=Phase;
end
sumRMS=0;
for r=1:size(DVF,2)
    sumRMS=sumRMS+abs(DVF(1,r))^2;
end
RMS1=(sumRMS)^0.5;
sumRMS=0;
for r=1:size(Deviation,2)
    sumRMS=sumRMS+abs(Deviation(1,r))^2;
end
RMS2=(sumRMS)^0.5;
RMS_VF=1-RMS1/RMS2;
```

Appendix B1 Stage 1-Identification of poles

```
npoles=size(a,1);
step1=npoles;
step3=npoles;
step4=npoles+npoles;
%Find zeros of sigma by a certain number of repetitions(maxrep=1000)
int=3;
RMS(1,1)=10^(50);
RMS(2,1)=10^(49);
while (RMS(int-1,1)<RMS(int-2,1))&&(int<maxrep)
        for i=1:nfrequencies
         for k=1:2:step1-1
             Asvd(i,k)=real((1/(s(1,i)-a(k,1)))+(1/(s(1,i)-
a(k+1,1))));
             Asvd(i,k+1)=real((1i/(s(1,i)-a(k,1)))-(1i/(s(1,i)-
a(k+1,1))));
             Asvd(i+nfrequencies,k)=imag((1/(s(1,i)-
a(k,1)))+(1/(s(1,i)-a(k+1,1))));
             Asvd(i+nfrequencies,k+1)=imag((1i/(s(1,i)-a(k,1)))-
(1i/(s(1,i)-a(k+1,1))));
         end
%          Asvd(i,step2)=1;
%          Asvd(i,step3)=real(s(1,i));
%          Asvd(i+nfrequencies,step2)=imag(1);
%          Asvd(i+nfrequencies,step3)=imag(s(1,i));
         for r=1+step3:2:step4-1
             Asvd(i,r)=real((-fs(1,i))/(s(1,i)-a(r-step3,1))+(-
fs(1,i))/(s(1,i)-a(r-step3+1,1)));
             Asvd(i,r+1)=real((-fs(1,i)*1i)/(s(1,i)-a(r-step3,1))-(-
fs(1,i)*1i)/(s(1,i)-a(r-step3+1,1)));
             Asvd(i+nfrequencies,r)=imag((-fs(1,i))/(s(1,i)-a(r-
step3,1))+(-fs(1,i))/(s(1,i)-a(r-step3+1,1)));
             Asvd(i+nfrequencies,r+1)=imag((-fs(1,i)*1i)/(s(1,i)-a(r-
step3,1))-(-fs(1,i)*1i)/(s(1,i)-a(r-step3+1,1)));
         end
        end
        %Least square solution
        for i=1:nfrequencies
         Refs(i,1)=real(fs(1,i));
         Imfs(i,1)=imag(fs(1,i));
        end
        flsq=[Refs;Imfs];
        Llsq=inv(Asvd'*Asvd)*Asvd'*flsq;

        %Calculation of residues of sigma for pole identification
        for k=1:2:npoles-1
        Csig(k,1)=Llsq(k+npoles,1);
        Csig(k+1,1)=Llsq(k+npoles+1,1);
        Csigma(k,1)=Csig(k,1)+1i*Csig(k+1,1);
        Csigma(k+1,1)=Csig(k,1)-1i*Csig(k+1,1);
        end
        %Calculation of sigma
        for i=1:nfrequencies
             sums(int,i)=0;
             for k=1:2:npoles-1
                sums(int,i)=sums(int,i)+Csigma(k,1)/(s(1,i)-
a(k,1))+Csigma(k+1,1)/(s(1,i)-a(k+1,1));
```

```
            end
            sigma(int,i)=sums(int,i)+1;
            Dsigma(int,i)=abs(sigma(int,i))-1;
        end
        sumRMS(int,1)=0;
        for r=1:size(Dsigma,2)
            sumRMS(int,1)=sumRMS(int,1)+Dsigma(int,r)^2;
        end

        RMS(int,1)=(sumRMS(int,1)/size(Dsigma,2))^0.5;
        if RMS(int,1)>RMS(int-1,1)
            FinalPoles=Holdpoles(:,int-1);
        else
%Separate Real and Imaginary part of the poles
            for h=1:npoles
             REpoles(h,1)=real(a(h,1));
             Impoles(h,1)=imag(a(h,1));
            end
            DiagRpoles=diag(REpoles);
            DiagImpoles=diag(Impoles);
            for h=1:2:npoles-1
             for d=1:2:npoles-1
                Apoles(h,d)=DiagRpoles(h,d);
                Apoles(h,d+1)=DiagImpoles(h,d);
                Apoles(h+1,d)=-DiagImpoles(h,d);
                Apoles(h+1,d+1)=DiagRpoles(h,d);
             end
            end
            for k=1:2:npoles-1
             b(k,1)=2;
             b(k+1,1)=0;
            end
            FinalPoles=eig(Apoles-b*Csig');
            for p=1:npoles
                if abs(imag(FinalPoles(p,1)))<1e-4
                    FinalPoles(p,1)=real(FinalPoles(p,1))+1i*0.001;
                end
            end
            Holdpoles(:,int)=a(:,1);
            a=FinalPoles; %New poles for the next interaction
        end
        int=int+1
end
```

Appendix B2 Stage 2-Vector fitting

```
npoles=size(FinalPoles,1);
step1=npoles;
for i=1:nfrequencies
 for k=1:2:step1-1
     Asvd(i,k)=real((1/(s(1,i)-FinalPoles(k,1)))+(1/(s(1,i)-
FinalPoles(k+1,1))));
     Asvd(i,k+1)=real((1i/(s(1,i)-FinalPoles(k,1)))-(1i/(s(1,i)-
FinalPoles(k+1,1))));
     Asvd(i+nfrequencies,k)=imag((1/(s(1,i)-
FinalPoles(k,1)))+(1/(s(1,i)-FinalPoles(k+1,1))));
     Asvd(i+nfrequencies,k+1)=imag((1i/(s(1,i)-FinalPoles(k,1)))-
(1i/(s(1,i)-FinalPoles(k+1,1))));
 end
end
%Least square solution
for i=1:nfrequencies
 Refs(i,1)=real(fs(1,i));
 Imfs(i,1)=imag(fs(1,i));
end
flsq=[Refs;Imfs];
Llsq=inv(Asvd'*Asvd)*Asvd'*flsq;
%Final Calculation of approximation function
for i=1:nfrequencies
    sum(1,i)=0;
    for k=1:2:npoles-1
        Cres(k,1)=Llsq(k,1)+Llsq(k+1,1)*1i;
        Cres(k+1,1)=Llsq(k,1)-Llsq(k+1,1)*1i;
        sum(1,i)=sum(1,i)+(Cres(k,1)/(s(1,i)-
FinalPoles(k,1)))+(Cres(k+1,1)/(s(1,i)-FinalPoles(k+1,1)));
    end
    d=0;
    h=0;
    fVF(1,i)=sum(1,i)+d+h*s(1,i);
    DVF(1,i)=fVF(1,i)-fs(1,i);
    Deviation(1,i)=(real(fs(1,i))-mean(real(fs)))+(imag(fs(1,i))-
mean(imag(fs)))*1i;
    Element=squeeze(fVF(1,i));
    [Phase] = Calc_Phase(Element);
    fVF_phase(1,i)=Phase;
end
sumRMS=0;
for r=1:size(DVF,2)
    sumRMS=sumRMS+abs(DVF(1,r))^2;
end
RMS1=(sumRMS)^0.5;
sumRMS=0;
for r=1:size(Deviation,2)
    sumRMS=sumRMS+abs(Deviation(1,r))^2;
end
RMS2=(sumRMS)^0.5;
RMS_VF=1-RMS1/RMS2;
```

Appendix B3 Poles and residues

```
ImPolesF=abs(imag(PolesF));
SORT=sort(ImPolesF,2);
PForder=zeros(ndirections,size(PolesF,2));
CresOrder=zeros(ndirections,size(PolesF,2));

%%First the poles with the same minimum imaginary part of 0.001
for d=1:ndirections
    n=0;
    for i=1:size(PolesF,2)
        if imag(PolesF(d,i))==0.001
            n=n+1;
            Hold(d,n)=i;
        end
    end
    for k=1:n
        PForder(d,k)=PolesF(d,Hold(d,k));
        CresOrder(d,k)=CresF(d,Hold(d,k));
    end

    for k=n+1:2:size(PolesF,2)-1
        min=SORT(1,k);
        for i=1:size(PForder,2)
            if imag(PolesF(d,i))>0
                if imag(PolesF(d,i))==min
                    PForder(d,k)=PolesF(d,i);
                    CresOrder(d,k)=CresF(d,i);
                end
            elseif imag(PolesF(d,i))<0
                if abs(imag(PolesF(d,i)))==min
                    PForder(d,k+1)=PolesF(d,i);
                    CresOrder(d,k+1)=CresF(d,i);
                end

            end
        end
    end
end
```

Appendix B4 Interpolation

```
for fr=1:size(CresOrder,2)
    xcreal=squeeze(real(CresOrder(:,fr)));
    xcimag=squeeze(imag(CresOrder(:,fr)));
    xdir=Wavedir';
    Crealint(:,fr)=interp(xcreal,3);
    Cimagint(:,fr)=interp(xcimag,3);
    Waveint=interp(xdir,3);
    Wavedirint=Waveint';
end
```

Appendix C1 Transformation of Hyd. data

```
userData= System.ModelData.Body.UserData;
userData.COG=COG_Original;
%Obtaines the hydrodynamic and hydrostatic data from the hydrodynamic
%database. And converts it to hydrostatic/dynamic data about the body
cog
%in local body coordinates.
%the hydrostatic/dynamic data from the database is given around the
%hydrodynamic origin in local hydrodynamic axis.
% userData.CoG_Original=[72.95;0;23.29];
deg2rad = pi/180;
Displ = 0;
Omg = 0;
WDir = 0;
Spring = zeros(6,6,1);
Amass = zeros(6,6,1);
Bdamp = zeros(6,6,1);
Fwave = zeros(6,1,1);
CoB = [0;0;0];
WL = [];
Error = 1;
IAmass = [];
IBdamp = [];
depth = [];

try
    if ~isempty(userData.HydFile)
        [hydBody,Error] =
read_hydfile(userData.HydFile,userData.BodyNo);
        if Error
            h = msgbox('Error reading .HYD file please check
format','!!ERROR!!',error);
            uiwait(h);
            return;
        end;
    else
        Error = 0;
        return
    end

    depth = hydBody.Depth;

    mode = 1:6;
    if hydBody.MultiBody
       mode = 6*hydBody.BodyNo-5:6*hydBody.BodyNo;
    end

    rot = userData.Rot;
    [Trot_g2l,Trot_l2g] = construct_rotmat(rot);
    rot(1) = 0;
    [Trot_h2l,Trot_l2h] = construct_rotmat(rot);
    rot = userData.Rot;
    rot(2) = 0;
    [Trot_g2h,Trot_h2g] = construct_rotmat(rot);

    shift = reshape(userData.HydOrg,3,1)-reshape(COG_Original,3,1);
    [Tm_ab,Tf_ab,Tm_ba,Tf_ba] = construct_tmat(shift);
```

```
    %please note that the local axis system is the hydrodynamic
database
    %axis system and the (temporary) global axis sytem is the local
body
    %axis system.

    CoB = Trot_h2l(1:3,1:3)*[hydBody.CoB;0;0];

    Displ = hydBody.Displ;
    Omg = hydBody.Omega;
    %%%%get global wave direction
    WDir = hydBody.Dir+userData.Rot(1);

    Amass = A_VF(mode,:,:);
    Bdamp = B_VF(mode,:,:);
%     Amass = hydBody.Amass(mode,:,:);
%     Bdamp = hydBody.Bdamp(mode,:,:);

    %%%%%adjust phase of force (relative to global origin i.s.o.
    %%%%%hydrodynamic origin of body
    dShift = Trot_l2g(1:3,1:3)*userData.HydOrg+userData.Org;
    ShiftDist =
repmat(dShift(1)*cos(deg2rad*WDir)+dShift(2)*sin(deg2rad*WDir),1,leng
th(Omg));
    WaveLength = repmat(get_length(Omg',depth),length(WDir),1);
    PhaseShift =
reshape(repmat(reshape(2*pi*ShiftDist./WaveLength,1,length(Omg)*lengt
h(WDir)),6,1),6,length(WDir),length(Omg));

    ftmp = FVF_amp.*cos(deg2rad*FVF_phase-
PhaseShift)+1i*FVF_amp.*sin(deg2rad*FVF_phase-PhaseShift);
    Fwave = ftmp;

    for iOmg = 1:length(Omg)
        tmp =
Trot_l2g*Tf_ba*Trot_h2l*squeeze(Amass(:,:,iOmg))*Trot_l2h*Tm_ab*Trot_
g2l;
%         Amass(1:6,1:6,iOmg) = 0.5*(tmp+tmp');
        Amass(1:6,1:6,iOmg) = tmp;
        tmp =
Trot_l2g*Tf_ba*Trot_h2l*squeeze(Bdamp(:,:,iOmg))*Trot_l2h*Tm_ab*Trot_
g2l;
%         Bdamp(1:6,1:6,iOmg) =  0.5*(tmp+tmp');
        Bdamp(1:6,1:6,iOmg) =  tmp;
        Fwave(1:6,1:length(WDir),iOmg) =
Trot_l2g*Tf_ba*Trot_h2l*squeeze(ftmp(:,:,iOmg));
    end;

    %%%%%%%%%%%%%%The wave force is already extrapolated to
smaller%%%%%%%%
    %%%%%%%%%%%%%%frequencies for additional
accuracy%%%%%%%%%%%%%%%%%%%%%%

    %Determine force amplitude at omg = 0
    zeroF =
[0;0;System.UserData.Rho*System.UserData.G*hydBody.Awl;0;-
System.UserData.Rho*System.UserData.G*hydBody.Awl*(hydBody.CoF-
hydBody.CoB);0];
    zeroF = Trot_l2g*Tf_ba*Trot_h2l*zeroF;
    amplFzero = zeros(6,length(WDir),1);
```

```
    for iMode = 1:6
        amplFzero(iMode,:,1) = zeroF(iMode);
    end

    % determine slope of phase near smallest frequency. Note: some
tricks
    % to prevent slope is determined at a change from 360->0
    mindphase = min((angle(Fwave(:,:,2))-
angle(Fwave(:,:,1)))./(Omg(2)-Omg(1)),(angle(Fwave(:,:,3))-
angle(Fwave(:,:,2)))./(Omg(3)-Omg(2)));
    maxdphase = max((angle(Fwave(:,:,2))-
angle(Fwave(:,:,1)))./(Omg(2)-Omg(1)),(angle(Fwave(:,:,3))-
angle(Fwave(:,:,2)))./(Omg(3)-Omg(2)));
    signphase = sign(sign(angle(Fwave(:,:,2))-
angle(Fwave(:,:,1)))+sign(angle(Fwave(:,:,3))-
angle(Fwave(:,:,2)))+sign(angle(Fwave(:,:,4))-angle(Fwave(:,:,3))));
    dphase = signphase.*min(abs(mindphase),abs(maxdphase));

    %use slope of phase plot to determine phase at omg = 0;
    phaseFzero = angle(Fwave(:,:,1))-Omg(1)*(angle(Fwave(:,:,2))-
angle(Fwave(:,:,1)))./(Omg(2)-Omg(1));

    %a range of frequencies between 0 and the smallest frequency in
the
    %hydfile is added. If only omg = 0 is added, the phase will
always be
    %extrapolated to zero (for many motions) because the amplitude is
zero
    nfreq = floor(Omg(1)/0.01);
    addfreq = [0:0.01:(nfreq-1)*0.01];
    addfreq(1) = 0.0001;

    %Extrapolate added mass (use smallest known added mass in hyd-
file)
    tmpMass = zeros(6,6,length(Omg)+nfreq);
    tmpMass(:,:,nfreq+1:end) = Amass;
    tmpMass(:,:,1:nfreq) = repmat(Amass(:,:,1),[1,1,nfreq]);
    Amass = tmpMass;

    %Extrapolate damping (extrapolate from smallest known to 0 at omg
= 0)
    tmpDamp = zeros(6,6,length(Omg)+nfreq);
    tmpDamp(:,:,nfreq+1:end) = Bdamp;
    for ifreq = 1:nfreq
        tmpDamp(:,:,ifreq) = addfreq(ifreq)/Omg(1)*Bdamp(:,:,1);
    end
    Bdamp = tmpDamp;

    %Extrapolate force (extrapolate from smallest known to value at
omg = 0) determined above
    sizeForce = size(Fwave);
    tmpForce = zeros(sizeForce(1),sizeForce(2),sizeForce(3)+nfreq);
    tmpForce(:,:,nfreq+1:end) = Fwave;
    amplF = zeros([sizeForce(1),sizeForce(2),nfreq]);
    phaseF = amplF;
    for ifreq = 1:nfreq
        amplF(:,:,ifreq) =
amplFzero+addfreq(ifreq)/Omg(1)*(abs(Fwave(:,:,1))-amplFzero);
        phaseF(:,:,ifreq) =
phaseFzero+addfreq(ifreq)/Omg(1)*(angle(Fwave(:,:,1))-phaseFzero);
```

```
    end;
    tmpForce(:,:,1:nfreq) = amplF.*cos(phaseF)+1i*amplF.*sin(phaseF);
    Fwave = tmpForce;

    [Spring,Error,WL] = spring_matrix(userData);


    if hydBody.MultiBody
        nbody = length(hydBody.Amass(:,1,1))/6;
        IAmass = cell(1,nbody);
        IBdamp = cell(1,nbody);
        for iBody = 1:nbody
            mode = 6*iBody-5:6*iBody;

            tmpMass = zeros(6,6,length(Omg)+nfreq);
            for iOmg = 1:length(Omg)
                tmpMass(:,:,nfreq+iOmg) =
Trot_l2g*Tf_ba*Trot_h2l*squeeze(hydBody.Amass(mode,:,iOmg));
            end
            tmpMass(:,:,1:nfreq) =
repmat(tmpMass(:,:,nfreq+1),[1,1,nfreq]);
            IAmass{hydBody.BodyNo,iBody} = tmpMass;

            tmpDamp = zeros(6,6,length(Omg)+nfreq);
            for iOmg = 1:length(Omg)
                tmpDamp(:,:,nfreq+iOmg) =
Trot_l2g*Tf_ba*Trot_h2l*squeeze(hydBody.Bdamp(mode,:,iOmg));
            end
            for ifreq = 1:nfreq
                tmpDamp(:,:,ifreq) =
addfreq(ifreq)/Omg(1)*tmpDamp(:,:,nfreq+1);
            end
            IBdamp{hydBody.BodyNo,iBody} = tmpDamp;

        end
    end


    %adjust frequency range
    Omg = [addfreq'; Omg];

    if Error
        h = msgbox(['error reading hydrodynamic spring matrix of
',userData.Name],'!!ERROR!!','error');
        uiwait(h)
        return;
    end;
    Error = 0;
catch
        h = msgbox(['error reading hydrodynamic data of
',userData.Name],'!!ERROR!!','error');
        uiwait(h)
end;


end
```

Appendix C2 Spring matrix transformation

```
SpringMat = zeros(6,6);
Error = 1;
WaterLine = [];
MultiBody = [];

try

    %%%Read Hyd-File
    if ~isempty(userData.HydFile)
        [hydBody,Error] =
read_hydfile(userData.HydFile,userData.BodyNo);
        if Error
            h = msgbox('Error reading .HYD file please check
format','!!ERROR!!','error');
            uiwait(h);
            return;
        end;
    else
        Error = 0;
        return
    end
    MultiBody = hydBody.MultiBody;

    %%Compute Rotation Matrices
    rot = userData.Rot;
    [Trot_g2l,Trot_l2g] = construct_rotmat(rot);% Global to local
axis
    rot(1) = 0;
    [Trot_h2l,Trot_l2h] = construct_rotmat(rot);% Hydro database to
local axis
    rot = userData.Rot;
    rot(2) = 0;
    [Trot_g2h,Trot_h2g] = construct_rotmat(rot);% Global to Hydro
database axis

    %%Compute cog and hydorg in local axis of hydrodynamic database
    cog = Trot_l2h(1:3,1:3)*userData.CoG; % COG in local axis of
liftdyn transformed to local axis of hydrodynamic database
    hydorg = Trot_l2h(1:3,1:3)*userData.HydOrg;% hydorigin (given in
local axis of liftdyn) transformed to local axis of hyd database

    tmpWL =
userData.Org+Trot_l2g(1:3,1:3)*(userData.HydOrg+Trot_h2l(1:3,1:3)*[0;
0;hydBody.WL]);
    WaterLine = tmpWL(3);

    %% Determine position of keel point(K) and vertical distance to
cog (KG)
    %k[x,y,z]: is the trasfer of the hyd origin which is in local hyd
axis to the keel point under the COG.
    k = hydorg;% Hyd origin is at CoF!
    k(1) = k(1) + hydBody.CoB; %The hyd origin is at the CoF and it
should be transferred to the CoB which is under the CoG
    k(3) = k(3) + hydBody.WL-hydBody.Draft; % 1)WL-Draft=Distance of
hyd orig and keel 2)k(3)=0
    kg = cog(3)-k(3); %Distance KG=cog(3)
```

```
    gmt = hydBody.KMT-kg-userData.GG(1);
    gml = hydBody.KML-kg-userData.GG(2);

    %construct hydrostatic spring matrix about virtual cog above cob
in
    %local database axis system
    spring = zeros(6,6);
    spring(3,3) = System.UserData.Rho*System.UserData.G*hydBody.Awl;
    spring(4,4) =
System.UserData.Rho*System.UserData.G*hydBody.Displ*gmt;
    spring(5,5) =
System.UserData.Rho*System.UserData.G*hydBody.Displ*gml;
    spring(3,5) = -
System.UserData.Rho*System.UserData.G*hydBody.Awl*(hydBody.CoF-
hydBody.CoB);
    spring(5,3) = spring(3,5);

    %transform matrix to true body cog in local body axis
    kcog = k;
    kcog(3) = kcog(3) + kg;
    shift = reshape(kcog,3,1)-reshape(cog,3,1);
    [Tm_ab,Tf_ab,Tm_ba,Tf_ba] = construct_tmat(shift);
    SpringMat = Trot_h2l*Tf_ba*spring*Tm_ab*Trot_l2h;
    Error = 0;

end;
```

Appendix D1 Golden section method

```
C= 0.61803399
%Triplet=[a,b,c1]
if (RMS_AllDofs_f2 < RMS_AllDofs_f1)
     a=x1;
     b=x2;
     c1=c1;
     if (abs(c1-b) > abs(b-a))
       x1=b;
       x2=b+(C)*abs(c1-b);
    else
       x2=b;
       x1=b-(C)*abs(b-a);
    end
else
     a=a;
     b=x1;
     c1=x2;
     if (abs(c1-b) > abs(b-a))
       x1=b;
       x2=b+(C)*abs(c1-b);
    else
       x2=b;
       x1=b-(C)*abs(b-a);
    end
end
```

Appendix D1 Identification of CoG

Identification of CoG: main script

```
close all
clear all
Omegaint=[0.01:0.01:1.7];

%% Data set
load('TestCase2b.mat');
Waves=Waves2;
ThialfHeading=ThialfHeading2;
Surge=Spec2{1,1};
Sway=Spec2{1,2};
Heave=Spec2{1,3};
Roll=Spec2{1,4};
Pitch=Spec2{1,5};
Yaw=Spec2{1,6};
%Wave Spectrum
for f=1:size(omega,2)
    WaveSpectra(f,:)=Waves(:,f)';
end
% Frequency interpolation
for dir=1:size(WavesHeading,2)
    Waveperdir=squeeze(WaveSpectra(:,dir))';
    [Inter_waves]=FrequencyInt_DATA(Omegaint,omega',Waveperdir);
    Wavesp(:,dir)=(Inter_waves(1,:)');
end
%Response Spectra
Responses=[Surge;Sway;Heave;Roll;Pitch;Yaw];
for dof=1:6
    RS_perdof=Responses(dof,:);
    [Inter_response]=FrequencyInt_DATA(Omegaint,omega',RS_perdof);
    Response_DATA(dof,:)=Inter_response(1,:);
end

%% Original vessel properties and approximation functions
load('thialf_22_deep2.mat');%Original properties
load('hyd_file'); %Hydrodynamic database from diffraction software
load('Forces_Approximation.mat'); %Approximation: wave forces
load('AB_Approximation.mat'); %Approximation: added mass-damp
% Select Matrices
Mass=System.ModelData.Body.UserData.MassMatrix;
Bad=System.ModelData.Body.UserData.Badd;
Bad(3,3)=3.09*Bad(3,3);
Sadd=System.ModelData.Body.UserData.Sadd;
COG_Original=[                ];
%HydFile
Omg=Hyd.body1.Omega;
Wavedir=Hyd.body1.WDir; %1X13
ndirections=size(Wavedir,2);
nfrequencies=size(Omg,2); %(0-1.6)rad/s
Famp=Hyd.body1.Famp;
Feps=Hyd.body1.Feps;
[Fhyd,Fhyd_phase] =
Forces_HydFile(ndirections,nfrequencies,Famp,Feps);
[Fhyd]=All_directions(Fhyd);
Ahyd=Hyd.body1.AdMass; %Added Mass
Bhyd=Hyd.body1.BDamp; %Damping
clear Wavedir ndirections
```

```
%% Transformation of matrices from hyd file
WDir=[0:15:345];
% Frequency interpolation
[Inter_Bhyd,Inter_Ahyd,Inter_Fhyd]=
FrequencyInterpolation_ABF(Omegaint,Bhyd,Ahyd,Fhyd,WDir,Omg,WDir);
[Fhyd_phase,Fhyd_amp]=Construct_Forces_Sens(Inter_Fhyd);
[Spring_hyd,Amass_hyd,Bdamp_hyd,Fwave_hyd,Error] =
TransformationCOG(COG_Original,Inter_Ahyd,Inter_Bhyd,Fhyd_phase,Fhyd_
amp,Omegaint',WDir');
clear Omg nfrequencies
Omg=Omegaint;
nfrequencies=size(Omegaint,2);
ndirections=size(WDir,2);

%% Response spectrum
[RAO,Bad_New]=NewRAO(ndirections,Omg,Amass_hyd,Bdamp_hyd,Mass,Bad,Spr
ing_hyd,Sadd,Fwave_hyd);
[RAONew,Wavedir]=transform_RAOsDir(Omegaint,RAO,WavesHeading,ThialfHe
ading);
clear RAO
RAO=RAONew;
[RS] =
Response_Spectra_Liftdyn(RAO,Wavesp,Wavedir,size(Wavedir,2),nfrequenc
ies,nperiods);
[RMS_Check]=Check_Response_COG(RS,Response_DATA);
MIN=min(RMS_Check);
RESPONSE={'Maximum Inaccuracy for Surge' 'Maximum Inaccuracy for
Sway' 'Maximum Inaccuracy for Heave' 'Maximum Inaccuracy for Roll'
'Maximum Inaccuracy for Pitch' 'Maximum Inaccuracy for Yaw'};
Title={'SURGE','SWAY','HEAVE','ROLL','PITCH','YAW'};
close all
for dof=1:6
       figure(p);
       subplot(2,3,dof)

plot(Omg(1:nfrequencies),squeeze(Response_DATA(dof,:)),'b',Omg(1:nfre
quencies),squeeze(RS(dof,:)),'r');%RS=DOFXfreqXPeakPeriods
        title(Title{dof});
        TeXStringX=texlabel('omega [rad/sec]');
        xlabel(TeXStringX,'Fontsize',14);
        if dof==1||dof==2||dof==3
            TeXStringY=texlabel('S(omega)  [m^(2)*s]');
            ylabel(TeXStringY,'Fontsize',14);
        else
            TeXStringY=texlabel('S(omega)  [degrees^(2)*s]');
            ylabel(TeXStringY,'Fontsize',14);
        end
       legend('Data','Calculations');
       hold on
end
%% check motion with maximum inaccuracies
for dof=1:6
    if MIN==RMS_Check(dof,1)
       h=msgbox(RESPONSE{1,dof});
       uiwait(h);
    end
end

clear RMS
```

```
%% X coordinate
Coordinate=1;
Lx=[redacted];
c1=0.4*Lx;
a=-0.40*Lx;
[FinalCOGX,FinalPerX,FinalRSX,MAX_RMSX,RMSX]=COG_InterationsGOLDEN(a,
c1,COG_Original,Coordinate,Inter_Ahyd,Inter_Bhyd,Fhyd_phase,Fhyd_amp,
Omg,WDir,Response_DATA,Mass,Bad,Sadd,Wavesp,nperiods,WavesHeading,Thi
alfHeading);
[RMS_CheckX]=Check_Response_COG(FinalRSX,Response_DATA);

%% Y coordinate
Coordinate=2;
Ly=[redacted];
c1=0.50*Ly;
a=-0.50*Ly;
[FinalCOGY,FinalPerY,FinalRSY,MAX_RMSY,RMSY]=COG_InterationsGOLDEN(a,
c1,COG_Original,Coordinate,Inter_Ahyd,Inter_Bhyd,Fhyd_phase,Fhyd_amp,
Omg,WDir,Response_DATA,Mass,Bad,Sadd,Wavesp,nperiods,WavesHeading,Thi
alfHeading);
[RMS_CheckY]=Check_Response_COG(FinalRSY,Response_DATA);

%% Z coordinate
Coordinate=3;
Lz=[redacted];
c1=Lz;
a=-COG_Original(Coordinate,1);
[FinalCOGZ,FinalPerZ,FinalRSZ,MAX_RMSZ,RMSZ]=COG_InterationsGOLDEN(a,
c1,COG_Original,Coordinate,Inter_Ahyd,Inter_Bhyd,Fhyd_phase,Fhyd_amp,
Omg,WDir,Response_DATA,Mass,Bad,Sadd,Wavesp,nperiods,WavesHeading,Thi
alfHeading);
[RMS_CheckZ]=Check_Response_COG(FinalRSZ,Response_DATA);
```

Frequency interpolation of data:

```
function[Inter]=FrequencyInt_DATA(Omegaint,omega_orig,mat)
Inter= zeros(1,size(Omegaint,2));
for iOmg = 1:size(Omegaint,2)
    omg = Omegaint(1,iOmg);
    matNew =freq_interp_Data(omg,omega_orig,mat,0);
    Inter(1,iOmg) = Inter(1,iOmg)+(matNew);
end

function matout = freq_interp_Data(freq,freqvec,mat,type)

        if freq<min(freqvec)
            if type == 0
                matout = freq/min(freqvec)*squeeze(mat(1,1));
                return;
            else
                matout = squeeze(mat(1,1));
                return;
            end
        end;

        if freq>max(freqvec)
                matout = squeeze(mat(1,end));
            return;
        end;
```

```
        mode = 1;
        [z] = ndgrid(freqvec);
        [z1] = ndgrid(freq);
        matout = squeeze(interp1(z,mat,z1));
```

Frequency interpolation of added mass, damping and wave forces:

```
function [Inter_Bdamp,Inter_Amass,Inter_Fwave]=
FrequencyInterpolation_ABF(Omega,Bdamp,Amass,Fwave,Dir_lifdyn,Omg,Dir
_Wamit)
Inter_Bdamp = zeros(6,6,size(Omega,2));
for iOmg = 1:size(Omega,2)
    omg = Omega(1,iOmg);
    hydDamp = freq_interp_mat(omg,Omg,Bdamp,0);
    Inter_Bdamp(1:6,1:6,iOmg) = Inter_Bdamp(1:6,1:6,iOmg)+(hydDamp);
end

Inter_Amass= zeros(6,6,size(Omega,2));
for iOmg = 1:size(Omega,2)
    omg = Omega(1,iOmg);
    hydAmass = freq_interp_mat(omg,Omg,Amass,0);
    Inter_Amass(1:6,1:6,iOmg) = Inter_Amass(1:6,1:6,iOmg)+(hydAmass);
end;

Inter_Fwave= zeros(6,size(Fwave,2),size(Omega,2));
for iOmg = 1:size(Omega,2)
    omg = Omega(1,iOmg);
    waveForce =
freq_interp_force(omg,Dir_lifdyn,Omg',Dir_Wamit,Fwave,1);
    Inter_Fwave(1:6,:,iOmg) = Inter_Fwave(1:6,:,iOmg) + waveForce;
end

function matout = freq_interp_mat(freq,freqvec,mat,type)

        if freq<min(freqvec)
            if type == 0
                matout = freq/min(freqvec)*squeeze(mat(:,:,1));
                return;
            else
                matout = squeeze(mat(:,:,1));
                return;
            end
        end;

        if freq>max(freqvec)
                matout = squeeze(mat(:,:,end));
            return;
        end;

        mode = 1:6;
        [x,y,z] = meshgrid(mode,mode,freqvec);
        [x1,y1,z1] = meshgrid(mode,mode,freq);
        matout = squeeze(interp3(x,y,z,mat,x1,y1,z1));


function matout =
freq_interp_force(freq,dir,freqvec,dirvec,force,type)

        if length(freqvec)==1 & freqvec(1)==0
            matout = zeros(6,length(dir),length(freq));
```

```
            return;
        end;
        if (dirvec(end)-dirvec(1))==360
            dirvec = dirvec(1:end-1);
            force = force(:,1:end-1,:);
        end

        sizeForce = size(force);
        tmpforce =
zeros([sizeForce(1),3*sizeForce(2),sizeForce(3)+2]);
        tmpforce(:,:,2:end-1) = [force,force,force];
        tmpforce(:,:,end) = tmpforce(:,:,end-1);
        tmpforce(:,:,1) = tmpforce(:,:,2);

        force = tmpforce;

        freqvec = [0;freqvec;max(freq(end),freqvec(end)+100)];
        dirvec = reshape(dirvec,1,length(dirvec));
        dirvec = [dirvec-360,dirvec,dirvec+360];

        mode = 1:6;
        [x,y,z] = meshgrid(dirvec,mode,freqvec);
        [x1,y1,z1] = meshgrid(dir,mode,freq);
        matout_real = interp3(x,y,z,real(force),x1,y1,z1,'linear');
        matout_imag = interp3(x,y,z,imag(force),x1,y1,z1,'linear');
        matout_ampl = interp3(x,y,z,abs(force),x1,y1,z1,'linear');
        matout_phase = angle(matout_real+i*matout_imag);
        matout =
matout_ampl.*cos(matout_phase)+i*matout_ampl.*sin(matout_phase);
```

Calculation of RAOS:

```
function[RAO,BadNew]=NewRAO(ndirections,Omg,Amass,Bdamp,Mass,Bad,Spri
ng,Sadd,Fwave)
for i=1:6
    for j=1:6
        for f=1:size(Omg,2)
            BadNew(i,j,f)=Bad(i,j);
        end
    end
end

for i=1:6
    for f=1:size(Omg,2)
        if
(Bdamp(i,i,f)+Bad(i,i))<(0.015*2*(((Mass(i,i)+Amass(i,i,f))*(Spring(i
,i)+Sadd(i,i)))^0.5))

BadNew(i,i,f)=(0.015*2*(((Mass(i,i)+Amass(i,i,f))*(Spring(i,i)+Sadd(i
,i)))^0.5))-Bdamp(i,i,f);
        end
    end
end
for f=1:size(Omg,2)
    AB(:,:,f)=Amass(:,:,f)-1i*Bdamp(:,:,f)/(Omg(1,f));
end
for i=1:ndirections
    for f = 1:size(Omg,2)
        HNew(:,:,f)=(-(Omg(1,f)^2)*Mass(:,:)-
(Omg(1,f)^2)*squeeze(AB(:,:,f))+1i*Omg(1,f)*squeeze(BadNew(:,:,f))+(S
pring(:,:))+Sadd(:,:))^(-1);
```

```
        RAO(:,f,i) = HNew(:,:,f)*(Fwave(:,i,f));
    end
end
```

Transformation of directional RAOs:

```
function
[RAO,Wavedir]=transform_RAOsDir(Omegaint,RAO,WavesHeading,ThialfHeadi
ng)
for i=1:6
    for f=1:size(Omegaint,2)
        RAONEW=abs(RAO(i,f,:));
        RAONEW_int(i,f,:)=interp(RAONEW,3);
    end
end
WavesHeadingNew=WavesHeading(1,1:size(WavesHeading,2)-1);
for dir=1:size(WavesHeadingNew,2)
    Wavedir(1,dir)=-WavesHeadingNew(1,dir)+ThialfHeading+180;
    if Wavedir(1,dir)<0
        Wavedir(1,dir)=360+Wavedir(1,dir);
    end
    if Wavedir(1,dir)>360
        Wavedir(1,dir)=Wavedir(1,dir)-360;
    end
    if Wavedir(1,dir)==360
        Wavedir(1,dir)=0;
    end
end
SORT=sort(Wavedir,2);
if SORT(1,1)==5
    clear RAO
    RAO(:,:,:)=RAONEW_int(:,:,2:2:size(RAONEW_int,3));
else
    clear RAO
    RAO(:,:,:)=RAONEW_int(:,:,1:2:size(RAONEW_int,3));
end

for k=1:size(Wavedir,2)
    min=SORT(1,k);
    for i=1:size(Wavedir,2)
        if Wavedir(1,i)==min
            RAO_Final(:,:,k)=RAO(:,:,i);
        end
    end
end
clear Wavedir
Wavedir=SORT;
RAO_Final(:,:,size(RAO_Final,3)+1)=RAO_Final(:,:,1);
clear RAO
RAO=RAO_Final;
Wavedir(1,size(Wavedir,2)+1)=Wavedir(1,size(Wavedir,2))+(Wavedir(1,2)
-Wavedir(1,1));
```

Calculation of response spectra:

```
function [RS] =
Response_Spectra_Liftdyn(RAO_ldyn,Wavesp,Wavedir,ndirections,nfrequen
cies,nperiods)
for i=4:6
    RAO_ldyn(i,:,:)=RAO_ldyn(i,:,:)*180/pi;
end

for i=1:6
    for dir=1:ndirections
```

```
        for f=1:nfrequencies
        RS_fdir(i,f,dir)=((RAO_ldyn(i,f,dir)))^2*Wavesp(f,dir);
        end
    end
end

%Response for all wave directions
for i=1:6
    for f=1:nfrequencies
        RS(i,f)=0;
        for dir=1:size(RS_fdir,3)
            RS(i,f)=RS(i,f)+RS_fdir(i,f,dir)*(Wavedir(1,2)-
Wavedir(1,1));
        end
    end
end
```

Calculation of NRMSE:

```
function [RMS_Check]=Check_Response_COG(RS,Response_DATA)
for dof=1:6
        sumRMS1=0;
        sumRMS2=0;
        for f=1:size(RS,2)
            Dif=(RS(dof,f)-Response_DATA(dof,f));
            Deviation=Response_DATA(dof,f)-
mean(squeeze(Response_DATA(dof,:)));
            sumRMS1=sumRMS1+Dif^2;
            sumRMS2=sumRMS2+Deviation^2;
            clear Dif Deviation
        end
        RMS_Check(dof,1)=1-(sumRMS1^0.5)/(sumRMS2^0.5);
end
```

Golden section for CoG:

```
function
[FinalCOG,FinalPer,FinalRS,MAX_RMS,RMS_perdof]=COG_InterationsGOLDEN(
a,c1,COG_Original,Coordinate,Ahyd,Bhyd,Fhyd_phase,Fhyd_amp,Omg,Wavedi
r,Response_DATA,Mass,Bad,Sadd,Wavesp,nperiods,WavesHeading,ThialfHead
ing)
R=0.61803399; %The golden ratios.
C=(1.0-R);
b=0;
x1=b;
x2=b+R*(c1-b);
while abs(c1-a) > 0.2 && abs(RMS_AllDofs_f2 - RMS_AllDofs_f1)>0.0001
    clear Spring_hyd Amass_hyd Bdamp_hyd Fwave_hyd RAO RAONew RS
COG_Change RS1_fdir RS2_fdir RS3_fdir RS4_fdir RS5_fdir RS6_fdir
    COG_Change=COG_Original;
    COG_Change(Coordinate,1)=COG_Original(Coordinate,1)+x1;
    [Spring_hyd,Amass_hyd,Bdamp_hyd,Fwave_hyd,Error] =
TransformationCOG(COG_Change,Ahyd,Bhyd,Fhyd_phase,Fhyd_amp,Omg',Waved
ir');

[RAO,Bad_New]=NewRAO(size(Wavedir,2),Omg,Amass_hyd,Bdamp_hyd,Mass,Bad
,Spring_hyd,Sadd,Fwave_hyd);

[RAONew,WavedirNew]=transform_RAOsDir(Omg,RAO,WavesHeading,ThialfHead
ing);
    [RS] =
Response_Spectra_Liftdyn(RAONew,Wavesp,WavedirNew,size(WavedirNew,2),
size(Omg,2),nperiods);
```

```
    COG_New_f1(:,1)=COG_Change;
    RS_New_f1(:,:)=RS(:,:);
    [RMS_AllDofs_f1,RMS_f1]=RMS_COG(RS,Response_DATA);
    clear Spring_hyd Amass_hyd Bdamp_hyd Fwave_hyd RAO RAONew RS
COG_Change RS1_fdir RS2_fdir RS3_fdir RS4_fdir RS5_fdir RS6_fdir
    COG_Change=COG_Original;
    COG_Change(Coordinate,1)=COG_Original(Coordinate,1)+x2;
    [Spring_hyd,Amass_hyd,Bdamp_hyd,Fwave_hyd,Error] =
TransformationCOG(COG_Change,Ahyd,Bhyd,Fhyd_phase,Fhyd_amp,Omg',Waved
ir');

[RAO,Bad_New]=NewRAO(size(Wavedir,2),Omg,Amass_hyd,Bdamp_hyd,Mass,Bad
,Spring_hyd,Sadd,Fwave_hyd);

[RAONew,WavedirNew]=transform_RAOsDir(Omg,RAO,WavesHeading,ThialfHead
ing);
    [RS] =
Response_Spectra_Liftdyn(RAONew,Wavesp,WavedirNew,size(WavedirNew,2),
size(Omg,2),nperiods);
    COG_New_f2(:,1)=COG_Change;
    RS_New_f2(:,:)=RS(:,:);
    [RMS_AllDofs_f2,RMS_f2]=RMS_COG(RS,Response_DATA);
    FinalPer_x1=x1;
    FinalPer_x2=x2;

[a,c1,x1,x2]=NewPoints(RMS_AllDofs_f2,RMS_AllDofs_f1,x1,x2,c1,a,C);
end
if (RMS_AllDofs_f1 > RMS_AllDofs_f2)
    MAX_RMS=RMS_AllDofs_f1;
    RMS_perdof=RMS_f1;
    FinalCOG(:,1)=squeeze(COG_New_f1(:,1));
    FinalPer(1,1)=FinalPer_x1;
    FinalRS(:,:)=squeeze(RS_New_f1(:,:));
else
    MAX_RMS=RMS_AllDofs_f2;
    RMS_perdof=RMS_f2
    FinalCOG(:,1)=squeeze(COG_New_f2(:,1));
    FinalPer(1,1)=FinalPer_x2;
    FinalRS(:,:)=squeeze(RS_New_f2(:,:));
end


function
[a,c1,x1,x2]=NewPoints(RMS_AllDofs_f2,RMS_AllDofs_f1,x1,x2,c1,a,C)
if (RMS_AllDofs_f2 > RMS_AllDofs_f1)
     a=x1;
     b=x2;
     c1=c1;
     if (abs(c1-b) > abs(b-a))
       x1=b;
       x2=b+(1-C)*abs(c1-b);
    else
       x2=b;
       x1=b-(1-C)*abs(b-a);
    end
else
     a=a;
     b=x1;
     c1=x2;
     if (abs(c1-b) > abs(b-a))
       x1=b;
```

```
        x2=b+(1-C)*abs(c1-b);
    else
        x2=b;
        x1=b-(1-C)*abs(b-a);
    end
end
```

Appendix D2 Identification of mass matrix

Identification of radii of gyration: main script

```
close all
clear all
Omegaint=[0.01:0.01:1.7];

%% Data set
load('TestCase2b.mat');
Waves=Waves2;
ThialfHeading=ThialfHeading2;
Surge=Spec2{1,1};
Sway=Spec2{1,2};
Heave=Spec2{1,3};
Roll=Spec2{1,4};
Pitch=Spec2{1,5};
Yaw=Spec2{1,6};
%Wave Spectrum
for f=1:size(omega,2)
    WaveSpectra(f,:)=Waves(:,f)';
end
% Frequency interpolation
for dir=1:size(WavesHeading,2)
    Waveperdir=squeeze(WaveSpectra(:,dir))';
    [Inter_waves]=FrequencyInt_DATA(Omegaint,omega',Waveperdir);
    Wavesp(:,dir)=(Inter_waves(1,:)');
end
%Response Spectra
Responses=[Surge;Sway;Heave;Roll;Pitch;Yaw];
for dof=1:6
    RS_perdof=Responses(dof,:);
    [Inter_response]=FrequencyInt_DATA(Omegaint,omega',RS_perdof);
    Response_DATA(dof,:)=Inter_response(1,:);
end

%% Original vessel properties and approximation functions
load('thialf_22_deep2.mat');%Original properties
load('hyd_file'); %Hydrodynamic database from diffraction software
load('Forces_Approximation.mat'); %Approximation: wave forces
load('AB_Approximation.mat'); %Approximation: added mass-damp
% Select Matrices
Mass=System.ModelData.Body.UserData.MassMatrix;
Bad=System.ModelData.Body.UserData.Badd;
Bad(3,3)=3.09*Bad(3,3);
Sadd=System.ModelData.Body.UserData.Sadd;
COG_Original=[                    ];
Rx=   ;%!!!!!!!!!!!!!!!!!!!!!!
Ry=   ;%!!!!!!!!!!!!!!!!!!!!!!!!!!!!
Rz=   ;%!!!!!!!!!!!!!!!!!!!!!!!!!!!!!!!!
%HydFile
Omg=Hyd.body1.Omega;
Wavedir=Hyd.body1.WDir; %1X13
ndirections=size(Wavedir,2);
nfrequencies=size(Omg,2); %(0-1.6)rad/s
Famp=Hyd.body1.Famp;
Feps=Hyd.body1.Feps;
[Fhyd,Fhyd_phase] =
Forces_HydFile(ndirections,nfrequencies,Famp,Feps);
```

```
[Fhyd]=All_directions(Fhyd);
Ahyd=Hyd.body1.AdMass; %Added Mass
Bhyd=Hyd.body1.BDamp; %Damping
clear Wavedir ndirections

%% Transformation of matrices from hyd file
WDir=[0:15:345];
% Frequency interpolation
[Inter_Bhyd,Inter_Ahyd,Inter_Fhyd]=
FrequencyInterpolation_ABF(Omegaint,Bhyd,Ahyd,Fhyd,WDir,Omg,WDir);
[Fhyd_phase,Fhyd_amp]=Construct_Forces_Sens(Inter_Fhyd);
[Spring_hyd,Amass_hyd,Bdamp_hyd,Fwave_hyd,Error] =
TransformationCOG(COG_Original,Inter_Ahyd,Inter_Bhyd,Fhyd_phase,Fhyd_
amp,Omegaint',WDir');
clear Omg nfrequencies
Omg=Omegaint;
nfrequencies=size(Omegaint,2);
ndirections=size(WDir,2);

%% Response spectrum
[RAO,Bad_New]=NewRAO(ndirections,Omg,Amass_hyd,Bdamp_hyd,Mass,Bad,Spr
ing_hyd,Sadd,Fwave_hyd);
[RAONew,Wavedir]=transform_RAOsDir(Omegaint,RAO,WavesHeading,ThialfHe
ading);
clear RAO
RAO=RAONew;
[RS] =
Response_Spectra_Liftdyn(RAO,Wavesp,Wavedir,size(Wavedir,2),nfrequenc
ies,nperiods);
RESPONSE={'Maximum Inaccuracy for Surge' 'Maximum Inaccuracy for
Sway' 'Maximum Inaccuracy for Heave' 'Maximum Inaccuracy for Roll'
'Maximum Inaccuracy for Pitch' 'Maximum Inaccuracy for Yaw'};
Title={'SURGE','SWAY','HEAVE','ROLL','PITCH','YAW'};
close all
for dof=1:6
       figure(p);
       subplot(2,3,dof)

plot(Omg(1:nfrequencies),squeeze(Response_DATA(dof,:)),'b',Omg(1:nfre
quencies),squeeze(RS(dof,:)),'r');%RS=DOFXfreqXPeakPeriods
        title(Title{dof});
        TeXStringX=texlabel('omega [rad/sec]');
        xlabel(TeXStringX,'Fontsize',14);
        if dof==1||dof==2||dof==3
            TeXStringY=texlabel('S(omega)  [m^(2)*s]');
            ylabel(TeXStringY,'Fontsize',14);
        else
            TeXStringY=texlabel('S(omega)  [degrees^(2)*s]');
            ylabel(TeXStringY,'Fontsize',14);
        end
       legend('Data','Calculations');
       hold on
end
dof=4;
[RMS_Check_X]=Check_Response_MassMatrix(dof,RS,Response_DATA);
dof=5;
[RMS_Check_Y]=Check_Response_MassMatrix(dof,RS,Response_DATA);
dof=6;
[RMS_Check_Z]=Check_Response_MassMatrix(dof,RS,Response_DATA);
if min([RMS_Check_Z RMS_Check_Y RMS_Check_X])==RMS_Check_Z
   h = msgbox('Change radius of gyration: Z axis');
```

```
    uiwait(h);
    Check=66;
elseif min([RMS_Check_Z RMS_Check_Y RMS_Check_X])==RMS_Check_Y
    h = msgbox('Change radius of gyration: Y axis');
    uiwait(h);
    Check=55;
elseif min([RMS_Check_Z RMS_Check_Y RMS_Check_X])==RMS_Check_X
    h = msgbox('Change radius of gyration: X axis');
    uiwait(h);
    Check=44;
end
%% Changing Mass Rxx
% Check=66;
if Check==44
   R=Rx;
   El_i=4;
   El_j=4;

[FinalMASSX,FinalPerX,FinalRSX,MAX_RMS_MX]=MassMatrix_InterationsGOLD
EN(R,El_i,El_j,Response_DATA,Mass,WDir,Omg,Amass_hyd,Bdamp_hyd,Spring
_hyd,Sadd,Bad,Fwave_hyd,Wavesp,nperiods,WavesHeading,ThialfHeading);
   FinalRS=FinalRSX;
end
%% Y Axis
if Check==55
    R=Ry;
    El_i=5;
    El_j=5;

[FinalMASSY,FinalPerY,FinalRSY,MAX_RMS_MY]=MassMatrix_InterationsGOLD
EN(R,El_i,El_j,Response_DATA,Mass,WDir,Omg,Amass_hyd,Bdamp_hyd,Spring
_hyd,Sadd,Bad,Fwave_hyd,Wavesp,nperiods,WavesHeading,ThialfHeading);
   FinalRS=FinalRSY;
end
%% Z Axis
clear RS RS_New Mass_New RMS RMS_AllDofs RMS_AllPeaks HNew RAO Dif
if Check==66
     R=Rz;
     El_i=6;
     El_j=6;

[FinalMASSZ,FinalPerZ,FinalRSZ,MAX_RMS_MZ]=MassMatrix_InterationsGOLD
EN(R,El_i,El_j,Response_DATA,Mass,WDir,Omg,Amass_hyd,Bdamp_hyd,Spring
_hyd,Sadd,Bad,Fwave_hyd,Wavesp,nperiods,WavesHeading,ThialfHeading);
   FinalRS=FinalRSZ;
End
```

NRMSE for radii of gyration:

```
function [RMS_Check]=Check_Response_MassMatrix(dof,RS,Response_DATA)
     sumRMS1=0;
     sumRMS2=0;
     for f=1:size(RS,2)
          Dif=(RS(dof,f)-Response_DATA(dof,f));
          Deviation=Response_DATA(dof,f)-
mean(squeeze(Response_DATA(dof,:)));
          sumRMS1=sumRMS1+Dif^2;
          sumRMS2=sumRMS2+Deviation^2;
          clear Dif Deviation
     end
     RMS_Check(1,1)=1-(sumRMS1^0.5)/(sumRMS2^0.5);
```

Golden section method for radii of gyration:

```
function
[FinalMASS,FinalPer,FinalRS,MAX_RMS_M]=MassMatrix_InterationsGOLDEN(R
adius,El_i,El_j,Response_DATA,Mass_Original,WDir,Omg,Amass,Bdamp,Spri
ng,Sadd,Bad,Fwave,Wavesp,nperiods,WavesHeading,ThialfHeading)
R=0.61803399; %The golden ratios.
C=(1.0-R);
a=-30;
c1=50;
b=0;
x1=b;
x2=b+R*abs(c1-b);
while abs(c1-a) > 0.2 && abs(RMS_AllDofs_f2 - RMS_AllDofs_f1)>0.0001
    Mass_Change=Mass_Original;
    Mass_Change(El_i,El_j)=(x1+Radius)^2*Mass_Original(1,1);

[RAO,Bad_New]=NewRAO(size(WDir,2),Omg,Amass,Bdamp,Mass_Change,Bad,Spr
ing,Sadd,Fwave);

[RAONew,Wavedir]=transform_RAOsDir(Omg,RAO,WavesHeading,ThialfHeading
);
    [RS] =
Response_Spectra_Liftdyn(RAONew,Wavesp,Wavedir,size(Wavedir,2),size(O
mg,2),nperiods);
    Mass_f1(:,:)=Mass_Change;
    RS_f1(:,:)=RS(:,:);
    [RMS_AllDofs_f1]=RMS_Mass(RS,El_i,Response_DATA);
    clear Mass_Change RS RAO
    Mass_Change=Mass_Original;
    Mass_Change(El_i,El_j)=(x2+Radius)^2*Mass_Original(1,1);

[RAO,Bad_New]=NewRAO(size(WDir,2),Omg,Amass,Bdamp,Mass_Change,Bad,Spr
ing,Sadd,Fwave);

[RAONew,Wavedir]=transform_RAOsDir(Omg,RAO,WavesHeading,ThialfHeading
);
    [RS] =
Response_Spectra_Liftdyn(RAONew,Wavesp,Wavedir,size(Wavedir,2),size(O
mg,2),nperiods);
    Mass_f2(:,:)=Mass_Change;
    RS_f2(:,:)=RS(:,:);
    [RMS_AllDofs_f2]=RMS_Mass(RS,El_i,Response_DATA);
    clear Mass_Change RS RAO
    FinalPer_x1=x1;
    FinalPer_x2=x2;
[a,c1,x1,x2]=NewPoints(RMS_AllDofs_f2,RMS_AllDofs_f1,x1,x2,c1,a,C);
end
if (RMS_AllDofs_f1 > RMS_AllDofs_f2)
    MAX_RMS_M=RMS_AllDofs_f1;
    FinalMASS(:,:)=(Mass_f1(:,:));
    FinalPer=FinalPer_x1;
    FinalRS(:,:)=(RS_f1(:,:));
else
    MAX_RMS_M=RMS_AllDofs_f2;
    FinalMASS(:,:)=(Mass_f2(:,:));
    FinalPer=FinalPer_x2;
    FinalRS(:,:)=(RS_f2(:,:));
end
```

Appendix D3 Identification of viscous damp.

Identification of viscous damping: main script

```
close all
clear all
Omegaint=[0.01:0.01:1.7];

%% Data set
load('TestCase2b.mat');
Waves=Waves2;
ThialfHeading=ThialfHeading2;
Surge=Spec2{1,1};
Sway=Spec2{1,2};
Heave=Spec2{1,3};
Roll=Spec2{1,4};
Pitch=Spec2{1,5};
Yaw=Spec2{1,6};
%Wave Spectrum
for f=1:size(omega,2)
    WaveSpectra(f,:)=Waves(:,f)';
end
% Frequency interpolation
for dir=1:size(WavesHeading,2)
    Waveperdir=squeeze(WaveSpectra(:,dir))';
    [Inter_waves]=FrequencyInt_DATA(Omegaint,omega',Waveperdir);
    Wavesp(:,dir)=(Inter_waves(1,:)');
end
%Response Spectra
Responses=[Surge;Sway;Heave;Roll;Pitch;Yaw];
for dof=1:6
    RS_perdof=Responses(dof,:);
    [Inter_response]=FrequencyInt_DATA(Omegaint,omega',RS_perdof);
    Response_DATA(dof,:)=Inter_response(1,:);
end

%% Original vessel properties and approximation functions
load('thialf_22_deep2.mat');%Original properties
load('hyd_file'); %Hydrodynamic database from diffraction software
load('Forces_Approximation.mat'); %Approximation: wave forces
load('AB_Approximation.mat'); %Approximation: added mass-damp
% Select Matrices
Mass=System.ModelData.Body.UserData.MassMatrix;
Bad=System.ModelData.Body.UserData.Badd;
Bad(3,3)=3.09*Bad(3,3);
Sadd=System.ModelData.Body.UserData.Sadd;
COG_Original=[[redacted]];
Rx=[redacted];%!!!!!!!!!!!!!!!!!!!!!
Ry=[redacted];%!!!!!!!!!!!!!!!!!!!!!!!!!!!!
Rz=[redacted];%!!!!!!!!!!!!!!!!!!!!!!!!!!!!!!!
%HydFile
Omg=Hyd.body1.Omega;
Wavedir=Hyd.body1.WDir; %1X13
ndirections=size(Wavedir,2);
nfrequencies=size(Omg,2); %(0-1.6)rad/s
Famp=Hyd.body1.Famp;
Feps=Hyd.body1.Feps;
[Fhyd,Fhyd_phase] =
Forces_HydFile(ndirections,nfrequencies,Famp,Feps);
[Fhyd]=All_directions(Fhyd);
```

```
Ahyd=Hyd.body1.AdMass; %Added Mass
Bhyd=Hyd.body1.BDamp; %Damping
clear Wavedir ndirections

%% Transformation of matrices from hyd file
WDir=[0:15:345];
% Frequency interpolation
[Inter_Bhyd,Inter_Ahyd,Inter_Fhyd]=
FrequencyInterpolation_ABF(Omegaint,Bhyd,Ahyd,Fhyd,WDir,Omg,WDir);
[Fhyd_phase,Fhyd_amp]=Construct_Forces_Sens(Inter_Fhyd);
[Spring_hyd,Amass_hyd,Bdamp_hyd,Fwave_hyd,Error] =
TransformationCOG(COG_Original,Inter_Ahyd,Inter_Bhyd,Fhyd_phase,Fhyd_
amp,Omegaint',WDir');
clear Omg nfrequencies
Omg=Omegaint;
nfrequencies=size(Omegaint,2);
ndirections=size(WDir,2);

%% Response spectrum
[RAO,Bad_New]=NewRAO(ndirections,Omg,Amass_hyd,Bdamp_hyd,Mass,Bad,Spr
ing_hyd,Sadd,Fwave_hyd);
[RAONew,Wavedir]=transform_RAOsDir(Omegaint,RAO,WavesHeading,ThialfHe
ading);
clear RAO
RAO=RAONew;
[RS] =
Response_Spectra_Liftdyn(RAO,Wavesp,Wavedir,size(Wavedir,2),nfrequenc
ies,nperiods);
RESPONSE={'Maximum Inaccuracy for Surge' 'Maximum Inaccuracy for
Sway' 'Maximum Inaccuracy for Heave' 'Maximum Inaccuracy for Roll'
'Maximum Inaccuracy for Pitch' 'Maximum Inaccuracy for Yaw'};
Title={'SURGE','SWAY','HEAVE','ROLL','PITCH','YAW'};
close all
for dof=1:6
       figure(p);
       subplot(2,3,dof)

plot(Omg(1:nfrequencies),squeeze(Response_DATA(dof,:)),'b',Omg(1:nfre
quencies),squeeze(RS(dof,:)),'r');%RS=DOFXfreqXPeakPeriods
        title(Title{dof});
        TeXStringX=texlabel('omega [rad/sec]');
        xlabel(TeXStringX,'Fontsize',14);
        if dof==1||dof==2||dof==3
            TeXStringY=texlabel('S(omega)  [m^(2)*s]');
            ylabel(TeXStringY,'Fontsize',14);
        else
            TeXStringY=texlabel('S(omega)  [degrees^(2)*s]');
            ylabel(TeXStringY,'Fontsize',14);
        end
       legend('Data','Calculations');
       hold on
end

dof=4;
[RMS_Check_X]=Check_Response_MassMatrix(dof,RS,Response_DATA);
dof=5;
[RMS_Check_Y]=Check_Response_MassMatrix(dof,RS,Response_DATA);
dof=6;
[RMS_Check_Z]=Check_Response_MassMatrix(dof,RS,Response_DATA);
```

```
if min([RMS_Check_Z RMS_Check_Y RMS_Check_X])==RMS_Check_Z
   h = msgbox('Change radius of gyration: Z axis');
   uiwait(h);
   Check=66;
elseif min([RMS_Check_Z RMS_Check_Y RMS_Check_X])==RMS_Check_Y
   h = msgbox('Change radius of gyration: Y axis');
   uiwait(h);
   Check=55;
elseif min([RMS_Check_Z RMS_Check_Y RMS_Check_X])==RMS_Check_X
   h = msgbox('Change radius of gyration: X axis');
   uiwait(h);
   Check=44;
end
%% B11
  El_i=1;
  El_j=1;
[FinalBad11,FinalPer11,FinalRS11,MAX_RMS_11]=ViscDamp_InterationsGOLD
EN(El_i,El_j,Response_DATA,Bad,WDir,Omg,Mass,Amass_hyd,Bdamp_hyd,Spri
ng_hyd,Sadd,Fwave_hyd,Wavesp,nperiods,WavesHeading,ThialfHeading);

%% B55
  El_i=2;
  El_j=2;
[FinalBad22,FinalPer22,FinalRS22,MAX_RMS_22]=ViscDamp_InterationsGOLD
EN(El_i,El_j,Response_DATA,Bad,WDir,Omg,Mass,Amass_hyd,Bdamp_hyd,Spri
ng_hyd,Sadd,Fwave_hyd,Wavesp,nperiods,WavesHeading,ThialfHeading);

%% B33
  El_i=3;
  El_j=3;
[FinalBad33,FinalPer33,FinalRS33,MAX_RMS_33]=ViscDamp_InterationsGOLD
EN(El_i,El_j,Response_DATA,Bad,WDir,Omg,Mass,Amass_hyd,Bdamp_hyd,Spri
ng_hyd,Sadd,Fwave_hyd,Wavesp,nperiods,WavesHeading,ThialfHeading);

%% B44
  El_i=4;
  El_j=4;
[FinalBad44,FinalPer44,FinalRS44,MAX_RMS_44]=ViscDamp_InterationsGOLD
EN(El_i,El_j,Response_DATA,Bad,WDir,Omg,Mass,Amass_hyd,Bdamp_hyd,Spri
ng_hyd,Sadd,Fwave_hyd,Wavesp,nperiods,WavesHeading,ThialfHeading);

%% B55
  El_i=5;
  El_j=5;
[FinalBad55,FinalPer55,FinalRS55,MAX_RMS_55]=ViscDamp_InterationsGOLD
EN(El_i,El_j,Response_DATA,Bad,WDir,Omg,Mass,Amass_hyd,Bdamp_hyd,Spri
ng_hyd,Sadd,Fwave_hyd,Wavesp,nperiods,WavesHeading,ThialfHeading);

%% B66

  El_i=6;
  El_j=6;
```

Golden section method for viscous damping:

```
function
[FinalBad,FinalPer,FinalRS,MAX_RMS_M]=ViscDamp_InterationsGOLDEN(El_i
,El_j,Response_DATA,Bad_Original,WDir,Omg,Mass,Amass,Bdamp,Spring,Sad
d,Fwave,Wavesp,nperiods,WavesHeading,ThialfHeading)
R=0.61803399; %The golden ratios.
```

```
C=(1.0-R);
a=0.2;
c1=50;
b=1;
x1=b;
x2=b+R*abs(c1-b);
while abs(c1-a) > 0.5 && abs(RMS_AllDofs_f2 - RMS_AllDofs_f1)>0.0001
    Bad_Change=Bad_Original;
    Bad_Change(El_i,El_j)=x1*Bad_Original(El_i,El_j);

[RAO,Bad_New]=NewRAO(size(WDir,2),Omg,Amass,Bdamp,Mass,Bad_Change,Spr
ing,Sadd,Fwave);

[RAONew,Wavedir]=transform_RAOsDir(Omg,RAO,WavesHeading,ThialfHeading
);
    [RS] =
Response_Spectra_Liftdyn(RAONew,Wavesp,Wavedir,size(Wavedir,2),size(O
mg,2),nperiods);
    Bad_f1(:,:)=Bad_Change;
    RS_f1(:,:)=RS(:,:);
    [RMS_AllDofs_f1]=RMS_Mass(RS,El_i,Response_DATA);
    clear Bad_Change RS RAO
    Bad_Change=Bad_Original;
    Bad_Change(El_i,El_j)=x2*Bad_Original(El_i,El_j);

[RAO,Bad_New]=NewRAO(size(WDir,2),Omg,Amass,Bdamp,Mass,Bad_Change,Spr
ing,Sadd,Fwave);

[RAONew,Wavedir]=transform_RAOsDir(Omg,RAO,WavesHeading,ThialfHeading
);
    [RS] =
Response_Spectra_Liftdyn(RAONew,Wavesp,Wavedir,size(Wavedir,2),size(O
mg,2),nperiods);
    Bad_f2(:,:)=Bad_Change;
    RS_f2(:,:)=RS(:,:);
    [RMS_AllDofs_f2]=RMS_Mass(RS,El_i,Response_DATA);
    clear Bad_Change RS RAO
    FinalPer_x1=x1;
    FinalPer_x2=x2;

[a,c1,x1,x2]=NewPoints(RMS_AllDofs_f2,RMS_AllDofs_f1,x1,x2,c1,a,C);
end
if (RMS_AllDofs_f1 > RMS_AllDofs_f2)
    MIN_RMS_M=RMS_AllDofs_f1;
    FinalBad(:,:)=(Bad_f1(:,:));
    FinalPer=FinalPer_x1;
    FinalRS(:,:)=(RS_f1(:,:));
else
    MIN_RMS_M=RMS_AllDofs_f2;
    FinalBad(:,:)=(Bad_f2(:,:));
    FinalPer=FinalPer_x2;
    FinalRS(:,:)=(RS_f2(:,:));
end
```

Appendix D4 Identification of added mass-damping

Identification of added mass and damping: main script

```
close all
clear all
Omegaint=[0.01:0.01:1.7];

%% Data set
load('TestCase2b.mat');
Waves=Waves2;
ThialfHeading=ThialfHeading2;
Surge=Spec2{1,1};
Sway=Spec2{1,2};
Heave=Spec2{1,3};
Roll=Spec2{1,4};
Pitch=Spec2{1,5};
Yaw=Spec2{1,6};
%Wave Spectrum
for f=1:size(omega,2)
    WaveSpectra(f,:)=Waves(:,f)';
end
% Frequency interpolation
for dir=1:size(WavesHeading,2)
    Waveperdir=squeeze(WaveSpectra(:,dir))';
    [Inter_waves]=FrequencyInt_DATA(Omegaint,omega',Waveperdir);
    Wavesp(:,dir)=(Inter_waves(1,:)');
end
%Response Spectra
Responses=[Surge;Sway;Heave;Roll;Pitch;Yaw];
for dof=1:6
    RS_perdof=Responses(dof,:);
    [Inter_response]=FrequencyInt_DATA(Omegaint,omega',RS_perdof);
    Response_DATA(dof,:)=Inter_response(1,:);
end

%% Original vessel properties and approximation functions
load('thialf_22_deep2.mat');%Original properties
load('hyd_file'); %Hydrodynamic database from diffraction software
load('Forces_Approximation.mat'); %Approximation: wave forces
load('AB_Approximation.mat'); %Approximation: added mass-damp
% Select Matrices
Mass=System.ModelData.Body.UserData.MassMatrix;
Bad=System.ModelData.Body.UserData.Badd;
Bad(3,3)=3.09*Bad(3,3);
Sadd=System.ModelData.Body.UserData.Sadd;
COG_Original=[[redacted]];
Rx=[redacted];%!!!!!!!!!!!!!!!!!!!!!!
Ry=[redacted];%!!!!!!!!!!!!!!!!!!!!!!!!!!!!
Rz=[redacted];%!!!!!!!!!!!!!!!!!!!!!!!!!!!!!!!!
%HydFile
Omg=Hyd.body1.Omega;
Wavedir=Hyd.body1.WDir; %1X13
ndirections=size(Wavedir,2);
nfrequencies=size(Omg,2); %(0-1.6)rad/s
Famp=Hyd.body1.Famp;
Feps=Hyd.body1.Feps;
```

```
[Fhyd,Fhyd_phase] =
Forces_HydFile(ndirections,nfrequencies,Famp,Feps);
[Fhyd]=All_directions(Fhyd);
Ahyd=Hyd.body1.AdMass; %Added Mass
Bhyd=Hyd.body1.BDamp; %Damping
clear Wavedir ndirections

%% Transformation of matrices from hyd file
WDir=[0:15:345];
% Frequency interpolation
[Inter_Bhyd,Inter_Ahyd,Inter_Fhyd]=
FrequencyInterpolation_ABF(Omegaint,Bhyd,Ahyd,Fhyd,WDir,Omg,WDir);
[Fhyd_phase,Fhyd_amp]=Construct_Forces_Sens(Inter_Fhyd);
[Spring_hyd,Amass_hyd,Bdamp_hyd,Fwave_hyd,Error] =
TransformationCOG(COG_Original,Inter_Ahyd,Inter_Bhyd,Fhyd_phase,Fhyd_
amp,Omegaint',WDir');
clear Omg nfrequencies
Omg=Omegaint;
nfrequencies=size(Omegaint,2);
ndirections=size(WDir,2);

%% Response spectrum
[RAO,Bad_New]=NewRAO(ndirections,Omg,Amass_hyd,Bdamp_hyd,Mass,Bad,Spr
ing_hyd,Sadd,Fwave_hyd);
[RAONew,Wavedir]=transform_RAOsDir(Omegaint,RAO,WavesHeading,ThialfHe
ading);
clear RAO
RAO=RAONew;
[RS] =
Response_Spectra_Liftdyn(RAO,Wavesp,Wavedir,size(Wavedir,2),nfrequenc
ies,nperiods);
[RMS_Check]=Check_Response_COG(RS,Response_DATA);
MIN=min(RMS_Check);
RESPONSE={'Maximum Inaccuracy for Surge' 'Maximum Inaccuracy for
Sway' 'Maximum Inaccuracy for Heave' 'Maximum Inaccuracy for Roll'
'Maximum Inaccuracy for Pitch' 'Maximum Inaccuracy for Yaw'};
Title={'SURGE','SWAY','HEAVE','ROLL','PITCH','YAW'};
close all
for dof=1:6
       figure(p);
       subplot(2,3,dof)

plot(Omg(1:nfrequencies),squeeze(Response_DATA(dof,:)),'b',Omg(1:nfre
quencies),squeeze(RS(dof,:)),'r');%RS=DOFXfreqXPeakPeriods
        title(Title{dof});
        TeXStringX=texlabel('omega [rad/sec]');
        xlabel(TeXStringX,'Fontsize',14);
        if dof==1||dof==2||dof==3
            TeXStringY=texlabel('S(omega)  [m^(2)*s]');
            ylabel(TeXStringY,'Fontsize',14);
        else
            TeXStringY=texlabel('S(omega)  [degrees^(2)*s]');
            ylabel(TeXStringY,'Fontsize',14);
        end
       legend('Data','Calculations');
       hold on
end

for dof=1:6
    if MIN==RMS_Check(dof,1)
       h=msgbox(RESPONSE{1,dof});
```

```
        uiwait(h);
        if dof==1|| dof==3|| dof==5
            Check=1;
        else
            Check=2;
        end
    end
end
clear RMS RMS_AllPeaks Omg
Omg=Hyd.body1.Omega;
%% Element 11
if Check==1
    i=1;
    j=1;
    PorderAB=PorderAB11;
    CresOrderAB=CresOrderAB11;
    dAB=dAB11;
    hAB=hAB11;

[MAX_RMS_AB11,Final_AB11,FinalPer_AB11,FinalRS_AB11]=Inter_ABresidues
_GOLDEN(i,j,BA_VF,PorderAB,CresOrderAB,dAB,hAB,Omegaint,Omg,Fhyd,WDir
,COG_Original,Mass,Sadd,Bad,Wavesp,nperiods,Response_DATA,WavesHeadin
g,ThialfHeading);
    RMS_AB11=max((MAX_RMS_AB11(1:2:size(MAX_RMS_AB11,1),1)));
    for c=1:2:size(CresOrderAB11,2)
        if RMS_AB11==MAX_RMS_AB11(c,1)
            c_AB11=c;
            AB11=squeeze(Final_AB11(c,:,:,:));
            Per_AB11=FinalPer_AB11(c,1);
            FinalResponse_AB11(:,:)=squeeze(FinalRS_AB11(c,:,:));
        end
    end

[RMS_CheckAB11]=Check_Response_COG(FinalResponse_AB11,Response_DATA);
    clear PorderAB CresOrderAB dAB hAB
end
%% Element 13
if Check==1
    i=1;
    j=3;
    PorderAB=PorderAB31;
    CresOrderAB=CresOrderAB31;
    dAB=dAB31;
    hAB=hAB31;

[MAX_RMS_AB13,Final_AB13,FinalPer_AB13,FinalRS_AB13]=Inter_ABresidues
_GOLDEN(i,j,BA_VF,PorderAB,CresOrderAB,dAB,hAB,Omegaint,Omg,Fhyd,WDir
,COG_Original,Mass,Sadd,Bad,Wavesp,nperiods,Response_DATA,WavesHeadin
g,ThialfHeading);
    RMS_AB13=max((MAX_RMS_AB13(1:2:size(MAX_RMS_AB13,1),1)));
    for c=1:2:size(CresOrderAB31,2)
        if RMS_AB13==MAX_RMS_AB13(c,1)
            c_AB13=c;
            AB13=squeeze(Final_AB13(c,:,:,:));
            Per_AB13=FinalPer_AB13(c,1);
            FinalResponse_AB13(:,:)=squeeze(FinalRS_AB13(c,:,:));
        end
    end

[RMS_CheckAB13]=Check_Response_COG(FinalResponse_AB13,Response_DATA);
    clear PorderAB CresOrderAB dAB hAB
```

```
end

%% Element 15
if Check==1
    i=1;
    j=5;
    PorderAB=PorderAB51;
    CresOrderAB=CresOrderAB51;
    dAB=dAB51;
    hAB=hAB51;

[MAX_RMS_AB15,Final_AB15,FinalPer_AB15,FinalRS_AB15]=Inter_ABresidues
_GOLDEN(i,j,BA_VF,PorderAB,CresOrderAB,dAB,hAB,Omegaint,Omg,Fhyd,WDir
,COG_Original,Mass,Sadd,Bad,Wavesp,nperiods,Response_DATA,WavesHeadin
g,ThialfHeading);
    RMS_AB15=max((MAX_RMS_AB15(1:2:size(MAX_RMS_AB15,1),1)));
    for c=1:2:size(CresOrderAB51,2)
        if RMS_AB15==MAX_RMS_AB15(c,1)
           c_AB15=c;
           AB15=squeeze(Final_AB15(c,:,:,:));
           Per_AB15=FinalPer_AB15(c,1);
           FinalResponse_AB15(:,:)=squeeze(FinalRS_AB15(c,:,:));
        end
    end

[RMS_CheckAB15]=Check_Response_COG(FinalResponse_AB15,Response_DATA);
    clear PorderAB CresOrderAB dAB hAB
end
%% Element 22
if Check==2
    i=2;
    j=2;
    PorderAB=PorderAB22;
    CresOrderAB=CresOrderAB22;
    dAB=dAB22;
    hAB=hAB22;

[MAX_RMS_AB22,Final_AB22,FinalPer_AB22,FinalRS_AB22]=Inter_ABresidues
_GOLDEN(i,j,BA_VF,PorderAB,CresOrderAB,dAB,hAB,Omegaint,Omg,Fhyd,WDir
,COG_Original,Mass,Sadd,Bad,Wavesp,nperiods,Response_DATA,WavesHeadin
g,ThialfHeading);
    RMS_AB22=max((MAX_RMS_AB22(1:2:size(MAX_RMS_AB22,1),1)));
    for c=1:2:size(CresOrderAB22,2)
        if RMS_AB22==MAX_RMS_AB22(c,1)
           c_AB22=c;
           AB22=squeeze(Final_AB22(c,:,:,:));
           Per_AB22=FinalPer_AB22(c,1);
           FinalResponse_AB22(:,:)=squeeze(FinalRS_AB22(c,:,:));
        end
    end

[RMS_CheckAB22]=Check_Response_COG(FinalResponse_AB22,Response_DATA);
    clear PorderAB CresOrderAB dAB hAB
end
%% Element 24
if Check==2
    i=2;
    j=4;
    PorderAB=PorderAB42;
    CresOrderAB=CresOrderAB42;
    dAB=dAB42;
```

```
    hAB=hAB42;

[MAX_RMS_AB24,Final_AB24,FinalPer_AB24,FinalRS_AB24]=Inter_ABresidues
_GOLDEN(i,j,BA_VF,PorderAB,CresOrderAB,dAB,hAB,Omegaint,Omg,Fhyd,WDir
,COG_Original,Mass,Sadd,Bad,Wavesp,nperiods,Response_DATA,WavesHeadin
g,ThialfHeading);
    RMS_AB24=max((MAX_RMS_AB24(1:2:size(MAX_RMS_AB24,1),1)));
    for c=1:2:size(CresOrderAB42,2)
        if RMS_AB24==MAX_RMS_AB24(c,1)
           c_AB24=c;
           AB24=squeeze(Final_AB24(c,:,:,:));
           Per_AB24=FinalPer_AB24(c,1);
           FinalResponse_AB24(:,:)=squeeze(FinalRS_AB24(c,:,:));
        end
    end

[RMS_CheckAB24]=Check_Response_COG(FinalResponse_AB24,Response_DATA);
    clear PorderAB CresOrderAB dAB hAB
end

%% Element 26
if Check==2
    i=2;
    j=6;
    PorderAB=PorderAB62;
    CresOrderAB=CresOrderAB62;
    dAB=dAB62;
    hAB=hAB62;

[MAX_RMS_AB26,Final_AB26,FinalPer_AB26,FinalRS_AB26]=Inter_ABresidues
_GOLDEN(i,j,BA_VF,PorderAB,CresOrderAB,dAB,hAB,Omegaint,Omg,Fhyd,WDir
,COG_Original,Mass,Sadd,Bad,Wavesp,nperiods,Response_DATA,WavesHeadin
g,ThialfHeading);
    RMS_AB26=max((MAX_RMS_AB26(1:2:size(MAX_RMS_AB26,1),1)));
    for c=1:2:size(CresOrderAB62,2)
        if RMS_AB26==MAX_RMS_AB26(c,1)
           c_AB26=c;
           AB26=squeeze(Final_AB26(c,:,:,:));
           Per_AB26=FinalPer_AB26(c,1);
           FinalResponse_AB26(:,:)=squeeze(FinalRS_AB26(c,:,:));
        end
    end

[RMS_CheckAB26]=Check_Response_COG(FinalResponse_AB26,Response_DATA);
    clear PorderAB CresOrderAB dAB hAB
end
%% Element 33
if Check==1
    i=3;
    j=3;
    PorderAB=PorderAB33;
    CresOrderAB=CresOrderAB33;
    dAB=dAB33;
    hAB=hAB33;

[MAX_RMS_AB33,Final_AB33,FinalPer_AB33,FinalRS_AB33]=Inter_ABresidues
_GOLDEN(i,j,BA_VF,PorderAB,CresOrderAB,dAB,hAB,Omegaint,Omg,Fhyd,WDir
,COG_Original,Mass,Sadd,Bad,Wavesp,nperiods,Response_DATA,WavesHeadin
g,ThialfHeading);
    RMS_AB33=max((MAX_RMS_AB33(1:2:size(MAX_RMS_AB33,1),1)));
    for c=1:2:size(CresOrderAB33,2)
```

```
        if RMS_AB33==MAX_RMS_AB33(c,1)
            c_AB33=c;
            AB33=squeeze(Final_AB33(c,:,:,:));
            Per_AB33=FinalPer_AB33(c,1);
            FinalResponse_AB33(:,:)=squeeze(FinalRS_AB33(c,:,:));
        end
    end

[RMS_CheckAB33]=Check_Response_COG(FinalResponse_AB33,Response_DATA);
    clear PorderAB CresOrderAB dAB hAB
end
%% Element 35
if Check==1
    i=3;
    j=5;
    PorderAB=PorderAB53;
    CresOrderAB=CresOrderAB53;
    dAB=dAB53;
    hAB=hAB53;

[MAX_RMS_AB35,Final_AB35,FinalPer_AB35,FinalRS_AB35]=Inter_ABresidues
_GOLDEN(i,j,BA_VF,PorderAB,CresOrderAB,dAB,hAB,Omegaint,Omg,Fhyd,WDir
,COG_Original,Mass,Sadd,Bad,Wavesp,nperiods,Response_DATA,WavesHeadin
g,ThialfHeading);
    RMS_AB35=max((MAX_RMS_AB35(1:2:size(MAX_RMS_AB35,1),1)));
    for c=1:2:size(CresOrderAB53,2)
        if RMS_AB35==MAX_RMS_AB35(c,1)
            c_AB35=c;
            AB35=squeeze(Final_AB35(c,:,:,:));
            Per_AB35=FinalPer_AB35(c,1);
            FinalResponse_AB35(:,:)=squeeze(FinalRS_AB35(c,:,:));
        end
    end

[RMS_CheckAB35]=Check_Response_COG(FinalResponse_AB35,Response_DATA);
    clear PorderAB CresOrderAB dAB hAB
end
%% Element 44
if Check==2
    i=4;
    j=4;
    PorderAB=PorderAB44;
    CresOrderAB=CresOrderAB44;
    dAB=dAB44;
    hAB=hAB44;

[MAX_RMS_AB44,Final_AB44,FinalPer_AB44,FinalRS_AB44]=Inter_ABresidues
_GOLDEN(i,j,BA_VF,PorderAB,CresOrderAB,dAB,hAB,Omegaint,Omg,Fhyd,WDir
,COG_Original,Mass,Sadd,Bad,Wavesp,nperiods,Response_DATA,WavesHeadin
g,ThialfHeading);
    RMS_AB44=max((MAX_RMS_AB44(1:2:size(MAX_RMS_AB44,1),1)));
    for c=1:2:size(CresOrderAB44,2)
        if RMS_AB44==MAX_RMS_AB44(c,1)
            c_AB44=c;
            AB44=squeeze(Final_AB44(c,:,:,:));
            Per_AB44=FinalPer_AB44(c,1);
            FinalResponse_AB44(:,:)=squeeze(FinalRS_AB44(c,:,:));
        end
    end

[RMS_CheckAB44]=Check_Response_COG(FinalResponse_AB44,Response_DATA);
```

```
    clear PorderAB CresOrderAB dAB hAB
end
%% Element 46
if Check==2
    i=4;
    j=6;
    PorderAB=PorderAB64;
    CresOrderAB=CresOrderAB64;
    dAB=dAB64;
    hAB=hAB64;

[MAX_RMS_AB46,Final_AB46,FinalPer_AB46,FinalRS_AB46]=Inter_ABresidues
_GOLDEN(i,j,BA_VF,PorderAB,CresOrderAB,dAB,hAB,Omegaint,Omg,Fhyd,WDir
,COG_Original,Mass,Sadd,Bad,Wavesp,nperiods,Response_DATA,WavesHeadin
g,ThialfHeading);
    RMS_AB46=max((MAX_RMS_AB46(1:2:size(MAX_RMS_AB46,1),1)));
    for c=1:2:size(CresOrderAB64,2)
        if RMS_AB46==MAX_RMS_AB46(c,1)
           c_AB46=c;
           AB46=squeeze(Final_AB46(c,:,:,:));
           Per_AB46=FinalPer_AB46(c,1);
           FinalResponse_AB46(:,:)=squeeze(FinalRS_AB46(c,:,:));
        end
    end

[RMS_CheckAB46]=Check_Response_COG(FinalResponse_AB46,Response_DATA);
    clear PorderAB CresOrderAB dAB hAB
end

%% Element 55
if Check==1
    i=5;
    j=5;
    PorderAB=PorderAB55;
    CresOrderAB=CresOrderAB55;
    dAB=dAB55;
    hAB=hAB55;

[MAX_RMS_AB55,Final_AB55,FinalPer_AB55,FinalRS_AB55]=Inter_ABresidues
_GOLDEN(i,j,BA_VF,PorderAB,CresOrderAB,dAB,hAB,Omegaint,Omg,Fhyd,WDir
,COG_Original,Mass,Sadd,Bad,Wavesp,nperiods,Response_DATA,WavesHeadin
g,ThialfHeading);
    RMS_AB55=max((MAX_RMS_AB55(1:2:size(MAX_RMS_AB55,1),1)));
    for c=1:2:size(CresOrderAB55,2)
        if RMS_AB55==MAX_RMS_AB55(c,1)
           c_AB55=c;
           AB55=squeeze(Final_AB55(c,:,:,:));
           Per_AB55=FinalPer_AB55(c,1);
           FinalResponse_AB55(:,:)=squeeze(FinalRS_AB55(c,:,:));
        end
    end

[RMS_CheckAB55]=Check_Response_COG(FinalResponse_AB55,Response_DATA);
    clear PorderAB CresOrderAB dAB hAB
end

%% Element 66
if Check==2
    i=6;
    j=6;
    PorderAB=PorderAB66;
```

```
    CresOrderAB=CresOrderAB66;
    dAB=dAB66;
    hAB=hAB66;

[MAX_RMS_AB66,Final_AB66,FinalPer_AB66,FinalRS_AB66]=Inter_ABresidues
_GOLDEN(i,j,BA_VF,PorderAB,CresOrderAB,dAB,hAB,Omegaint,Omg,Fhyd,WDir
,COG_Original,Mass,Sadd,Bad,Wavesp,nperiods,Response_DATA,WavesHeadin
g,ThialfHeading);
    RMS_AB66=max((MAX_RMS_AB66(1:2:size(MAX_RMS_AB66,1),1)));
    for c=1:2:size(CresOrderAB66,2)
        if RMS_AB66==MAX_RMS_AB66(c,1)
           c_AB66=c;
           AB66=squeeze(Final_AB66(c,:,:,:));
           Per_AB66=FinalPer_AB66(c,1);
           FinalResponse_AB66(:,:)=squeeze(FinalRS_AB66(c,:,:));
        end
    end

[RMS_CheckAB66]=Check_Response_COG(FinalResponse_AB66,Response_DATA);
    clear PorderAB CresOrderAB dAB hAB
end
%% Total MIN
if Check==1
    ELEMENTS={'Element 11' 'Element 13' 'Element 15' 'Element 33'
'Element 35' 'Element 55'};
    MAX_TOTAL=[RMS_AB11 RMS_AB13 RMS_AB15 RMS_AB33 RMS_AB35
RMS_AB55];

save('FinalRMS_AB_TC2.mat','RMS_CheckAB11','RMS_CheckAB13','RMS_Check
AB15','RMS_CheckAB33','RMS_CheckAB35','RMS_CheckAB55');

save('Adjust_ResiduesAB_TC5.mat','RMS_AB11','c_AB11','AB11','Per_AB11
','FinalResponse_AB11','RMS_AB13','c_AB13','AB13','Per_AB13','FinalRe
sponse_AB13','RMS_AB15','c_AB15','AB15','Per_AB15','FinalResponse_AB1
5','RMS_AB33','c_AB33','AB33','Per_AB33','FinalResponse_AB33','RMS_AB
35','c_AB35','AB35','Per_AB35','FinalResponse_AB35','RMS_AB55','c_AB5
5','AB55','Per_AB55','FinalResponse_AB55');
else
    ELEMENTS={'Element 22' 'Element 24' 'Element 26' 'Element 44'
'Element 46' 'Element 66'};
    MAX_TOTAL=[RMS_AB22 RMS_AB24 RMS_AB26 RMS_AB44 RMS_AB46
RMS_AB66];

save('FinalRMS_AB_TC2.mat','RMS_CheckAB22','RMS_CheckAB24','RMS_Check
AB26','RMS_CheckAB44','RMS_CheckAB46','RMS_CheckAB66');

save('Adjust_ResiduesAB_TC5.mat','RMS_AB22','c_AB22','AB22','Per_AB22
','FinalResponse_AB22','RMS_AB24','c_AB24','AB24','Per_AB24','FinalRe
sponse_AB24','RMS_AB26','c_AB26','AB26','Per_AB26','FinalResponse_AB2
6','RMS_AB44','c_AB44','AB44','Per_AB44','FinalResponse_AB44','RMS_AB
46','c_AB46','AB46','Per_AB46','FinalResponse_AB46','RMS_AB66','c_AB6
6','AB66','Per_AB66','FinalResponse_AB66');
end

for i=1:size(MAX_TOTAL,2)
    if max(MAX_TOTAL)==MAX_TOTAL(1,i)
       h = msgbox(ELEMENTS{1,i});
       uiwait(h);
    end
end
```

Golden section method for added mass and damping:

```
function
[MAX_RMS_AB,Final_AB,FinalPer_AB,FinalRS_AB]=Inter_ABresidues_GOLDEN(
i,j,BA_VF,PorderAB,CresOrderAB,dAB,hAB,Omegaint,Omega,Fhyd,Wavedir,CO
G_Original,Mass,Sadd,Bad,Wavesp,nperiods,Response_DATA,WavesHeading,T
hialfHeading)
for c=1:2:size(CresOrderAB,2)
    R=0.61803399; %The golden ratios.
    C=(1.0-R);
    a=-50;
    c1=50;
    b=1;
    x1=b;
    x2=b+R*(c1-b);
   while abs(c1-a)> 0.1 && abs(RMS_AllDofs_AB_f2(1,c) -
RMS_AllDofs_AB_f1(1,c))>0.001

[sum]=NewAB(CresOrderAB,x1,c,Omega,PorderAB,size(BA_VF,3),dAB,hAB);
        BA_VF(i,j,:)=sum(1,:);
        BA_VF(j,i,:)=BA_VF(i,j,:);
        BA_VFNew_f1(c,:,:,:)=BA_VF;
        for f=1:size(BA_VF,3)
            A_Change(:,:,f)=real(squeeze(BA_VF(:,:,f)));
            B_Change(:,:,f)=-imag(squeeze(BA_VF(:,:,f)))*Omega(1,f);
        end
        % Frequency interpolation
        clear Inter_Bhyd Inter_Ahyd Inter_Fhyd
        [Inter_Bhyd,Inter_Ahyd,Inter_Fhyd]=
FrequencyInterpolation_ABF(Omegaint,B_Change,A_Change,Fhyd,Wavedir,Om
ega,Wavedir);
        clear B_Change A_Change
        B_Change=Inter_Bhyd;
        A_Change=Inter_Ahyd;
        Fhydint =Inter_Fhyd;
        nfrequencies=size(Omegaint,2);
        [Fhyd_phase,Fhyd_amp]=Construct_Forces_Sens(Fhydint);
        [Spring_hyd,Amass_hyd,Bdamp_hyd,Fwave_hyd,Error] =
TransformationCOG(COG_Original,A_Change,B_Change,Fhyd_phase,Fhyd_amp,
Omegaint',Wavedir');

[RAO,Bad_New]=NewRAO(size(Wavedir,2),Omegaint,Amass_hyd,Bdamp_hyd,Mas
s,Bad,Spring_hyd,Sadd,Fwave_hyd);

[RAONew,WavedirNew]=transform_RAOsDir(Omegaint,RAO,WavesHeading,Thial
fHeading);
        [RS] =
Response_Spectra_Liftdyn(RAONew,Wavesp,WavedirNew,size(WavedirNew,2),
size(Omegaint,2),nperiods);
        RS_New_f1(c,:,:)=RS(:,:);
        [RMS_AllDofs_f1]=RMS(i,RS,Response_DATA);
        RMS_AllDofs_AB_f1(1,c)=RMS_AllDofs_f1;
        clear B_Change A_Change Fhyd_phase Fhyd_amp Spring_hyd
Amass_hyd Bdamp_hyd Fwave_hyd Error RAO RAONew Bad_New RS1_fdir
RS2_fdir RS3_fdir RS4_fdir RS5_fdir RS6_fdir RS


[sum]=NewAB(CresOrderAB,x2,c,Omega,PorderAB,size(BA_VF,3),dAB,hAB);
        BA_VF(i,j,:)=sum(1,:);
        BA_VF(j,i,:)=BA_VF(i,j,:);
        BA_VFNew_f2(c,:,:,:)=BA_VF;
        for f=1:size(BA_VF,3)
```

```
            A_Change(:,:,f)=real(squeeze(BA_VF(:,:,f)));
            B_Change(:,:,f)=-imag(squeeze(BA_VF(:,:,f)))*Omega(1,f);
        end
        % Frequency interpolation
        clear Inter_Bhyd Inter_Ahyd Inter_Fhyd
        [Inter_Bhyd,Inter_Ahyd,Inter_Fhyd]=
FrequencyInterpolation_ABF(Omegaint,B_Change,A_Change,Fhyd,Wavedir,Om
ega,Wavedir);
        clear B_Change A_Change
        B_Change=Inter_Bhyd;
        A_Change=Inter_Ahyd;
        Fhydint =Inter_Fhyd;
        nfrequencies=size(Omegaint,2);
        [Fhyd_phase,Fhyd_amp]=Construct_Forces_Sens(Fhydint);
        [Spring_hyd,Amass_hyd,Bdamp_hyd,Fwave_hyd,Error] =
TransformationCOG(COG_Original,A_Change,B_Change,Fhyd_phase,Fhyd_amp,
Omegaint',Wavedir');

[RAO,Bad_New]=NewRAO(size(Wavedir,2),Omegaint,Amass_hyd,Bdamp_hyd,Mas
s,Bad,Spring_hyd,Sadd,Fwave_hyd);

[RAONew,WavedirNew]=transform_RAOsDir(Omegaint,RAO,WavesHeading,Thial
fHeading);
        [RS] =
Response_Spectra_Liftdyn(RAONew,Wavesp,WavedirNew,size(WavedirNew,2),
size(Omegaint,2),nperiods);
        RS_New_f2(c,:,:)=RS(:,:);
        [RMS_AllDofs_f2]=RMS(i,RS,Response_DATA);
        RMS_AllDofs_AB_f2(1,c)=RMS_AllDofs_f2;
        FinalPer_x1(c,1)=x1;
        FinalPer_x2(c,1)=x2;
        clear B_Change A_Change Fhyd_phase Fhyd_amp Spring_hyd
Amass_hyd Bdamp_hyd Fwave_hyd Error RAO RAONew Bad_New RS1_fdir
RS2_fdir RS3_fdir RS4_fdir RS5_fdir RS6_fdir RS

[a,c1,x1,x2]=NewPoints(RMS_AllDofs_f2,RMS_AllDofs_f1,x1,x2,c1,a,C);
    end
    if (RMS_AllDofs_AB_f1(1,c) > RMS_AllDofs_AB_f2(1,c))
        MAX_RMS_AB(c,1)=RMS_AllDofs_AB_f1(1,c);
        Final_AB(c,:,:,:)=squeeze(BA_VFNew_f1(c,:,:,:));
        FinalPer_AB(c,1)=FinalPer_x1(c,1);
        FinalRS_AB(c,:,:)=squeeze(RS_New_f1(c,:,:));
    else
        MAX_RMS_AB(c,1)=RMS_AllDofs_AB_f2(1,c);
        Final_AB(c,:,:,:)=squeeze(BA_VFNew_f2(c,:,:,:));
        FinalPer_AB(c,1)=FinalPer_x2(c,1);
        FinalRS_AB(c,:,:)=squeeze(RS_New_f2(c,:,:));
    end
    clear RMS_AllDofs_f2 RMS_AllDofs_f1 a c1 x1 x2 b
end
```

Appendix D5 Identification of wave forces

Identification of wave forces: main script

```
close all
clear all
Omegaint=[0.01:0.01:1.7];

%% Data set
load('TestCase2b.mat');
Waves=Waves2;
ThialfHeading=ThialfHeading2;
Surge=Spec2{1,1};
Sway=Spec2{1,2};
Heave=Spec2{1,3};
Roll=Spec2{1,4};
Pitch=Spec2{1,5};
Yaw=Spec2{1,6};
% [px1, py1] = PolarContour(Waves, WavesHeading, omega');
% mdir=-120+ThialfHeading+180
mdir=30;
%Wave Spectrum
for f=1:size(omega,2)
    WaveSpectra(f,:)=Waves(:,f)';
end
% Frequency interpolation
for dir=1:size(WavesHeading,2)
    Waveperdir=squeeze(WaveSpectra(:,dir))';
    [Inter_waves]=FrequencyInt_DATA(Omegaint,omega',Waveperdir);
    Wavesp(:,dir)=(Inter_waves(1,:)');
end
%Response Spectra
Responses=[Surge;Sway;Heave;Roll;Pitch;Yaw];
for dof=1:6
    RS_perdof=Responses(dof,:);
    [Inter_response]=FrequencyInt_DATA(Omegaint,omega',RS_perdof);
    Response_DATA(dof,:)=Inter_response(1,:);
end

%% Original vessel properties and approximation functions
load('thialf_22_deep2.mat');%Original properties
load('hyd_file'); %Hydrodynamic database from diffraction software
load('Forces_Approximation.mat'); %Approximation: wave forces
load('AB_Approximation.mat'); %Approximation: added mass-damp
% Select Matrices
Mass=System.ModelData.Body.UserData.MassMatrix;
Bad=System.ModelData.Body.UserData.Badd;
Bad(3,3)=3.09*Bad(3,3);
Sadd=System.ModelData.Body.UserData.Sadd;
COG_Original=[[redacted]];
Rx=[redacted];%!!!!!!!!!!!!!!!!!!!!!!
Ry=[redacted];%!!!!!!!!!!!!!!!!!!!!!!!!!!!!
Rz[redacted];%!!!!!!!!!!!!!!!!!!!!!!!!!!!!!!!
%HydFile
Omg=Hyd.body1.Omega;
Wavedir=Hyd.body1.WDir; %1X13
ndirections=size(Wavedir,2);
nfrequencies=size(Omg,2); %(0-1.6)rad/s
Famp=Hyd.body1.Famp;
Feps=Hyd.body1.Feps;
```

```
[Fhyd,Fhyd_phase] =
Forces_HydFile(ndirections,nfrequencies,Famp,Feps);
[Fhyd]=All_directions(Fhyd);
Ahyd=Hyd.body1.AdMass; %Added Mass
Bhyd=Hyd.body1.BDamp; %Damping
clear Wavedir ndirections

%% Transformation of matrices from hyd file
WDir=[0:15:345];
% Frequency interpolation
[Inter_Bhyd,Inter_Ahyd,Inter_Fhyd]=
FrequencyInterpolation_ABF(Omegaint,Bhyd,Ahyd,Fhyd,WDir,Omg,WDir);
[Fhyd_phase,Fhyd_amp]=Construct_Forces_Sens(Inter_Fhyd);
[Spring_hyd,Amass_hyd,Bdamp_hyd,Fwave_hyd,Error] =
TransformationCOG(COG_Original,Inter_Ahyd,Inter_Bhyd,Fhyd_phase,Fhyd_
amp,Omegaint',WDir');
clear Omg nfrequencies
Omg=Omegaint;
nfrequencies=size(Omegaint,2);
ndirections=size(WDir,2);

%% Response spectrum
[RAO,Bad_New]=NewRAO(ndirections,Omg,Amass_hyd,Bdamp_hyd,Mass,Bad,Spr
ing_hyd,Sadd,Fwave_hyd);
[RAONew,Wavedir]=transform_RAOsDir(Omegaint,RAO,WavesHeading,ThialfHe
ading);
clear RAO
RAO=RAONew;
[RS] =
Response_Spectra_Liftdyn(RAO,Wavesp,Wavedir,size(Wavedir,2),nfrequenc
ies,nperiods);
[RMS_Check]=Check_Response_COG(RS,Response_DATA);
MIN=min(RMS_Check);
RESPONSE={'Maximum Inaccuracy for Surge' 'Maximum Inaccuracy for
Sway' 'Maximum Inaccuracy for Heave' 'Maximum Inaccuracy for Roll'
'Maximum Inaccuracy for Pitch' 'Maximum Inaccuracy for Yaw'};
Title={'SURGE','SWAY','HEAVE','ROLL','PITCH','YAW'};
close all
for dof=1:6
       figure(p);
       subplot(2,3,dof)

plot(Omg(1:nfrequencies),squeeze(Response_DATA(dof,:)),'b',Omg(1:nfre
quencies),squeeze(RS(dof,:)),'r');%RS=DOFXfreqXPeakPeriods
        title(Title{dof});
        TeXStringX=texlabel('omega [rad/sec]');
        xlabel(TeXStringX,'Fontsize',14);
        if dof==1||dof==2||dof==3
            TeXStringY=texlabel('S(omega)  [m^(2)*s]');
            ylabel(TeXStringY,'Fontsize',14);
        else
            TeXStringY=texlabel('S(omega)  [degrees^(2)*s]');
            ylabel(TeXStringY,'Fontsize',14);
        end
       legend('Data','Calculations');
       hold on
end

for dof=1:6
    if MIN==RMS_Check(dof,1)
       h=msgbox(RESPONSE{1,dof});
```

```
        uiwait(h);
        if dof==1|| dof==3|| dof==5
            Check=1;
        else
            Check=2;
        end
    end
end
clear RMS RMS_AllPeaks Omg
Omg=Hyd.body1.Omega;
[Fhyd]=All_directions(Fhyd);
[DIRECTION,holddir]=Choose_WaveDirections(mdir,ndirections,WDir);
%% Wave Force 1
if Check==1
   dof=1;
    for j=1:size(holddir,2)
        if holddir(1,j)>13
            CresOrder=CresOrder1(24-holddir(1,j)+2,:);
            PForder=PForder1(24-holddir(1,j)+2,:);
        else
            CresOrder=CresOrder1(holddir(1,j),:);
            PForder=PForder1(holddir(1,j),:);
        end
        dir=holddir(1,j);
        for c=1:2:size(CresOrder,2)

[MAX_RMS_F1,Final_F1,Per_F1,FinalRS_F1]=Inter_FresiduesGolden(c,dof,d
ir,Fhyd,Bhyd,Ahyd,WDir,Omegaint,PForder,CresOrder,Omg,COG_Original,Ma
ss,Sadd,Bad,Wavesp,nperiods,Response_DATA,WavesHeading,ThialfHeading)
;
            RMS_RES_F1(c,1)=MAX_RMS_F1;
            RES_F1(c,:,:,:)=Final_F1;
            RES_PerF1(c,1)=Per_F1;
            RES_RSF1(c,:,:)=FinalRS_F1;
            clear Cres_Change MIN_RMS_F3 Final_F3 Per_F3 FinalRS_F3
        end
        RMS_DIR_F1(j,1)=max(RMS_RES_F1(1:2:size(RMS_RES_F1,1),1));
        for c=1:2:size(CresOrder,2)
            if RMS_RES_F1(c,1)==RMS_DIR_F1(j,1)
                DIR_F1(j,:,:,:)=(RES_F1(c,:,:,:));
                DIR_PerF1(j,1)=RES_PerF1(c,1);
                DIR_RSF1(j,:,:)=(RES_RSF1(c,:,:));
                c_F1(j,1)=c;
            end
        end
        clear CresOrder PForder
    end
    for j=1:size(holddir,2)
        if max(RMS_DIR_F1)==RMS_DIR_F1(j,1)
           DIR1=DIRECTION(1,j);
           C1=c_F1(j,1);
           F1(:,:,:)=squeeze(DIR_F1(j,:,:,:));
           PerF1(1,1)=DIR_PerF1(j,1);
           FinalResponse_F1(:,:)=squeeze(DIR_RSF1(j,:,:));
           MAXRMS_F1=max(RMS_DIR_F1);
        end
    end
   [RMS_CheckF1]=Check_Response_COG(FinalResponse_F1,Response_DATA);
end
%% Wave Force 2
if Check==2
```

```
   dof=2;
    for j=1:size(holddir,2)
        if holddir(1,j)>13
            CresOrder=CresOrder2(24-holddir(1,j)+2,:);
            PForder=PForder2(24-holddir(1,j)+2,:);
        else
            CresOrder=CresOrder2(holddir(1,j),:);
            PForder=PForder2(holddir(1,j),:);
        end
        dir=holddir(1,j);
        for c=1:2:size(CresOrder,2)

[MAX_RMS_F2,Final_F2,Per_F2,FinalRS_F2]=Inter_FresiduesGolden(c,dof,d
ir,Fhyd,Bhyd,Ahyd,WDir,Omegaint,PForder,CresOrder,Omg,COG_Original,Ma
ss,Sadd,Bad,Wavesp,nperiods,Response_DATA,WavesHeading,ThialfHeading)
;
            RMS_RES_F2(c,1)=MAX_RMS_F2;
            RES_F2(c,:,:,:)=Final_F2;
            RES_PerF2(c,1)=Per_F2;
            RES_RSF2(c,:,:)=FinalRS_F2;
            clear Cres_Change MIN_RMS_F3 Final_F3 Per_F3 FinalRS_F3
        end
        RMS_DIR_F2(j,1)=max(RMS_RES_F2(1:2:size(RMS_RES_F2,1),1));
        for c=1:2:size(CresOrder,2)
            if RMS_RES_F2(c,1)==RMS_DIR_F2(j,1)
                DIR_F2(j,:,:,:)=squeeze(RES_F2(c,:,:,:));
                DIR_PerF2(j,1)=RES_PerF2(c,1);
                DIR_RSF2(j,:,:)=squeeze(RES_RSF2(c,:,:));
                c_F2(j,1)=c;
            end
        end
        clear CresOrder PForder
    end
    for j=1:size(holddir,2)
        if max(RMS_DIR_F2)==RMS_DIR_F2(j,1)
           DIR2=DIRECTION(1,j);
           C2=c_F2(j,1);
           F2(:,:,:)=squeeze(DIR_F2(j,:,:,:));
           PerF2(1,1)=DIR_PerF2(j,1);
           FinalResponse_F2(:,:)=squeeze(DIR_RSF2(j,:,:));
           MAXRMS_F2=max(RMS_DIR_F2);
        end
    end
   [RMS_CheckF2]=Check_Response_COG(FinalResponse_F2,Response_DATA);
end
%% Wave Force 3
if Check==1
   dof=3;
    for j=1:size(holddir,2)
        if holddir(1,j)>13
            CresOrder=CresOrder3(24-holddir(1,j)+2,:);
            PForder=PForder3(24-holddir(1,j)+2,:);
        else
            CresOrder=CresOrder3(holddir(1,j),:);
            PForder=PForder3(holddir(1,j),:);
        end
        dir=holddir(1,j);
        for c=1:2:size(CresOrder,2)

[MAX_RMS_F3,Final_F3,Per_F3,FinalRS_F3]=Inter_FresiduesGolden(c,dof,d
ir,Fhyd,Bhyd,Ahyd,WDir,Omegaint,PForder,CresOrder,Omg,COG_Original,Ma
```

```
ss,Sadd,Bad,Wavesp,nperiods,Response_DATA,WavesHeading,ThialfHeading)
;
            RMS_RES_F3(c,1)=MAX_RMS_F3;
            RES_F3(c,:,:,:)=Final_F3;
            RES_PerF3(c,1)=Per_F3;
            RES_RSF3(c,:,:)=FinalRS_F3;
            clear Cres_Change MIN_RMS_F3 Final_F3 Per_F3 FinalRS_F3
        end
        RMS_DIR_F3(j,1)=max(RMS_RES_F3(1:2:size(RMS_RES_F3,1),1));
        for c=1:2:size(CresOrder,2)
            if RMS_RES_F3(c,1)==RMS_DIR_F3(j,1)
                DIR_F3(j,:,:,:)=squeeze(RES_F3(c,:,:,:));
                DIR_PerF3(j,1)=RES_PerF3(c,1);
                DIR_RSF3(j,:,:)=squeeze(RES_RSF3(c,:,:));
                c_F3(j,1)=c;
            end
        end
        clear CresOrder PForder
    end
    for j=1:size(holddir,2)
        if max(RMS_DIR_F3)==RMS_DIR_F3(j,1)
           DIR3=DIRECTION(1,j);
           C3=c_F3(j,1);
           F3(:,:,:)=squeeze(DIR_F3(j,:,:,:));
           PerF3(1,1)=DIR_PerF3(j,1);
           FinalResponse_F3(:,:)=squeeze(DIR_RSF3(j,:,:));
           MAXRMS_F3=max(RMS_DIR_F3);
        end
    end
   [RMS_CheckF3]=Check_Response_COG(FinalResponse_F3,Response_DATA);
end
%% Wave Force 4
if Check==2
   dof=4;
    for j=1:size(holddir,2)
        if holddir(1,j)>13
            CresOrder=CresOrder4(24-holddir(1,j)+2,:);
            PForder=PForder4(24-holddir(1,j)+2,:);
        else
            CresOrder=CresOrder4(holddir(1,j),:);
            PForder=PForder4(holddir(1,j),:);
        end
        dir=holddir(1,j);
        for c=1:2:size(CresOrder,2)

[MAX_RMS_F4,Final_F4,Per_F4,FinalRS_F4]=Inter_FresiduesGolden(c,dof,d
ir,Fhyd,Bhyd,Ahyd,WDir,Omegaint,PForder,CresOrder,Omg,COG_Original,Ma
ss,Sadd,Bad,Wavesp,nperiods,Response_DATA,WavesHeading,ThialfHeading)
;
            RMS_RES_F4(c,1)=MAX_RMS_F4;
            RES_F4(c,:,:,:)=Final_F4;
            RES_PerF4(c,1)=Per_F4;
            RES_RSF4(c,:,:)=FinalRS_F4;
            clear Cres_Change MIN_RMS_F3 Final_F3 Per_F3 FinalRS_F3
        end
        RMS_DIR_F4(j,1)=max(RMS_RES_F4(1:2:size(RMS_RES_F4,1),1));
        for c=1:2:size(CresOrder,2)
            if RMS_RES_F4(c,1)==RMS_DIR_F4(j,1)
                DIR_F4(j,:,:,:)=squeeze(RES_F4(c,:,:,:));
                DIR_PerF4(j,1)=RES_PerF4(c,1);
                DIR_RSF4(j,:,:)=squeeze(RES_RSF4(c,:,:));
```

```
                c_F4(j,1)=c;
            end
        end
        clear CresOrder PForder
    end
    for j=1:size(holddir,2)
        if max(RMS_DIR_F4)==RMS_DIR_F4(j,1)
           DIR4=DIRECTION(1,j);
           C4=c_F4(j,1);
           F4(:,:,:)=squeeze(DIR_F4(j,:,:,:));
           PerF4(1,1)=DIR_PerF4(j,1);
           FinalResponse_F4(:,:)=squeeze(DIR_RSF4(j,:,:));
           MAXRMS_F4=max(RMS_DIR_F4);
        end
    end
   [RMS_CheckF4]=Check_Response_COG(FinalResponse_F4,Response_DATA);
end
%% Force 5
if Check==1
   dof=5;
    for j=1:size(holddir,2)
        if holddir(1,j)>13
            CresOrder=CresOrder5(24-holddir(1,j)+2,:);
            PForder=PForder5(24-holddir(1,j)+2,:);
        else
            CresOrder=CresOrder5(holddir(1,j),:);
            PForder=PForder5(holddir(1,j),:);
        end
        dir=holddir(1,j);
        for c=1:2:size(CresOrder,2)

[MAX_RMS_F5,Final_F5,Per_F5,FinalRS_F5]=Inter_FresiduesGolden(c,dof,d
ir,Fhyd,Bhyd,Ahyd,WDir,Omegaint,PForder,CresOrder,Omg,COG_Original,Ma
ss,Sadd,Bad,Wavesp,nperiods,Response_DATA,WavesHeading,ThialfHeading)
;
            RMS_RES_F5(c,1)=MAX_RMS_F5;
            RES_F5(c,:,:,:)=Final_F5;
            RES_PerF5(c,1)=Per_F5;
            RES_RSF5(c,:,:)=FinalRS_F5;
            clear Cres_Change MIN_RMS_F3 Final_F3 Per_F3 FinalRS_F3
        end
        RMS_DIR_F5(j,1)=max(RMS_RES_F5(1:2:size(RMS_RES_F5,1),1));
        for c=1:2:size(CresOrder,2)
            if RMS_RES_F5(c,1)==RMS_DIR_F5(j,1)
                DIR_F5(j,:,:,:)=squeeze(RES_F5(c,:,:,:));
                DIR_PerF5(j,1)=RES_PerF5(c,1);
                DIR_RSF5(j,:,:)=squeeze(RES_RSF5(c,:,:));
                c_F5(j,1)=c;
            end
        end
        clear CresOrder PForder
    end
    for j=1:size(holddir,2)
        if max(RMS_DIR_F5)==RMS_DIR_F5(j,1)
           DIR5=DIRECTION(1,j);
           C5=c_F5(j,1);
           F5(:,:,:)=squeeze(DIR_F5(j,:,:,:));
           PerF5(1,1)=DIR_PerF5(j,1);
           FinalResponse_F5(:,:)=squeeze(DIR_RSF5(j,:,:));
           MAXRMS_F5=max(RMS_DIR_F5);
        end
```

```
    end
   [RMS_CheckF5]=Check_Response_COG(FinalResponse_F5,Response_DATA);
end
%% Force 6
if Check==2
   dof=6;
    for j=1:size(holddir,2)
        if holddir(1,j)>13
            CresOrder=CresOrder6(24-holddir(1,j)+2,:);
            PForder=PForder6(24-holddir(1,j)+2,:);
        else
            CresOrder=CresOrder6(holddir(1,j),:);
            PForder=PForder6(holddir(1,j),:);
        end
        dir=holddir(1,j);
        for c=1:2:size(CresOrder,2)

[MAX_RMS_F6,Final_F6,Per_F6,FinalRS_F6]=Inter_FresiduesGolden(c,dof,d
ir,Fhyd,Bhyd,Ahyd,WDir,Omegaint,PForder,CresOrder,Omg,COG_Original,Ma
ss,Sadd,Bad,Wavesp,nperiods,Response_DATA,WavesHeading,ThialfHeading)
;
            RMS_RES_F6(c,1)=MAX_RMS_F6;
            RES_F6(c,:,:,:)=Final_F6;
            RES_PerF6(c,1)=Per_F6;
            RES_RSF6(c,:,:)=FinalRS_F6;
            clear Cres_Change MIN_RMS_F3 Final_F3 Per_F3 FinalRS_F3
        end
        RMS_DIR_F6(j,1)=max(RMS_RES_F6(1:2:size(RMS_RES_F6,1),1));
        for c=1:2:size(CresOrder,2)
            if RMS_RES_F6(c,1)==RMS_DIR_F6(j,1)
                DIR_F6(j,:,:,:)=squeeze(RES_F6(c,:,:,:));
                DIR_PerF6(j,1)=RES_PerF6(c,1);
                DIR_RSF6(j,:,:)=squeeze(RES_RSF6(c,:,:));
                c_F6(j,1)=c;
            end
        end
        clear CresOrder PForder
    end
    for j=1:size(holddir,2)
        if max(RMS_DIR_F6)==RMS_DIR_F6(j,1)
           DIR6=DIRECTION(1,j);
           C6=c_F6(j,1);
           F6(:,:,:)=squeeze(DIR_F6(j,:,:,:));
           PerF6(1,1)=DIR_PerF6(j,1);
           FinalResponse_F6(:,:)=squeeze(DIR_RSF6(j,:,:));
           MAXRMS_F6=max(RMS_DIR_F6);
        end
    end
   [RMS_CheckF6]=Check_Response_COG(FinalResponse_F6,Response_DATA);
end
%% Total MAX
if Check==1
    MAX_F1= MAXRMS_F1;
    MAX_F3= MAXRMS_F3;
    MAX_F5= MAXRMS_F5;
    FORCES={'FORCE 1' 'FORCE 3' 'FORCE 5'};
    MAX_TOTAL=[MAX_F1 MAX_F3 MAX_F5];

save('FinalRMS_F_TC2b1.mat','RMS_CheckF1','RMS_CheckF3','RMS_CheckF5'
);
```

```
save('Adjust_ResiduesForces_TC2b1.mat','MAXRMS_F5','C5','F5','PerF5',
'FinalResponse_F5','DIR5','MAXRMS_F3','C3','F3','PerF3','FinalRespons
e_F3','DIR3','MAXRMS_F1','C1','F1','PerF1','FinalResponse_F1','DIR1')
else
    MAX_F2=MAXRMS_F2;
    MAX_F4=MAXRMS_F4;
    MAX_F6=MAXRMS_F6;
    FORCES={'FORCE 2' 'FORCE 4' 'FORCE 6'};
    MAX_TOTAL=[MAX_F2 MAX_F4 MAX_F6];

save('FinalRMS_F_TC2b1.mat','RMS_CheckF2','RMS_CheckF4','RMS_CheckF6'
);

save('Adjust_ResiduesForces_TC2b1.mat','MAXRMS_F6','C6','F6','PerF6',
'FinalResponse_F6','DIR6','MAXRMS_F4','C4','F4','PerF4','FinalRespons
e_F4','DIR4','MAXRMS_F2','C2','F2','PerF2','FinalResponse_F2','DIR2')
end

for i=1:size(MAX_TOTAL,2)
    if min(MAX_TOTAL)==MAX_TOTAL(1,i)
       h = msgbox(FORCES{1,i});
       uiwait(h);
    end
end
```

Golden section method for wave forces:

```
function
[MAX_RMS_F,Final_F,FinalPer_F,FinalRS_F]=Inter_FresiduesGolden(c,dof,
dir,F_VF,Bhyd,Ahyd,Wavedir,Omegaint,PForder,CresOrder,Omega,COG_Origi
nal,Mass,Sadd,Bad,Wavesp,nperiods,Response_DATA,WavesHeading,ThialfHe
ading)
R=0.61803399; %The golden ratios.
C=(1.0-R);
a=-10;
c1=10;
b=1;
x1=b;
x2=b+R*(c1-b);
while abs(c1-a) > 0.1  && abs(RMS_AllDofs_f2 - RMS_AllDofs_f1)>0.001
    [sum]=NewForce(CresOrder,x1,c,Omega,PForder,size(F_VF,3));
    F_VF(dof,dir,:)=sum(1,:);
    F_VF_f1(:,:,:)=F_VF;
    [FVF_phase,FVF_amp]=Construct_Forces_Sens((F_VF_f1(:,:,:)));
    % Frequency interpolation
    clear Inter_Bhyd Inter_Ahyd Inter_Fhyd
    [Inter_Bhyd,Inter_Ahyd,Inter_Fhyd]=
FrequencyInterpolation_ABF(Omegaint,Bhyd,Ahyd,F_VF,Wavedir,Omega,Wave
dir);
    [Fhyd_phase,Fhyd_amp]=Construct_Forces_Sens(Inter_Fhyd);
    [Spring_hyd,Amass_hyd,Bdamp_hyd,Fwave_hyd,Error] =
TransformationCOG(COG_Original,Inter_Ahyd,Inter_Bhyd,Fhyd_phase,Fhyd_
amp,Omegaint',Wavedir');

[RAO,Bad_New]=NewRAO(size(Wavedir,2),Omegaint,Amass_hyd,Bdamp_hyd,Mas
s,Bad,Spring_hyd,Sadd,Fwave_hyd);

[RAONew,WavedirNew]=transform_RAOsDir(Omegaint,RAO,WavesHeading,Thial
fHeading);
```

```
    [RS] =
Response_Spectra_Liftdyn(RAONew,Wavesp,WavedirNew,size(WavedirNew,2),
size(Omegaint,2),nperiods);
    RS_f1(:,:)=RS(:,:);
    [RMS_AllDofs_f1]=RMS(dof,RS_f1,Response_DATA);
    clear Inter_Bhyd Inter_Ahyd Inter_Fhyd Fhyd_phase Fhyd_amp
Spring_hyd RAONew Amass_hyd Bdamp_hyd Fwave_hyd Error RAO Bad_New
RS1_fdir RS2_fdir RS3_fdir RS4_fdir RS5_fdir RS6_fdir RS

    [sum]=NewForce(CresOrder,x2,c,Omega,PForder,size(F_VF,3));
    F_VF(dof,dir,:)=sum(1,:);
    F_VF_f2(:,:,:)=F_VF;
    [FVF_phase,FVF_amp]=Construct_Forces_Sens((F_VF_f1(:,:,:)));
    % Frequency interpolation
    clear Inter_Bhyd Inter_Ahyd Inter_Fhyd
    [Inter_Bhyd,Inter_Ahyd,Inter_Fhyd]=
FrequencyInterpolation_ABF(Omegaint,Bhyd,Ahyd,F_VF,Wavedir,Omega,Wave
dir);
    [Fhyd_phase,Fhyd_amp]=Construct_Forces_Sens(Inter_Fhyd);
    [Spring_hyd,Amass_hyd,Bdamp_hyd,Fwave_hyd,Error] =
TransformationCOG(COG_Original,Inter_Ahyd,Inter_Bhyd,Fhyd_phase,Fhyd_
amp,Omegaint',Wavedir');

[RAO,Bad_New]=NewRAO(size(Wavedir,2),Omegaint,Amass_hyd,Bdamp_hyd,Mas
s,Bad,Spring_hyd,Sadd,Fwave_hyd);

[RAONew,WavedirNew]=transform_RAOsDir(Omegaint,RAO,WavesHeading,Thial
fHeading);
    [RS] =
Response_Spectra_Liftdyn(RAONew,Wavesp,WavedirNew,size(WavedirNew,2),
size(Omegaint,2),nperiods);
    RS_f2(:,:)=RS(:,:);
    [RMS_AllDofs_f2]=RMS(dof,RS_f2,Response_DATA);
    clear Inter_Bhyd Inter_Ahyd Inter_Fhyd Fhyd_phase Fhyd_amp
Spring_hyd RAONew Amass_hyd Bdamp_hyd Fwave_hyd Error RAO Bad_New
RS1_fdir RS2_fdir RS3_fdir RS4_fdir RS5_fdir RS6_fdir RS
    FinalPer_x1=x1;
    FinalPer_x2=x2;

[a,c1,x1,x2]=NewPoints(RMS_AllDofs_f2,RMS_AllDofs_f1,x1,x2,c1,a,C);
end

if (RMS_AllDofs_f1 > RMS_AllDofs_f2)
    MAX_RMS_F=RMS_AllDofs_f1;
    Final_F(:,:,:)=(F_VF_f1(:,:,:));
    FinalPer_F=FinalPer_x1;
    FinalRS_F(:,:)=(RS_f1(:,:));
else
    MAX_RMS_F=RMS_AllDofs_f2;
    Final_F(:,:,:)=(F_VF_f2(:,:,:));
    FinalPer_F=FinalPer_x2;
    FinalRS_F(:,:)=(RS_f2(:,:));
end
```